Role of MAPK and NF-κB signalling pathways in the regulation of the human GM-CSF gene in normal and leukaemic blood cells

Martina Canestraro

A thesis submitted to the University of Birmingham for the degree of
DOCTOR OF PHILOSOPHY

Institute of Biomedical Research,
School of Immunity and Infection,
College Of Medical and Dental Sciences,
University of Birmingham

October 2014

ABSTRACT

GM-CSF is an important haematopoietic growth factor and immune modulator. Studies on T cells revealed that efficient activation of the human GM-CSF gene is dependent upon the activation of an enhancer located 3 kb upstream of the promoter, inducible by phorbol myristate acetate and calcium ionophore (PMA/I) via kinase- and Ca^{2+}-dependent signalling pathways, respectively. This enhancer is often aberrantly remodelled as a constitutive DNase hypersensitive site (DHS) in acute myeloid leukaemia (AML). To investigate the role of MAPKs in enhancer activity and chromatin remodelling, I used activated T blasts and human leukaemic cell lines as inducible model systems. The combination of MEK and p38 MAPK inhibitors reduced PMA/I-induced GM-CSF gene expression and the DHS at the enhancer. This was associated with a reduction in DNA-binding activity for the MAPK-inducible AP-1 and in the phosphorylation of MSK1, which in turn stimulates NF-κB transcriptional activity by phosphorylating p65 at Ser276. The combination of MEK and p38 inhibitors also reduced the PMA/I-mediated recruitment of AP-1, MSK1 and NF-κB at the enhancer.

These data demonstrate a cross-talk between the MAPK and NF-κB signalling pathways in regulating GM-CSF gene transcription and therefore represent potential targets for the treatment of AML cases where aberrant chromatin remodelling occurs.

A mamma e papà

ACKNOWLEDGEMENTS

I would like to thank my supervisor Peter Cockerill and my co-supervisor Costanze Bonifer for making this work possible and for all I have learnt in these four years.

Thanks to all the people in the lab, from the ones in Leeds to the last arrived in Birmingham. It has been a pleasure to work with them.

A special thank you to Sarah and Monika for their patience with me in and out of the lab, respectively.

Thanks to Alessandra (the “big” one) and Alessandra (the “little” one), two wonderful friends who I was so lucky to meet here in Birmingham.

And last but not least, special thanks to Laura for her precious help and support.

TABLE OF CONTENTS

LIST OF FIGURES

LIST OF TABLES

LIST OF ABBREVIATIONS

Ab	Antibody
AcH3	Acetylated Histone 3
AML	Acute Myeloid Leukaemia
AP-1	Activator Protein 1
APS	Ammonium Persulfate
ATP	Adenosine Triphosphate
BAF	BRG1/BRM associated factors
bp	Base Pairs
Brg1	Brahma related gene 1
BSA	Bovine Serum Albumin
$CaCl_2$	Calcium Chloride
CBP	CREB binding protein
CDK	Cyclin Dependent Kinase
cDNA	Complementary DNA
ChIP	Chromatin Immunoprecipitation
CLPs	Common Lymphoid Progenitors
CML	Chronic Myeloid Leukaemia
CMPs	Common Myeloid Progenitors
CO_2	Carbon Dioxide
CREB	cAMP response element (CRE)-binding protein
CsA	Cyclosporin A
CTAB	Cetyltrimethyl ammonium bromide
CTCF	CCCTC-binding factor

CTD	Carboxy-Terminal Domain
dATP	Deoxyadenosine Triphosphate
dCTP	Deoxycytidine Triphosphate
dGTP	Deoxyguanosine Triphosphate
DHSs	DNase I Hypersensitive Sites
DMS	Dimethyl Sulphide
DMSO	Dimethyl Sulfoxide
DNA	Deoxyribonucleic Acid
DNase	Deoxyribonuclease
DNMT	DNA Methyltransferases
dNTP	Deoxyribonucleotide Triphosphate
DPE	Downstream Promoter Element
ds	Double Strand
DTT	Dithiothreitol
dTTP	Deoxythymidine Triphosphate
EDTA	Ethylene Diamine Tetra-acetic Acid
EGTA	Ethylene Glycol Tetra- acetic Acid
EMSA	Electrophoretic Mobility Shift Assay
ERK	Extracellular Regulated Kinase
FAB	French American British
FCS	Foetal Calf Serum
FLT3	Fms-like tyrosine kinase 3 (FLT3)
GAPDH	Glyceraldehyde-3-Phosphate Dehydrogenase
G-CSF	Granulocyte Colony-Stimulating factor
GM-CSF	Granulocyte-Macrophage Colony-Stimulating Factor

GTP	Guanosine Triphosphate
h	Human
H3K9ac	histone 3 tail acetylation at lysine 9
H3K27ac	histone 3 tail acetylation at lysine 27
HAT	Histone Acetyltransferase
HDAC	Histone Deacetylase
HMT	Histone Methyl Transferase
HP1	Heterochromatin Protein 1
HS	Hypersensitive Site
HSC	Haematopoietic Stem Cell
I	Ionophore
IFN	Interferon
Ig	Immunoglobulin
IL	Interleukin
IMDM	Iscove's Modified Eagle’s Medium
ING2	Inhibitor of growth family 2
Inr	Initiator elements
IP	Immuno Precipitation
JAKs	Janus Kinases
JNK	c-Jun NH_2-terminal kinase
kb	kilo base
KCl	Potassium Chloride
kD	kilo Daltons
LiCl	Lithium Chloride
LCR	Locus Control Region

LT-HSC	Long Term Haemopoietic Stem Cell
Lys	Lysine
m	Mouse
mA	milli Ampere
MAPK	Mitogen-Activated Protein Kinase
MBT	Malignant Brain Tumor
Me	Methyl Group
$MgCl_2$	Magnesium Chloride
MHC	Major Histocompatibility complex
ml	milli Litre
miRNA	microRNA
MkE	Megakaryocyte/erthyroid
mM	milli Molar
M-MLV	Moloney Murine Leukemia Virus
MPP	Multipotent Progenitors
mRNA	Messenger RNA
MSK	Mitogen and Stress activate Protein Kinase
MTG	3-Mercapto 1,2-Propanediol
NFAT	Nuclear Factor of Activated T cells
ng	nano gram
NK	Natural Killer cells
NP-40	Nonidet P-40
ORF	Open Reading Frame
PBS	Phosphate Buffered Saline
PCC	Polycomb Core Complex

PcG	Polycomb Group
PCR	Polymerase Chain Reaction
PHD	Plant Homeodomain
PIC	Pre Initiation Complex
PMA	Phorbol 12-Myristate 13-Acetate
PMSF	Phenylmethanesulphonylfluoride
Pol II	RNA Polymerase II
RISC	RNA-Induced Silencing Complex
RNA	Ribonucleic Acid
RNAi	RNA interference
RNaseA	Ribonuclease A
rpm	Rotation Per Minute
RT	Reverse Transcription
RTKs	Receptor Tyrosine Kinases
SD	Standard deviation
SDS	Sodium Dodecyl Sulphate
SE	Standard error
siRNA	small interfering RNA
ss	Single Strand
STAT	Signal Transducer and Activator of Transcription
SUMO	Small Ubiquitin-like Modifier
SV40	Simian Virus 40
SWI/SNF	Switch/Sucrose Nonfermentable
T cells	Thymus dependent lymphocytes
TAF	TBP Associated Factor

T-bet	T-box expressed in T cells
TBP	TATA Binding Protein
TF	Transcription Factor
TRIS	TRIS(Hydroxymethyl)Methylamine
U	Unit
UV	Ultraviolet
X	Times
WHO	World Health Organisation

1. INTRODUCTION

1.1 HAEMATOPOIESIS

1.1.1 Haematopoietic cascade

Haematopoiesis is the process responsible for the formation and development of all types of blood cells from common multipotent haematopoietic stem cells (HSCs). Haematopoiesis is usually represented as a hierarchical cascade, where progenitors and precursors originate from HSCs through single or multiple pathways directed by specific cytokines and growth factors (Figure 1.1.1). Progress through the pathways is mediated by alterations of gene expression.

HSCs have the potential to differentiate into various progenitor cells and divide to generate more HSCs (self-renewal ability) [1]. During the differentiation process HSCs gradually lose their self-renewal ability. At every step of differentiation, cells are characterised by specific cell surface markers. HSCs are lin^- (lineage negative, meaning they don't show on their surface any marker of differentiated immune cells), Sca-1^+ and c-kit^+ (LSK) [2]. In humans, lineage negative cells are negative for CD3 (T lymphocytes), CD14 (monocytes), CD16 (NK cells, granulocytes), CD19 (B lymphocytes), CD20 (B lymphocytes), and CD56 (NK cells). LSK cells can be subdivided into long-term (LT-) HSCs (Thy-1^{low}Flk2/Flt3^-), short-term (ST-) HSCs (Thy-1^{low}Flt3^+) and multipotent progenitors (MPPs) (Thy-1^-Flt3^+) [3, 4]. LT-HSCs differentiate into multipotent ST-HSCs, which maintain self-renewal capability for about 6 weeks in vivo.

ST-HSCs differentiate into MPPs, which retain multi-lineage differentiation potential but lack self-renewal capability [3].

MPPs can differentiate into common lymphoid progenitors (CLPs) and common myeloid progenitor (CMPs). CLPs give rise to all classes of lymphocytes (B, T and NK cells) [5, 6]. CMPs in turn give rise to early precursors for megakaryocyte and erythroid progenitors (MEPs) and granulocyte, macrophage progenitors (GMPs) [7]. Both CLPs and CMPs can give rise to dendritic cells (DCs) [8].

Adolfsson and colleagues [9] have identified a class of progenitor cells with lymphoid and myeloid potential but little or no megakaryocyte-erythrocyte potential. These cells, termed lymphoid-primed multi-potent progenitors (LMPPs), are $Lin^{-}Sca\text{-}1^{+}c\text{-}kit^{+}CD34^{+}$ (LSK) and express high level of Flt3.

This discovery led to the proposal of an alternative HSC differentiation program where LMPPs can differentiate into all different haematopoietic cell types apart from megakaryocytes and erythrocytes and GMPs can be generated by both CMPs and LMPPs (Figure 1.1.2).

Figure 1.1.1 ***Hierarchy of hematopoietic differentiation***

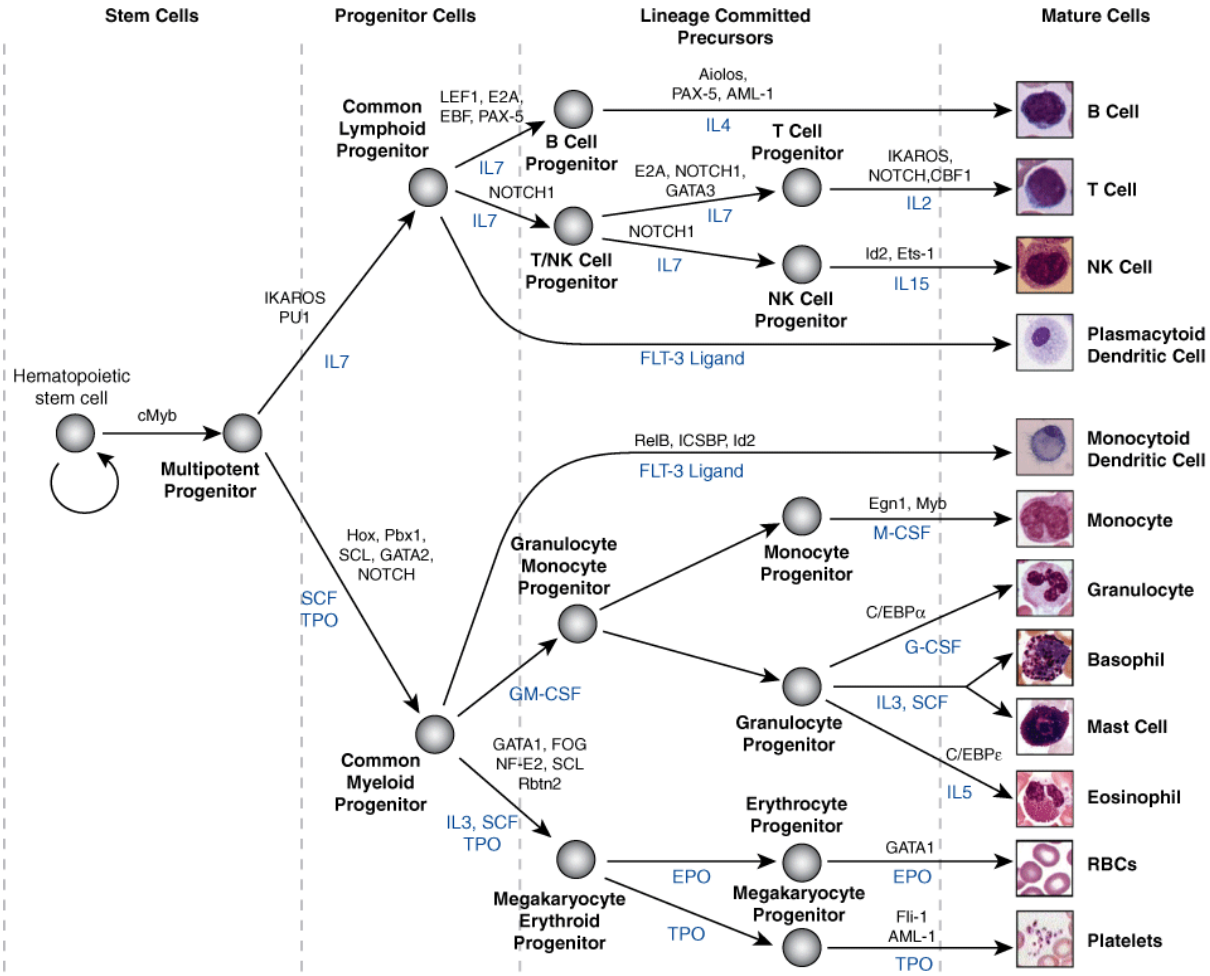

Transcription factors involved in cell transitions are illustrated on the arrows; soluble factors that contribute to the differentiation process are written in blue. SCF, stem cell factor; EPO, erythropoietin; TPO, thrombopoietin. *Taken from Fauci A.S. 2008 [10].*

Figure 1.1.2 ***Hierarchy of differentiation in the haematopoietic system***

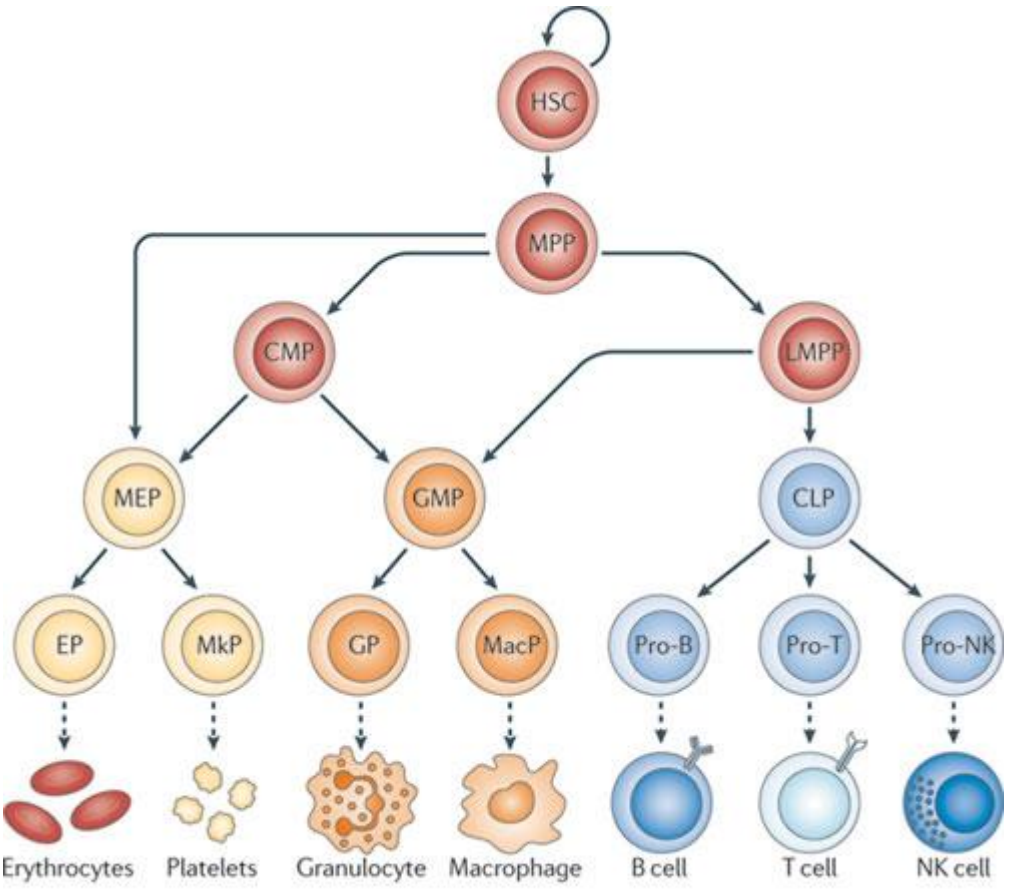

CLP: common lymphoid progenitor; CMP: common myeloid progenitor; EP: erythrocyte progenitor; GMP: granulocyte–macrophage progenitor; GP: granulocyte progenitor; LMPP: lymphoid primed multipotent progenitor; MacP: macrophage progenitor; MEP: megakaryocyte–erythrocyte progenitor; MkP: megakaryocyte progenitor; MPP: multipotent progenitor; NK: natural killer. *Taken from Cedar and Bergman, 2011 [11].*

1.1.2 Lymphoid development

MPPs go through a series of developmental stages where they gradually lose their myeloid lineage differentiation potential to become lymphoid-committed CLPs. In a study conducted by Lai and Kondo, MPPs were subdivided into three groups: FLT3^{low}VCAM-1^{+}, FLT3^{high}VCAM-1^{+} and FLT3^{high}VCAM-1^{-} [12]. Flt3^{low}VCAM-1^{+} MPPs represent the most primitive multi-lineage progenitors: they retain the ability to give rise to MegE, macrophages, granulocytes and lymphoid lineages [13] and they are the only ones which can give rise to CMPs. Flt3^{high}VCAM-1^{+} MPPs correspond to the LMPPs population defined by Adolfsson; they have lost MegE differentiation potential, but they can still differentiate into macrophages/granulocytes and lymphocytes both *in vitro* and *in vivo* [13].

The most developmentally advanced Flt3^{high}VCAM-1^{-} MPPs are lymphoid-specified progenitors, meaning they predominately give rise to lymphocytes *in vivo.* CLPs are characterized by the expression of IL-7Rα surface marker and IL-7/IL-7R signalling is essential for both T and B cell development [14, 15].

1.1.2.1 B cell development

B lymphocytes derive from CLPs through several stages. The first step is represented by Ly6D positive B-primed lymphoid progenitor (BLP), that differentiate into pre-pro-B cell (B220^{int}CD43^{high}) and then into pro-B cell (B220^{high}CD19^{high}). The last stage is represented by CD25 positive pre-B cell [16]. The main transcription factors involved in B cell development are PU.1, Ikaros, EBF, E2A and PAX5. PU.1, encoded by the *SFPI1* gene, is an ETS

transcription factor essential for both myeloid and lymphoid cell development, but not for normal erythroid differentiation [17]. High levels of PU.1 drive myeloid differentiation, whereas low levels promote B-cell differentiation. In MPPs PU.1 levels are under control of the zinc-finger transcription protein Gfi1 (Growth factor independence 1), which represses the *SFPI1* gene. Interestingly, Ikaros promotes Gfi1 and antagonizes PU.1 expression in MPPs [18]. PU.1 and Ikaros have been demonstrated to work together in also regulating Flt3 and IL-7R expression in CLPs [19]. The ability of Ikaros to repress myeloid genes is also linked to its capability to associate with transcription repressive complexes, such as the histone deacetylase (HDAC)-containing complexes NURD or Sin3 [20].

Loss of either E2A, a basic helix-loop-helix E protein, or the early B cell factor EBF leads to a block in B cell development at the pro-B stage, before B cell receptor (BCR) rearrangement occurs [21, 22]. E2A and EBF collaborate at the promoters of target genes, such as genes encoding proteins necessary for BCR rearrangement and signalling [23]. The transcription factor PAX5 is regulated by both E2A and EBF as well as by PU.1, IRF4 and IRF8. PAX5 is expressed only in B cells and it is essential for progression of B cell development beyond the early pro-B cell stage [24]. PAX5 sustains B-cell differentiation by both activating B cell specific genes, including genes modulating homing and migration of B cell progenitors, and suppressing alternate lineage specific genes, such as s Csf1r, Flt3, and Notch1 [25].

1.1.2.2 T cell development

Different to other haematopoietic lineages, that complete their differentiation within the bone marrow, T lymphocytes mature in the thymus. Mature T cells are characterized by the expression of T-cell receptors (TCR) and of the co-receptor molecules CD4 or CD8. Most T cells (> 95%) express a TCR composed of two glycoprotein chains called α and β. Just a small subset of T lymphocytes expresses a TCR that is made up of one γ and one δ chain. CD4 positive cells are defined as T helper or regulatory T cells and they recognize antigens presented by the MHC class II complex expressed on the surface of antigen-presenting cells (APC); CD8 positive cells are known as cytotoxic T cells and they recognize antigens presented by the MHC class I complex. Both CD4 and CD8 positive cells can become memory T cells. These cells persist a long time after an infection has been resolved. They quickly expand to large numbers of effector T cells upon re-exposure to the same infection/antigen thus providing an immune memory. The first step of T cell maturation is the differentiation of CLPs into double negative early T-cell progenitors (ETPs or DN), $CD4^-$ and $CD8^-$, that still maintain their ability to give rise to myeloid cells, dendritic cells and natural killer (NK) [26]. DN thymocytes undergo four further differentiation steps according to the surface expression of CD25 and CD44 (DN1: $CD44^+CD25^-$; DN2: $CD44^+CD25^+$; DN3: $CD44^-CD25^+$; and DN4: $CD44^-CD25^-$) [27]. T lineage commitment occurs at DN3 stage, since DN1 and DN2 populations maintain differentiation potential for other lineages. DN3 cells express a pre-TCR α, encoded by a non-rearranging locus, and a rearranged TCR β chain; the pre-TCR $\alpha\beta$ associates with the CD3 protein complex, involved in signal transduction [28]. During the last stage of maturation a newly

rearranged TCR α chain replaces the pre-TCR α chain and cells start expressing CD4 and CD8, forming the double positive population (DP). DP cells interact with cortical epithelial cells that express high density of both MHC class I and II molecules associated with self-peptides. Just a few TCRs adequately bind to self-peptide-MHC ligands: most of the time this interaction is too weak (death by neglect) or too strong (negative selection) and cells undergo apoptosis. How DP cells become CD4 or CD8 single positive (SP) cells is still a matter of debate. In the "stochastic" (or "selection") model it is assumed that either CD4 or CD8 is randomly switched off. Instead, in the "instruction" model the binding of the TCR αβ to a certain class of MHC molecules would generate a specific signal instructing the DP precursors to switch off the expression of either CD4 or CD8 [29]. A schematic representation of T cell development is shown in Figure 1.1.3.

Notch1 and GATA-3 are key regulatory factors required for development of T cell lineage. Notch1 triggers T cell program in DN cells mediating the upregulation of GATA-3 [30, 31]. A proper balance of GATA-3 and PU.1 expression is also essential. Opposite to GATA-3, PU.1 levels are high in DN1 cells and decrease towards the DN3 stage. The absence of PU.1 causes a block of T cell differentiation at the early stages [32]. PU.1 levels are in turn regulated by RUNX1, which is also required for proper T-lineage commitment [33].

Figure 1.1.3 T cell development in the thymus

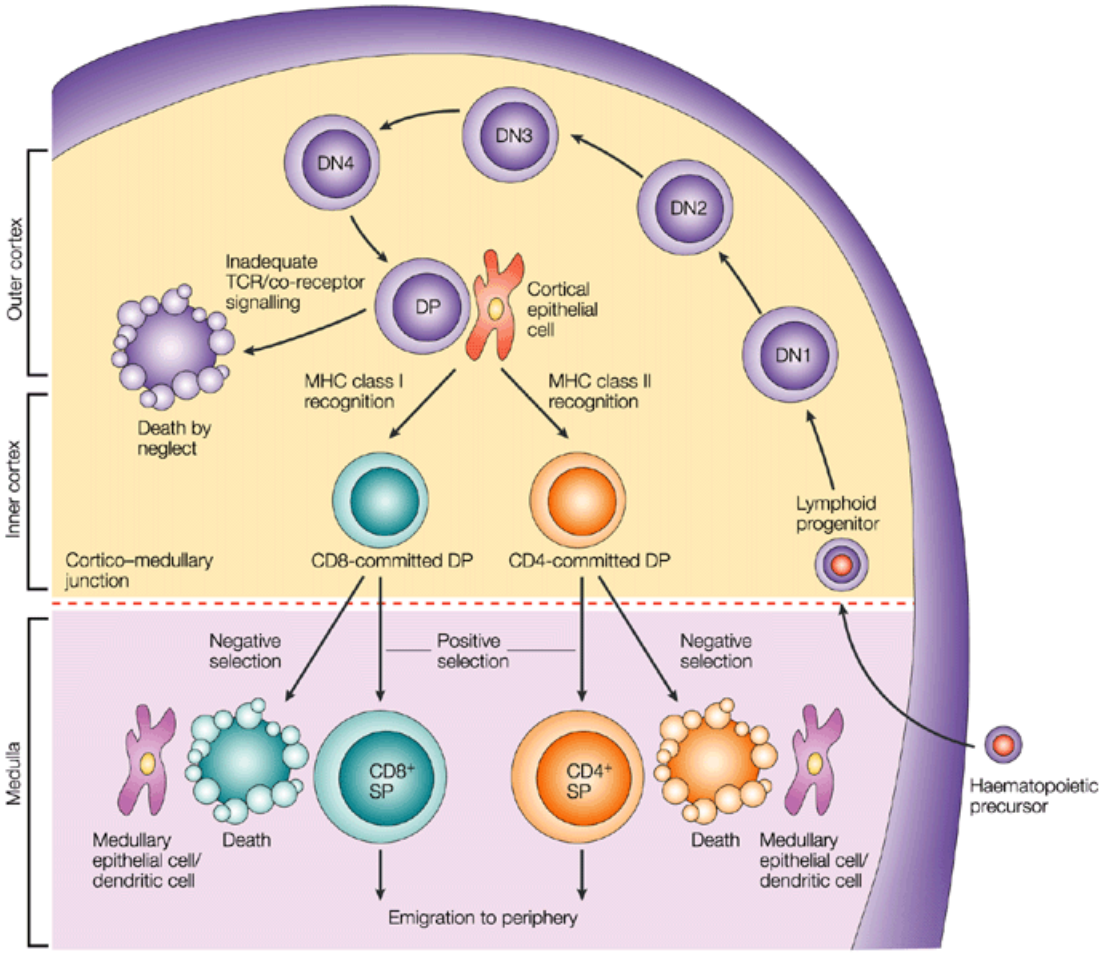

The first step of T cell maturation is the differentiation lymphoid progenitors into double negative (DN) cells, $CD4^-$ and $CD8^-$. DN thymocytes undergo four further differentiation before becoming double positive (DP). DP cells interact with cortical epithelial cells that express high density of both MHC class I and II molecules associated with self-peptides. After this interaction DP cells become CD4 or CD8 committed. The final step of differentiation into single positive (SP) cells occurs in the medulla. *Taken from Germain R.N., 2002* [28].

1.1.3 T cell receptor (TCR) signalling

CD4 and CD8 SP T cells are released from the thymus into the bloodstream as naïve T cells. They become active as they encounter antigen presented by MHC molecules on APC in the peripheral lymphoid organs, mainly lymph nodes and spleen.

TCR forms a complex with CD3, containing the motif for tyrosine phosphorylation ITAMs (Immunoreceptor Tyrosine-based Activation Motifs).

Simultaneous binding of the MHC molecules by TCR complex and CD4 or CD8 co-receptor triggers the signal. The contact with the antigen recruits the Src family kinases Lck and Fyn, activated through their dephosphorylation by CD45. Lck and Fyn initiate the signal by phosphorylating the ITAMs on the CD3. This recruits ZAP-70 [34], which in turn phosphorylates LAT (Linker Activator for T cells). LAT attracts PLC-γ1 [35, 36] which cleaves PIP2 (Phosphatidylinositol-4,5-Bisphosphate) into DAG (Diacylglycerol) and IP3 (Inositol Triphosphate). IP3 leads to an increase of cytoplasmatic level of Ca^{2+}, both because of the release of Ca^{2+} from the endoplasmic reticulum and because of an increased entry of extracellular Ca^{2+} into the cell. The increased Ca^{2+} levels disrupt the interaction between calcineurin and its inhibitory protein calmodulin. Active calcineurin dephosphorylates the transcription factor NFAT (Nuclear Factor of Activated T cells), allowing it to enter the nucleus and to cooperate with other transcription factors to bind promoters and regulate gene transcription [37]. The NFAT family consists of five members: NFATc1-c4 and NFAT5, which is the only one not regulated by calcium signalling [38].

Phosphorylated LAT recruits additional proteins through different members of the GRB2 family proteins. One of these is SLP-76, which in turn recruits Vav

and triggers the p38 and JNK/MAPK pathways [39]. Another example is the recruitment of SOS1 which activates Ras and ERK/MAPK pathway [40]. AP-1 is one of the main transcription factors activated by MAPK signal pathway and involved in TCR receptor signalling (see section 1.5.4). A schematic representation of TCR signalling is shown in Figure 1.1.4. Essential for TCR signalling is the stimulation of the coreceptor CD28, which interacts with CD80 (B7.1) and CD86 (B7.2) molecules on activated APC, and stimulates IL-2 production and T cell proliferation.

TCR activation, together with CD28 costimulation, leads also to the activation of NF-κB pathway. DAG activates Protein kinase C (PKCθ), which in combination with the PKB/Akt, activated by the CD28 co-receptor, is able to regulate NF-κB activity through the IKK complex [41]. This phosphorylates IκB (Inhibitor of Kappa Light Chain Gene Enhancer in B-Cells) and leads to its degradation, causing the release of NF-κB into the nucleus where it activates gene transcription.

Figure 1.1.4 ***TCR signal transduction***

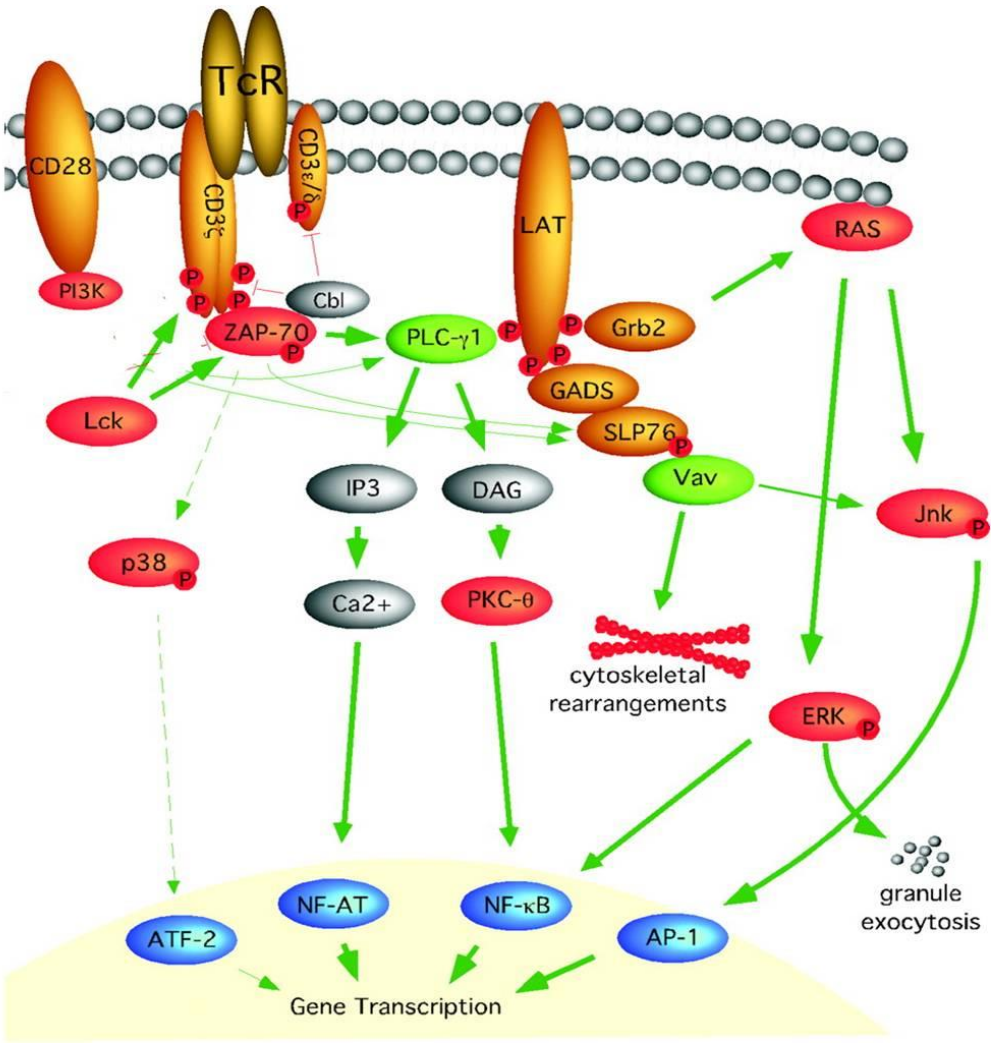

TCR forms a complex with CD3. The contact with the antigen recruits Lck, activated through their dephosphorylation by CD45. Lck initiates the signal by phosphorylating CD3. This recruits ZAP-70, which in turn phosphorylates LAT. LAT attracts PLC-γ1, which cleaves PIP2 (Phosphatidylinositol-4,5-Bisphosphate) into DAG (Diacylglycerol) and IP3 (Inositol Triphosphate). IP3 leads to an increase of cytoplasmatic level of Ca^{2+}. The increased Ca^{2+} levels activates Calcineurin, which dephosphorylates the transcription factor NFAT (Nuclear Factor of Activated T cells), allowing it to enter the nucleus and to cooperate with other transcription factors to bind promoters and regulate gene transcription. Phosphorylated LAT recruits additional proteins through different members of the GRB2 family proteins. One of these is SLP-76, which in turn recruits Vav and triggers the JNK/MAPK pathway. TCR activation, together with CD28 costimulation, leads also to the activation of NF-κB pathway, through DAG and Protein kinase C (PKCθ) activation. *Taken from Jerome 2008 [42].*

1.1.4 Myelopoiesis

Myelopoiesis is the generation of myeloid cells (erythroid, megakaryocytic, granulocytic and monocytic cells) in the bone marrow. GMPs can be generated by either LMPPs or CMPs and they are LSK expressing the FcγR and CD34 surface markers. GMPs can give rise to granulocytes (neutrophils, eosinophils and basophils) or macrophages and essential transcription factors in their regulation are PU.1 and C/EBPα. PU.1 expression in early progenitor cells is induced by Runx1 [33] and it is required for both lymphopoiesis and myelopoiesis. However, high levels of PU.1 in LMPPs drive the myeloid cell development at the expense of B-cell differentiation [43]. C/EBPα regulates the expression of M-CSF and G-CSF receptors and its absence arrests myeloid differentiation prior to the GMPs stage [44]. C/EBPα also regulates the differentiation of eosinophils and basophils, together with GATA-2. Iwasaki and co-workers [45] demonstrated that eosinophils are generated if C/EBPα expression is induced before GATA-2; in contrast if GATA-2 is expressed first followed by C/EBPα, then basophils are generated.

CMPs can also differentiate into megakaryocytes-erythroid progenitor cells (MEPs). Megakaryocytes and erythrocytes differentiation is mainly regulated by PU.1 and GATA-1. GATA-1 is essential for the maturation of megakaryocytes [46] and it collaborates with FOG-1 (Friend of GATA-1) during erythropoiesis.

1.2 LEUKAEMIA

1.2.1 Acute myeloid leukaemia (AML)

Several types of committed precursors (monocyte, granulocyte, erythrocyte, megakaryocyte precursors) can originate from CMPs, giving rise to different final mature cells. A block of the differentiation at any stage of the cascade leads to an abnormal proliferation of myeloid progenitor cells in the bone marrow and defines the characteristics associated with myeloid leukaemia (AML).

To establish a diagnosis of AML ≥ 20% myeloblasts need to be present in the blood or bone marrow. Myeloblasts can be identified by the presence of Auer rods (cytoplasmatic clumps of azurophilic granular material forming elongated needles), by myeloperoxidase (MPO) cytochemical staining or by the expression of myeloid markers such as CD13, CD33 or CD117 [47]. An exception in which a diagnosis of AML can be made irrespective of blast count is the evidence of cytogenetic abnormalities such as t(15;17), inv(16)/t(16;16) or t(8;21).

According to the two-hit model of AML pathogenesis, AML is the result of two types of genetic alterations. Class I mutations support proliferation/survival of hematopoietic progenitors [48, 49]; they typically involve alterations in receptor tyrosine kinase (RTK) signalling pathways such as mutations in FMS-like tyrosine kinase 3 (Flt3), c-Kit and Ras or activation of PI3K/Akt pathways. Acting in cooperation, class II mutations lead to impaired haematopoietic differentiation [48] and typically involve alterations of transcription factors required for normal myeloid cell differentiation. Class II mutations include fusion

proteins such as RUNX1-ETO, CBFβ-MYH11, PML-RAR [48, 50] and mutations of the transcription factors RUNX1, mixed lineage leukaemia (MLL), C/EBPα or nucleophosmin 1 (NPM1) [51].

In the last 5 years a comprehensive genomic analysis has been used to find new gene mutations, such as those in TET2, isocitrate dehydrogenase 1/2 (IDH1/2), DNMT3A, which directly targets epigenetic control such as DNA or histone methylation status [52]. Some authors, including Naoe and Kiyoi, have called this last class of gene mutations “class III” and they have proposed a model in which the three classes of mutations are functionally linked to generate AML [53].

1.2.1.1 Epigenetics in AML

Many fusion proteins generated by chromosomal translocations have a critical role in leukaemogenesis because their target genes are involved in stem cell development or lineage differentiation in haematopoiesis. These chimeric fusion oncoproteins are capable of directly interacting with chromatin remodelling complexes or histone modifier enzymes, leading to gene deregulation and a differentiation block [54].

So far more than 50 different fusion partners of the MLL gene have been identified in both AML and acute lymphoblastic leukaemia (ALL). MLL methylates lysine 4 at histone 3 through its SET domain. Moreover, it is part of a large complex of proteins able to interact with chromatin remodelers, HATs, HDACs and other histone modifiers [55]. MLL fusion proteins, such as MLL-CBP or MLL-p300, lack the SET domain but they retain the bromodomain and HAT domain and so they increase the acetylation and the expression of target genes

(e.g. Hox genes), which are normally highly expressed in pluripotent haematopoietic stem cells and downregulated upon differentiation; MLL fusion proteins act as constitutive activators, preventing proper cell differentiation (Figure 1.2.1).

The t(8;21) translocation generates the RUNX1-ETO fusion protein. RUNX1 is part of the core-binding factor (CBF) complex, together with CBFβ subunit. RUNX1 can function as either a transcriptional activator or repressor, whereas its partner ETO binds co-repressors such as HDACs, Sin3, N-CoR and SMRT [56]. RUNX1-ETO recruits the co-repressors N-CoR/Sin3/HDAC1 complex at RUNX1 target genes, leading to transcriptional repression [57].

Acute promyelocytic leukaemia is also characterised by the translocation of the retinoic acid receptor alpha (RARα) and one of five different partner genes, amongst which the most frequent is PML. In the absence of retinoic acid (RA), RAR binds to specific DNA sequences on target genes (called RA responsive elements or RARE) and represses transcription by recruiting repressive complexes such as NCoR-HDAC. Physiological doses of RA promote the dissociation of the co-repressor complexes and the recruitment of co-activators, leading to transcriptional activation of target genes and promoting cell differentiation. The fusion protein PML-RARα binds the co-repressor complexes with higher efficiency than RARα and it is responsible for the differentiation block. Pharmacological doses of all-*trans*-RA are able to remove these repressive complexes and recruit HATs, inducing re-expression of the silenced genes and differentiation of the promyelocytic cells [58] (Figure 1.2.1).

Figure 1.2.1 ***Model of gene repression mediated by leukaemia fusion proteins***

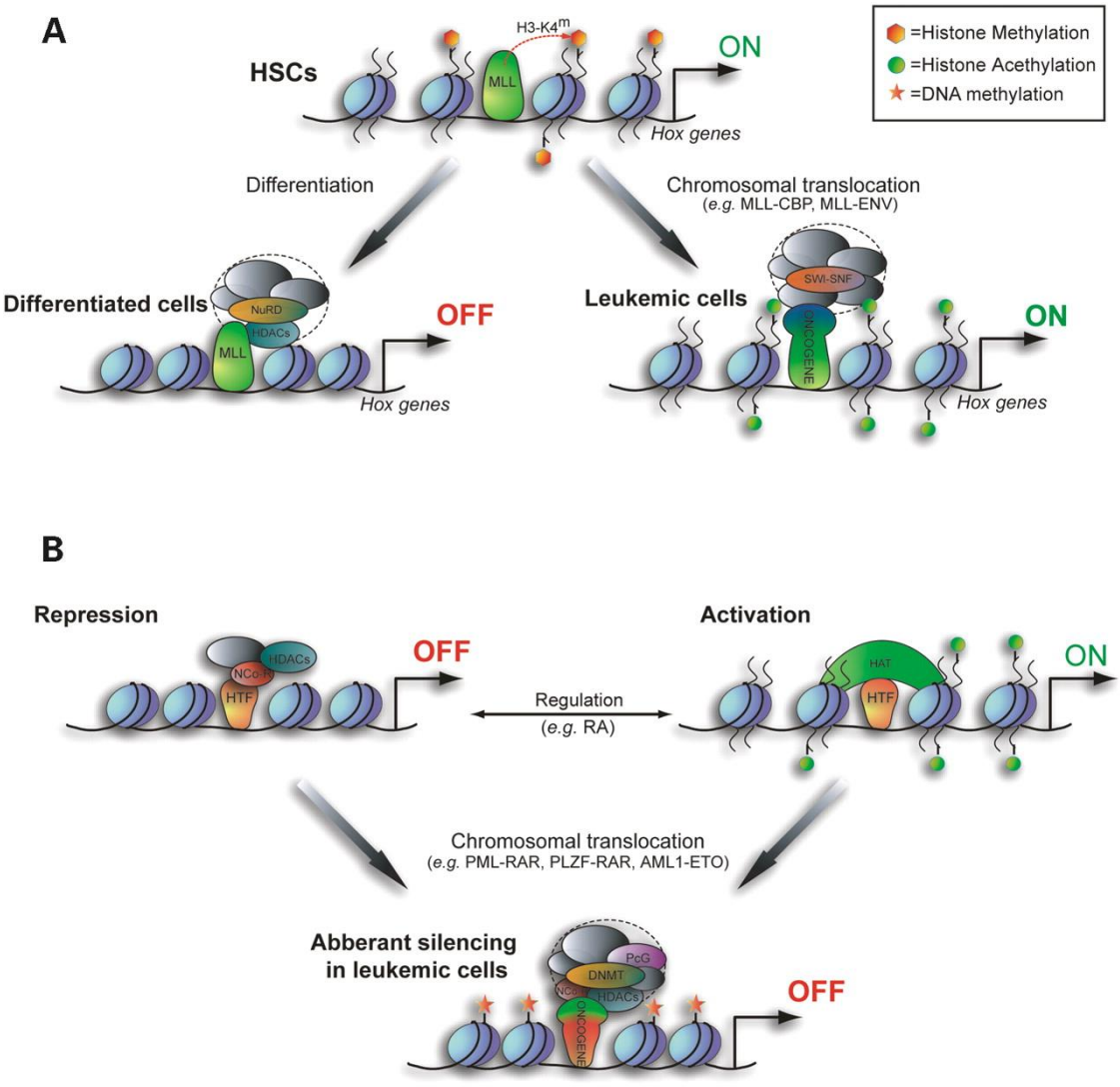

(A) In leukaemic cells, MLL fusion proteins block cell differentiation acting as constitutive activators of target genes critical for normal haematopoietic development. (B) Haematopoietic transcription factors (HTF) regulate cell differentiation via interaction with either co-activator (HAT) or co-repressor (HDAC). Fusion proteins, such as PML–RARα and RUNX1–ETO, show a constitutively repressed gene transcription because of their stronger affinity for co-repressor complexes.

Taken from Di Croce L., 2005 [59].

Both PML-RARα and RUNX1-ETO are able to interact with DNMTs, leading to methylation of CpG islands of target promoters [58, 60]. Aberrant DNA methylation is a common feature in AML [61] and it has been shown that there is an increase of DNMT1, DNMT3A and DNMT3B levels in AML blasts [62, 63].

1.2.2 T cell acute lymphoblastic leukaemia (T-ALL)

T cell acute lymphoblastic leukaemia (T-ALLs) is an aggressive haematological tumour resulting from the malignant transformation of lymphoid progenitors cells. Normally immature $CD34^+$ cells leave the bone marrow and enter the thymus, where they differentiate through progressive stages into mature T-cells harbouring a functional TCR receptor. However, in primary T-ALL patient samples there is a clonal expansion of malignant T-cells arrested at a specific stage during T-cell differentiation. The T cell transformation process is regulated by different genetic alterations that contribute to alter the normal process of T cell growth and differentiation. The most relevant oncogenic pathway in T cell transformation is governed by NOTCH1 signalling (Figure 1.2.2) [64].

Figure 1.2.2 ***Schematic representation of NOTCH1 signalling in T cell progenitors***

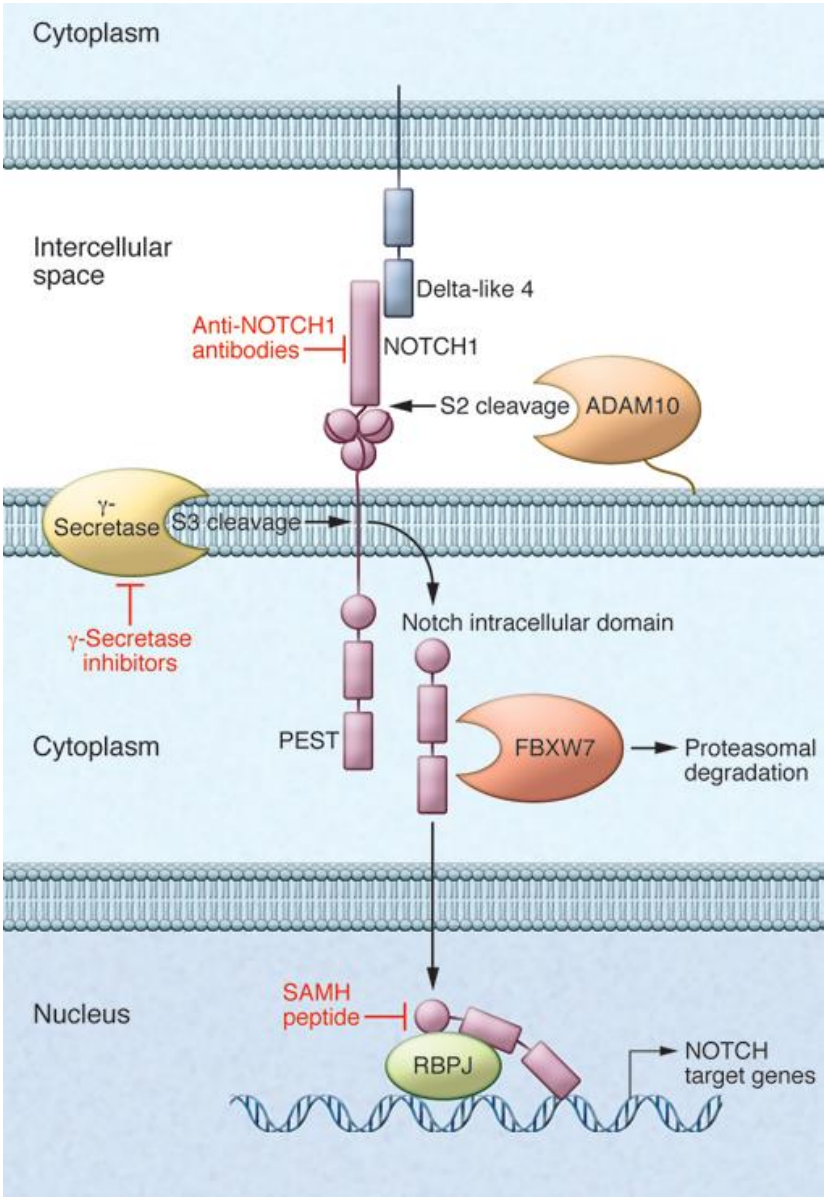

Interaction of the NOTCH ligand delta-like 4 with NOTCH1 triggers a double cleavage of the receptor, first by the metalloprotease ADAM10 and subsequently by the γ-secretase complex. Release of the intracellular domains of NOTCH1 from the membrane activates the expression of NOTCH target genes in the nucleus. FBXW7 recognizes the PEST domain of activated NOTCH1 and terminates NOTCH signalling through its proteasome degradation. *Taken from Van Vlierberghe et al., 2012 [64].*

Activating mutations of NOTCH1 signalling have been found in over 50% of T-ALLs cases [65]. Constitutive activation of NOTCH1 signalling often cooperates with alterations of cell cycle regulators, such as deletions of the cyclin-dependent kinase inhibitor 2A (CDKN2A) [66].

Moreover, T-ALLs show chromosomal translocations that place T-ALL transcription factor oncogenes under the control of strong T-cell specific enhancers located in the TCRβ and TCRαδ loci, leading to their aberrant expression in T cell progenitors. Examples of these transcription factors are TAL1 [67] and TAL2 [68] belonging to the basic helix-loop-helix (bHLH) family; LIM-only domain (LMO) genes such as LMO1 and LMO2 [69]; the HOX transcription factors HOXA [70]; MYC [71] and MYB [72].

Important signal transduction pathways are also altered in T-ALLs. Constitutive activation of PI3K-AKT [73], RAS and JAK/STAT [74, 75] signalling pathways has been found in about 5-10% of T-ALLs.

1.3 TRANSCRIPTION

1.3.1 Basal transcription machinery

Messenger RNAs (mRNAs) are transcribed by the DNA-dependent RNA polymerase II (Pol II) machinery. The process of transcription starts at the transcription start site (TSS) located in the core promoter element (see section 1.3.2.1) with the assembly of the 'transcription machinery'. The assembled apparatus contains a 12-subunit (Rpb1-Rpb12) RNA polymerase II core complex, general transcription factors (GTFs) (TFIIA, TFIIB, TFIID, TFIIE, TFIIF, TFIIH) and co-activators [76]. Co-regulators are often multiprotein complexes, many of which can interact directly with Pol II and GTFs and influence expression, or have chromatin remodelling activity changing the chromatin architecture of the gene. The activity of co-regulators influences transcription-factor association and the transcriptional status [77].

In vitro studies demonstrated a stepwise recruitment of the GTFs to form a stable pre-initiation complex (PIC) at the core promoter region. TFIID first binds to the promoter, followed by TFIIA and TFIIB that help stabilize promoter-bound TFIID, and then the recruitment of RNA Pol II/TFIIF. After formation of a stable complex, TFIIE and TFIIH are recruited (Figure 1.3.1) [78].

The largest subunit of RNA Pol II (Rpb1) contains a carboxy-terminal repeat domain (CTD) consisting of 52 (in human) repeats of Tyr-Ser-Pro-Thr-Ser-Pro-Ser. The Cdk7 subunit of TFIIH is able to phosphorylate CTD at Ser5 (as well as at Ser7) and this phosphorylation allows transcriptional initiation to occur. RNA Pol II complex transcribes about 20-30 base pairs and then pauses. Transcription is resumed and transcriptional elongation occurs once CTD has

been phosphorylated at Ser2 by CDK9 and cyclin T subunits of the positive transcription elongation factor b (pTEFb). TFIIF moves along with the RNA Pol II enzyme, whereas TFIIA and TFIID remain attached to the promoter and promotes the subsequent recruitment of TFIIB and RNA Pol II for repeated cycles of transcription.

RNA polymerase II produces not only coding mRNAs that will be translated into proteins, but also transcripts called noncoding RNAs (ncRNA)s which have regulatory functions and do not encode proteins. ncRNAs can regulate gene expression through several mechanisms, for example interacting with transcriptional coregulators that can influence their recruitment to specific transcriptional control regions [79].

Different ncRNAs have been identified, among which long non coding RNAs (lncRNAs), longer than 200 nucleotides, and the small double-stranded (ds) siRNAs and miRNAs. siRNAs and miRNAs are involved in translation arrest, mRNA stability and gene silencing, a phenomenon called RNA interference (RNAi).

Figure 1.3.1 ***Sequential assembly pathway of the basal transcription machinery***

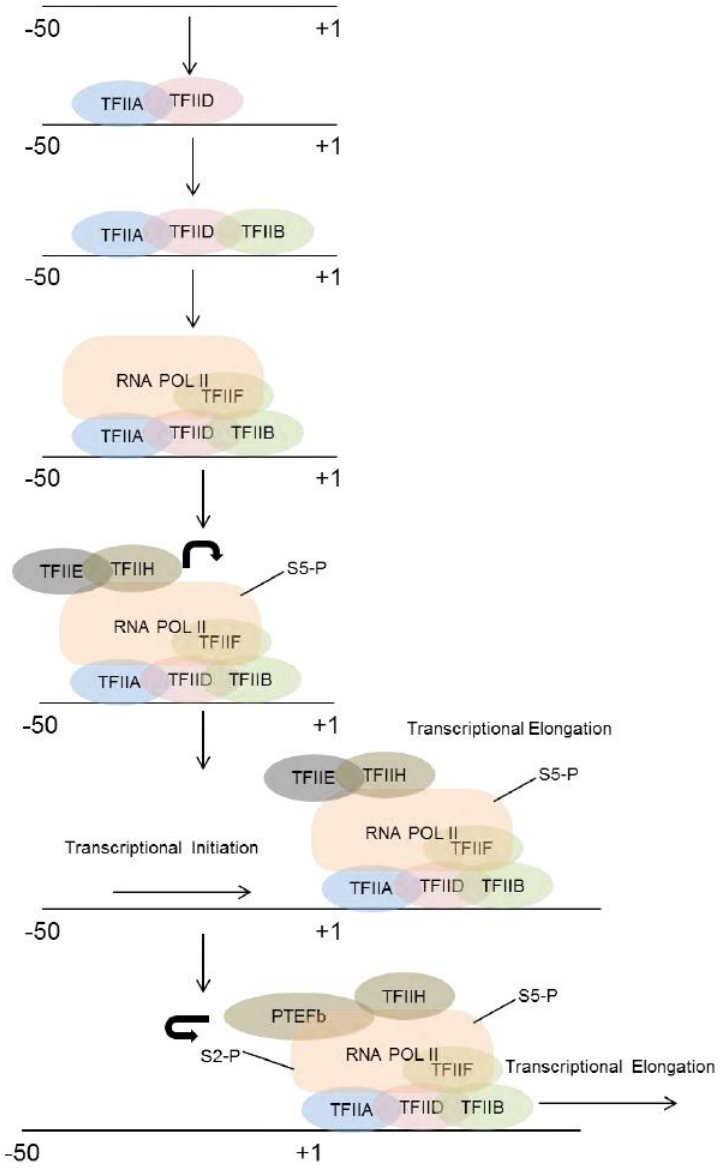

Picture represents a stepwise recruitment of the general transcription factors to form stable pre-initiation complex at the core promoter region. TFIID first binds to the promoter, followed by TFIIA and TFIIB that help stabilize promoter-bound TFIID, and then the recruitment of RNA Pol II/TFIIF. After formation of a stable complex, TFIIE and TFIIH are recruited. TFIIH phosphorylates RNA Pol II at Ser5 and this phosphorylation allows transcriptional initiation to occur. RNA Pol II complex transcribes about 20-30 base pairs and then pauses. Transcription is resumed and transcriptional elongation occurs once CTD has been phosphorylated at Ser2 by positive transcription elongation factor b (pTEFb). *Taken from D.Ray's PhD thesis, University of Birmingham 2012.*

1.3.2 *Cis*-regulatory elements and DNAse I hypersensitive sites (DHSs)

The information about when and where a gene is going to be expressed resides in defined genomic elements called *cis*-regulatory elements. These are regions of DNA or RNA that regulates the expression of genes located on that same molecule of DNA. They contain binding sites for *trans*-acting proteins involved in the positioning of the basic transcriptional machinery and in the regulation of transcription. Promoters are DNA regions used to position the basic transcriptional machinery, which is a DNA-dependent RNA polymerase (RNA Pol). Other DNA *cis*-regulatory elements are enhancer, silencers, insulators, locus control regions (LCRs). Active *cis*-regulatory elements are typically characterized by an enhanced sensitivity to DNase I digestion [80]. DNase I is a nuclease that cleaves DNA (single-stranded DNA, double-stranded DNA and chromatin) preferentially at phosphodiester linkages adjacent to a pyrimidine nucleotide, yielding 5'-phospho-polynucleotides with a free hydroxyl group on position 3', on average producing tetranucleotides. Most of the DNA in the nucleus is relatively inaccessible to proteins, because it exists as condensed chromatin. However, about 1% of the genome exists as regions of decondensed chromatin called DNAse I hypersensitive sites (DHSs), which are usually nucleosome-free and provide increased access for factors to interact with DNA [81, 82]. The normal process of gene activation involves the recruitment of factors that bind the DNA in a cooperative manner and can create these nucleosome-free regions which are the DHSs. Indeed, genes that are being transcribed are normally characterized by the presence of DHSs, which are indication of a more open chromatin structure [83, 84].

1.3.3 General structure of a typical eukaryotic gene

1.3.3.1 Promoters

In eukaryotes messenger RNAs (mRNAs) are transcribed by the RNA polymerase II (RNA Pol II) machinery. Promoters usually encompass upstream promoter elements (UPEs) and a core promoter. The core promoter is a region around the transcriptional start site (TSS) of a gene and contains DNA elements that promote the binding of regulatory transcription factors and the formation of the pre-initiation complex (PIC) (See section 1.3.3.3). Core promoters contain an AT-rich sequence called the TATA box. The TATA box binds the TATA-binding protein (TBP) [85] which, together with TATA-associated factors form the complex TFIID. Most of the time TFIID is recruited by other elements within the core promoter, such as the initiator (Inr) and the downstream promoter element (DPE). The BRE region recognizes TFIIB complex. Core promoters can be divided into two classes: focused core promoters, with a single TSS or a cluster of TSSs over a narrow region of several nucleotides, and dispersed core promoters, that have a dispersed range of potential TSSs over a 50-100 bp region [86]. The TATA box is the most ancient promoter element. Its consensus sequence is TATAWAAR and it is preferably located 30-31 bp upstream from the TSS in mammals [87].

The Inr straddles the TSS. It is the most prevalent region in focused core promoters [88] and contains the consensus sequence YY*A*NWYY in humans, where the *A* frequently represents the TSS. The BRE region can be located upstream as well as downstream of the TATA box and has both activating or inhibitory effect on transcription [89].

The downstream promoter element (DPE) cooperates with the Inr and is located between +28 and +33 bp from the TSS.

Other known elements are the motif ten element (MTE), conserved from *Drosophila* to mammals, located between +18 and +27 bp from the TSS.

Usually core promoters contain either both a TATA box and an Inr element or an Inr and a downstream promoter element (DPE) [90]. There is also evidence that a DPE and a TATA elements can co-exist in the same gene, and that some genes have neither a DPE or a TATA region [91]. However, some promoters do not contain any of the three core regulatory regions defined in *Drosophila* [92].

1.3.3.2 Silencers

Silencers are *cis*-regulatory elements responsible for the downregulation of gene expression. Two different classes of silencers exist: classical silence elements and negative regulatory elements (NREs). Classical silence elements are short, position-independent motifs that interfere with the PIC assembly through the binding of repressor proteins and are normally found upstream of the TSS. The NREs are position-dependent silencers that prevent the binding of transcription factors to their respective *cis*-regulatory motifs and are found within introns and exons, both up- and downstream of the TSS [93].

1.3.3.3 Enhancers and locus control regions (LCR)

Enhancers are *cis*-acting DNA regions containing binding sites for activator transcription factors and they increase the rate of transcription in a manner that is independent of their orientation and distance from the TSS. In fact they can be located upstream or downstream of the TSS (even thousands of base pairs distant from the gene that they regulate) within introns or exons and in the 5' or 3' untranslated (UTR) gene regions [94]. Transcription factors and co-activators bind enhancers forming a complex defined as an "enhanceosome", which is able to directly or indirectly interact with the pre-initiation complex (PIC) of the transcription machinery, stabilizing its binding at the promoter and increasing transcription. It seems that the interaction between enhancer and promoter occurs through chromatin looping, but it's not clear whether the contact happens by chance, due to free motion of the chromatin strand or through the action of protein complexes that bind the enhancer and track the chromatin strand until it encounters the promoter [95]. During development, transcriptional specificity is guaranteed by both the enhancer-promoter and the tissue specificities (enhancers get activated by specific transcription factors in specific cell types only).

Locus control regions (LCRs) are DNA regulatory elements consisting of multiple activator binding sites. Contrary to enhancers, LCR stimulate transcription independently of their site of integration into native chromatin and their effect is limited by distance and orientation [76].

1.3.3.4 Insulators

Two different types of insulators have been identified: enhancer-blocking insulators and barrier insulators. The enhancer-blocking insulators are located between the enhancer and the promoter and block the signal between the two elements. This also represents a way to guarantee the enhancer-promoter selectivity preventing interactions with inappropriate promoters. Barrier insulators block heterochromatin spreading by promoting enzymatic activities like HATs and chromatin remodelling complexes, thus recruiting euchromatin.

Three different models for enhancer-blocking activities have been identified [96]. In the decoy model the insulator competes with the promoter for the contact with the enhancer (Figure 1.3.2a). In the facilitator model the contact between the insulator and the facilitator proteins interrupts the signal between enhancer and promoter (Figure 1.3.2b). In the looping model insulators organise chromatin looping by promoting contacts between insulators or with other genomic structures (Figure 1.3.2c). Interaction between enhancers and promoters can only occur if they are located in the same loop. Looping can either interfere with enhancer-promoter interaction (thus mediating the enhancer-blocking function of insulators) or it can assist in increasing enhancer-promoter contact, resulting in an active gene.

Figure 1.3.2 Structural models for enhancer-blocking activities

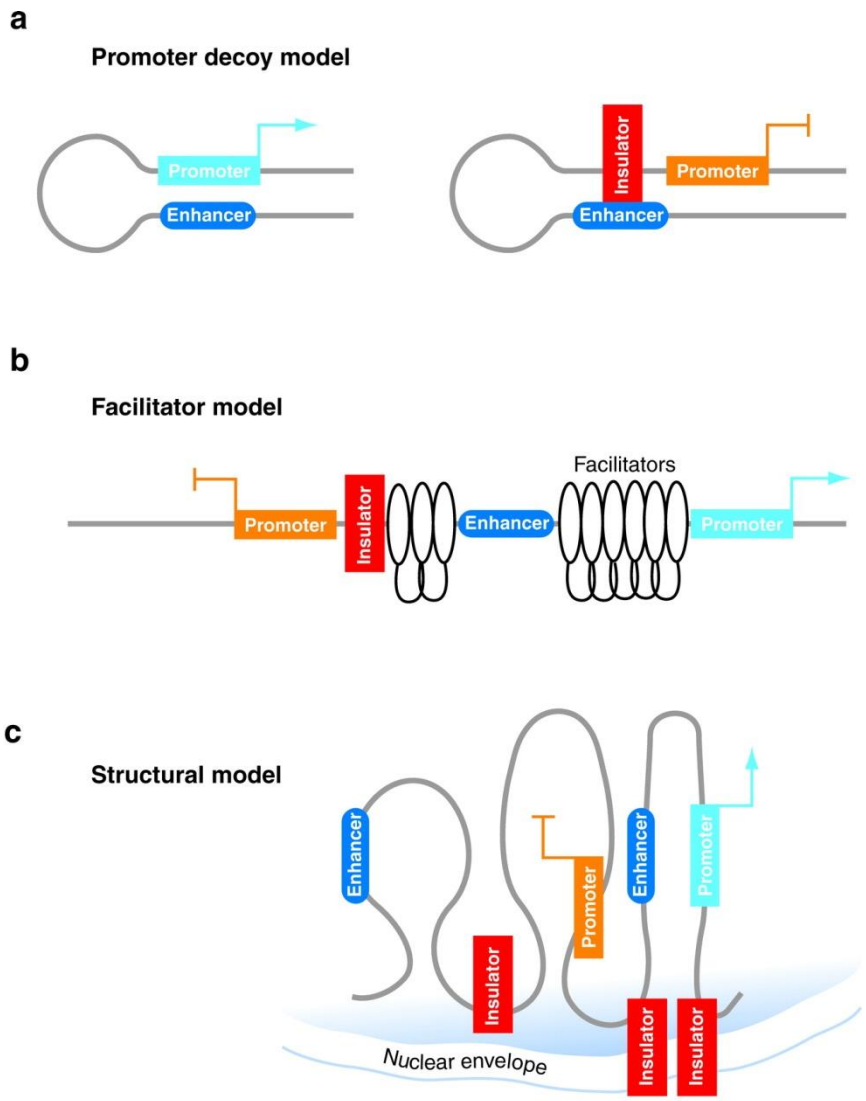

Picture represents three different models for enhancer-blocking activities. In the decoy model the insulator competes with the promoter for the contact with the enhancer (Figure 1.3.2a). In the facilitator model the contact between the insulator and the facilitator proteins interrupts the signal between enhancer and promoter (Figure 1.3.2b). In the looping model insulators organise chromatin looping by promoting contacts between insulators or with other genomic structures (Figure 1.3.2c). *Taken from Valenzuela et al., 2006* [96].

In vertebrates all the identified enhancer-blocking insulators contain cis-regulatory binding motifs for the CCCTC-binding factor (CTCF). CTCF was one of the first proteins demonstrated to be involved in chromatin looping. Initially CTCF was described as a transcriptional repressor of the chicken *c-myc* gene [97]. The versatile role of CTCF is confirmed by the fact that its binding sites can be found at boundaries that separate active and inactive domains but also at enhancer, gene promoters and inside gene bodies. CTCF functions were initially studied at the β-globin locus and the imprinted H19-Igf2 locus. The human β-globin locus contains five developmentally regulated beta-type globin genes, under the control of one locus control region (LCR) and it is flanked by CTCF binding sites [98]. In erythroid progenitor cells CTCF binding sites interact with each other to create an inactive chromatin hub in which LCR and the β-globin genes are not in contact. Upon erythroid differentiation specific transcription factors and cohesin promote the formation of a chromatin hub where the LCR interacts with the β-globin genes and enhance transcription (Figure 1.3.4a).

However, CTCF functions were initially studied at the chicken β-globin locus.

A schematic picture of the locus is represented in picture 1.3.3.

Figure 1.3.3 The chicken β-globin locus

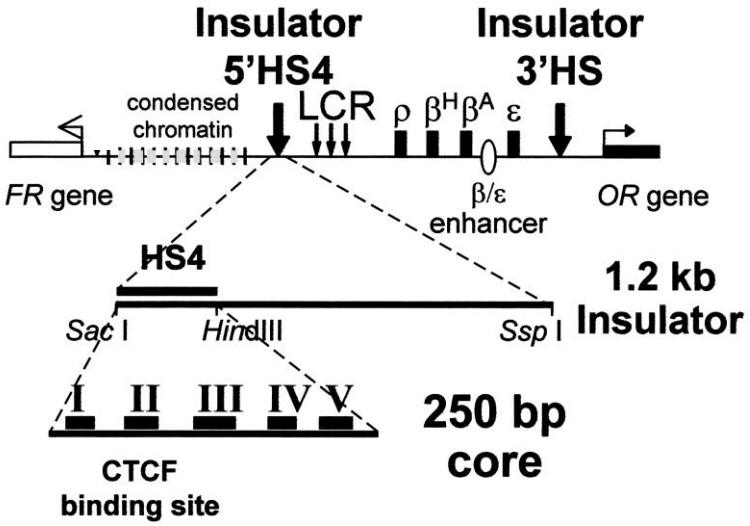

The locus control region (LCR) is located between the 5'HS4 and the ρ gene. The insulator region is defined by the SacI and SspI retriction enzymes; it is 1.2 kb long and it contains the CTCF binding site. Picture taken from Targa et al, 2002 [99].

The 30 kb chicken β-globin gene locus includes four globin genes that are developmentally regulated and expressed in erythroid cells [100]: rho (ρ), beta H (β^H), beta A (β^A), epsilon (ε) (5'-3' direction). There are two insulator regions. The 1.2 kb insulator region at 5' includes the DNase I-hypersensitive site 5′HS4, which has both enhancer-blocking and barrier properties. The region II depicted in the picture below contains the CTCF binding motif. Upstream of the 5'HS4 is a 16 kb condensed chromatin region, followed by a folate receptor gene (FR) [101]. The constitutive hypersensitive site, 3′HS, has enhancer-blocking properties, and beyond a gene for an odorant receptor (OR) is located [102].

The H19/Igf2 locus contains an imprinting control region (ICR) between the H19 and the Igf2 genes. On the maternal allele CTCF binds the unmethylated ICR and blocks the communication between the Igf2 gene and the distal enhancer, leading to H19 expression. On the paternal allele ICR is methylated; this prevents CTCF binding and allows the distal enhancer to interact with the Igf2 genes and to enhance its expression (Figure 1.3.4b) [103].

ChIP-Seq analysis revealed that more than 14,000 CTCF binding sites are present in the human genome and more than 5000 sites are ultra-conserved between tissues and species and bind CTCF with high affinity [104]. Genome-wide analysis also revealed that CTCF globally co-localises with cohesin, which has been demonstrated to have a role in looping formation [105]. Cohesin localization to CTCF sites is dependent on CTCF binding; on the contrary CTCF can bind its DNA binding motifsin the absence of cohesin binding. CTCF shares binding sites with several other factors, such as the histone deacetylase SIN3 [106], nucleophosmin [107], FOXA1 and the oestrogen receptor (ER).

Figure 1.3.4 CTCF activity at β-globin and H19/Igf2 loci

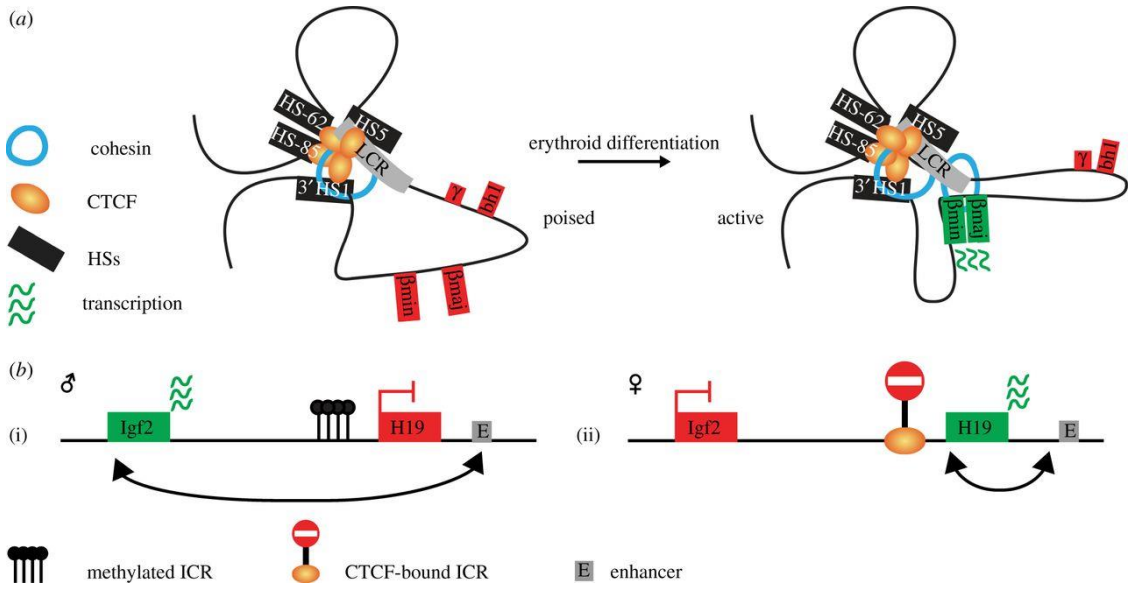

a) In erythroid progenitor cells CTCF binding sites interact with each other to create an inactive chromatin hub in which LCR and the β-globin genes are not in contact. Upon erythroid differentiation specific transcription factors and cohesin promote the formation of a chromatin hub where the LCR interacts with the β-globin genes and enhance transcription. b) The H19/Igf2 locus contains an imprinting control region (ICR) between the H19 and the Igf2 genes. On the paternal allele ICR is methylated; this prevents CTCF binding and allows the distal enhancer to interact with the Igf2 genes and to enhance its expression (i). On the maternal allele CTCF binds the unmethylated ICR and blocks the communication between the Igf2 gene and the distal enhancer, leading to H19 expression (ii). Taken from Holwerda et al., 2013 *[103]*.

1.3.4 Transcriptional activators and repressors

Gene expression is regulated by the interaction in *trans* of specific transcription factors (TFs), activators or repressors, with the *cis* regulatory elements present on the DNA. Transcription factors are proteins that recognize and bind specific DNA sequences. Activators consist of two different domains: a DNA binding domain and an activator domain that recruits and stimulates the activity of the transcription apparatus. The main DNA binding domains can be classified as:

1) basic leucine zipper (bZIP) motifs, found in dimeric complexes of two proteins that each contains short α-helices with a leucine residue at every seventh position and an adjacent basic DNA-binding domain. Leucines in the two helices interact with each other forming a Y shape which bifurcates to enable α-helix to interact with the major groove of the DNA. The c-Fos and c-Jun components of the activator protein AP-1 are leucine zipper regulatory proteins;

2) zinc finger domains, characterized by the coordination of one or more zinc ions in order to stabilize the fold. The most common zinc fingers are the Cys_2His_2-like proteins, where the zinc finger motif consists of an α helix and an antiparallel β and the zinc ion is coordinated by two histidines and two cysteine residues;

3) basic-helix-loop-helix (bHLH) domains are characterized by two α-helices connected by a flexible loop;

4) helix-turn-helix (HTH) domains, composed of two $\underline{\alpha}$ helices joined by a short strand of amino acids [108].

Enhancers and promoters can encompass multiple DNA binding sites for TFs, so that they can bind in a cooperative way and provide a mechanism for combinatorial control. In fact the presence of a binding site of a TF is usually insufficient to generate a functional productive interaction in terms of transcriptional regulation. Some TFs are also able to recruit and regulate the activity of chromatin-modifying complexes and the transcription machinery, promoting or repressing gene transcription. Histone acetylases are components of many transcriptional coactivators. Transcriptional repressors can be divided into two categories: general and gene specific.

Many general repressors interact with the TATA-binding protein (TBP) and prevent the formation of the transcription initiation complex. An example is represented by Mot1, which causes the dissociation of TBP from DNA in an ATP-dependent manner [109]. Gene specific repressors can either bind to activators or compete for activator binding sites. Deacetylase complexes such as mSin3A and NuRD have a repressor activity and they can be recruited to DNA by DNA-binding proteins or through corepressors such as N-Cor [110].

1.4 CHROMATIN

1.4.1 Chromatin structure

Chromosomal DNA, which contains the genome of eukaryotic cells, exists in association with histone proteins as chromatin [111]. The repeating unit of chromatin is the nucleosome, where about 146 base pairs (bp) of DNA are typically wrapped around a core histone octamer formed by two of each of the histones H2A, H2B, H3 and H4 [112] (Figure 1.4.1A). Core particles are connected by linker regions, which are typically 40 to 60 bp long. Considering the length of core and linker region, nucleosomes are regularly spaced at 180-200 bp intervals. Linker histones such as H1 and its isoforms are involved in chromatin compaction and bind to DNA at the point where it exits the nucleosome [113]. However, under normal conditions, chains of nucleosomes spontaneously fold into a more compact and stable 30 nm diameter fibres, even when H1 histone is absent. Through interactions with nuclear scaffolding proteins, the 30 nm diameter fibers form a series of loops and coils and become more and more condensed, reaching an approximately packing ratio of 1000 during the interphase and 10000 in mitotic chromosomes (Figure 1.4.1B).

As observed by electron microscopy (EM), chromatin exists as two different forms: euchromatin and heterochromatin [114]**.** Euchromatin is a lightly packed form of chromatin enriched for genes undergoing active transcription. Heterochromatin is a tightly packed form of chromatin less accessible to proteins and transcription factors (TFs) thus showing very little transcriptional activity. Heterochromatin is mostly present at telomeres, centromeres and repetitive DNA elements but at some specific loci it is able to switch into euchromatin conformation in response to developmental signals.

A) High-resolution crystal structure of the nucleosome, an octamer formed by two of each of the histones H2A, H2B, H3 and H4, shown in different colours. H3 is represented in blue, H4 in green, H2A in yellow and H2B in red, the DNA is shown in grey. 146 base pairs of DNA are wrapped around the histone octamer. H3/H4 tetramer makes up the inner core, the two dimers H2A/H2B bind DNA at entry and exit points of the nucleosomes. On the left the nucleosome core particle is viewed down the superhelical axis. On the right the same structure is rotated by 90° around the y-axis. *α*-helices of the histone proteins are shown as spirals. *Picture taken from Luger et al., 1997 [112].*

B) Folding of DNA into nucleosomes (1-5). 1: DNA wraps around a histone octamer to form the nucleosome core; 2: chains of nucleosomes fold into a more compact and stable 30 nm diameter fibres; 3: through interactions with nuclear scaffolding proteins, the 30 nm diameter fibres form a series of loops and coils and become more and more condensed, reaching an approximately packing ratio of 1000 during the interphase (4) and 10000 in mitotic chromosomes (5).

The structure and organization of chromatin loops inside the chromosome is still matter of debates. The models proposed are the forms of solenoid, zigzag, nucleosomes or a hybrid of those [115]. *Picture taken from the website http://www.mechanobio.info.*

Figure 1.4.1 ***Structure of nucleosome core and chromatin organisation***

A

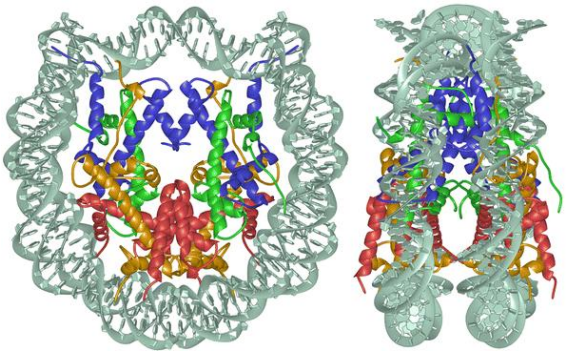

B

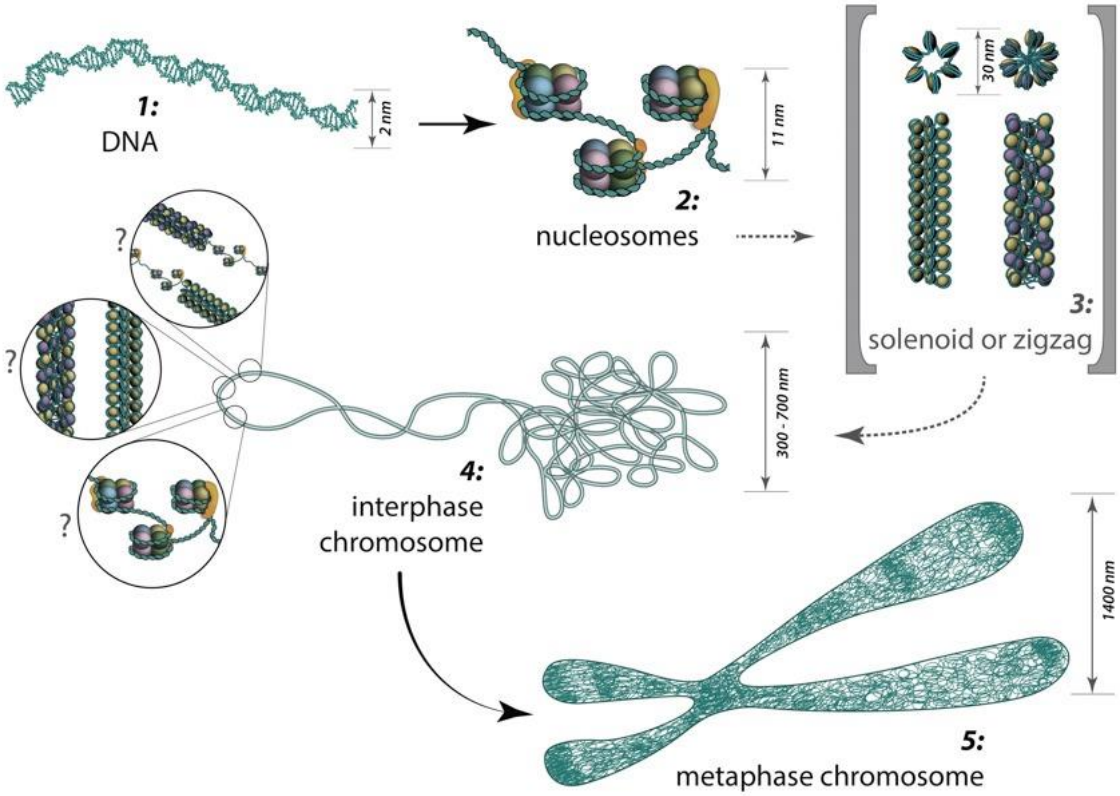

1.4.2 Gene regulation and chromatin remodelling

Eukaryotic cells use many different ways to regulate genes and the accessibility of chromatin to transcription factors. During all DNA-templated cellular processes chromatin structures undergo dynamic remodelling (opening and closing of higher-order structures) to allow access to associated DNA segments [116]. Chromatin remodelling can be achieved through different but interconnected mechanisms: 1) covalent histone modifications, 2) DNA methylation, 3) utilization of histone variants, 4) ATP-dependent chromatin remodelling [117]. These mechanisms allow optimal chromatin remodelling for efficient transcriptional regulation, DNA replication and repair.

Epigenetics studies all the modifications of DNA and histones that do not change the genetic code but have an effect on gene expression or chromatin condensation. The entire collection of epigenetic modifications of DNA and histones in the genome of a tissue is defined as the *epigenome* [118].

Some of these changes, such as promoter methylation, determine an “ON” or “OFF” state in gene expression; some others, such as enhancer methylation, modulate gene expression levels. All these epigenetic changes require enzymes called “writers” that add the modification to the DNA or histone (such as DNA and histone methyltransferases or histone acetyltransferases), “readers” enzyme that mediate the interaction of protein/protein complexes with the modification (such as MeCP2, methyl-CpG-binding protein 2, that recognizes methylated CpG) and “erasers” enzymes that modify or remove the modification (such as histone deacetylases) [118].

1.4.2.1 Chromatin modifications

The N-terminal tails of histones are subject to several post-translational modifications. At least eight different types of modifications have been identified: acetylation, methylation, phosphorylation, ubiquitination, sumoylation, ADP ribosylation, deimination and proline isomerisation [119]. These modifications define the “histone code” hypothesis, where the specific combination of modifications forms the recognition surface for chromatin regulatory factors [120]. Lysine, arginine, serine, threonine and proline are the amino acids modified (Figure 1.4.2). Lysines can be mono-, di- or trimethylated, arginines can be mono- or dimethylated, with either two methyl groups on one nitrogen (asymmetric methylation) or one methyl group on both nitrogens (symmetric methylation). Since a large variety of modifications occur at the same lysine residue some modifications are mutually exclusive.

Histone modifications influence different cellular processes, including transcription, replication, cell cycle progression and DNA repair [121]. To perform these functions, contacts between nucleosomes have to be disrupted in order to create a more relaxed form of chromatin; in this regard acetylation is the most potential modification because it neutralizes the basic charge of the lysine. Non-neutralising modifications such as methylation may have less impact on structure, but they might serve as docking sites for chromatin remodelling factors [119]. Regulatory proteins are recruited to modified sites via specific domains: plant homeodomains (PHDs) and chromo-like domains (chromo, tudor, Malignant Brain Tumor MBT) recognize methylated histones whereas bromodomains recognise acetylated histones.

Figure 1.4.2 ***Post-translational modifications of human histones***

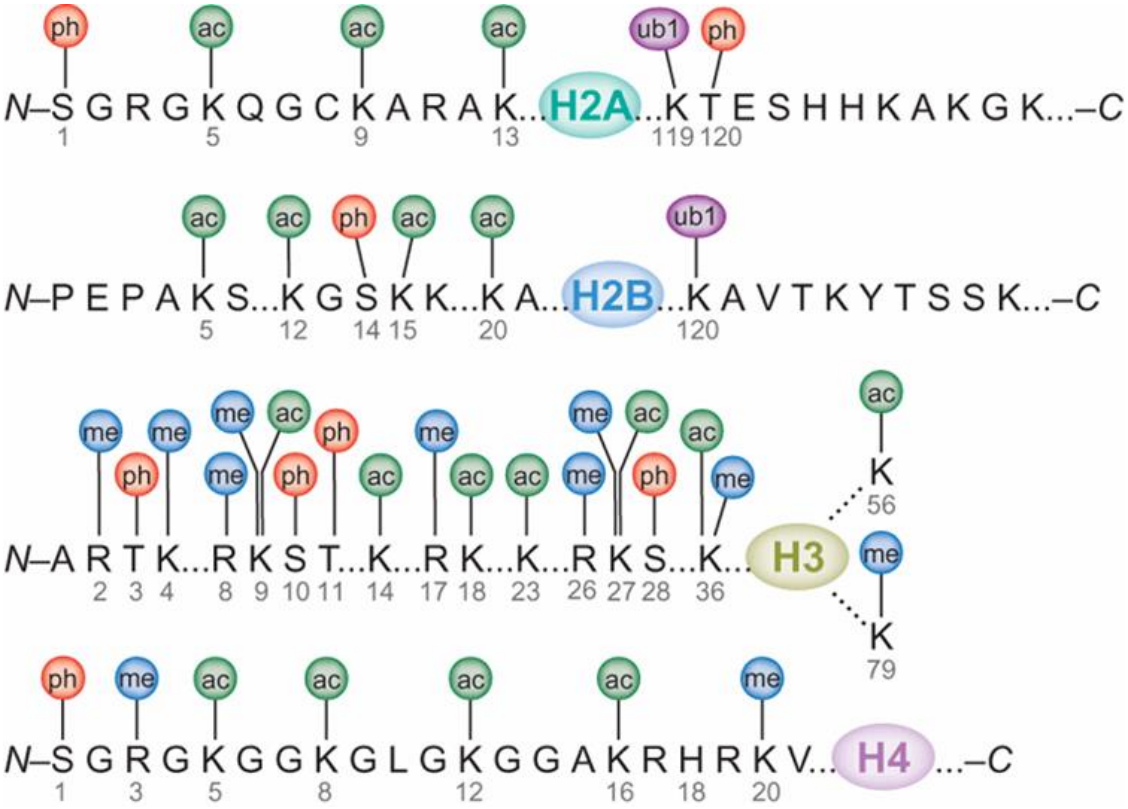

Most of the known histone modifications occur on the N-terminal tails, with exceptions in the C-terminal tails and in the globular domain of H3. ac = acetylation, me = methylation, ph = phosphorylation, ub1 = ubiquitination. Globular domains of each core histone are represented as coloured ovals. *Taken from Bhaumik et al., 2007 [122]*.

However, so far no chromo or MBT domain containing protein has been shown to recognize R-methyl marks. So far only Tudor domains and the BRCT domain of BRCA1 have been shown to bind methylated R-residues. Proteins that bind histone modifications can have enzymatic activity; for instance JMJD2A is a histone lysine demethylase that interacts with H3K4-methylated histone tails through a tudor domain. Other proteins can either tether chromatin remodelling complexes or are part of the complex itself. For example Inhibitor of growth family 2 (ING2) recognises a bromodomain and tethers the repressive mSin3a-HDAC1 histone deacetylases complex [123] whereas BPTF, subunit of the NURF chromatin remodelling complex, recognises H3K4me3 via a PHD domain [124]. Some modifications can disrupt the binding of a protein or, on the contrary, they can help the protein to bind more effectively. The vast array of possible modifications gives great potential for functional responses but the timing of the appearance of a modification depends on the signalling conditions within the cells [119]. In fact, a close relationship has been demonstrated between chromatin-associated proteins and important signal transduction pathways during processes like differentiation and development and a lot of ongoing research is aimed to understand the linking between cell signalling and epigenetics [125]. Most histone modifications are dynamic. Specific enzymes that modify histone tails as well as enzymes that remove the modification have been identified. Some of them are listed in Table 1.1. The only exception is the methylation of arginines, where demethylating enzymes have yet to be identified. Histone modifying enzymes can often be found in complexes and in some cases the specificity of the enzyme can be influenced by the association with other proteins [126].

Table 1.1 ***Enzymes that modify histones and residues modified***

Enzymes that Modify Histones	*Residues Modified*
Acetyltransferase	
HAT1	H4 (K5, K12)
CBP/P300	H3 (K14, K18) H4 (K5, K8) H2A (K5) H2B (K12, K15)
PCAF/GCN5	H3 (K9, K14, K18)
TIP60	H4 (K5, K8, K12, K16) H3 K14
Deacetylases	
SirT2 (ScSir2)	H4K16
Lysine Methyltransferase	
SUV39H1/2, G9a, RIZ1	H3K9
MLL1/2/3/4/5	H3K4
SET1B	H3K4
ASH1	H3K4
SET2 ,NSD1, SYMD1	H3K36
DOT1	H3K79
SUV420H1/H2	H4K20
EZH2	H3K27
Lysine Demethylases	
LSD1/BHC110	H3K4
JHDM1a/1b	H3K36
JHDM2a/2b	H3K9
JMJD2A/2B/2C/2D	H3K9
Arginine Methlytransferases	
CARM1	H3 (R2, R17, R26)
PRMT4	H4R3
PRMT5	H3R3, H4R8
Serine/Thrionine Kinases	
MSK1/2	H3 (S10, S28)
CKII	H4S1
Mst1	H2BS14
Ubiquitilases	
Bmi/Ring1A	H2AK119
RNF20/RNF40	H2BK120

Taken from Kouzarides 2007 [119].

1.4.2.1.1 Histone acetylation

Histone acetylation occurs at specific lysines of the four core histones and it is catalyzed by histone acetyltransferases (HATs); some HATs can modify more than one lysine residue, some others are more specific. Type A HATs are localized in nuclei and preferably acetylate nuclear factors; type B HATs are localized in the cytoplasm and they acetylate newly synthesized histones. Histone acetylation can be reversed by histone deacetylases (HDACs). Histone acetylation can create a more relaxed chromatin structure and for this reason it is associated with active chromatin. Many transcriptional coactivators, such as CBP and p300, possess intrinsic HAT activity, while conversely, some transcriptional corepressor complexes (e.g. mSin3a) contain subunits with HDAC activity. In ChIP-Seq analysis, Wang et al. [127] demonstrated that different acetylations are concentrated in different regions of genes. For example, H3K9ac, H3K27ac and H3K36ac are mainly located around the TSS, whereas other such as H3K4ac, H4K12ac and H4K16ac are elevated in the promoter and transcribed regions of active genes. H3K27 acetylation (H3K27ac) and H3K4 mono-methylation (H3K4me1) are usually marks of active enhancers. However, these modifications are also associated with other regions downstream of (H3K4me1) and around (H3K27ac) the TSSs of actively transcribed genes [128].

1.4.2.1.2 Histone phosphorylation

Phosphorylation targets serine residues on H3, H4 and H2B and threonine residues on H3. Phosphorylation is also likely to affect chromatin structure via a change in charge on amino acid residues in the histone tails [129]. Distinct kinases are required for the phosphorylation of histones on different residues. In humans MSK1/2 and RSK2 phosphorylate Ser10 on histone H3. Phosphorylation at histone H3Ser10 and H3Ser28 during mitosis is regulated by Aurora kinases. Phosphorylation of H3Ser10 has been shown to be involved in the activation of NF-κB regulated genes as well as immediate early genes such as *jun* and *fos* [130].

1.4.2.1.3 Histone methylation

Methylation occurs on lysine and arginine residues on histones H3 and H4 [131]. In eukaryotes, arginine residues can be mono- or dimethylated by protein arginine methyltransferases (PRMTs). Coactivator arginine methyltransferases 1 (CARM1) is a PRMT family member. Lysines can be mono-, di- or trimethylated on position 4, 9, 27 36 and 79 of histone H3 and on position 20 of histone H4. Histone methyltransferases typically contain a SET domain and are more specific than HATs with respect to their histone targets.

Methylation of H3K9 and H3K27 is associated with transcriptional repression via two distinct mechanisms. H3K9me3 is highly correlated with constitutive heterochromatin. It recruits heterochromatin protein 1 (HP1) which leads to further modifications, including histone deacetylation and DNA methylation and results in chromatin compaction and gene silencing [132, 133]. H3K27

methylation is associated with gene repression by Polycomb Repressive Complex (PRC) 1 and 2. Establishment of H3K27me3 by PRC2 complex can induce the recruitment of PRC1; once recruited, PRC1 induces transcriptional repression of target genes by catalyzing the ubiquitination of lysine 119 on histone H2A or by an H2Aub-independent mechanism [134, 135].

In contrast, methylation of H3K4 and H3K36 is correlated with transcriptional activation. H3K4me2 marks promoters that are poised for activation [136]. A genome-wide analysis demonstrated that enhancers are characterized by the monomethylation of lysine 4 of histone H3 (H3K4me1+/H3K4me3-) [137]. H3K36me3 and H3K79me3 are found in the gene body of transcribed genes [138], suggesting the possible interaction of methyltransferases with the elongating RNA Polymerase II [139].

Two families of demethylases reverse lysine methylation: amine oxidases, such as LSD1, which demethylate only mono- and dimethylated lysines, whereas hydroxylases of the JmjC family also demethylate trimethylated lysines and they have unique substrate specificity [140].

1.4.2.2 DNA methylation

DNA methylation has been implicated in numerous biological processes, including genomic imprinting and X chromosome inactivation [141]. DNA methylation occurs predominantly in the context of CpG (C followed by G) dinucleotides. *De novo* methylation is established by DNA methyltransferases DNMT3A and DNMT3B [142] and it is maintained after cell division by DNMT1, which fully methylates the hemi-methylated CpG sites [143]. Passive DNA demethylation is achieved during DNA replication in the absence of DNMT1

activity; active DNA demethylation is the enzymatic removal of the methyl group from 5-methylcytosine (5meC) and is often carried out by several DNA repair enzymes [141]. Alternatively, ten-eleven-translocation (TET) proteins are capable of hydrolysing 5meC to produce 5-hydroxymethylcytosine (5hmC) [144]. DNA methylation is generally associated with transcriptional repression [145], with the majority of CpGs in the human genome being methylated. Active promoters (as well as enhancers and boundary elements) generally lack DNA methylation. Gene repression occurs when increased DNA methylation either prevents the binding with a transcriptional activator or promotes the recruitment of corepressor complexes associated with HDAC activity [146]. Generally this recruitment is mediated by methyl-binding domain (MBD) proteins, that are specialized in the recognition of methyl-CpGs. However, about 70% of mammalian promoters are characterized by GC-rich regions containing a greater content of CpG dinucleotides called CpG islands (CGIs) which are predominantly not methylated. Most CGIs are sites of transcription initiation and are also marked specifically by histone acetylation (H3/H4Ac) and methylation (H3K4me3) which is directed by Cfp1, and show Kdm2a-dependent H3K36me2 depletion (Figure 1.4.3)

Figure 1.4.3 ***Chromatin state at CpG islands***

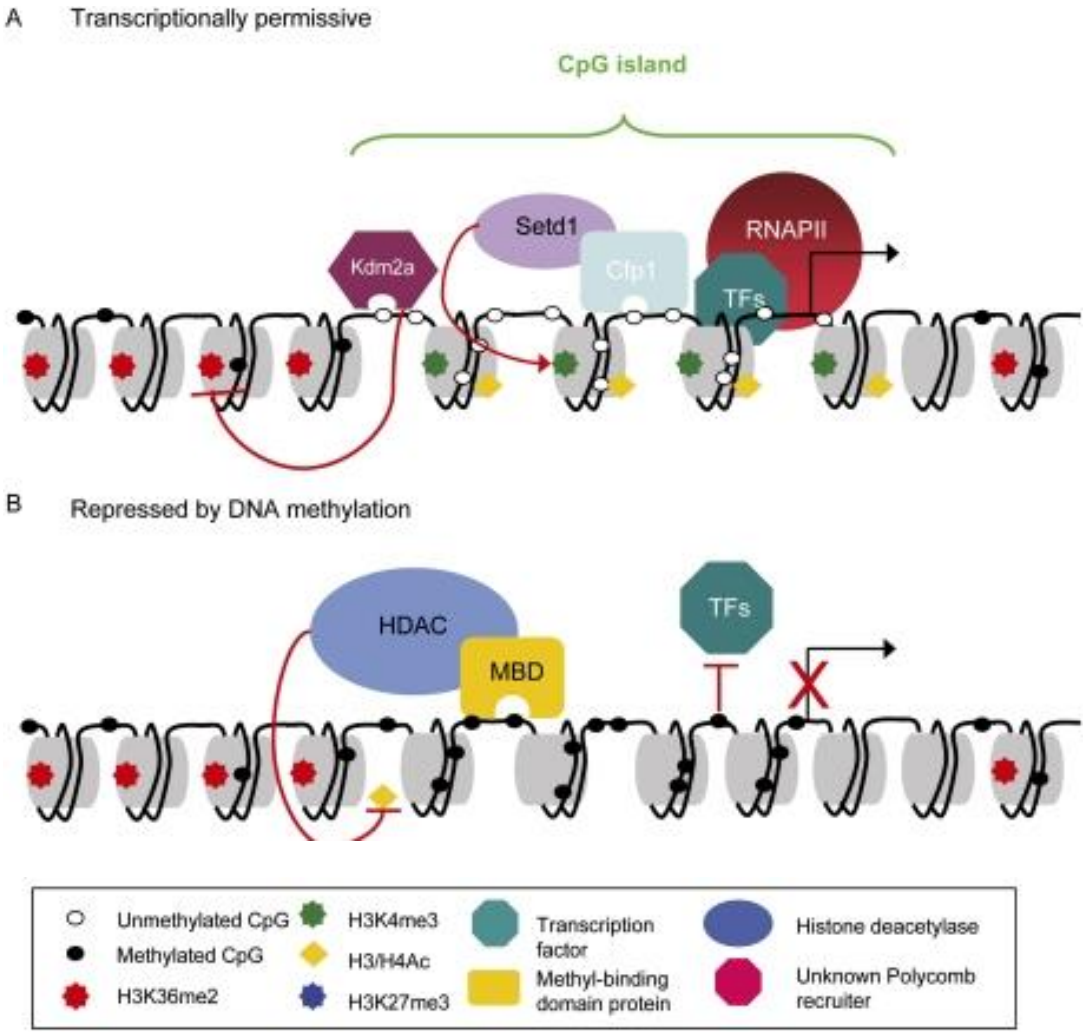

A) Transcriptionally permissive state at CpG islands. In this case CpG islands are marked specifically by histone acetylation (H3/H4Ac) and show Kdm2a-dependent H3K36me2 depletion. Cfp1 binds unmethylated DNA and interacts with Setd1 to direct H3K4me3. *B*) Repressed transcription status at CpG islands is characterized by DNA methylation. DNA methylation can inhibit the binding of transcription factors (TFs) or recruit histone deacetylase complexes (HDAC) through methyl-binding domain (MBD) proteins. *Taken from Deaton and Bird, 2011 [147]*

1.4.2.3 Histone variants

The canonical histones H2A, H2B, H3 and H4 are almost exclusively expressed during the S-phase of the cell cycle and incorporated into chromatin in a DNA replication-dependent way. Histone variants can be subsequently incorporated into chromatin by specific histone chaperones in the absence of DNA replication, replacing the equivalent canonical histones. Introduction of histone variants affects nucleosome stability and chromatin conformation [148]. In mammals three ubiquitously expressed H3 variants are known (H3.1, H3.2, H3.3), which have the same molecular weight and differ by only four to five amino acid residues [149] (Figure 1.4.4). Four H2A histone variants have been reported in mammals: H2A.Z, H2A.X, H2A.Bdb and macroH2A, which contains a large (200 residue) C terminal domain called “macro domain” that shares no sequence similarity with any other histone [150].

Figure 1.4.4 ***Schematic representations of histone H3 and H2A variants***

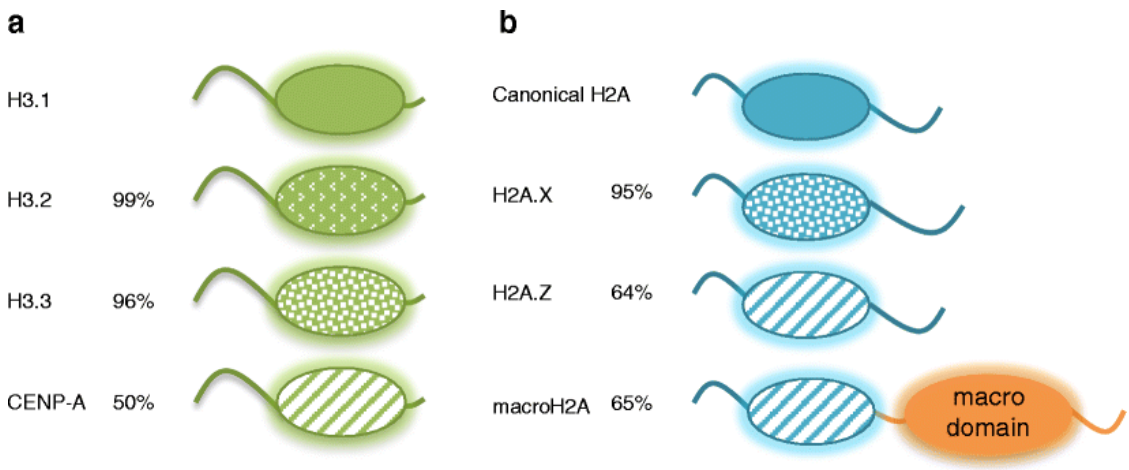

Schematic representations of histone H3 (a) and H2A (b) variants. Ovals and lines represent globular domains and flexible N- or C-terminal tails respectively. Difference in amino acid sequence of the variant compared to the canonical histone is represented by patterning in white. Percentage of similarity is also shown. *Taken from Biterge and Schneider, 2014 [148].*

1.4.2.4 ATP-dependent chromatin remodelling complexes

ATP-dependent chromatin remodelling complexes are highly conserved from yeast to humans. These complexes contain a catalytic ATPase subunit and, utilising energy from ATP hydrolysis, can mobilise nucleosomes along DNA, evict histones or promote the exchange of histone variants [116]. Four families of chromatin remodelling ATPases can be distinguished in mammals: 1) the SWI/SNF family, 2) the ISWI family, 3) the NuRD/Mi.2/CHD family and 4) the INO80 family.

The SWI/SNF (switching defective/sucrose non-fermenting) complexes comprise nine or more proteins, including both conserved (core) and non conserved subunits [151], which can help to target the complex to a specific DNA region. The catalytic core contains one of two closely related alternative ATPases: Brahma (BRM) or Brahma-related gene 1 (BRG1). These subunits also contain a BROMO domain, important in recognizing acetylated histones.

SWI/SNF remodelling complexes mainly disorganise and reorganise nucleosome positioning to promote accessibility for transcription-factor binding and gene activation [151]; however, under certain conditions, they can also promote transcriptional-repressor binding and gene repression [152].

ISWI (Imitation of SWItch) complexes also exist as multi protein complexes, but it exhibits a more limited range in subunit composition. SNF2H and SNF2L subunits have a SANT (‘SWI3, ADA2, NCOR and TFIIIB’) domain and a SLIDE (SANT-like ISWI) domain that mediate interaction with unmodified histone tails and linker DNA respectively. ISWI complexes primarily organise nucleosome positioning to induce gene repression, but they have also been shown to mediate transcriptional activation and elongation [153].

CHDs 1-5, members of NuRD (nucleosome remodelling and deacetylation) /Mi.2/CHD (chromodomain, helicase, DNA binding) family, have unique tandem chromodomains that recognize methylated histones. This family of chromatin remodelers is primarily involved in transcriptional repression in the nucleus and in the transcriptional activation of rRNAs in the nucleolus [154].

The INO80 (INOsitol requiring 80) subfamily includes the INO80 remodelling complex and the SWR1 remodelling complex which are characterized by split ATPase domains and the presence of two RuvB-like proteins, Rvb1 and Rvb2. The INO80 complex, as well as the SWI/SNF family remodelers, participates in DNA double-strand break (DSB) repair. The SWR1 complex was found to be able to specifically exchange histone H2A in nucleosomes for its variant H2A.Z [155].

1.5 SIGNAL TRANSDUCTION PATHWAYS

1.5.1 Mitogen-activated protein kinase (MAPK) signalling pathways

Mitogen-activated protein kinases (MAPKs) are a family of serine/threonine kinases. They are expressed ubiquitously and they are involved in physiological processes such as cell growth, differentiation and apoptosis [156, 157]. In humans, the MAPK family consists of six subgroups according to sequence similarity: 1) ERK1, ERK2; 2) ERK3; 3) ERK5; 4) ERK7; 5) p38 MAPKs (p38α, β, γ, δ); 6) JNK1, JNK2, JNK3.

Each group represents a distinct kinase cascade. Growth factors, cytokines, radiation and different stimuli activate the pathway. The MAPK module is formed of an initial MAPKKK, which phosphorylates and activates a downstream MAPKK, which in turn phosphorylates the last MAPK on threonine and tyrosine residues (Figure 1.5.1). This last phosphorylation leads to a conformational change that increases substrate accessibility and increases enzyme activity [158]. GTPases belonging to Ras or Rho families relay signals from the receptor to the first MAPKKK. MAPKs associate with many regulatory proteins such as phosphatases and scaffold proteins. Phosphatases dephosphorylate and inactivate the protein kinases; scaffold proteins often direct the pathway to specific substrates or co-localise pathway components.

Figure 1.5.1 ***MAPK signalling pathways***

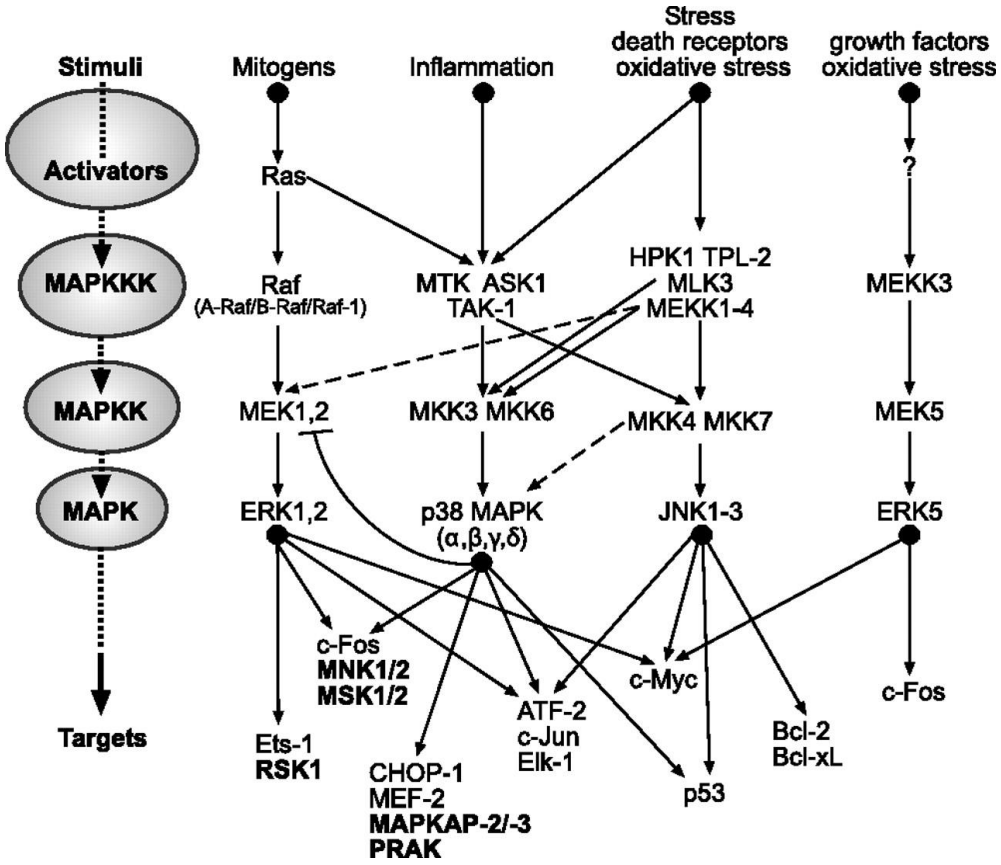

Picture representing the main MAPK pathways (ERK, p38, JNK and ERK5) and their cross-talk. Each pathway can be activated by different stimuli, which activate the MAPK cascade. An initial MAPKKK (or MEKK) phosphorylates and activates a downstream MAPKK (or MEK), which in turn phosphorylates the last MAPK on threonine and tyrosine residues. Different MAPK pathways have mutual downstream effectors, usually transcription factors able to enter the nucleus and activate the transcription of several target genes. *Taken from Juntilla M.R. 2008 [159].*

1.5.1.1 ERK pathway

ERK1 and ERK2, also known as $p44^{MAPK}$ and $p42^{MAPK}$ respectively, are activated mainly by growth factors and mitogens and are associated with cell growth, proliferation and survival [159]. As a result of stimulation of the Ras, Raf and MEK1 or MEK2 pathway, ERK1 or ERK2 can translocate to the nucleus and activate transcription factors such as c-Fos, c-Jun, ATF-2 and Ets family members. Activated ERK1/2 can also phosphorylate cytoplasmic and nuclear kinases such as the 90 kDa ribosomal protein S6 kinase 1 (RSK1), the MAP kinase-interacting kinases 1/2 (MNK1/2), and the mitogen- and stress-activated protein kinases 1/2 (MSK1/2). MSK1 can in turn activate CREB and NF-κB and is also implicated in chromatin remodelling [160].

The ERK pathway is also required for normal haematopoiesis. In ERK1 knockout mice defects in T cell development, mesoderm development and placenta function are observed [161], whereas in ERK2 knockout mice defects in Th2 differentiation and T cell activation are evident [162].

ERK1/2 phosphorylates C/EBPα on Ser21, inhibiting granulocyte differentiation [163]. Several studies have also demonstrated the importance of the ERK pathway in the survival of erythroid $CD34^+$ progenitors. Treatment of $CD34^+$ cells with a MEK1/2 inhibitor induced cell apoptosis due to the abrogation of anti-apoptotic Bcl-X_L levels [164].

1.5.1.2 p38 MAPK pathway

p38 MAPK family is formed from four different splice variants: p38α, p38β, p38γ and p38δ. p38α and p38β are expressed ubiquitously whereas the other two are

more tissue-specific [165]. p38 MAPKs are stimulated mainly by inflammatory cytokines or cellular stress such as hypoxia or UV radiation but they can mediate either apoptosis or survival depending on the kind of stimuli and on cellular conditions. Some of the substrates are ATF-1/2, STAT1 and STAT3, protein kinases such as p90 RSK and MSK1/2 (as for ERK pathway).

p38α(-/-) deficiency is embryonic lethal and causes defects in EPO production [166]. Mice deficient in the other p38 isoforms survive normally. p38 MAPKs also have a role in regulating neonatal haematopoiesis, phosphorylating and reducing the transcriptional repressor ability of TEL (a member of Ets family) [167]. p38 MAPKs are also involved in regulation of erythroid and myeloid differentiation. Moreover, specific expression of the four different p38 isoforms has been found to occur at different specific stages of erythroid differentiation [168]. Geest et al. [169] demonstrated that p38 MAPK inhibits neutrophil development through phosphorylation of C/EBPα on Ser21.

1.5.1.3 JNK pathway

Three different genes have been identified: JNK1, JNK2 and JNK3. JNK1 and JNK2 are ubiquitously expressed, JNK3 is expressed mainly in brain, heart and testis. Mice lacking one of the JNK proteins are viable, a double knockout of JNK1 and JNK2 shows defects in T cell activation [170].

As for the p38 MAPK pathway, JNKs are activated by inflammatory cytokines and cellular stress. Among the downstream substrates of JNKs are c-Jun, ATF-2, Elk-1, p53 and NFAT. However, JNK proteins are also activated by growth factors such as EPO, TPO, IL-3 and GM-CSF [171]. JNK proteins and the upstream MEKK1-JNK connection are involved in the regulation of

erythropoiesis [172] and treatment with SP600125 (JNK1/2/3 inhibitor) inhibited EPO-dependent proliferation of several erythroid cell lines [173]. Instead the MKK7-JNK signalling pathway functions as a negative regulator of mast cells growth [174].

1.5.2 MAPK signalling in haematological malignancies

Since MAPK pathways play a role in regulation of haematopoiesis, their aberrant activation has been found in many haematological diseases. Sustained activation of the MEK-ERK pathway has been reported in a large percentage of AML and CML [175, 176]. Raf/Ras mutations as well as FLT3 mutations mediate their effects through the activation of the downstream MEK-ERK pathway. Moreover in patients with FLT3 mutations the activation of MEK-ERK pathway contributes to the granulocytic differentiation block, through the phosphorylation on C/EBPα on Ser21.

The role of p38 MAPK and JNK pathways in haematological disorders is less defined. p38 has been found to be constitutively activated in myeloproliferative disorders and myelodysplastic syndromes [177] and, since it is involved in the regulation of cell cycle checkpoint controls, it could contribute to tumorigenesis.

Analysis of AML patients with t(8;21), t(15;17) or inv(16) showed increased expression of c-Jun, and in RUNX1-ETO cells this expression has been found to be JNK-dependent. Also both the BCR-ABL fusion gene (in CML) and FLT3 mutations lead to the activation of the JNK pathway [178-180].

1.5.3 MAPKs and transcription

The MAPKs signalling pathway is also involved in transcriptional regulation. The advent of next-generation sequencing technologies helped to clarify how MAPK proteins can bind to chromatin and promote or inhibit transcriptional outputs, with different modes of interaction with chromatin being identified [181]:

1) *direct DNA binding:* ERK2 has been demonstrated to bind to DNA *in vitro* at the defined DNA motif C/GAAAG/C [182];

2) *binding to histone modifiers:* ERK1/2 can phosphorylate and activate p300 [183];

3) *binding to chromatin remodelling complexes:* an example is the recruitment of SWI/SNF complex by p38 during cardiomyocyte differentiation [184];

4) *binding to RNA Polymerase II:* in yeast, Mpk1 (functionally similar to ERK5) drives transcription by binding the Paf1 elongation complex [185].

5) *binding to transcription factor substrates:* in response to stress, p38 phosphorylates and recruits ELK1 to the c-Fos promoter [186], while in response to mitogens ELK1 recruits ERK to the same promoter and to the promoter of other immediate-early genes (IEGs) [187]. ERK1/2 and p38MAPKs can drive histone modification and chromatin remodelling by phosphorylating the mitogen- and stress-activated protein kinase 1 and 2 (MSK1/2).

1.5.4 Activator protein-1 (AP-1)

The mammalian activator protein-1 (AP-1) is a homodimer or heterodimer composed of proteins from the Jun family (c-Jun, JunB, JunD) and the Fos family (c-Fos, FosB, Fra-1, Fra-2), and the closely related activating transcription factors (ATFs), the cyclic AMP response element binding proteins (CREB) and the Maf subfamily [188]. Several kinases (including MAPKs) have been demonstrated to phosphorylate and activate AP-1, which regulates the expression of different genes and also auto-regulates itself, thus amplifying the signal [189]. AP-1 is essential in normal cell growth and development and genes which play important roles in differentiation, inflammation, apoptosis and immune response contain AP-1 binding site(s) in their promoter and/or enhancer regions [190]. Thus, alterated AP-1 protein activation or expression by toxicants can lead to the development of various diseases. Fos and Jun proteins belong to the basic region-leucine zipper (bZIP) group of DNA binding proteins. They contain a positively charged DNA binding domain (DBD) and a leucine-zipper domain (LZD) containing a heptad repeat of leucine residues located immediately downstream of the DBD (Figure 1.5.2). The LZD mediates the dimerisation of proteins, bringing two DBDs into juxtaposition and facilitating the interaction with DNA. Because of their LZD composition, Fos proteins cannot form homodimers. Instead, Jun-Fos heterodimers are more stable and have a higher DNA binding activity than Jun-Jun homodimers. As shown in Figure 1.5.2 Jun proteins contain the transactivation domain (TAD) at their amino terminal region whereas c-Fos and FosB contain the TADs at both amino and carboxy terminal regions. AP-1 homo- and heterodimers can bind the 7 bp DNA sequence 5'-TGA(G/C)TCA-3', known as 12-*O*-tetradecanoylphorbol-13-

acetate (TPA)-responsive element (TRE), as well as the two variant sequences 5'-TTAGTCA-3' and 5'-TGATTCA-3' [191]. AP-1 heterodimers containing ATF or CREB proteins, prefer to bind to the cyclic-AMP-responsive element (CRE), the 8 bp DNA sequence 5'-TGACGTCA-3'. Jun and Fos AP-1 dimers have a lower affinity to the CRE [189].

As mentioned above, AP-1 proteins can be phosphorylated by a number of kinases, such as protein kinase C (PKC) [192], protein kinase A (PKA) [193] and MAPKs. Most cells possess already a level of pre-existing Jun and Fos proteins but they can also be induced by different stimuli [194]. JNKs and ERKs phosphorylate both pre-existing and newly synthesized AP-1 proteins. JNKs mainly phosphorylate Jun proteins on Ser63 and Ser73 in its TAD [194], whereas ERKs mainly phosphorylate Fos proteins on serine and/or threonin residues within their carboxy terminal domain [195]. c-Fos is phosphorylated by ERKs on Ser374 [196] whereas FosB can be phosphorylated on different serine residues (284, 297, 299, 302, 303) [197]. ERKs can also phosphorylate Fra-1 and Fra-2 at different sites both *in vivo* and *in vitro* [198, 199]. p38 MAPKs regulate *jun* and *fos* gene transcription through phosphorylation of transcription factors able to bind *jun* and *fos* promoter elements (e.g. ATF-2, Elk1, CCAAT enhancer binding proteins (C/EBPs), SAP-1).

Figure 1.5.2 ***Structure, dimerisation and DNA binding properties of Jun and Fos proteins***

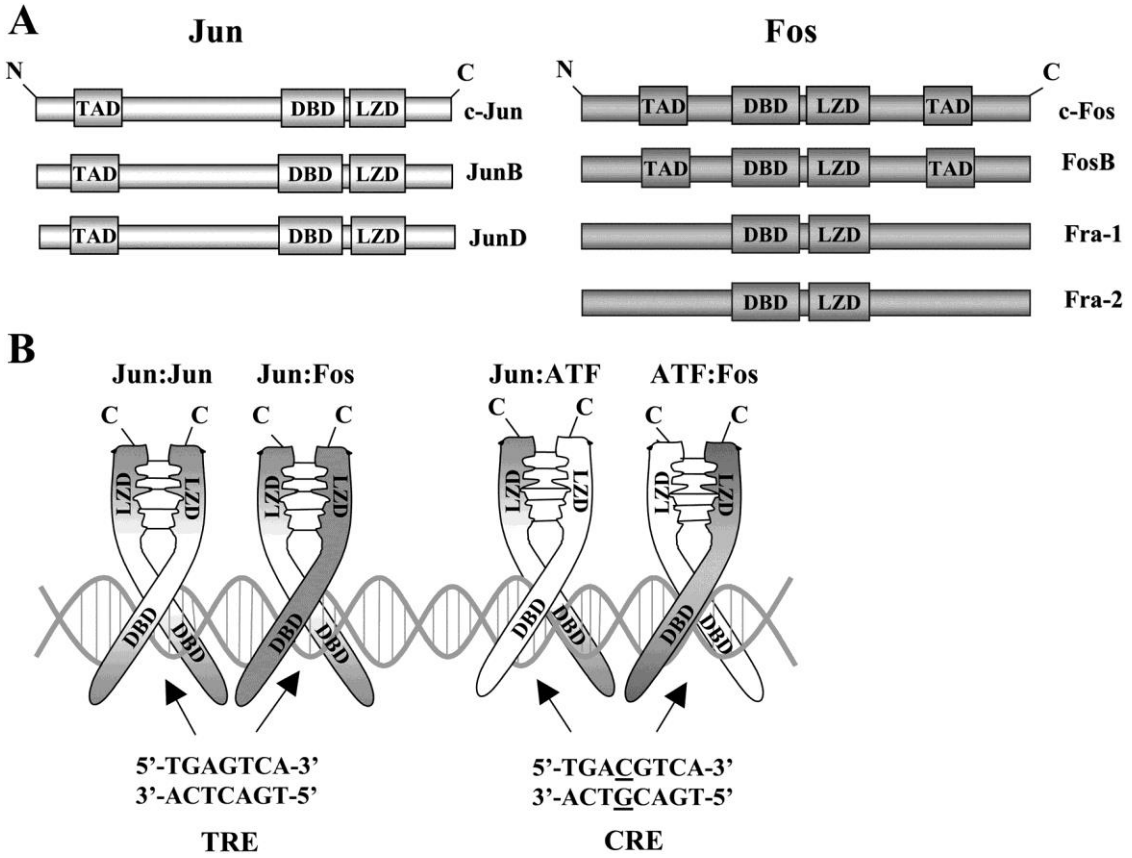

A) Structure of Fos and Jun proteins. TAD = transcription-activating domain; LZD = leucine-zipper domain; DBD = DNA binding domain; N = amino terminus; C = carboxyl terminus. *B*) LZD-mediated dimerisation of Fos and Jun proteins and their binding to DNA. ATF = activation transcription factor; TRE = 12-*O*-tetradecanoylphorbol-13-acetate(TPA)-responsive element; CRE = cyclic AMP-responsive element. *Taken from Reddy S.P.M. and Mossman B.T., 2002 [189].*

1.5.5 Mitogen- and stress-activated protein kinase 1 and 2 (MSK1/2)

Mitogen- and stress-activated protein kinase 1 and 2 (MSK1/2) can be activated by agents that trigger ERK and p38 MAPK pathways and by other agents such as arsenite, fibroblast growth factor (FGF), transforming growth factor β (TGFβ). MSKs show a large structural homology with the ribosomal S6 kinase (RSKs). There is a nuclear localization sequence in their C-terminal region and they are mainly found in the nucleus [200]. In MSK proteins, an N-terminal kinase domain (NKD) and a C-terminal kinase domain are connected by a linker region. In the case of human MSK1, either ERK or p38 MAPK pathways, or both, phosphorylate Ser360, Thr581 and Thr700. Among these, phosphorylation of Thr581 is essential for MSK1 activity. Then the activated CKD phosphorylates Ser212 (in the NKD), Ser376 and Ser381(in the linker region). Finally the active NKD phosphorylates MSK substrates as well as the MSK1 C-terminal region [160] (Figure 1.5.3). MSK2 activation seems to be very similar to MSK1 activation [200].

The first MSK target to be identified was cAMP response element (CRE)-binding protein (CREB). MSKs phosphorylate CREB at Ser133, promoting the recruitment of CREB-binding protein (CBP) and p300. These two proteins acetylate histone tails, leading to a more relaxed chromatin structure and gene activation [201]. RSKs and PKA are alternative kinases able to phosphorylate CREB [202]. MSKs can also phosphorylate activating transcription factor 1 (ATF1) at Ser63, which is a member of the same class of CRE-binding factors [202].

Figure 1.5.3 ***Schematic view of MSK1 structure and activation***

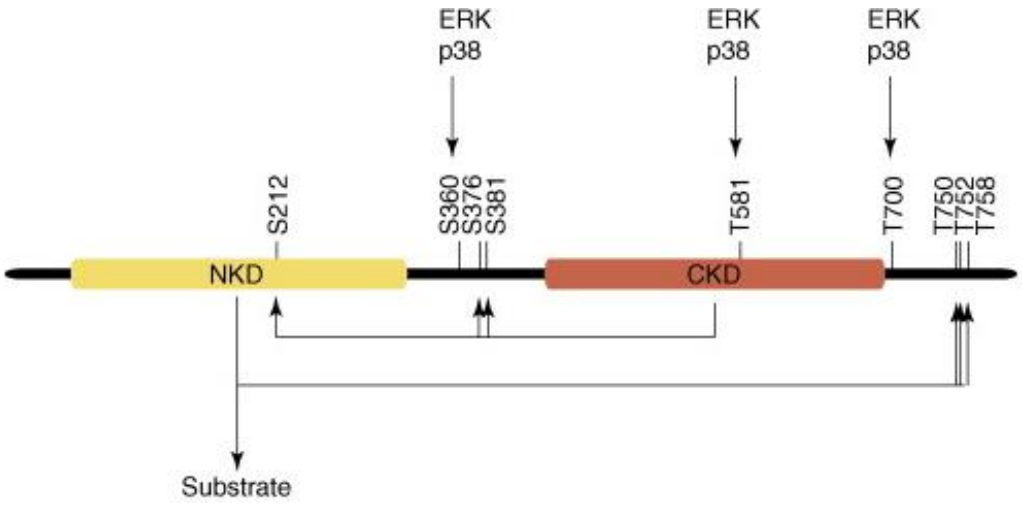

Picture represents the structure of MSK1 and its activation. An N-terminal kinase domain (NKD) and a C-terminal kinase domain are connected by a linker region. Either ERK or p38 MAPK pathways, or both, phosphorylate Ser360, Thr581 and Thr700. Then the activated CKD phosphorylates Ser212 in the NKD, Ser376 and Ser381 in the linker region. Finally the active NKD phosphorylates MSK substrates as well as the MSK1 C-terminal region [160]. *Taken from Vermeulen et al, 2009 [160]*

Another interesting MSKs target is NF-κB p65. Phosphorylation at Ser276 by MSKs (or PKA) recruits CBP and p300 [203]. Beyond acetylating histones, CBP and p300 can also acetylate p65 itself, resulting in an enhanced transcriptional activity [204].

MSKs also regulate chromatin environment, phosphorylating histone 3 at Ser10 and Ser28 (H3Ser10 and H3Ser28). Vicent at al. [205] demonstrated that the phosphorylation of H3Ser10 displaces an HP1-containing repressor complex and promotes the recruitment of BRG1, PCAF and RNA polymerase II to initiate transcription. Interestingly Duncan and colleagues [206] reported that MSK1/2 is necessary for epidermal growth factor (EGF)- but not for TNFα-induced H3Ser10 phosphorylation of the *c-fos* promoter.

Phosphorylation of H3Ser28 by MSKs is also related to gene activation. Lau et al. [207] demonstrated that H3Ser28 phosphorylation induces a methyl-acetylation switch of the adjacent K27 residue. MSK1 and H3Ser28 phosphorylation antagonize polycomb silencing through the displacement of PRCs and the removal of H3K27me3. This double mark can recruit specific chromatin modifiers or transcription regulators to further modulate gene expression. JNKs also seem to be implicated in the phosphorylation of H3Ser10 and H3Ser28 during the differentiation of stem cells into neurons but it has not been investigated whether this effect is mediated by MSK1/2 [208].

1.5.6 Nuclear factor kappa B (NF-κB) signalling pathway

Nuclear factor kappa B (NF-κB) was identified in 1986 as a transcription factor present in the nucleus of B cells that bound to the enhancer of the immunoglobulin κ light chain gene [209]. It is involved in the regulation of immune and inflammatory response as well as in carcinogenesis. NF-κB consists of a family of proteins that share a highly conserved dimerisation and DNA-binding domain called Rel homology domain (RHD). The family includes Rel A (p65), Rel B, c-Rel, p50 (NF-κB1) and p52 (NF-κB2). Phosphorylation-dependent cleavage of inactive p100 gives rise to active p52, whereas cleavage of p105 yields p50 [210]. NF-κB proteins form different homo- and heterodimers and their activity is regulated by two main pathways: the canonical and the alternative pathways. The canonical pathway is activated in response to infections or pro-inflammatory cytokines. In this pathway the heterodimer p50-p65 is held in the cytoplasm as an inactive form, bound to a specific inhibitor which masks the nuclear localization sequence of associated Rel proteins (Inhibitor of kB: IκBα, IκBβ, IκBγ or NEMO: NF-κB essential modulator). Triggering of the canonical pathway activates IκB kinase (IKK) protein complex and leads to IκB phosphorylation. Then phosphorylated IκB gets ubiquitinated and degraded by the 26S proteasome, releasing the p50-p65 heterodimer that translocates to the nucleus and binds to specific κB sites within the promoter and enhancer regions of NF-κB target genes [211, 212].

The alternative pathway preferentially affects the p100-Rel B heterodimer and it is activated by members of the TNF-α cytokine family. These cytokines selectively activate IKKα and lead to the cleavage of p100, allowing the p52-Rel

B heterodimer to translocate to the nucleus (Figure 1.5.4). Once in the nucleus, the transcriptional functions of NF-κB are further modulated by post-translational modification. NF-κB target genes belong to four different categories: inflammatory and immunoregulatory genes (i.e. IL-6, IL-8); anti-apoptotic genes, such as BCL-X_L, c-FLIP, c-IAPs; genes that positively regulate cell proliferation (Cyclin D1, c-MYC) and genes that encode negative regulators of NF-κB (i.e. IκBα, IκBβ). Genes of all four categories can contribute to tumorigenesis [210].

1.5.6.1 NF-κB signalling pathway in inflammation and cancer

Inflammation and cancer are tightly related. Inflammation is the response of the innate immune system to physiological and/or oxidative stress and it is associated with activation of the canonical NF-κB pathway [213]. On one hand, NF-κB targets and tries to eliminate cancer cells. On the other hand, NF-κB is constitutively activated in a number of haematological and solid tumours and it can exert pro-tumorigenic functions. In acute inflammation NF-κB activation is accompanied by a high activity of cytotoxic immune cells against transformed cells [214]. However cancer cells tend to “escape” and outperform the immune system and this establishes a chronic inflammatory condition with moderately elevated levels of NF-κB activity, related to a high risk to develop cancer. In fact, NF-κB activation usually leads to cell survival through the up-regulation of anti-apoptotic genes. Moreover, NF-κB induces cytokines such as IL-8, IL-6, IL-1 and TNF-α that recruits leukocytes and granulocytes to the sites of inflammation.

Figure 1.5.4 ***Canonical and alternative NF-κB activation pathways***

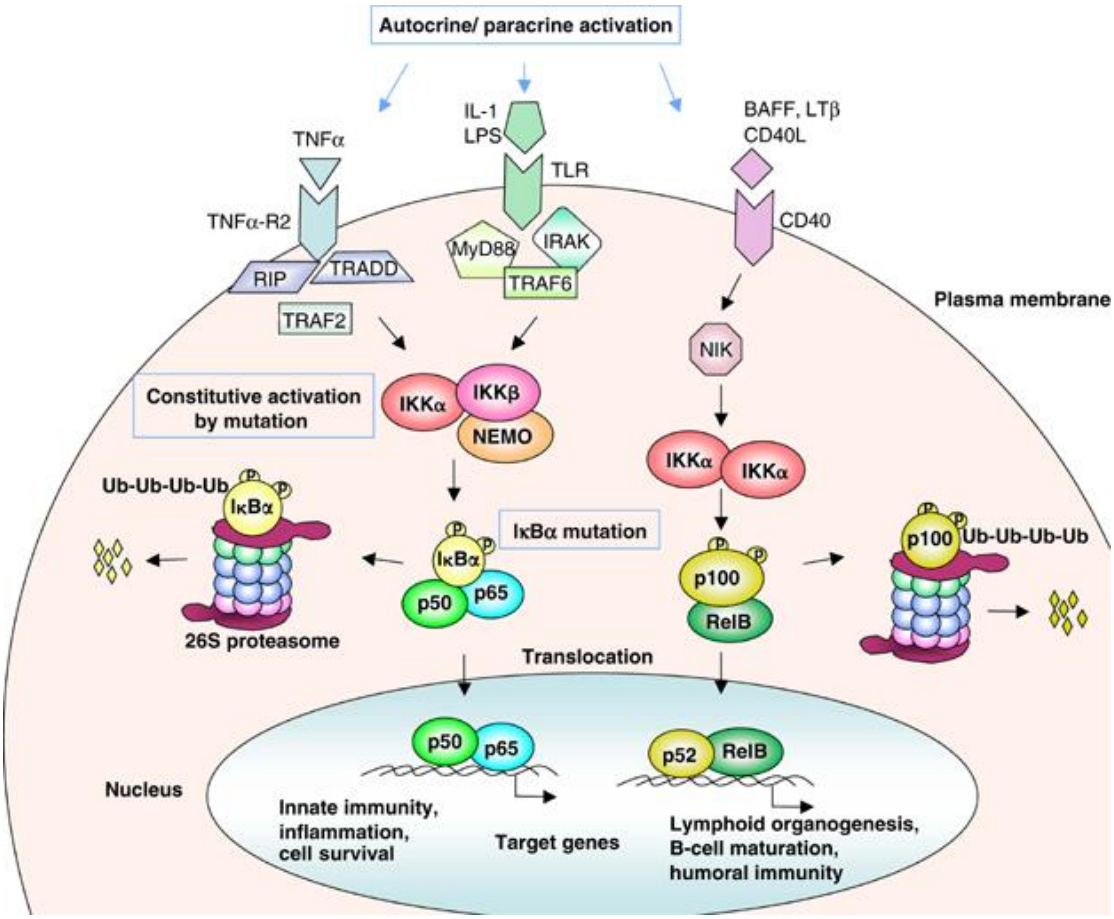

In the canonical pathway the heterodimer p50-p65 is held in the cytoplasm as an inactive form, bound to the specific inhibitor of κB (IκB). Triggering of this pathway activates IκB kinase (IKK) protein complex and leads to IκB phosphorylation. Then phosphorylated IκB gets ubiquitinated and degraded by the proteasome, releasing the p50-p65 heterodimer that translocates to the nucleus and binds to specific κB sites within the promoter of NF-κB target genes [211, 212]. In the alternative pathway activated IKKα leads to the cleavage of p100, allowing the p52-Rel B heterodimer to translocate to the nucleus. BAFF= B-cell activating factor; CD40L= CD40 ligand; IL= interleukin; IRAK= IL-1R-associated kinase; FADD= Fas-associated death domain protein; LPS= lipopolysaccharides; LTb= lymphotoxin b; NEMO=NF-κB essential modulator; NF-κB= nuclear factor kappa B; NIK= NF-κB-inducing kinase; RIP= receptor interacting protein; TLR= toll-like receptor; TNF= tumour necrosis factor; TRADD= TNF receptor-associated protein with a death domain; TRAF= TNF receptor-associated factor; Ub, ubiquitin. *Taken from Braun et al., 2006 [209].*

The release of reactive oxygen species (ROS) by neutrophils might cause DNA-damage and genetic mutations, triggering tumour initiation [215].

NF-κB has been shown to contribute to tumour progression and metastasis formation. In fact, it can control the epithelial-mesenchymal transition (EMT) [216], it is often related to high levels of matrix metalloproteinases (MMPs) [217] and it can control vascularisation of tumours via upregulation of vascular endothelium growth factor (VEGF) and its receptors [218]. In tumours, high level of NF-κB activity can be induced by either mutations of NF-κB genes and/or genes that activate the NF-κB pathways or through an increased release of cytokines from the tumour microenvironment [219].

1.5.6.2 NF-κB signalling pathway in solid and haematological tumours

In solid tumours there is often an aberrant activity of IKK proteins, which leads to an aberrant sustained NF-κB activity. An example is prostate cancer, where the gene fusion between IKK2 and TNPO1 (transportin 1) leads to an increase in IKK2 expression [220]. Other alterations occur at NF-κB1 and/or NF-κB2 level [221]. In haematological malignancies the underlying pathways are quite different. These include: the short half-life of IκBα in B-cell lymphoma, the mutation of IκBα in Hodgkin's lymphoma, TNFα production in Burkitt's lymphoma and cutaneous T-cell lymphoma [222]. In B-/T-cell lymphomas and in myelomas, alterations or deletions of p52 locus result in the cleavage of p100 and the generation of constitutive active p52 protein. Increased degradation of IκBα has been reported in T cell leukaemia [223]. In Philadelphia positive acute lymphoblastic leukaemias BCR/ABL1 expression promotes nuclear

translocation of NF-κB [224]. High IKK kinase activity [225] and high production of IL-1β has also been demonstrated in AML cells. It is possible that NF-κB stimulates IL-1β expression, which in turn activates NF-κB and promotes AML cell proliferation [226].

1.5.6.3 NF-κB and transcription

NF-κB proteins bind to a variation of the consensus DNA sequence of 5'-GGGRNYYYCC-3' (where R is a purine, Y is a pyrimidine and N is any nucleotide) called κB sites [227]. NF-κB activation can be regulated by post-translational modifications on IκB and Rel subunits. Acetylation and phosphorylation of Rel subunits (especially p65 subunit) and the recruitment of HATs and HDACs control NF-κB activation and transcriptional activity [228] and generate a "NF-κB-signalling code" which could regulate biological responses in an inducer-, cell line- and promoter-dependent manner [229]. p65 phosphorylation on Ser536 accelerates p65 nuclear localization and binding to DNA because this phosphorylated form cannot interact with cytosolic IκB [230]. Phosphorylation of p65 on Thr254 by Pin1 also decreases the affinity for IκB leading to p65 nuclear translocation and increasing DNA binding activity [231].
PKA and MSK1/2 can phosphorylate p65 on Ser276 in response to different stimuli [232-234]. It has been shown that Ser276 phosphorylated p65 is recruited to several NF-κB-dependent genes and is required for P-TEFb recruitment [235]. p65 phosphorylation on Ser276 and Ser536 promote interaction with CBP/p300, which in turn acetylates p65 at Lys310 and promotes Brd4 and P-TEFb recruitment and transcriptional activity [236]. Brd4 is a

bromodomain-containing protein of the BET family and it has the ability to interact with acetylated lysines on histones and on P-TEFb. This latter interaction leads to the recruitment of P-TEFb to promoters where it phosphorylates the Pol II CTD to stimulate elongation [237] (Figure 1.5.5).

Brd4 and P-TEFb can also be recruited through histone acetylation [238].

p65 NF-κB subunit can also be acetylated by p300 and PCAF and deacetylated by SIRT or HDAC-3. Acetylation of Lys221 and Lys218 impairs the interaction between p65 and IκB, increasing p65 DNA binding and prolonging the NF-κB response in the nucleus [239]. Thus, p65 deacetylation of these two lysines by HDAC-3 promotes the interaction with IκB and NF-κB nuclear export [240]. The same effect of dissociation from DNA and successive nuclear export has been seen after acetylation of p65 at Lys122 and Lys123 [241] .

When NF-κB enters the nucleus it activates two types of promoters: those that are already accessible due to acetylated before stimulation and those that require stimulus-dependent chromatin remodelling in order to make NF-κB site accessible [242]. An example is the *mcp-1* gene, which requires AP-1 binding to the promoter and subsequent ATP-dependent chromatin remodelling by the SWI/SNF complex. This remodelling leads to the recruitment of NF-κB and HATs, promoting gene activation.

Figure 1.5.5 ***Role of phosphorylation of serine 276 and 536 in the regulation of RelA (p65) acetylation***

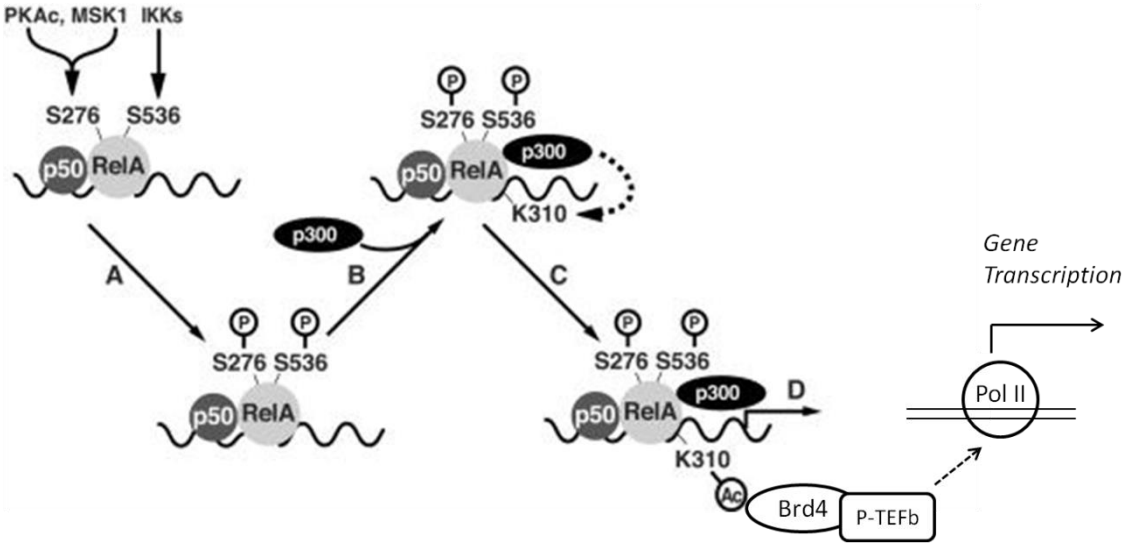

Phosphorylation of RelA at serine 276 by PKA or MSK1 or phosphorylation at serine 536 by IKK (A) leads to the recruitment of p300 (B). p300 acetylates lysine 310 (C) and promotes Brd4 and P-TEFb recruitment, thus leading to transcriptional activation (D). Adapted from Chen at al., 2005 [243].

1.6 CYTOKINES

1.6.1 Cytokines and their role in haematopoiesis and immune system

Cytokines are proteins, peptides or glycoproteins which mediate communication among cells and between cells and tissues and are secreted by numerous cells of the immune system at nano to picomolar concentration. Cytokines act on specific receptors whose cytoplasmic domains contain specialized regions able to initiate different responses such as proliferation, survival, differentiation commitment, and functional activation [244]. Cytokines are fundamental to the development of immune system and in the regulation of an immune response.

Cytokines are also essential in normal haematopoiesis, either acting in a lineage-specific manner or directing more than one lineage at the same time. Some cytokines are known as Interferons (IFNs) because they are involved in antiviral responses, whilst others are called Interleukins (ILs) since initially they were thought to be produced and act upon leukocytes only. Chemokines are involved in chemotaxis whereas colony stimulating factors (CSF) or growth factors induce clone formation in liquid or semi-solid media and support cell growth of specific cell types (such as IL-3 and GM-CSF). Cytokines such as IL-1, TNFα and β, IFN-γ stimulate in turn the release of other haematopoietic cytokines [245] whereas others (e.g. IL-1, IL-2, IL-5, IL-6) synergise with effectors proteins to promote cell growth and differentiation.

Cytokine genes are deregulated in a number of immune-related diseases, confirming the importance of cytokines in the development and regulation of the immune system and its responses.

1.6.2 Granulocyte-Macrophage Colony-Stimulating Factor (GM-CSF) and Interleukin-3 (IL-3)

Granulocyte-Macrophage Colony-Stimulating Factor (GM-CSF) and Interleukin-3 (IL-3) are pro-inflammatory cytokines produced at sites of inflammation which also regulate growth, differentiation and survival of several haematopoietic lineages.

GM-CSF regulates the terminal differentiation of granulocytes and macrophages and it is produced by different cell types including activated T cells, NK cells, mast cells, basophils, eosinophils, megakaryocytes, endothelial cells, epithelial cells and fibroblasts [246, 247]. IL-3 is only produced by activated T cells, mast cells, NK cells and eosinophils but it supports development and proliferation of almost all types of myeloid progenitor cells [248] and promotes the self-renewal of haematopoietic progenitor cells [249].

However, IL-3 and GM-CSF expression in bone marrow stroma cells is minimal. For this reason it seems that the stimulation of haematopoietic cells by these cytokines is associated with the inflammatory reaction [250]. In the inflammatory response IL-3 induces the proliferation of macrophages and mast cells and promotes the synthesis of histamine by mast cells and phagocytosis in macrophages.

IL-3, GM-CSF and also IL-5 exert very similar biological activities on their common target cells. This is due in part to the fact that their high-affinity receptors, consisting of two subunits, alpha and beta, share the same β_c subunit. The α subunit is specific for the different cytokines [250] and although none of these receptor subunits has intrinsic kinase activity, these cytokines induce protein tyrosine phosphorylation and activation of several cellular

proteins, including JAK kinases [251], phosphoinositide 3 (PI-3) kinase, Ras, Raf-1 and MAPKs as well as the transcriptional activation of nuclear proto-oncogenes such as *c-myc*, *c-fos* and *c-jun* [252].

1.6.3 Cytokines and AML

The role of specific growth factors in controlling the proliferation of haematopoietic cells has been demonstrated in *in vitro* clonogenic assays with AML blasts [253]. IL-3 and GM-CSF demonstrated an equivalent activity, greater than G-CSF, in stimulating progenitor cell proliferation. In this regard, combination of G-CSF with GM-CSF showed a synergistic effect, but IL-3 combined with GM-CSF did not synergize [254]. This suggests that G-CSF acts upon a different population within the same clone, whereas the other two cytokines act upon the same population.

IL-1α acts synergistically with GM-CSF in supporting AML blast cell colony formation [255]. Endogenous IL-1 secretion varies among individual patients. Despite this variation, IL-1 inhibition significantly decreases both spontaneous blast proliferation and blast secretion of IL-1α, GM-CSF, G-CSF, IL-6 and TNF-α. Moreover, it has been shown that IL-1 induces GM-CSF production by AML blasts but its proliferative effect is inhibited by neutralizing antibodies to GM-CSF. This suggests that IL-1 effects are mediated by an autocrine GM-CSF secretion [256].

TNF-α synergizes with IL-3 and GM-CSF to stimulate AML blasts proliferation [257]. Similarly to IL-1, IL-6 synergises with GM-CSF in stimulating AML blast cell growth and enhances IL-3 dependent proliferation of normal pluripotent stem cells [258]. Several studies have reported the presence of GM-CSF mRNA

in AML blasts and secretion of GM-CSF [259-261]. AML samples which express GM-CSF often express also G-CSF, TNF-α, IL-1β and IL-6 [262].

1.6.4 The IL-3/GM-CSF locus

The human GM-CSF and IL-3 genes reside on chromosome 5, separated by just 10.5 kb and by approximately 500 kb from the genes encoding IL-5, IL-13 and IL-4 [263]. GM-CSF and IL-3 are expressed in all T cells subtypes following activation of TCR receptor and in mast cells after IgE receptor activation. GM-CSF and IL-3 can also be expressed by myeloid progenitor cells [259, 264], and by epithelial and endothelial cells after stimulation with inflammatory cytokines [247]. IL-3 and GM-CSF mRNA are controlled at both transcriptional and post-transcriptional level. In fact their transcripts include an AU-rich sequence in the 3' untranslated region (3'-UTR), required for the binding of a transcription factor which mediates mRNA decay [265, 266].

1.6.4.1 DHSs within the IL-3 gene

The IL-3/GM-CSF locus contains many different regulatory elements, most of which were first identified as inducible or tissue-specific DHSs (Figure 1.6.1a) [267].

The lL-3 gene has a highly inducible promoter and three inducible enhancers at -37 kb, -14 kb and -4.5 kb which have different tissue-specificities and can increase IL-3 promoter activity (Figure 1.6.1b) [264, 268-270].

The IL-3 promoter is located within the first 315 bp upstream of the TSS. A TATA box is present between -25 and -30 bp from the TSS. Essential for

efficient promoter activity is a region at -300 bp from TSS, containing an AP-1 binding site, and a highly conserved region from -160 to -100 bp, called activator-1 (ACT-1). This region contains the element ATGAATAAT [270], which is a binding site for the T cell specific protein NFIL-3A, but is also an imperfect consensus sequence for AP-1 and Oct-1. A RUNX1 and GATA binding sites are also present downstream of the ACT-1, and they are occupied *in vivo* only upon T cell activation. Between these two elements, there is CK1 consensus element, which is not necessary for the promoter activity, that seems to represent a strong NFAT binding site [267]. Between the GATA region and the TATA box there is a GC-rich region which can bind several Zn-finger proteins, including the Early growth response factor 1 and 2 (ERG1, ERG2) and the constitutive factor Sp1. The IL-3 promoter can also be negatively regulated by the binding of the nuclear inhibitory protein NIP to a region located between -271 and -250 bp [271].

The -4.5 kb inducible enhancer is active in induced human T cells and mast cells, where is activated via Ca^{2+} and kinase-signalling pathways and shows high homology with the mouse genome. Essential for its enhancer activity is the presence of three NFAT binding sites in the core region [269]. RUNX-1, AP-1, Sp1 and GATA3 binding sites are also present in this region.

In contrast to the -4.5 kb enhancer, the -14 kb enhancer is only known to function in two T cell lines, Jurkat and CEM cells and it doesn't show any mouse homology. This enhancer encompasses four NFAT binding sites, with an essential core region spanning two of them. One of the NFAT binding site overlaps an Oct-1 element, and is essential for its activity and its T cell specificity, together with the recruitment of OCA-B, a lymphoid-specific Oct-1 factor [268, 272].

The -37 kb enhancer is also strictly inducible in T blast cells and leukaemic cell lines such as Jurkat and KG1a (AML cell line) and it is 10-20 times more powerful than either the -14 or the -4.5 kb enhancers. It is highly conserved and contains consensus sequences for the Ca^{2+}-inducible factor NFAT and the MAPK-inducible factor AP-1, suggesting a cooperation between these two pathways in the activation of the IL-3 locus. Moreover, the -37 kb enhancer encompasses also ETS-1, GATA and PU.1 binding sites, although these last two sites are not required for enhancer activity in Jurkat cells [264].

Other constitutive DHSs are present both downstream and upstream of the IL-3 gene. The downstream sites are present in every lineage, they bind the insulator factor CTCF, and they function as an insulator between the IL-3 and GM-CSF genes [273]. The upstream DHSs are tissue-specific and are present in T cells and myeloid cells [268, 274]. Of particularly interest is the -4.1 kb DHS, which lacks any classical enhancer activity, and is present in all cells expressing IL-3, in leukaemic cells and in primitive $CD34^+$ myeloid cells which do not yet express IL-3. These observations suggest that this DHS might represent a locus that has been primed for activation by other inducible pathway [267]. This is consistent with the observation that the -4.1 kb DHS is marked by histone H3K4me2 and is stably maintained in circulating $CD4^+$ memory T cells, but is absent in the thymus and in naive T cells [274]. This observation raised the suggestion that some elements in the genome, such as the -4.1 kb element, may serve the function of maintaining an epigenetic activation signature that allows more efficient reactivation.

1.6.4.2 DHSs within the GM-CSF gene

All the gene regulatory elements required for the efficient activation of the human GM-CSF gene in transgenic mice are located on a 10 kb segment of DNA that extends to 5 kb upstream of the GM-CSF promoter [246]. This implies that the GM-CSF gene is regulated independently of the IL-3 gene, consistent with the presence of an enhancer-blocking insulator between the two genes [273] (Figure 1.6.1A). At least three DHSs exist upstream of the GM-CSF gene: one inducible at the promoter; another inducible enhancer at -3 kb in all the cells expressing GM-CSF and a constitutive site at -4.1 kb characteristic of the myeloid lineage [275-277]. The -3 kb enhancer encompasses four NFAT binding sites, defined as the GM170, GM330, GM420 and GM550 elements, according to their positions in a 717 bp Bgl II fragment that defines the enhancer [276]. Three of these sites show a cooperation with AP-1 binding, suggesting a collaboration between the Ca^{2+} signalling pathway, mediated by NFAT, and kinase signalling pathways, mediated by AP-1 [275, 276, 278, 279].

The two central composite NFAT/AP-1 binding sites (GM330 and GM420) are essential for the enhancer activity in T cells. One Sp1 and two GATA sites are present upstream of the core region, whereas two RUNX1 sites are located downstream [280]. The GATA elements and the adjacent GM170 AP-1 site are required for efficient enhancer activation in mast cells but not in T cell lines [281]. The RUNX element is a member of an unusual class whereby it binds two molecules of RUNX1 to overlapping binding sites and requires both sites for full activity [280].

Moreover, GM-CSF enhancer also contains a NFAT/κB binding motif (at GM220 in the Bgl II fragment), suggesting that NF-κB pathway might have a

role in GM-CSF gene regulation. Unpublished data from luciferase assays performed in Peter Cockerill's lab showed that modification of the NFAT/κB binding site at GM220 significantly decreases the enhancer activity in Jurkat cells.

A scheme of the 717 bp Bgl II fragment that defines the enhancer and the location of the regulatory elements within it is represented in Figure 1.6.1B.

The GM-CSF DHS at -4.1 kb is restricted to the myeloid lineage and it encompasses consensus sequences for RUNX1, AP-1 and for the specific myeloid lineage PU.1, suggesting its possible role in regulating myeloid cells [267]. The GM-CSF promoter is highly inducible by AP-1 and NF-κB/rel upon activation of kinase signalling pathways (e.g. TNF-α can activate both transcription factors) or upon activation of Ca^{2+} signalling and NFAT recruitment. The core of the GM-CSF promoter consists of a TATA element and a CLE0 element (conserved lymphokine element 0) just upstream. The CLE0 element is activated by Ca^{2+}/calcineurin and kinase signalling pathway and it represents a composite AP-1/Ets element able to bind also NFAT with low affinity. Upstream of CLE0 there are a RUNX1 and a κB site. This κB site, located at -86, binds p65/p50 complexes in response to signal activation by agents such as IL-1, LPS or TNF-α. The κB site overlaps with a Sp1 site, creating a composite element that has the ability to recruit BRG1-containing complexes, leading to chromatin remodelling [282].

A) Map of the DHSs in the IL-3/GM-CSF locus in activated T blast cells and myeloid progenitor (MP) cells. Gray arrows indicate constitutive DHSs, black arrows indicate PMA/I-inducible DHSs. E, enhancer; Prom, promoter. *Taken from Baxter at al., 2012 [264].*

B) Map of the human GM-CSF enhancer, defined in a Bgl II fragment, and the sequence of the regions containing the NFAT, AP-1 and kB binding motifs. Perfect consensus sequences are: (A/T)GGAAA for NFAT, TGAGTCA for AP-1 and GGGRNYYYCC for NF-κB (where R is a purine, Y is a pyrimidine and N is any nucleotide). The four NFAT binding sites are located in the regions defined as GM170, GM330, GM420 and GM550 elements, according to their positions in the Bgl II fragment [276]. Three of these sites show a cooperativity with AP-1 binding. GM330 contains a perfect consensus sequence for AP-1. The NFAT/kb site is located at GM220. *Adapted from Bert et al., 2007 [281].*

Figure 1.6.1 ***Map of the DHSs in the IL-3/GM-CSF locus and location of the regulatory elements in the GM-CSF enhancer***

A

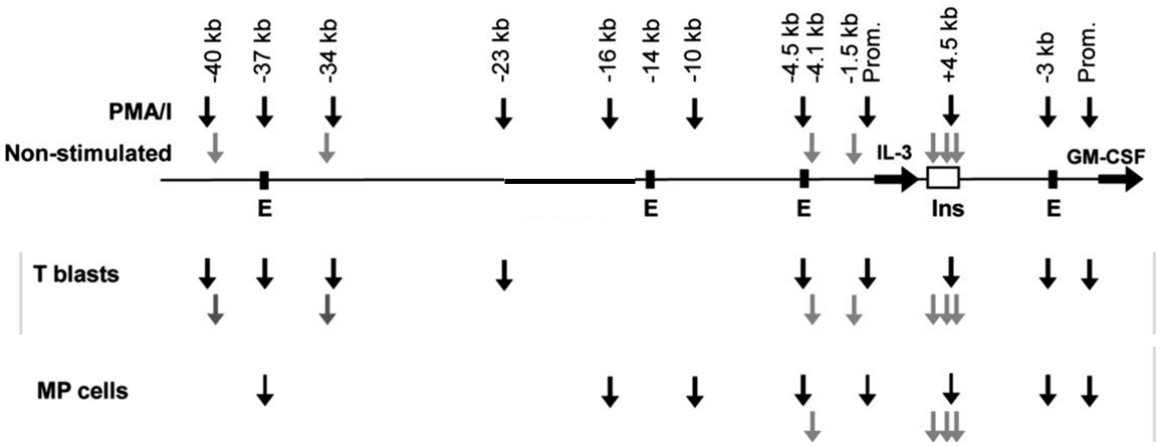

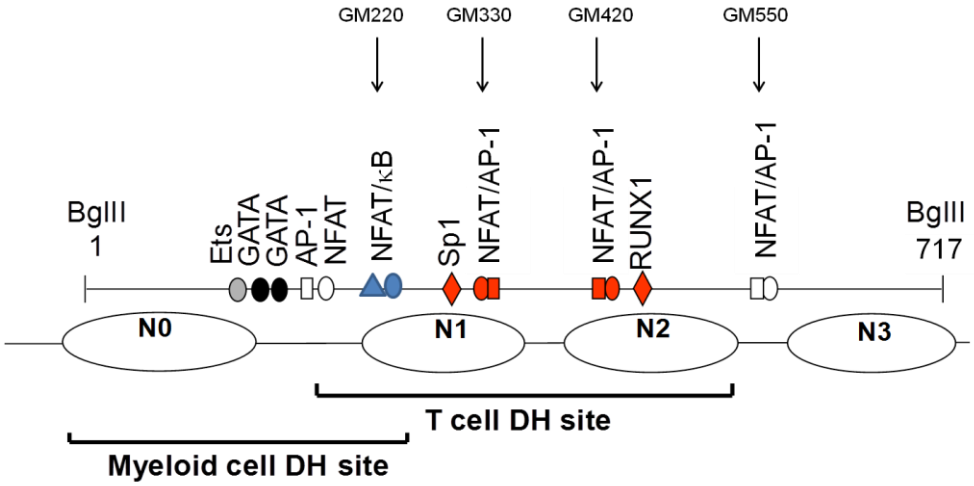

GM220	AGGAAACTCCT
GM330	CGGAGCCCCTGAGTCA
GM420	TGGAAAGATGACATCA
GM550	AGGAAAGCAAGAGTCA

Upstream of the κB site is a CK1 element, an atypical NF-κB site able to bind p65/cRel complexes in response to CD28 activation in T cells as well as NFAT [283].

1.6.4.3 Activation of GM-CSF enhancer and chromatin remodelling

In contrast to the promoter, the GM-CSF enhancer requires both Ca^{2+} and kinase signalling pathways for activity. The GM-CSF enhancer contains four NFAT binding sites: three of them bind cooperatively with AP-1 and two are essential for the enhancer activity.

In T cells the DHS at the enhancer is highly inducible within 20 min of stimulation with the PKC activator phorbol myristate acetate (PMA) and calcium ionophore (I) and its induction is associated with increased GM-CSF gene expression [275]. In fact, the induction of GM-CSF gene expression in T cells is the result of both a Ca^{2+}-dependent signal pathway, mediated by the nuclear factor of activated T cells (NFAT), and a kinase signal pathway, mediated by several transcription factors, such as AP-1. Ca^{2+} activates calcineurin, which interacts with and dephosphorylates NFAT. This dephosphorylation allows NFAT to enter the nucleus and bind DNA, promoting gene transcription. On the other hand, PMA activates different PKC isoforms. Some of them, such as PKCθ, activates NF-κB [42] and some others, such as PKCα or δ, activate different MAPK pathways [284, 285], which have AP-1 as downstream mutual transcription factor.

A schematic representation of the signalling pathways cooperating in GM-CSF gene expression after TCR activation or PMA/I-treatment is shown in Figure 1.6.2.

Figure 1.6.2 ***Schematic representation of the signalling pathways cooperating in GM-CSF expression after TCR activation or PMA/I-treatment***

A

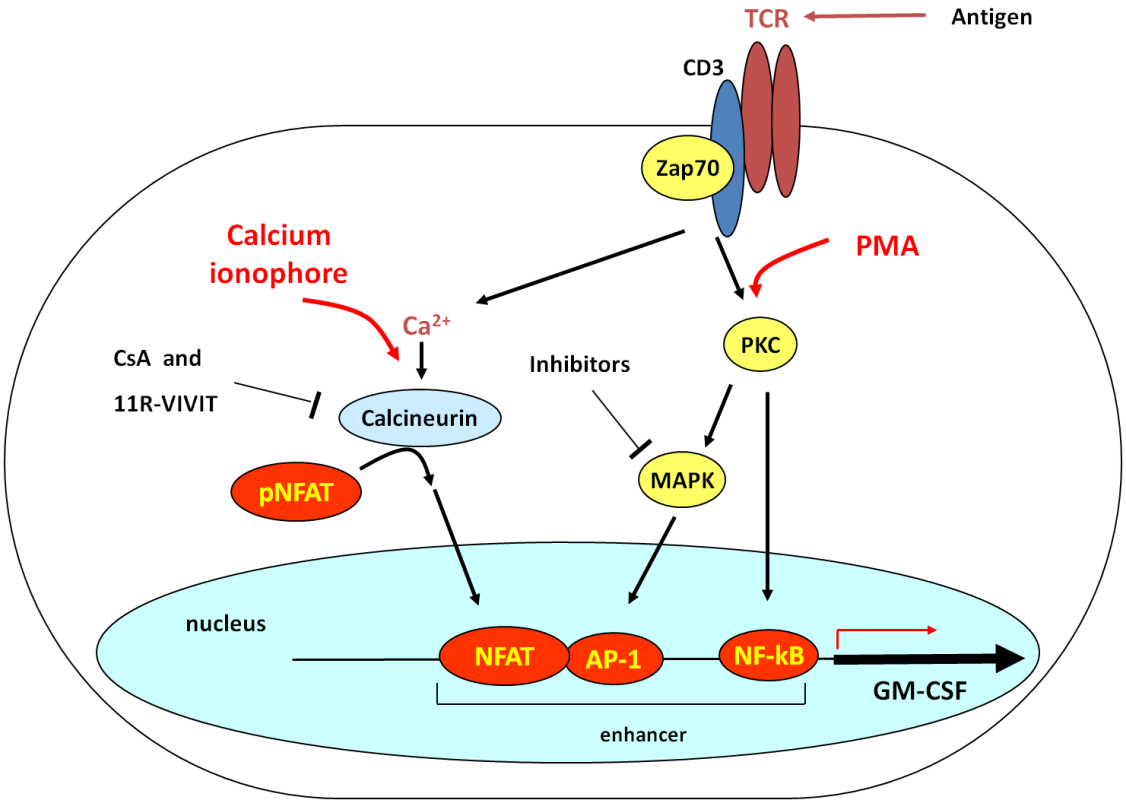

Picture shows the cooperation between the Ca^{2+} signal pathway, mediated by NFAT, and the kinase pathways, mediated by AP-1 and NF-κB, in the induction of GM-CSF gene expression. The different pathways can be activated either by TCR antigen stimulation or with phorbol myristate/calcium ionophore (PMA/I) treatment (adapted *from a figure made by Peter Cockerill*).

The -3 kb DHS is inducible in all the cells expressing GM-CSF. In some cells, such as T cells, it is entirely inducible upon stimulation. In others, like mast cells and myeloid cells, it is partly inducible and partly pre-existing [281]. As shown schematically in figure 1.6.2, the location of this DHS is also different, because in myeloid cells there are different transcription factors involved in specific gene expression, such as GATA-2.

The difference between T cells and myeloid cells has been confirmed in leukaemic cell lines. In the human cell lines Jurkat (T-ALL leukaemia model) and CEM (T cell lymphoma model) the DHS is entirely inducible. In several myeloid cell lines, the DHS is already present before the stimulation, with the exception of the AML cell line KG1a, where the DHS is entirely inducible [281].

Moreover, unpublished data from our lab show that, in some AML patients, both DHSs at the GM-CSF promoter and enhancer are already present before stimulation with IL-1, indicating that the gene is already primed for activation with the characteristics of open chromatin.

The activation of the GM-CSF enhancer in T cells requires the recruitment of two multi-protein complexes able to disrupt two positioned nucleosomes (N1 and N2). It seems that NFAT first induces the chromatin remodelling and, through the cooperation with AP-1 binding, it creates a more accessible environment for the binding of other transcription factors such as Sp1 and RUNX1. Indeed, *in vivo* footprinting of the RUNX motifs revealed complete occupancy of these sites after induction, but no detectable binding before stimulation [280]. Both NFAT and AP-1 can recruit CBP and p300 (two HATs) as well as chromatin remodelling complexes like SWI/SNF (Figure 1.6.3) [81].

Mirabella et al. [274] showed that active forms of RNA Pol II are bound within the DHSs in the IL-3 and GM-CSF locus after induction, including at the GM-

CSF enhancer, indicating that both GM-CSF and IL-3 enhancers could generate intergenic transcripts. The presence of non coding RNAs, which could be responsible for nucleosome mobilization, has been demonstrated at both the IL-3 [274] and GM-CSF enhancer (unpublished data from Cockerill's laboratory). However, their role in gene regulation has not been investigated.

Figure 1.6.3 ***Anatomy of the inducible DHS in the GM-CSF enhancer in activated T cells***

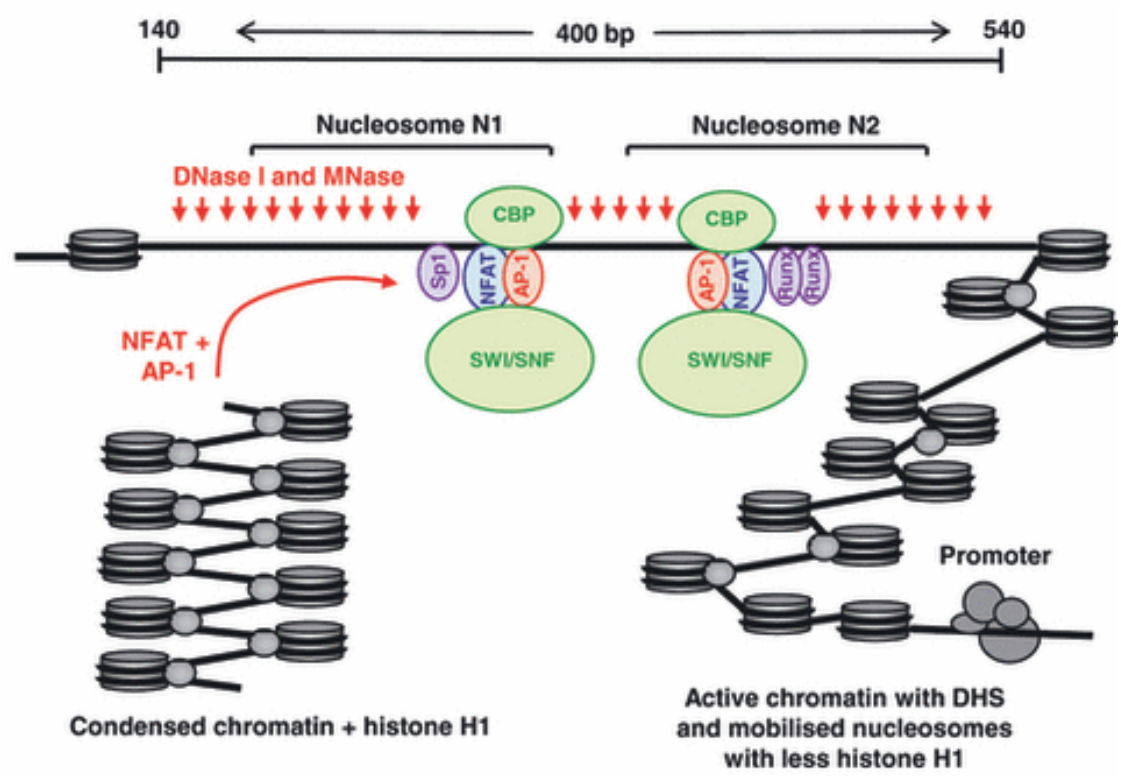

Picture represents the DHS formation and nucleosome mobilization at the human GM-CSF locus. The activation of the GM-CSF enhancer in T cells requires the recruitment of two multi-protein complexes able to disrupt two positioned nucleosomes (N1 and N2). It seems that NFAT first induces the chromatin remodelling and, through the cooperation with AP-1 binding, it creates a more accessible environment for the binding of other transcription factors such as Sp1 and RUNX1. Both NFAT and AP-1 can recruit CBP and p300 as well as chromatin remodelling complexes like SWI/SNF. *Taken from Cockerill P.N. 2011 [81].*

AIMS OF THE PROJECT:

1) To define the role of signalling transduction pathways, focusing on MAPK and NF-κB signalling, in the regulation of the PMA/I-induced GM-CSF gene expression and chromatin remodelling. Activated T blasts, which physiologically produce GM-CSF, and a T-ALL leukaemia cell line, which shows an inducible GM-CSF gene activation and DHS at the enhancer will be used. In order to do this selective kinase inhibitors will be tested;

2) GM-CSF has been demonstrated to be produced by AML blasts to support their growth and proliferation and GM-CSF enhancer is often aberrantly remodelled as a constitutive DHS in AML. For these reasons, two AML cell lines will be used to study the role of signalling pathways in the regulation of the GM-CSF gene transcription as in 1);

3) to study the role of single MAPK and NF-κB downstream transcription factors in order to find a possible cross-talk between the two signalling pathways in the regulation of the PMA/I-induced GM-CSF gene expression in leukaemia cell lines;

4) this study could represent the starting point for a genome-wide DHS analysis on AML samples, in order to find specific remodelled target genes and to investigate which transcription factors and signalling pathways are responsible for their regulation.

   Consequently, these pathways might represent potential targets for the treatment of AML cases where aberrant DHSs exist.

2. MATERIALS AND METHODS

2.1 Tissue culture procedures

2.1.1 Cell culture

Jurkat (human T cell leukaemia), KG1a (human acute myeloid leukaemia) and HEL (human erythroleukaemia) cells were grown in GIBCO^{TM} 1640 RPMI + Glutamax^{TM} medium supplemented with 10% heat inactivated fetal calf serum (GIBCO), 100 U/ml Penicillin, 100 mg/ml Streptomycin. According to the DSMZ cell bank's protocol, Jurkat and KG1a cells were passaged 1:2 to 1:3 every 2-3 days, maintaining them at 0.5-1.5 x 10^6 cells/ml; HEL cells were grown to 0.2-1.0 x 10^6 cells/ml, before passaging them 1:3 to 1:5 every 2-3 days.

Human GM-CSF transgenic mouse T blast cells were isolated from spleen and cultured in Iscove's modified Dulbecco's medium + Glutamax^{TM}, supplemented as above plus 150 μM Monothioglycerol.

All cells were incubated the cells at 37 °C, in a humidified atmosphere containing 5% CO_2.

2.1.2 Preparation and expansion of splenic primary T blast cells from transgenic mice

Actively dividing T lymphoblastoid cells (to be referred to as T blast cells) were prepared from the spleen and cultured in Iscove's modified Dulbecco's medium + Glutamax^{TM}(Gibco) supplemented as above plus 150 μM Monothioglycerol.

To prepare a suspension of lymphocytes, the spleen was isolated from C42 transgenic mice containing six copies of an Age I fragment encompassing the entire human IL-3/GM-CSF locus. The spleen was minced to small pieces using sterilised scissors, before crushing in 5 ml of fresh medium and passing through a 70 μM cell strainer.

To induce the transformation of T lymphocytes to T blast cells, purified cells were incubated with 2 μg/ml Concanavalin A (GE Healthcare) for 48h. Afterwards Concavalin A was removed and replaced with 50 U/ml recombinant mouse (rm) IL-2 (Peprotech Inc.) for 3 or 4 more days to stimulate proliferation, passaging every day to maintain them at a concentration not higher than $2x10^6$ cells/ml.

2.1.3 Stimulation and treatments

All cells were pre-treated for 45 minutes to 4 hours (depending on the experiment) with 20 ng/ml phorbol 12-myristate 13-acetate (PMA) and 2 μM calcium ionophore A23187 (I). To test inhibitors, cells were pre-treated for 1 h with each inhibitor before stimulation, either alone or in combination. Inhibitors of MEK (PD98059), p38 (SB202190), JNK (SP600125), NFAT (11R-VIVIT), MSK1 (H89 dihydrocloride hydrate) and the proteasome inhibitor MG132 were purchased from Calbiochem/Merck. The calcineurin inhibitor Cyclosporin A (CsA) was obtained from Sigma-Aldrich. All inhibitors were dissolved in sterile dimethyl sulfoxide (DMSO)-Hybri-Max® (Sigma-Aldrich) and stored as a 10 mM stock at -80 °C.

2.2 DNase I treatment

Permeabilized cell digestions were performed by suspending the cells at a concentration of $3x10^6$ cell/100 μl in nuclei digestion buffer (60 mM KCl, 15 mM NaCl, 5 mM $MgCl_2$, 10 mM Tris pH 7.4, 0.3 M sucrose) at 21 °C. Usually $18x10^6$ cells were required per treatment, in order to test three different concentrations of DNase I in a range from 6 to 16 μg/ml to obtain optimally digested samples in which constitutive and inducible DHSs could be efficiently detected. Therefore, $6 x10^6$ cells were resuspended in 200 μl in nuclei digestion buffer; then DNase I (Worthington) was added in an equal volume of digestion buffer containing 0.4% Nonidet P-40 and 2 mM $CaCl_2$. After exactly 3 minutes the digestion was terminated with a double volume (400 μl) of nuclei lysis buffer containing 0.3 M sodium acetate pH 7.0, 0.5% SDS, 5 mM EDTA and 1 mg/ml proteinase K (PK), giving a final volume of about 800 μl. Samples were incubated at 55°C for 1 h and then at 37 °C for 18 hours. The rate of digestion of the samples was analysed via 0.8% agarose gel electrophoresis using 1X TAE buffer (40 mM Tris, 20 mM acetic acid and 1 mM EDTA) and 0.5 μg/ml ethidium bromide. 8 μl of lysate solution (8 μl from 800 μl lysate = 1% of $6 x 10^6$ cells = ~ 300 ng DNA) were loaded per well and electrophoresis was performed at 30 Volts for 15-16 h and visualised under UV. Samples which showed optimal extents of DNase I digestion were selected, using as reference a λ DNA-HindIII Digest ladder (New England BioLabs). Picture 2.1 shows a representative gel with an explaination on how samples were identified and selected for subsequent Southern Blot analysis. Afterwards 100 μg/ml of RNase A were added and samples were incubated for 1 h at 37 °C before an extra PK treatment at 55 °C for 1 h.

Figure 2.1 ***Check gel for DNAse I digestion***

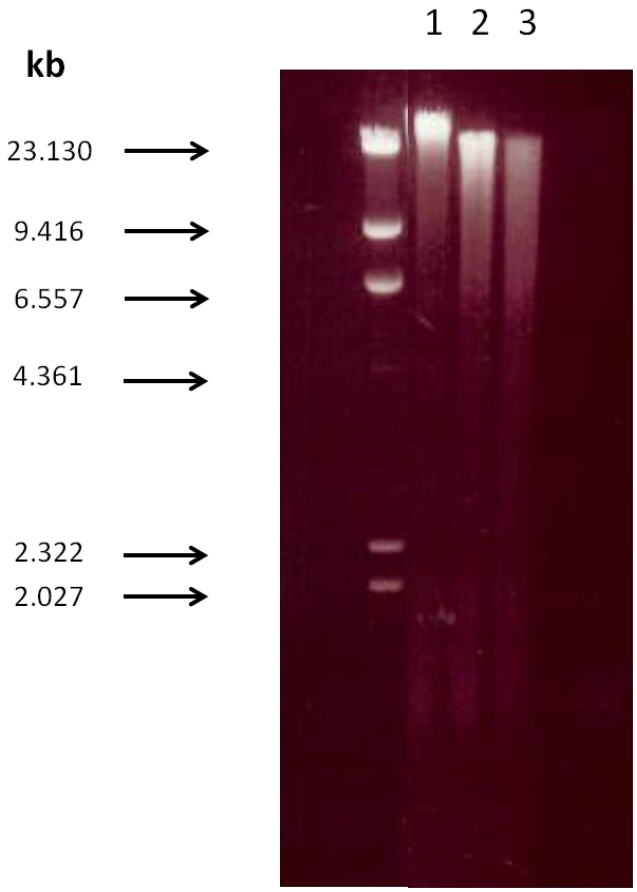

Picture represents a 0.8% agarose gel after an overnight run at 30 V.

Lanes 1, 2 and 3 show about 300 ng of DNA from KG1a cells treated with 6, 10 and 12 μg/ml of DNAse I, respectively. On the left 1 μg of λ DNA-HindIII Digest ladder has been loaded (molecular weight of the bands is indicated by the arrows).

In this analysis most of the DNA of sample 3 has been digested into fragments smaller than 23 kb. For this reason, I decided to exclude sample 3 and to use the samples 1 and 2 for Southern blot analysis of DHSs.

2.3 DNA purification

After selecting samples with an optimal rate of digestion, DNA was purified using phenol/chloroform. An equal volume of phenol was added to the genomic DNA solution and the mixture was incubated with rotation at RT for 1 hour. Following centrifugation for 5 minutes at 13000 rpm, the aqueous phase was transferred to a fresh eppendorf and an equal volume of phenol:chloroform (1:1) solution added, incubated at RT for 30 minutes under constant rotation and then centrifuged as before. An equal volume of chloroform was then added to the aqueous phase, incubated with rotation at RT for 20 minutes and centrifuged; then the DNA was precipitated using 2 volume of absolute ethanol, in the presence of salt (sodium acetate 0.3 M pH 5.2) and 20 μg glycogen on ice for 5 minutes and then centrifuged at 13000 rpm for 10 minutes at 4 °C. The pellet was washed with 70% ethanol before air drying and then resuspended in 1X TE (10 mM Tris-HCl, 1 mM EDTA, pH 7.4).

2.4 DNase hypersensitive site (DHSs) mapping and Southern blot

After purification 5 μg of DNA were digested with 30 Units of either EcoR I or BamH I (New England BioLabs Inc.) in 17.5 μl solution containing 1X NEBuffer and 0.1 mg/ml BSA using the recommended NEBuffer 2 for EcoR I digestion (100 mM Tris-HCl, 50 mM NaCl, 10 mM $MgCl_2$ 0.025% Triton® X-100, pH 7.5 at 25°C) and NEBuffer 3 for BamH I digestion (100 mM NaCl, 50 mM Tris-HCl, 10 mM $MgCl_2$, 100 μg/ml BSA, pH 7.9 at 25°C). After 3-4 hours at 37 °C the digestion was stopped with 4 ml of stop buffer containing 1 % SDS, 20% ficoll and Orange G dye. In this study the DHSs

across a 9.4 kb EcoRI fragment spanning the GM-CSF enhancer and promoter were mapped, using a 1.5 kb BamH I fragment of DNA as a probe. The DHSs spanning the insulator downstream of the IL-3 gene were mapped in a BamHI fragment, using a 1 kb Bgl I/BamH I fragment as a probe. A schematic representation of the technique used to identify cis-regulatory elements by Southern blot and the strategy used to map the DHSs in the GM-CSF/IL-3 locus is represented in Figure 2.2.

Digested DNA was analysed on a 0.8% agarose gel made up with 1X TAE buffer (Tris base, acetic acid and EDTA) and 0.5 μg/ml ethidium bromide and run at 30 Volts for 15-16 hours. Afterwards, the gel was washed twice for 15 minutes in a solution containing 0.5 M NaOH and 1.5 M NaCl to denature the DNA and then twice for 20 minutes in a neutralization solution containing 1 M Tris pH 7.0 and 1.5 NaCl. Denatured DNA was transferred onto Hybond-XL membrane (Amersham) in 10X SSC buffer (0.15 M sodium citrate, 1.5 M NaCl plus 0.1 M EDTA). The filter was washed in 2X SSC and then the DNA fixed onto the membrane using UV at 0.07 Joules/cm^2.

Figure 2.2 ***Identification of cis-regulatory elements by Southern blot and strategy of the DHSs mapping in the GM-CSF/IL-3 locus***

A

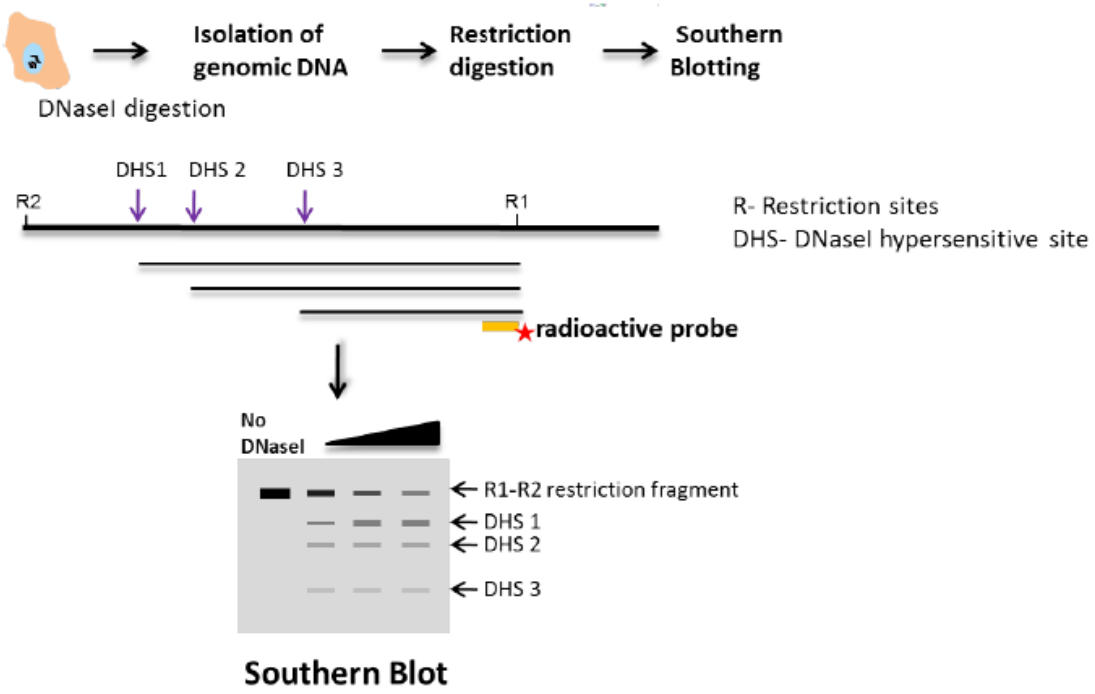

B

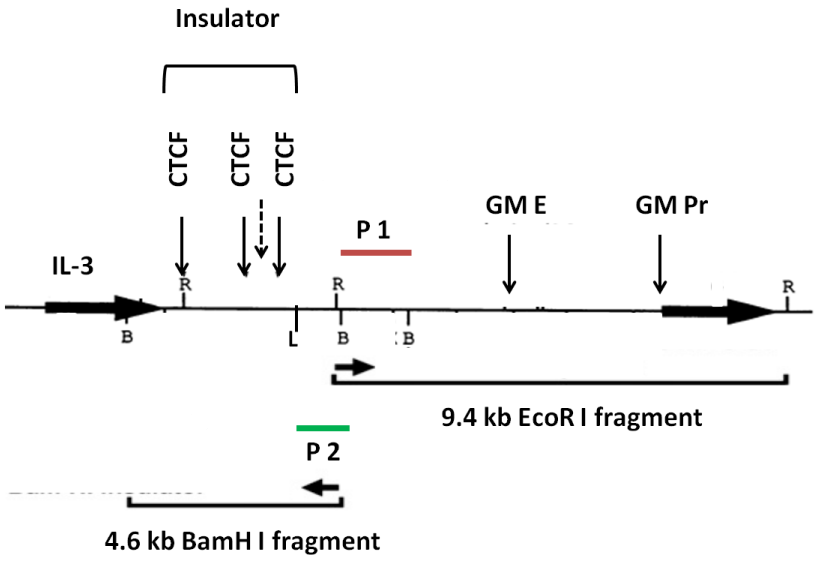

Schematic representation of the identification of cis-regulatory elements by Southern blotting. B) Strategy of DHSs mapping. DHSs within a 9.4 kb EcoR I fragment were identified by using a 1.5 kb BamH I fragment as a probe (P 1). DHSs spanning the insulator region downstream of the IL-3 gene were identified in a BamH I fragment using a 1.0 kb Bgl I/BamH I fragment as a probe (P 2). R, EcoR I site; B, BamH I site; L, Bgl I site.

2.5 Southern blot hybridization

After DNA transfer to membranes, DHSs were mapped by indirect end-labelling as follows. The membrane following Southern Blot was incubated with rotation for at least 2 hours at 65°C with 20 ml of RapidHyb buffer (Amersham) containing 0.25 mg/ml heat denaturated sonicated herring sperm DNA. Probes were prepared using an Amersham kit. To prepare a specific probe, 30 ng of DNA probe was combined with 5 μl of random primers in a final volume of 33 μl water, and heated at 99°C for 5 min. After cooling the mixture briefly on ice, 10 μl of labelling buffer, 2 μl (1 U/μl) of Klenow fragment of DNA polymerase (Amersham) and 5 μl ^{32}P dCTP were added and incubated at 37 ˚C for 20-30 minutes. To purify the probe from free ^{32}P-dCTP, the probe was centrifuged through Sephadex G50 spin columns (GE Healthcare). The probe was heat denaturated in the presence of 0.5 ml of 10 mg/ml herring sperm DNA at 99°C for 5 minutes, cooled on ice, and then added to the hybridization buffer. After hybridization (2 hours at 65°C) the filter was washed twice for 15 minutes with 2X SSC containing 25 mM NaPhosphate and 0.1 % SDS, then twice for 20 minutes with pre-warmed 0.1X SSC wash buffer containing 1 mM sodium pyrophosphate pH 7 and 0.1% SDS. The final wash was in a high salt buffer (2X SSC, 50 mM $NaPO_4$, 10 mM NaPyrophosphate, 0.5% SDS) for 15 minutes to reduce the background. The labelled membrane was then exposed to a Kodak phosphorimager screen and visualised using a PharoxFX™ phosphoimager (Bio-Rad). Images were analysed using Bio-Rad Quantity One® Software.

2.6 mRNA extraction and purification

$5x10^6$ cells were incubated with 1 ml Trizol® (Invitrogen) for 5-10 minutes before addition of 0.2 ml of chloroform and centrifugation at 13000 rpm for 15 min at 4°C. The supernatant was removed and the RNA was precipitated by adding 500 μl of isopropanol. Samples were incubated for 10 minutes at RT and then centrifuged at 13000 rpm for 10 min at 4°C. The pellet was washed in 70% ethanol, air dried and resuspended in 20-40 μl of DEPC treated water. Genomic DNA was removed by digestion with 2 U of TURBO™ DNase I (Ambion), after adding 0.1 volume of 10X TURBO™ DNase I buffer. After 30 min at 37°C digestion was stopped with 0.1 volume of 10X TURBO™ DNase I inactivation buffer. Finally the samples were centrifuged at 7500 *g* for 1.5 min and the supernatant containing the purified mRNA transferred to a fresh eppendorf.

2.7 Reverse transcription and Real Time PCR

1 μg of purified mRNA was mixed with 0.5 mM of each of dCTP, dGTP, dATP, TTP and 1 μl of 176 μM oligo dT primers and incubated for 5 min at 95°C. Then 4 μl of 5X first strand buffer, 1 μl of RNase out recombinant ribonuclease inhibitor, 10 mM DTT and 1 μl of M-MLV Reverse transcriptase (Invitrogen) were added and incubated at 37°C for 50 min. M-MLV enzyme was inactivated at 70°C for 15 min.

Quantitative Reverse Transcriptase PCR experiments (qRT-PCR) were performed using the Applied Biosystem® 7500 System. PCR conditions were: 50˚C for 2 minutes, 95˚C 10 minutes, then 40 cycles of 95˚C for 15 seconds and 60 ˚C for 1 minute. To measure the levels of expression of each gene, I used 20

μl of a mix containing a 2X Sybr Green Master Mix (Applied Biosystem) (1X final concentration), 500 ng of forward and reverse primers and 2 μl of cDNA, previously diluted 1:20 or 1:100 (in the case of GAPDH). Data from the threshold values for each amplification was analysed against a standard curve prepared using serial dilutions (usually 1:20, 1:100, 1:1000 and 1:10000) of cells stimulated with PMA/I and normalised to glyceraldehyde-3-phosphate dehydrogenase (GAPDH) gene values.

Primer pairs were designed using the aid of Primer3 software and were made by Sigma-Aldrich. The sequences used as primers in Real Time experiments are listed in table 2.1.

In every biological experiment, the expression of the genes was measured in triplicate after each treatment and the average was calculated. Values with threshold cycles > or < 0.5 compared to the other two were excluded. Statistical difference in gene expression between two different groups (e.g treated vs untreated cells) was determined using the student *t*-test (samples different if value ≤ 0.05).

Table 2.1 ***Primers used in Real Time PCR***

Primer name	***Sequence 5'-3'***
h GM-CSF forward	CACTGCTGCTGAGATGAATGAAA
h GM-CSF reverse	GTCTGTAGGCAGGTCGGCTC
m GAPDH forward	AACAGCGACACCCACTCCTC
m GAPDH reverse	CATACCAGGAAATGAGCTTGACAA
h GAPDH forward	CCCACTCCTCCACCTTTGAC
h GAPDH reverse	ACCCTGTTGCTGTAGCCAAAT
m c-Fos forward	TCCAAGCGGAGACAGATCAAC
m c-Fos reverse	TTTTTCCTTCTCTTTCAGCAGATTG
m c-Jun forward	GCCGGAAAAGGAAGCTGGAGC
m c-Jun reverse	CTGTTCCCTGAGCATGTTGGC
h c-Fos forward	AGGCCGAGCGCAGAGCATTG
h c-Fos reverse	CGGTTGCGGCATTTGGCTGC
h c-Jun forward	GTTTGCAACTGCTGCGTTAG
h c-Jun reverse	CAGGTGGCACAGCTTAAACA
h Fra-1 forward	CTGCAGCCCAGATTTCTCAT
h Fra-1 reverse	AACCGGAGGAAGGAACTGAC
h Fra-2 forward	ATCAAGACCATTGGCACCAC
h Fra-2 reverse	GACGCTTCTCCTCCTCTTCA
h JunB forward	CACCTCCCGTTTACACCAAC
h JunB reverse	GGAGGTAGCTGATGGTGGTC
h JunD forward	TTGACGTGGCTGAGGACTTT
h JunD reverse	CGCCTGGAAGAGAAAGTGAA

m = mouse h = human

2.8 siRNA genes knock-down in KG1a cells

SignalSilence® p44/42 MAPK ERK1/2 siRNA (#6560) was purchased from Cell Signaling Technology; p38α (sc-29433) and c-Jun (sc-29223) siRNA (h) were purchased from SantaCruz Biotechnology. siRNAs were resuspended in nuclease free water according to the manufacturer's protocol and stored at -80°C. MISSION® siRNA Universal Negative Control #1 from Sigma-Aldrich (SIC001) was used as a control for nonsequence-specific effects. Up to $2X10^7$ KG1a or Jurkat cells were transfected with 100-200 nM siRNA in RPMI media (10% FCS, L-Glutamine and antibiotics) using a Fischer 3500 electroporator (Fischer, Heidelberg, Germany) at 350 Volts with an electrical pulse of 10 msec. Following electroporation, the transfected cells were seeded in pre-warmed medium at a concentration of $5x10^5$ cells/ml and incubated at 37°C with 5% CO_2. mRNA levels were analysed via qRT-PCR 48h after transfection, and protein levels via western blotting after 72 h. In the case of ERK1/2 and p38, the cells were transfected again and the level of protein expression was verified after further 24 h.

Although exogenous siRNAs can be introduced in the cells to silence specific genes, endogenous siRNAs have been identified in various organisms. In human siRNA-mediated RNAi the RNAse enzyme Dicer can convert both hairpin RNAs and lncRNAs into 21-23 nucleotides (nt) siRNAs, carrying a phosphate group at 5' end and a 2-nt overhangs at the 3' end. These dsRNAs assemble into a RNA-induced silencing complex (RISC), containing Dicer, AGO2 and other protein subunits. RISC complex containing the antisense strand (called guide strand) binds the target mRNA and leads to its cleavage and degradation. After cleavage, RISC is recycled (Figure 2.3) [286].

Figure 2.3 siRNA gene silencing mechanism

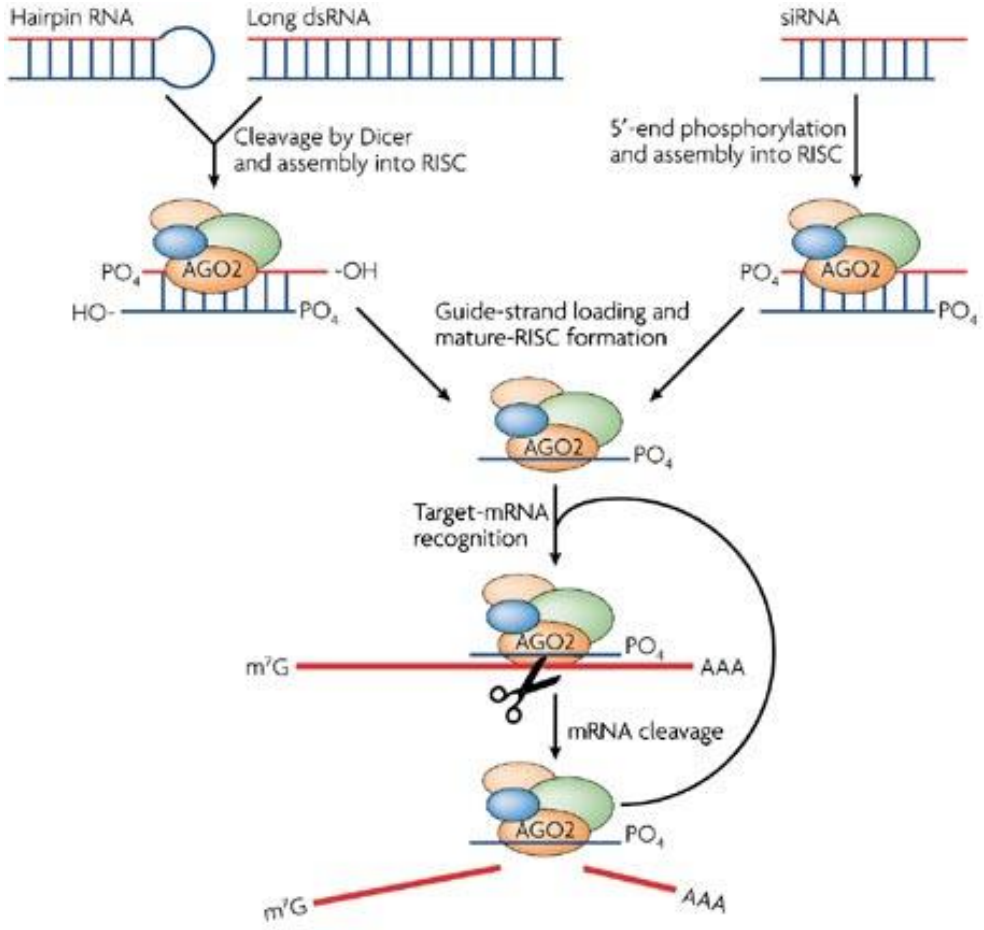

The RNAse enzyme Dicer can convert both hairpin RNAs and lncRNAs into 21-23 nucleotides (nt) siRNAs, carrying a phosphate group at 5' end and a 2-nt overhangs at the 3' end. These dsRNAs assemble into a RNA-induced silencing complex (RISC), containing Dicer, AGO2 and other protein subunits. The RISC complex containing the antisense strand (called guide strand) binds the target mRNA and leads to its cleavage and degradation [286]. Taken from Rana T.M., 2007 *[286]*.

2.9 Electrophoretic Mobility Shift Assay (EMSA)

2.9.1 Nuclear extract preparation

Nuclear extracts were obtained from Jurkat and KG1a cells by homogenizing the cells in ice cold buffer A, containing 10 mM HEPES, 10 mM KCl, 1.5 mM $MgCl_2$, 0.5 mM DTT, 0.5 mM PMSF, 50 μg/ml aprotinin and leupeptin [60]. After centrifugation at 1500 rpm for 5 minutes the pellet was resuspended in buffer A and 4 volumes of buffer C (20 mM HEPES, 0.42 M NaCl, 1.5 mM $MgCl_2$, 0.2 mM EDTA, 0.5 mM DTT, 0.5 mM PMSF, 50 μg/ml aprotinin and 50 μg/ml leupeptin). Following centrifugation at 13000 rpm for 10 minutes protein concentration was determined by the Bradford assay (Pierce), following the manufacturer's instructions.

A known volume of sample (2-5 μl) was mixed with 1 ml of Bradford reagent (which contains the protein stain Coomassie Blue G250) and after 5 minutes the absorbance was read at a wavelength of 595 nm using a spectrophotometer. Concentration of the samples was determined using a calibration curve made of serial dilutions of BSA.

2.9.2 Labelling and purification of EMSA probes

The probes used for AP-1 and Oct-1 EMSA assays were duplexes of DNA oligonucleotides containing either the AP-1 or Oct-1 consensus sequence (Stromelysin gene AP-1 site: GCAAGGATGAGTCAAGCTGCGGGTGATCC; Oct-1 consensus: TGGACACCAAATTTGCATAAATC).

To anneal the forward and reverse oligonucleotides 100 μl of sample containing 50 μM of both oligos in TE plus 50 mM NaCl was incubated at 90 °C for 5 minutes and left to cool slowly. The probe was then radiolabelled as follows. In the labelling reaction 25 ng of oligonucleotide duplex in TE + 50 mM NaCl were mixed with 0.5-2 units T4 DNA polymerase, 1 μl 10X T4 DNA polymerase buffer, 3 μl 0.33 mM dCTP + dATP + TTP and 5 ul ^{32}P dCTP. After 10 minutes at RT, 3 μl 20% ficoll + Bromophenol Blue were added and, in order to purify the EMSA probe from free radioactive, the mixture was loaded onto a 7.5% polyacrylamide TAE gel, which had been pre-run for 1 hour at 150 V. After 45-50 minutes at 250 V in TAE buffer the run was stopped; the gel was sealed in a plastic bag and exposed to an X-Ray film (Amersham), using luminous stars that had been previously exposed to light to help localise the position of the probe on the gel. The radioactive probe was excised from the gel, transferred onto a midi D-tube dialyser (Merck Millipore) with 300 μl TAE buffer and placed it in a mini-agarose gel tank in TAE buffer for 20-30 minutes at 80 V for eletroelution. After elution the gel slice was dialysed in 1X TE + 50 mM NaCl overnight at 4°C.

2.9.3 EMSA gel shift

Each EMSA was performed using a 4% polyacrylamide gel in 25 mM Tris borate/0.5 mM EDTA (TBE). The gel was pre-run at 200 V for 1 hour and left to cool down. In each assay, 4 μg of nuclear protein, 4 μg of poly(dI·dC) and 0.2 ng of radiolabeled DNA probe were incubated for 10 min at room temperature in

a final 20 μl of 18 mM HEPES, 45 mM NaCl, 15 mM KCl, 10% glycerol, 0.1 mM PMSF, 1 mM DTT, 5 μg/ml aprotinin and 5 μg/ml leupeptin.

In competition assays and supershift assays an excess of unlabeled specific competitor or 1 μg of specific antibody was added, respectively, to the nuclear extracts and incubated for 10 minutes at RT before adding the radioactive probe. At the end of the incubation samples were loaded on the gel including a Bromophenol Blue marker on one side lane only. The gel was run at 200 V for exactly 1.5 hours, when the dye migrated about 9.5 cm. Then the gel was fixed in 0.5% Cetyl Trimethyl Ammonium Bromide, 50 mM NaAcetate pH 5.5 for about 45-60 minutes to reduce the risk of diffusion of probe during drying. After fixation the gel was transferred on one sheet of Whatman 3MM, covered in clingfilm and dried at 80°C for approximately 1 hour.

Autoradiography was performed using a Kodak phosphorimager. Images were visualised using a PharoxFX™ phosphoimager (Bio-Rad) and analysed using Bio-Rad Quantity One® Software.

2.10 Western blotting

2.10.1 Whole protein extraction

10^7 cells were harvested by centrifugation at 1200 rpm for 5 minutes, washed twice in PBS after treatments and then resuspended in 1X RIPA buffer (20 mM Tris-HCl pH 7.5, 150 mM NaCl, 1 mM Na_2EDTA, 1 mM EGTA, 1% NP-40, 1% sodium deoxycholate, 2.5 mM sodium pyrophosphate, 1 mM β-glycerophosphate, 1 mM Na_3VO_4, 1 μg/ml leupeptin). After 30 minutes at 4°C cells were centrifuged at 16000 g at 4°C for 15 minutes. The resulting pellet was

discarded and the supernatant was either used for western blotting or stored at -20°C. Protein concentration was determined by Bradford assay as described above.

2.10.2 SDS – Polyacrylamide gel electrophoresis (PAGE)

30 μg of total proteins was mixed with a 2x Laemmli sample buffer from Bio-Rad (65.8 mM Tris-HCl, pH 6.8, 2.1% SDS, 26.3% (w/v) glycerol, 0.01% bromophenol blue), supplemented with 5% (v/v) β-mercaptoethanol and heated at 100 °C for 5 minutes. Then samples were loaded onto a 10% polyacrylamide gel containing SDS or onto a 4-20% Mini-PROTEAN®TGX™ Precast Gels (Bio-Rad). The 10% polyacrylamide + SDS gel was formed of 2 parts: a resolving gel (375 mM Tris-HCl pH 8.8, 10% (w/v) acrylamide/bis-acrylamide (37.5:1) (Bio-Rad), 0.1% (w/v) SDS, polymerised with 0.04% (w/v), ammonium persulphate (APS) and 0.08% (v/v) TEMED) and a stacking gel (125 mM Tris-HCl pH 6.8, 4.5% (w/v) acrylamide/bis-acrylamide (37.5:1), 0.1% (w/v) SDS, polymerised with 0.05% (w/v) APS and 0.125% (v/v) TEMED). Gel electrophoresis was performed at constant voltage (100V) for about 1.5 hours in 1X Running buffer (25 mM Tris-HCl, glycine 192 mM, 0.1% (w/v) SDS) using a Mini-PROTEAN tetra electrophoresis system (Bio-Rad). To determine molecular weight of proteins of interest the Full Range Rainbow Molecular Weight marker was used (GE Healthcare). After electrophoresis, proteins were transferred to nitrocellulose membrane (Thermo scientific, Pierce) using Mini-Trans blot cell (Bio-Rad) at 100 Volts for 1 h at 4 °C in transfer buffer (25 mM Tris-HCl, 192 mM glycine, 20% (v/v) methanol). Membranes were then blocked at room temperature for 1 h with 5% (w/v) milk powder in TBS-Tween 20 (0.1%) (TBST).

After brief washes with 1X TBST, membranes were incubated first overnight at 4°C with primary antibody (1:1000 in 5% (w/v) BSA in TBST) (Table 2.2). Membranes were washed 3 times for 5 minutes with 1X TBST and then they were incubated for 1h at room temperature with an anti-rabbit IgG, HRP-linked secondary antibody diluted 1:10000 in 5% BSA in TBST (#7074 Cell Signaling Technology). Before detection, membranes were washed again 3 times for 5 minutes with 1X TBST. Membranes were developed using the ECL Plus Western Blotting detection system (GE Healthcare) according to the manufacturer's protocol and the signal was detected using x-ray films.

The intensity of the band was measured using Image J software and results were expressed as relative to either a housekeeping protein (e.g. GAPDH) or, in case of a phosphorylated protein, to its total form (e.g. MAPK proteins).

Antibody	*Cat. No.*	*Company*
p44/42 MAPK (ERK1/2) Rabbit mAb	4695	Cell Signaling Tech.
p38 MAPK Rabbit mAb	9212	Cell Signaling Tech.
SAPK/JNK Rabbit mAb	9252	Cell Signaling Tech.
Phospho-p44/42 MAPK (Erk1/2) (Thr202/Tyr204) Rabbit mAb	9101	Cell Signaling Tech.
Phospho-p38 MAPK (Thr180/Tyr182) (3D7) Rabbit mAb	9215	Cell Signaling Tech.
Phospho-SAPK/JNK (Thr183/Tyr185) (98F2) Rabbit mAb	4671	Cell Signaling Tech.
MSK1 (C27B2) Rabbit mAb	3489	Cell Signaling Tech.
Phospho-MSK1 (Thr581) Rabbit mAb	9595	Cell Signaling Tech.
c-Fos	4384	Cell Signaling Tech.
c-Jun (60A8) Rabbit mAb	9165	Cell Signaling Tech.
Phospho-c-Jun (Ser63) (54B3) Rabbit mAb	2361	Cell Signaling Tech.
NF-κB p65 Antibody	3034	Cell Signaling Tech.
Phospho-NF-κB p65 (Ser276) Antibody	ab106129	Abcam
Phospho-NF-κB p65 (Ser536) Rabbit mAb	3033	Cell Signaling Tech.
GAPDH (14C10) Rabbit mAb	2118	Cell Signaling Tech.

Table 2.2 ***List of primary antibodies used in Western blot analysis***

2.11 Chromatin immunoprecipitation (ChIP)

2.11.1 Chromatin preparation

For histone modification ChIPs, a single cross-linking protocol with formaldehyde was used, starting from $1.5x10^7$ cells. Alternatively, when an antibody against a transcription factor was used, a double cross-linking protocol was performed, starting from $5x10^7$ cells. In this case cells were washed three times with PBS after treatments. Then they were resuspended in 15 ml PBS and DNA-protein interactions were first cross-linked for 45 minutes at RT by the addition of 12.5 mg disuccinimidyl glutarate (DSG). Cells were then washed four times with PBS and a second cross-linking was performed by adding 16% formaldehyde to a final concentration of 1%. For all ChIP assays, after 10 minutes at RT, the cross-linking was stopped by addition of glycine to a final concentration of 0.125 M. Cells were washed twice with cold PBS and resuspended in ice cold Buffer A (10 mM Hepes 1 M pH 8, 10 mM EDTA 0.5 M pH 8, 0.5 mM EGTA 0.2 M pH 8, 0.25% TritonX100 10%) plus a protease inhibitor cocktail and rotated on a rotating wheel at 4°C for 5-10 min. Then pellet was spun down and resuspended in ice cold Buffer B (10 mM Hepes pH 8, 200 mM NaCl, 1 mM EDTA pH 8, 0.5 mM EGTA pH 8, 0.01% TritonX100) and rotated again on a rotating wheel for 5-10 min. For sonication, chromatin was resuspended in 300 μl IP buffer I (25 mM Tris pH 8, 150 mM NaCl, 2 mM EDTA pH 8, 1% TritonX100, 0.25% SDS) and was shredded in order to obtain ~ 200-500 bp DNA fragments using Bioruptor™ (Diagenode) at 240W for 15 cycles of 30 sec on and 30 sec off at 5°C. Samples were then centrifuged at 16000 g, 10 min at 4°C and the supernatant was diluted by adding 2 volumes of ice-cold IP

buffer II (0.083% SDS, 5% glycerol final concentration). The chromatin solution was then split into two aliquots to be used for two immunoprecipitations. 10% input material was taken from one of the aliquots.

To verify the size of chromatin after sonication, a few microlitres of input were loaded onto a 0.8% agarose gel made up with TBE buffer (89 mM Tris borate, 0.01 M EDTA, pH 8.2-8.4 at 25 °C). The gel was run at 50 V for about 45 minutes using 1 μg of 100 bp DNA ladder (New England BioLabs) as reference and then visualised under UV light. A picture of a typical gel is shown in Figure 2.4.

2.11.2 Immunoprecipitation and DNA quantification

15 μl Dynabeads were incubated for 2 hours with 10 μg antibody (against a transcription factor) or 2 μg antibody (against a histone modification) (Table 2.3) together with 0.5% BSA to reduce the non-specific binding. Then, antibodies were added to 450 μl chromatin and samples were rotated at 4 degrees. After 4 hours of incubation samples were washed once with Wash Buffer I (20 mM Tris pH 8, 150 mM NaCl, 2 mM EDTA pH 8, 1% TritonX100, 0.1% SDS), then twice with Wash Buffer II (20 mM Tris pH 8, 500 mM NaCl, 2 mM EDTA pH 8, 1% TritonX100, 0.1% SDS), once with LiCl Buffer (10 mM Tris pH 8, 250 mM LiCl, 1 mM EDTA pH 8, 0.5% NP40, 0.5% Na-deoxycholate) and twice with TE/NaCl buffer (10 mM Tris pH 8, 50 mM NaCl, 1 mM EDTA pH 8). Histone complexes were eluted with 100 μl Elution Buffer (1% SDS, 0.1 M $NaHCO_3$).

Figure 2.4 ***Agarose gel to check chromatin size after sonication***

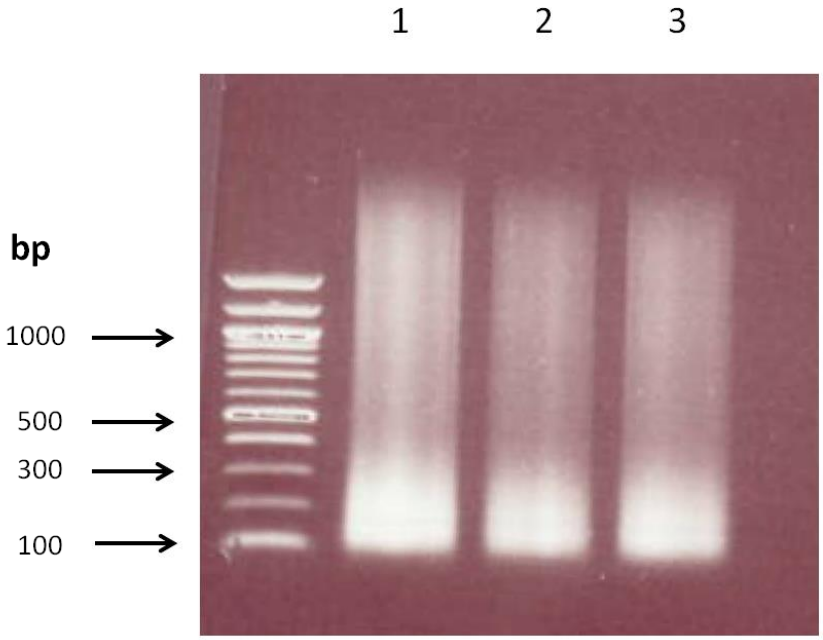

The gel shows input fractions from KG1a untreated (1), treated with PMA/I for 1.5 h (2) and pretreated for 1 h with the combination of MEK and p38 inhibitors before PMA/I stimulation (3). In the three samples, most of the chromatin shows a size between 100 and 300 bp. On the right side, arrows indicate the molecular weights corresponding to the bands of the 100 bp DNA ladder.

Input samples were also diluted in Elution Buffer up to 100 μl. 1 μl RNaseA (10 mg/ml) was added to the samples and incubated for 30 min at 37°C. Then 4 μl 5 M NaCl and 2 μl 0.5 M EDTA were added and cross-linking was reversed by adding 0.5 μl Proteinase K (50 mg/ml) and heating at 65°C overnight. For input samples, 1 μl Proteinase K (50 mg/ml) was used. The following day samples were purified by using 180 μl Agencourt AMPure reagent (Beckman Coulter Genomics). They were washed twice with 750 μl EtOH 70% and then resuspended in 100 μl 0.1 X TE.

The qRT-PCR reaction and analysis were performed as described before, using 4 μl of DNA sample in 20 μl PCR reaction and the primers listed in Table 2.4. Input samples were diluted 1:10. For each ChIP analysis, an IgG antibody has been used as control for non specific binding.

For c-Fos and c-Jun ChIP assays, primers were designed in order to span the NFAT/AP-1 site GM420 [276]; in MSK1 and NF-κB ChIPs, primers are spanning the κb site at GM220 [281]. Finally, for analysis at histone modifications analysis, primers were designed at the edge of the DHS, spanning the region between positions 600 and 717 of the Bgl II fragment spanning the GM-CSF enhancer, in the proximity of a positioned nucleosome referred to as N3, and were indicated as GM-N3. Data were normalised to either IVL or Chr18, two gene desert regions. A schematic representation of the GM-CSF enhancer, including the position of the primers, is shown in Figure 2.5.

Table 2.3 ***List of antibodies used in ChIP assays***

Antibody	*Catalogue number*	*Company*
Normal Rabbit IgG	12-370	Merck Millipore
p300 (C-20)	sc-585	Santa Cruz Biotech.
MSK1 (H-65)	sc-25417	Santa Cruz Biotech.
c-Fos (H-125)	sc-7202X	Santa Cruz Biotech.
c-Jun (H-79)	sc-1694X	Santa Cruz Biotech.
NF-kB p65	ab7970	Abcam
Histone H3	ab1791	Abcam
Acetyl-Histone H3 (Lys27)	07-360	Millipore

Table 2.4 ***List of Real time PCR primers used in ChIP assays***

Primer name	*Sequence 5'-3'*
GM-CSF enhancer (GM420) Fw	GGAGCCCCTGAGTCAGCAT
GM-CSF enhancer (GM420) Rev	CATGACACAGGCAGGCATTC
GM-CSF enhancer (GM-N3) Fw	CTTGCCCATCTGTTATGTCC
GM-CSF enhancer (GM-N3) Rev	AGCGGTACATGTCTGTGTGG
GM-CSF enhancer (GM220) Fw	GGTGGACACGCATAGGAAAC
GM-CSF enhancer (GM220) Rev	ATGGGTGGTATGACCCCTCT
IVL Fw	GCCGTGCTTTGGAGTTCTTA
IVL Rev	CCTCTGCTGCTGCCACTT
Chr18 Fw	ACTCCCCTTTCATGCTTCTG
Chr18 Rev	AGGTCCCAGGACATATCCATT

Figure 2.5 ***Schematic view of the GM-CSF enhancer, including the position of the primers used in ChIP assays***

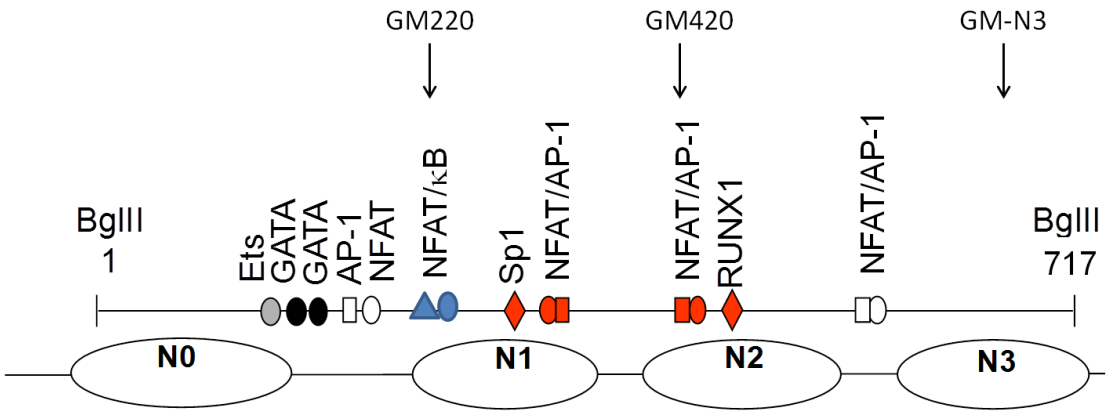

The diagram shows the Bgl II fragment which defines the GM-CSF enhancer, including the location of the binding sites for the different transcription factors. Arrows indicate the region amplified by the primers used in ChIP-Real Time PCR assays.

3. RESULTS

3.1 The NFAT inhibitor 11R-VIVIT doesn't reduce the PMA/I-induced GM-CSF mRNA levels and chromatin remodelling at the GM-CSF enhancer

GM-CSF has been demonstrated to be produced by AML blasts thus supporting their growth and proliferation [259-261]. The aim of this study is to understand the mechanism by which GM-CSF gene is expressed and regulated in an AML model, focusing especially on the signalling pathways involved in its regulation. However, before studying GM-CSF gene regulation in pathological conditions such as AML, I decided to first study it in T blast cells, which physiologically produce GM-CSF when activated. It has been already demonstrated that, beyond TCR activation, treatment with phorbol myristate acetate (PMA) and calcium ionophore A23187 (I), which activate PKC and the Ca^{2+}-dependent signal pathways respectively, can induce GM-CSF gene expression in T blast cells [274]. In fact, the induction of GM-CSF gene expression in T cells is the result of both a Ca^{2+}-dependent signal pathway and a kinase signal pathway. Ca^{2+} activates calcineurin, which interacts with and dephosphorylates NFAT. This dephosphorylation allows NFAT to enter the nucleus and bind DNA, promoting the transcription of several genes, including GM-CSF. Alternatively, PKC activates several specific kinase pathways, such as NF-κB [287] and MAPKs, which have the transcription factor AP-1 as a downstream target [288]. A schematic representation of the signalling pathways cooperating in GM-CSF expression after TCR activation or PMA/I-treatment is shown in Figure 3.1.

Figure 3.1 ***Schematic representation of the signalling pathways cooperating in GM-CSF gene expression after TCR activation or PMA/I-treatment***

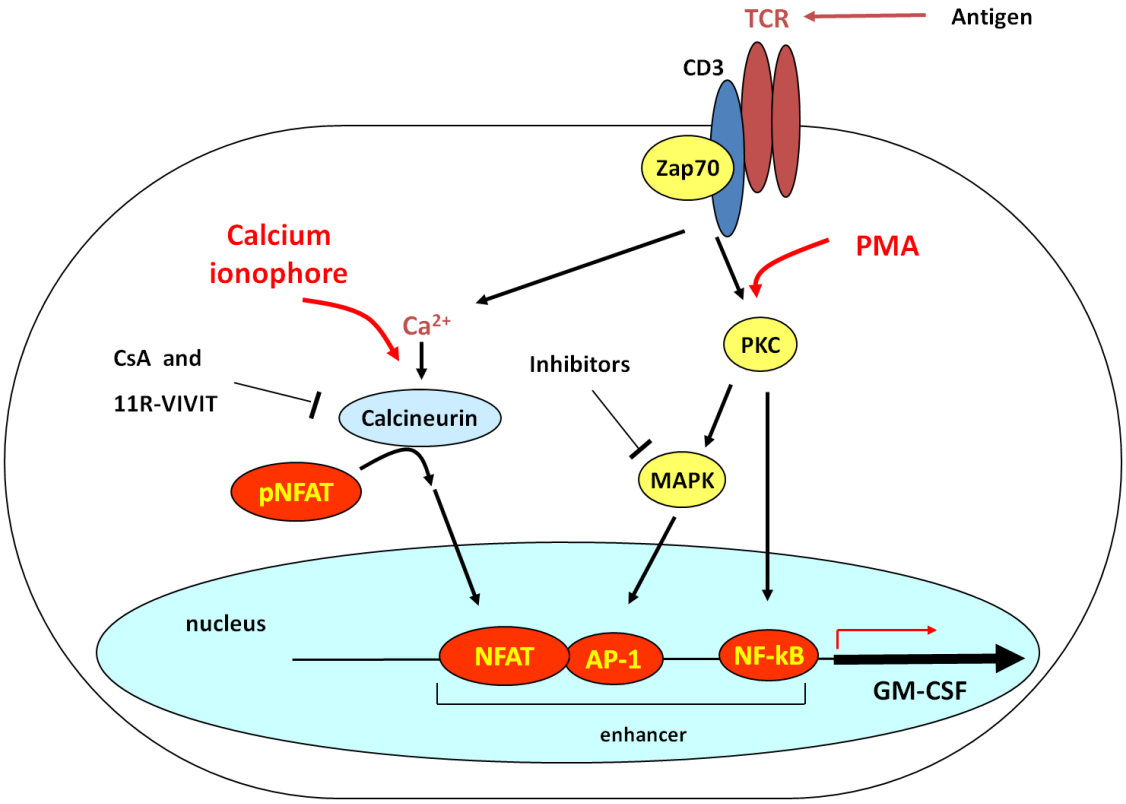

The diagram shows the cooperation between the Ca^{2+} signalling pathway, mediated by NFAT, and the kinase pathways, mediated by AP-1 and NF-κB, in the induction of GM-CSF gene expression. The different pathways can be activated either by TCR antigen stimulation or with phorbol myristate and calcium ionophore (PMA/I) treatment (adapted *from a figure made by Peter Cockerill*).

Because it is difficult to reliably obtain uniform batches of human T cells, in this study I used T cells isolated from a well characterised transgenic mouse strain which contains six copies of a 130 kb Age I fragment spanning the entire human IL-3/GM-CSF locus (Figure 3.2A) and produces high levels of IL-3 and GM-CSF following activation. To prepare large quantities of actively dividing T blast cells, I first isolated T cells from the spleen of these mice and I put them in culture in the presence of Concanavalin A (ConA) to activate them to become T blasts. After two days, I removed the ConA and I expanded the cells by culturing them in the presence of mouse recombinant IL-2 for a further three days, before stimulating them with PMA and ionophore A23187 (PMA/I) to induce the production of IL-3 and GM-CSF (Figure 3.2B). Following extraction of the mRNA, I performed a qRT-PCR to measure GM-CSF gene expression. Figure 3.3 shows that PMA/I treatment led to about a 400 fold induction of GM-CSF gene expression in transgenic T blast cells, compared to untreated cells. mRNA levels were normalised using the mouse *GAPDH* gene as an internal control.

Figure 3.2 ***Schematic representation of T cells activation and stimulation***

A

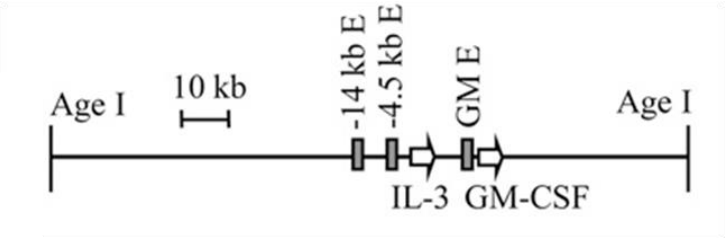

B

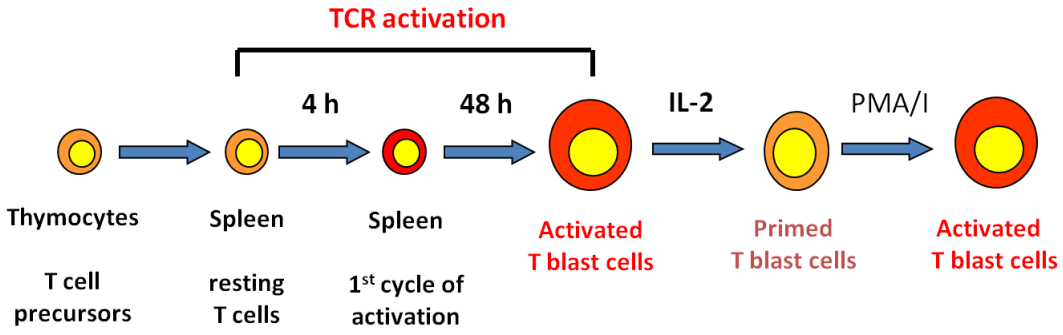

A) Scheme of one of the six Age I fragments spanning the entire IL-3/GM-CSF locus present in the transgenic mice used in this study. B) Representation of the procedure used to isolate T cells from the spleen of transgenic mice and following T cell activation, expansion and stimulation with PMA/I. T cells were cultured in presence of 2 μg of Concanavalin A (ConA) for 2 days to activate them to T blasts. Then T cells were expanded by using 10 U of recombinant mouse IL-2 per ml of culture for a further three days at a density of 0.5 X 10^6 to 1.5 X 10^6. Finally, I stimulated them for 4 h with 20 ng/ml PMA and 2 μM ionophore A23187 (PMA/I) to induce the production of IL-3 and GM-CSF. *Figure made by Peter Cockerill.*

I first confirmed the induction of GM-CSF gene expression by PMA/I treatment (about 1200 times higher than in unstimulated cells) (Figure 3.3), as demonstrated previously by Cockerill et al. [289]. My main aim, however, was to study the role of the Ca^{2+} signalling pathway and other kinase pathways in its regulation. To do this, I used specific inhibitors in order to interfere with these pathways.

I first focused on the Ca^{2+}-dependent pathway involved in GM-CSF activation and I tested the calcineurin inhibitor Cyclosporin A (CsA) and the NFAT inhibitor 11R-VIVIT, using concentrations previously described in the literature [274, 290, 291]. I pretreated the cells for 1 h with CsA and 11R-VIVIT before stimulating them for 4 h with PMA and ionophore A23187 (PMA/I). Figure 3.3 shows that CsA abolished PMA/I-induced GM-CSF gene expression whereas 11R-VIVIT only reduced it by about 20%.

Because it is well established that changes in gene expression are often accompanied by changes in chromatin structure, I next examined the regulation of DHSs in the GM-CSF locus. PMA/I has already been described to induce chromatin remodeling at the GM-CSF enhancer in T blast cells, and this is inhibited by CsA [289]. In order to confirm this result and to test whether the NFAT inhibitor 11R-VIVIT reduced the PMA/I-induced chromatin remodelling at the GM-CSF enhancer, I studied chromatin conformation in a DNase hypersensitive site (DHSs) assay, using Southern blot DNA hybridization analysis.

Figure 3.3 ***Effect of Ca^{2+} signal pathway inhibitors on PMA/I-induced GM-CSF gene expression in transgenic T blast cells***

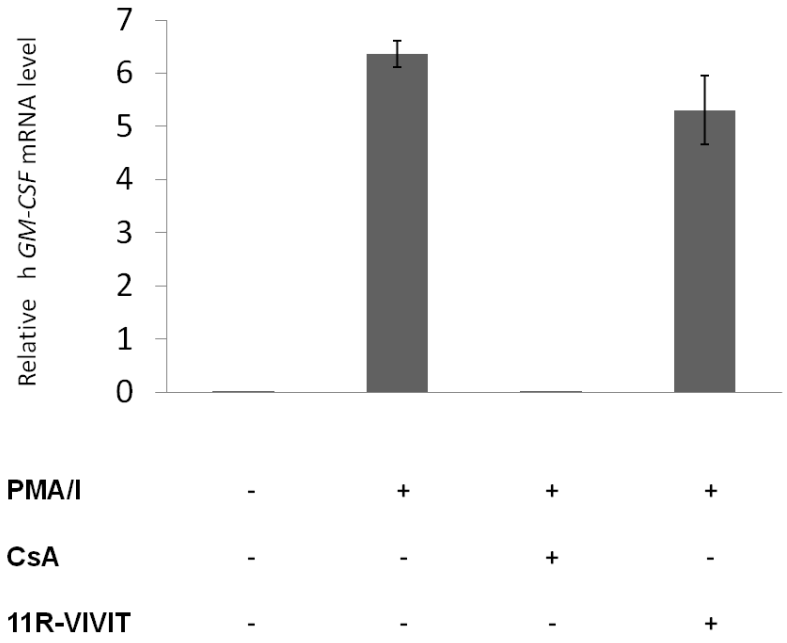

Cells were pre-treated with CsA 0.1 μM and NFAT inhibitor 11R-VIVIT 1 μM for 1 h and then stimulated for 4 h with 20 ng/ml PMA and 2 μM ionophore A23187 (PMA/I). Human GM-CSF mRNA levels were measured by qRT-PCR. Data shown are normalised to mouse GAPDH gene. Each bar represents the average of three technical replicates. Error bars represent SE.

For the DHS analyses, I used DNase I-digested samples from cells either untreated or treated with the same concentration of inhibitors used in the previous qRT-PCR analysis prior to the 4 h PMA/I stimulation. I used increasing concentrations of DNAse I (range 8-12 μg/ml) in order to identify the optimal rate of digestion able to show clearly all the DHSs in the fragment (see Materials and methods). Then, I purified the DNA and digested it with EcoR I. A schematic representation of the strategy is represented in Figure 3.4A. To identify the DHSs within the 9.4 kb EcoR I fragment spanning the GM-CSF enhancer and promoter, I performed an electrophoresis on a 0.8% agarose gel, blotted the DNA onto a Hybond N membrane, and hybridized it to a ^{32}P-labeled 1.4 kb BamHI fragment located at the 5' end of the EcoRI fragment. In Figure 3.4B the highest band detected in the upper blot represents the full length 9.4 kb EcoR I fragment. The lower band indicates DNaseI digestion at the DHS at the -3kb enhancer, whereas the middle one represents cleavage at GM-CSF promoter. PMA/I treatment induced a strong DHS at the enhancer which was strongly inhibited by CsA treatment. In contrast, the NFAT inhibitor 11R-VIVIT does seem not to have a strong effect in reducing chromatin remodelling. The DHS at the promoter appears to be present also in unstimulated cells and showed minimal changes under any of the conditions tested.

As an internal control I reprobed the same membrane with a ^{32}P-labeled 1 kb Bgl I/BamH I fragment, which extends upstream of the EcoR I fragment previously examined. This was in order to identify the constitutive DHSs corresponding to the CTCF insulator region between the GM-CSF and the IL-3 loci. This blot was used as loading control as well as a control for the overall extent of DNase I digestion [246]. Beyond the ubiquitous CTCF sites, in this fragment I also detected the presence of another inducible hypersensitive site

between them, located 4.5 kb downstream of the IL-3 promoter, which was partially inhibited by CsA but not by 11R-VIVIT. A previous study demonstrated that this +4.5 kb DHS can function as an inducible non-coding promoter in Jurkat T cells, but this study did not show that the DHS is partially inhibited by CsA [264].

Undigested genomic DNA was also included as an additional control and showed no additional bands, confirming that the DHS bands defined above were products of the DNase I digestion, and not unrelated or non-specific bands.

These results confirm that the treatment with PMA/I induces chromatin remodelling at the enhancer and this change in chromatin conformation corresponds to an increase of GM-CSF gene expression. The role of the Ca^{2+} signalling pathway in GM-CSF gene regulation is confirmed by the inhibitory effect of CsA, whereas the NFAT inhibitor 11R-VIVIT didn’t show the same strong effect.

A) Strategy of DHS mapping. DHSs within a 9.4 kb EcoR I fragment were identified by using a 1.5 kb BamH I fragment as a probe (P 1). DHSs spanning the insulator region downstream of the IL-3 gene were identified in an EcoR I fragment using a 1.0 kb Bgl I/BamH I fragment as a probe (P 2). R, EcoR I site; B, BamH I site; L, Bgl I site. B) The upper blot shows the mapping of DHSs in a 9.4 kb EcoR I fragment, encompassing the GM-CSF enhancer and promoter. The lower panel represents the same blot after reprobing it to map DHSs in the insulator region between the GM-CSF and the IL-3 loci in the EcoR I fragment. Black triangles indicate increasing concentrations of DNase I. 8, 10 and 12 μg/ml of DNAse I were used for the untreated cells, whereas just 8 and 12 μg/ml were used for the others. Genomic DNA serves as control for DNA not digested with DNAse I. The dashed arrow indicates an inducible DHS at +4.5 kb within the insulator region.

Figure 3.4 ***Mapping of DHSs between the IL-3 and GM-CSF genes in transgenic T blast cells***

A

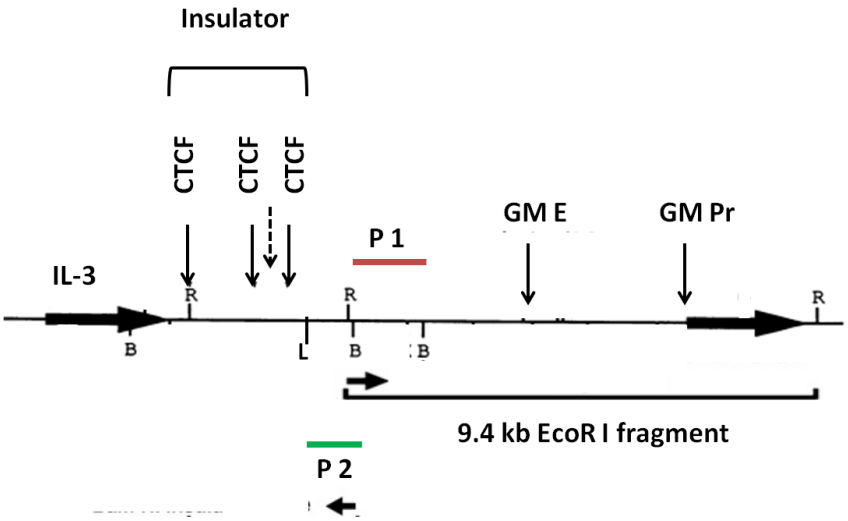

B

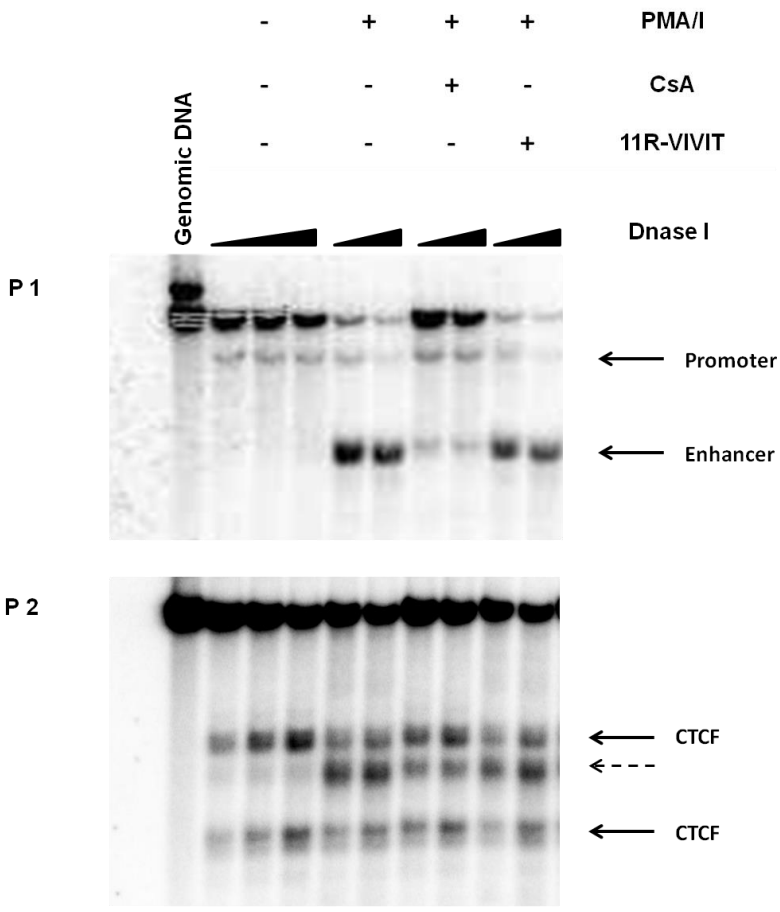

3.2 PMA/I treatment activates MAPK signalling pathways in transgenic T blast cells

GM-CSF gene activation is dependent on the cooperation between a Ca^{2+}-dependent signal pathway and kinase pathways, among which are the MAPK and NF-κB pathways. After investigating the role of the Ca^{2+}-signalling pathway on GM-CSF gene regulation by using its inhibitors CsA and 11R-VIVIT, I decided to focus on the kinase pathways, starting with MAPKs. First of all I studied the effect of PMA/I on the activation of the main MAPK pathways: MEK/ERK, p38 and SAPK/JNK (Figure 3.5). For this purpose, I treated T blast cells with PMA/I for 1 hour and then extracted the whole cell proteins to perform a western blot analysis. I used antibodies against the total forms of ERK1/2, p38 and JNK and also antibodies against their phosphorylated forms, which represent the active form of the pathways. Figure 3.5B shows that ERK1/2 and JNK were strongly activated by PMA/I. In both cases, two bands were visible on the blot. In fact ERK1/2 could be also called p44/42 MAPK, where 44 and 42 are the molecular weights in kDa of ERK1 and ERK2 respectively. A weak level of ERK1/2 activation and p38 is visible on the blot before PMA/I stimulation, maybe due to the fact that cells were cultured in presence of IL-2, which can activate MAPKs. The antibody against SAPK/JNK recognises the p46 and p54 SAPK/JNK isoforms, where 46 and 54 represent the molecular weight in kDa. The level of the total form of the protein didn't change upon PMA/I treatment and it was used as a loading control. Interestingly, the effect of PMA/I on p38 activation wasn't as strong as on ERK and JNK pathways.

Figure 3.5 ***PMA/I treatment phosphorylates MAPK proteins in T blast cells***

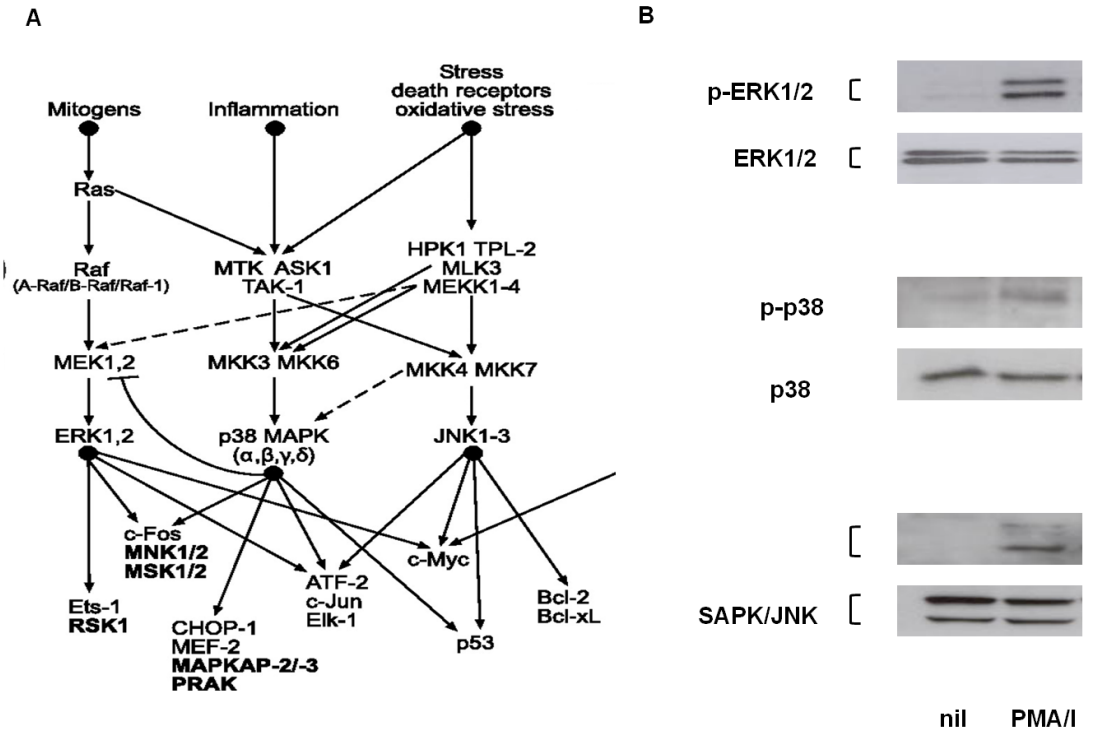

A) Schematic representation of MAPK signal pathways and their crosstalk. Taken from Junttila et al. [159]. B) Western blot of whole-cell lysates prepared from T blast cells before (nil) and after 1h stimulation with 20 ng/ml PMA and 2 µM ionophore A23187 (PMA/I). A representative experiment of two biological replicates is shown.

3.3 MAPK inhibitors decrease PMA/I-induced GM-CSF gene expression and chromatin remodelling at GM-CSF enhancer

After verifying that the three MAPK pathways were activated by PMA/I treatment in T blast cells, I investigated which specific pathways have a role in the PMA/I-induced GM-CSF gene expression and chromatin remodelling. To do this, I tested the effect of MAPK inhibitors and their combinations on PMA/I-treated T blast cells, using concentrations previously described in the literature [292-294]. I used three selective inhibitors: the MEK inhibitor PD98059, which can also block the downstream proteins ERK1/2, the p38 inhibitor SB202190 and the JNK inhibitor SP600125. Pre-treatments of the cells before PMA/I stimulation was for 1 h, after which I performed a Trypan Blue exclusion test to make sure that cell viability was not affected. Before PMA/I treatment, cell viability was about 90%; none of the inhibitors, used singularly or in combination, decreased cell viability to under 80% (data not shown). After 1h pretreatment with MAPK inhibitors, I stimulated the cells for 4 h with PMA/I as described before. To measure GM-CSF gene expression, I extracted the mRNA and converted it to cDNA before performing qRT-PCR analysis (Figure 3.6). The MEK inhibitor, PD98059 (50 μM) and the JNK inhibitor, SP600125 (50 μM) showed only a small effect in reducing PMA/I-induced GM-CSF gene expression (between 10 and 20%), whereas the p38 MAPK inhibitor, SB202190 (25 μM) reduced mRNA level by about 50%. The combination of MEK and JNK inhibitors had about the same effect as the p38 inhibitor alone, whereas the most effective treatment was the combination of MEK and p38 inhibitors. Interestingly, the three inhibitors together were not more effective than the combination of MEK and p38 inhibitors, although the effect was much stronger than all the inhibitors alone.

Figure 3.6 ***Effect of MAPK inhibitors on PMA/I-induced GM-CSF gene expression in transgenic T blast cells***

A

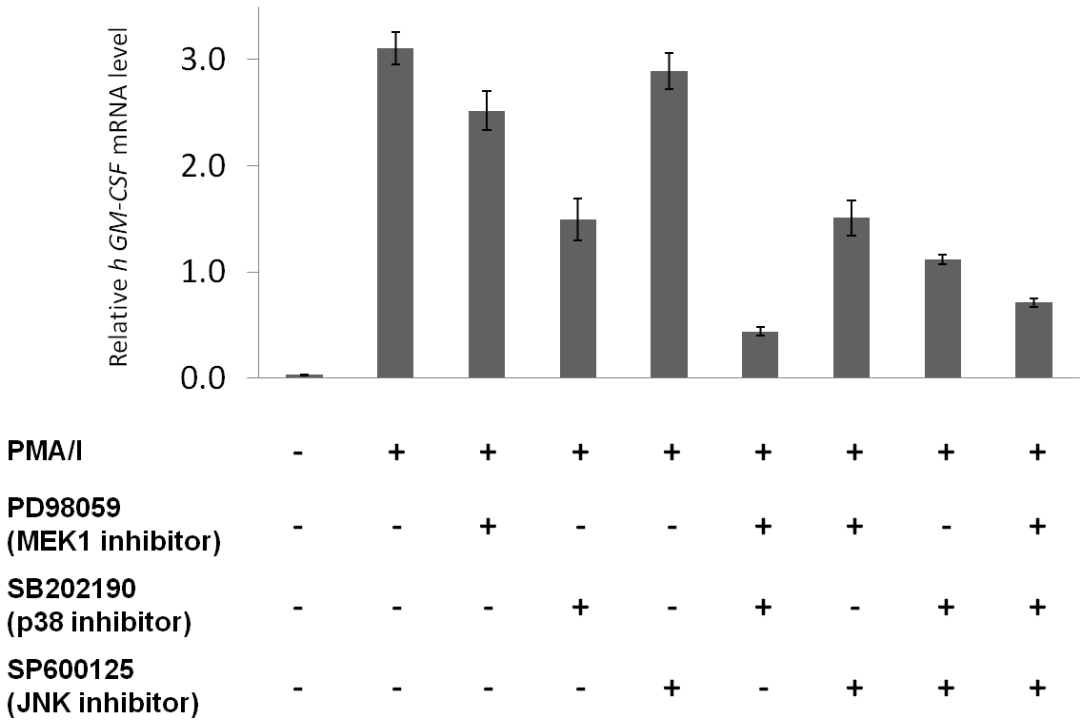

T blast cells were pre-treated for 1 h with MAPK inhibitors, singularly or in combination (MEK inhibitor PD98059 50 μM; p38 inhibitor SB202190 25 μM; JNK inhibitor SP600125 50 μM) and then stimulated for 4h with 20 ng/ml PMA and 2 μM ionophore A23187 (PMA/I). GM-CSF mRNA levels were measured by qRT-PCR. Y-axis shows expression relative to murine GAPDH expression. Error bars represent SE of at least three biological replicates.

Results are expressed as relative to murine GAPDH mRNA expression. In these studies, I used GAPDH as a control housekeeping gene, since none of the treatments above affected its expression as a proportion of total mRNA (data not shown).

Using the same strategy as before (section 3.1), I performed a DHSs analysis using DNase I-digested samples from either untreated cells or cells treated with the same concentration of inhibitors used in the previous RT-PCR analysis prior 4h PMA/I stimulation. I used increasing doses of DNAse I in order to identify the optimal rate of digestion able to clearly detect all the DHSs in the fragment. As before, I ran the digested DNA on a 0.8% agarose gel and I excluded the samples which showed a too high level of DNA digestion (data not shown). Purified DNA was digested with either EcoR I or BamH I. Distinct from the previous DHSs analysis shown in Figure 3.4B, here I used a BamH I fragment to identify the DHSs spanning the insulator region. The data obtained with the EcoR I fragment show that PMA/I treatment induced a strong DHS at the enhancer, whereas the DHS at the promoter appeared to be present also in unstimulated cells. The DHS at the enhancer became weaker after treatment with either the combination of the MEK inhibitor PD98059 and the p38 inhibitor SB202190 or the combination of the two plus the JNK inhibitor SP600125. The reduction of the signal for the DHS at the enhancer by the combinations of inhibitors corresponded well to the reduction of GM-CSF mRNA levels shown in Figure 3.6. Figure 3.7 shows the DHSs between the IL-3 and GM-CSF genes in a BamH I fragment. As observed previously, beyond the three pre-existing CTCF sites, in this fragment I also confirmed the presence of the inducible +4.5 kbDHS located downstream of the IL-3 gene, which was not inhibited by any of the MAPK inhibitors or their combinations.

Overall, these results strongly suggest that the PMA/I-induced GM-CSF gene expression and its chromatin remodelling at the enhancer are dependent on MAPK pathways in T blast cells.

3.4 PMA/I treatment activates MAPK signalling pathways in Jurkat and KG1a leukaemia cell lines

In the above studies, I tested MAPK inhibitors on cultured transgenic mouse T cells, which produce GM-CSF upon TCR activation. I questioned whether these inhibitors would have the same effect on different human leukaemic cell lines, where the GM-CSF enhancer is also entirely inducible upon treatment with PMA/I, as in T blast cells. Bert et al. [281] already demonstrated that the leukaemic T cell line Jurkat and the AML cell line, KG1a show an inducible DHS at the enhancer and this change in chromatin structure is associated with an increase in GM-CSF gene expression. Moreover, AML blast cells have been demonstrated to produce GM-CSF and its production supports blast cell growth and proliferation [259-261].

Mapping of DHSs in a 9.4 kb EcoR I fragment encompassing the GM-CSF enhancer and promoter. Mapping of DHSs in a 4.6 kb BamH I fragment downstream of the IL3 gene showing three constitutive CTCF sites plus one inducible DHS (dashed arrow) located at +4.5 kb relative to the IL-3 gene. To perform both Southern blots, T blasts were pre-treated for 1 h with MAPK inhibitors, singularly or in combination (MEK inhibitor, PD98059 50 μM; p38 inhibitor, SB202190 25 μM; JNK inhibitor, SP600125 50μM) and then stimulated for 4h with 20 ng/ml PMA and 2 μM ionophore A23187 (PMA/I). Black triangles indicate increasing concentrations of DNase I and genomic DNA is used as control.

Figure 3.7 ***Mapping of DHSs in the region between the IL-3 and the GM-CSF gene in transgenic T blast cells***

EcoR I fragment

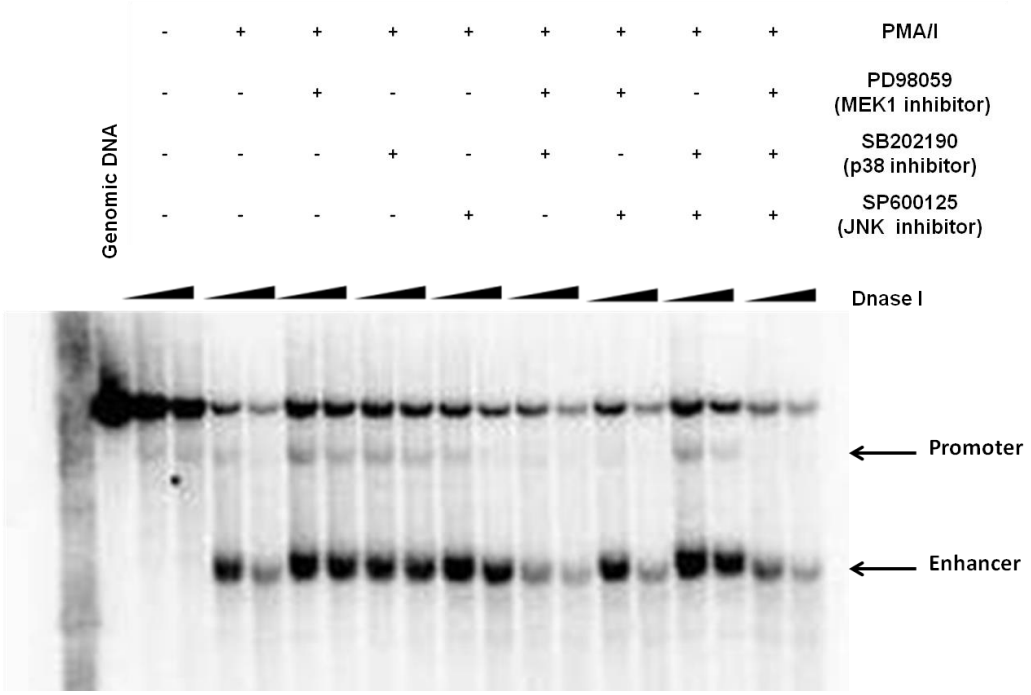

BamH I fragment

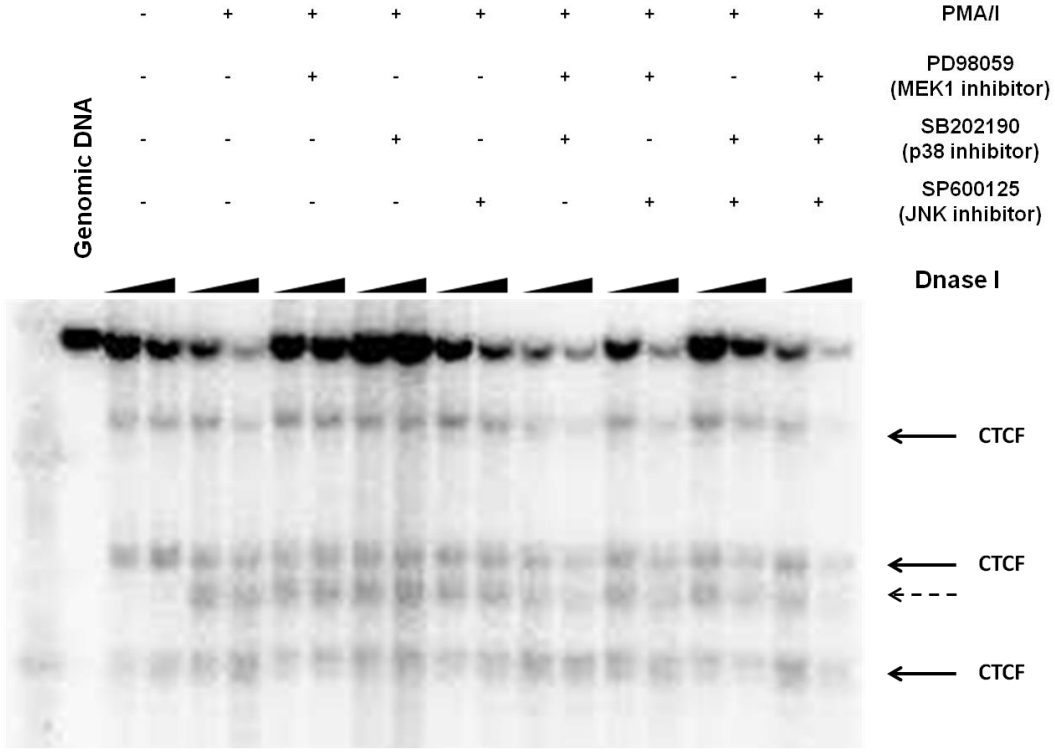

One of my aims is to understand the mechanisms by which GM-CSF is expressed and regulated in a model of AML. Amongst many different AML cell lines, I chose to use KG1a cells as a model because they show an inducible DHS at the GM-CSF enhancer, whereas in other myeloid tumour cell lines, this site is already present prior to PMA/I stimulation [281]. As for T blasts, I tested the phosphorylation of the different MAPK pathways upon treatment with PMA/I. I treated Jurkat and KG1a cells with PMA/I for 1 hour before extracting the whole cell lysate. I performed a western blot, and labelled antibodies against the total and phosphorylated form of ERK1/2, p38 and JNK. As for T blast cells, western blot analysis confirmed that all three MAPK pathways (ERK, p38 and JNK) were activated by PMA/I treatment (Figure 3.8).

Interestingly, quite a strong level of p38 phosphorylation was detected in untreated KG1a (as previously reported by Kale V.P. in 2004 [295]), which was not evident in Jurkat cells. This is not surprising because KG1a is a cancer cell line and many tumour cells show constitutively activation of specific signal pathways. This difference in p38 activation between KG1a and Jurkat should be taken into account in order to explain their possible different response to specific stimuli or treatment.

Figure 3.8 ***PMA/I treatment phosphorylates MAPK proteins in Jurkat and KG1a cell lines***

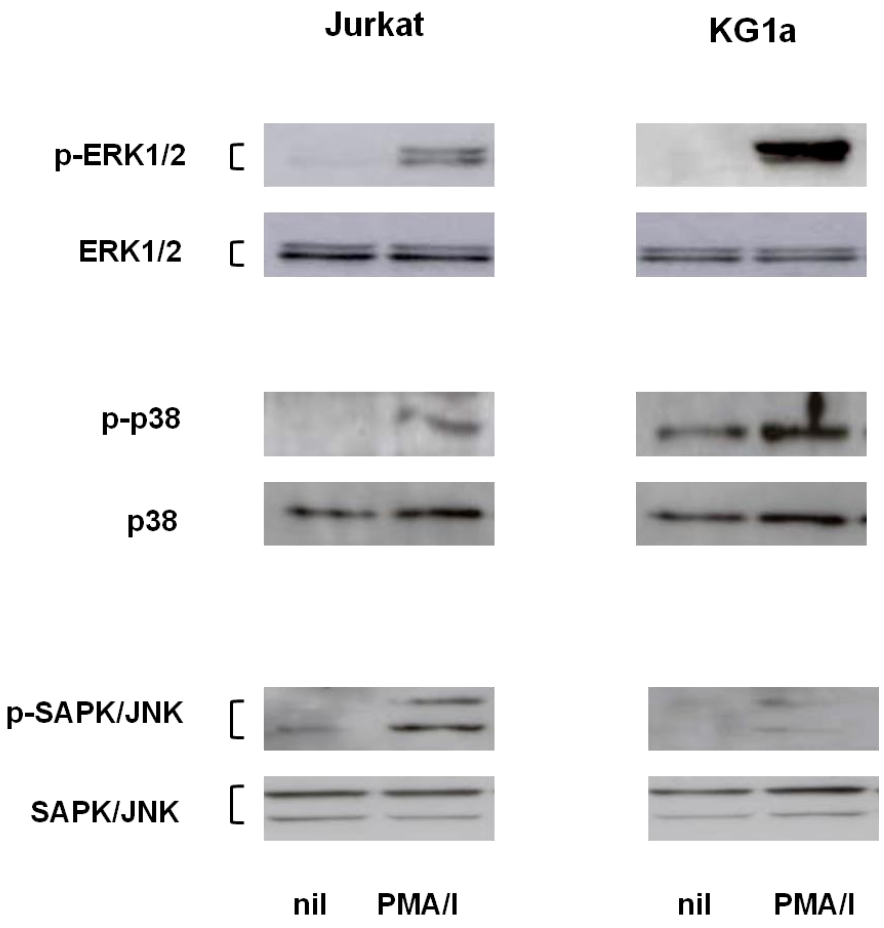

Western blot of whole-cell lysates prepared from Jurkat and KG1a cell lines before (nil) and after 1h stimulation with 20 ng/ml PMA and 2 µM ionophore A23187 (PMA/I). A representative experiment of two biological replicates is shown.

3.5 The MEK inhibitor PD98059 and p38 inhibitor SB202190 inhibit PMA/I-induced GM-CSF gene expression and chromatin remodelling at the GM-CSF enhancer in Jurkat and KG1a leukaemia cell lines

After demonstrating that PMA/I treatment activated MAPK pathways in the leukaemic cell lines Jurkat and KG1a and knowing that both cell lines show an inducible DHS at the GM-CSF enhancer upon PMA/I treatment [281], I decided to test the role of the different MAPK pathways in the PMA/I-induced GM-CSF chromatin remodelling. In order to do this, I pre-treated the cells with MAPK inhibitors before PMA/I stimulation and then performed a DHS analysis.

Since the combination of MEK and p38 inhibitors was the most effective in reducing PMA/I-induced GM-CSF mRNA levels and its chromatin remodelling in T blast cells, I decided to focus on the study ERK/MEK and p38 pathways in these cell lines. After 1 h pre-treatment with the inhibitors, I stimulated the cells for 4 h with PMA/I and then I performed a DHS analysis. I treated the cells with increasing concentrations of DNAse I (range 6-16 μg/ml) in order to achieve a suitable rate of digestion, which varies amongst different cell types. 50 μM of MEK inhibitor, PD98059 and especially 25 μM of p38 MAPK inhibitor, SB202190 alone reduced the DHS at the GM-CSF enhancer induced by PMA/I in KG1a but not in Jurkat cells, whereas the combination of both inhibitors resulted in a loss of the DHS in both cell lines (Figure 3.9A). These results suggest that MAPKs are involved in the regulation of the PMA/I-induced DHS at the GM-CSF enhancer in Jurkat cells and KG1a cells.

The parallel analyses of the same samples using the BamH I fragment confirmed that a similar amount of DNA was loaded because the bands belonging to one sample have similar intensity to the bands belonging to the

other samples; moreover, in most of the treatments a good rate of digestion was achieved because all the DHSs are clearly visible. Interestingly, the inducible DHS located 4.5 kb downstream of the IL-3 gene, between two of the CTCF sites, seemed to be inhibited by the combination of MAPK inhibitors in KG1a cells. To confirm this result, I repeated the experiment pre-treating the cells just with the combination of MEK and p38 inhibitors. Figure 3.9B shows more clearly that the inducible +4.5 kb DHS disappeared after treatment with the inhibitors in KG1a. Figure 3.9A is not very clear on the Jurkat side, but it seems that the DHS was still present in Jurkat cells, maybe a bit weaker, after the treatment with inhibitors. A further experiment with a stronger overall signal would be needed to confirm its presence.

These data suggest that the IL-3 +4.5 kb DHS is regulated differently in KG1a cells compared to T blast cells. The function of this non-coding promoter element is not known, but it would be interesting to further investigate the role of this DHS in the regulation of the GM-CSF/IL-3 locus.

Figure 3.9 ***Effect of MEK and p38 inhibitors on PMA/I-induced GM-CSF chromatin remodelling in Jurkat and KG1a cells***

A EcoR I fragment

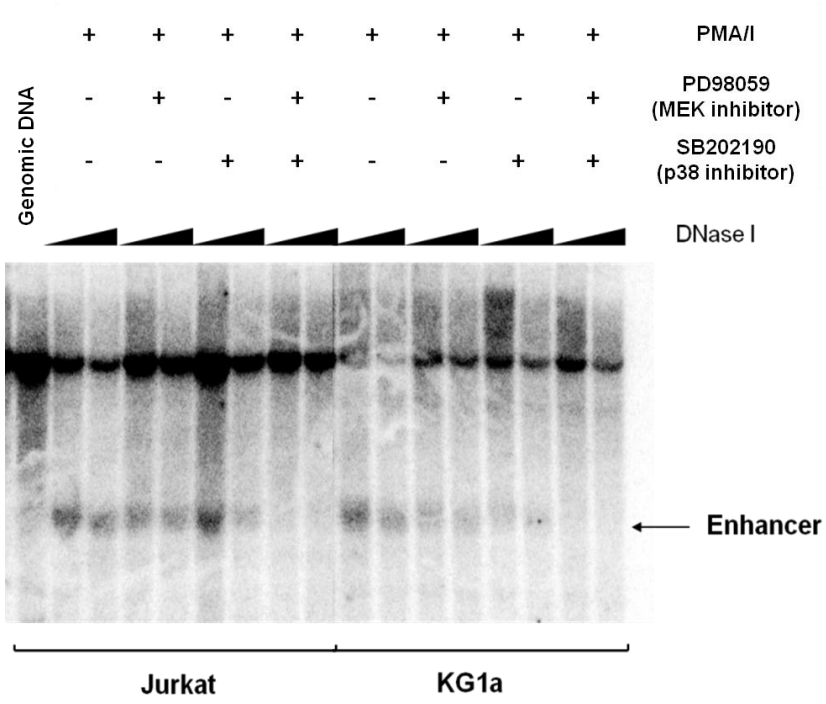

BamH I fragment

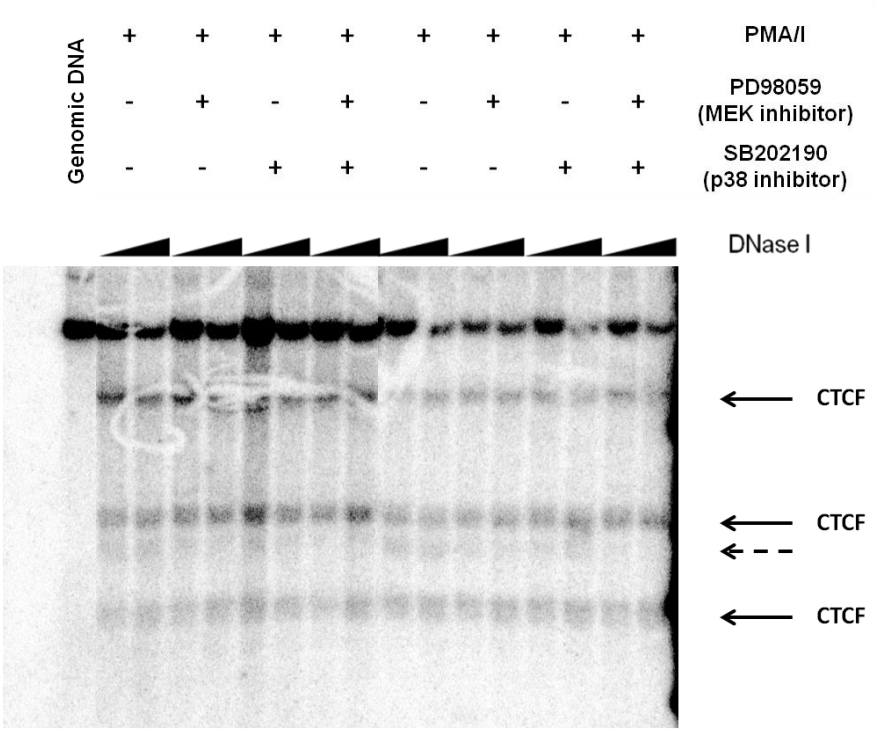

Figure 3.9 ***Effect of MEK and p38 inhibitors on PMA/I-induced GM-CSF chromatin remodelling in Jurkat and KG1a cells***

B BamH I fragment

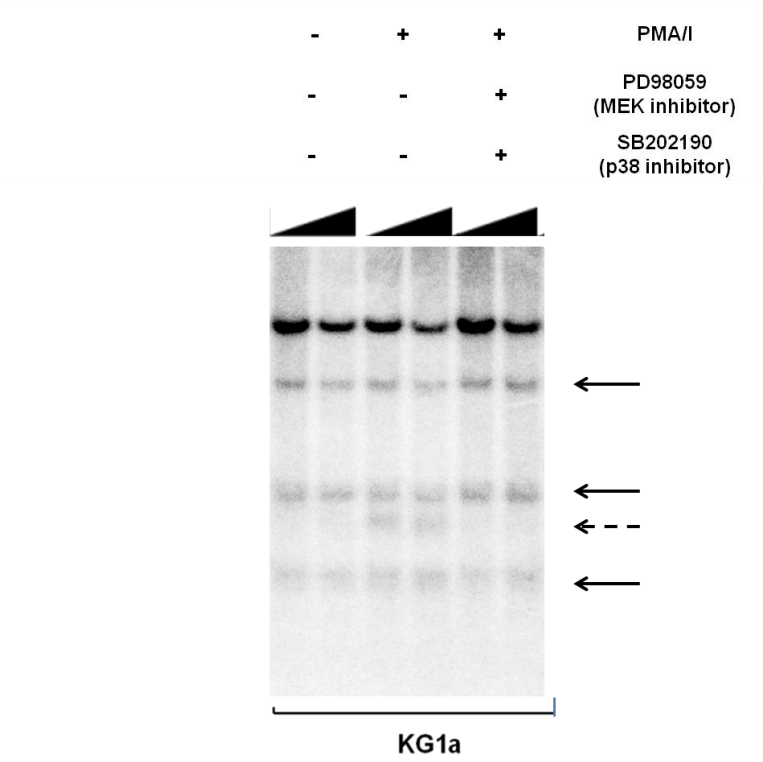

A and B) DHS analyses of permeabilised Jurkat and KG1a cells, before and after treatment with inhibitors in a 9.4 kb EcoR I fragment of the GM-CSF locus (B, upper blot). Mapping of DHSs in a 4.6 kb BamH I fragment downstream of the IL3 gene showing 3 constitutive CTCF sites (B, lower blot and C). The dashed arrow indicates an inducible DHS located 4.5 kb downstream of the IL-3 promoter. For each Southern Blot cells were pre-treated for 1 h with MEK and p38 inhibitors, singularly or in combination (MEK inhibitor PD98059 50 μM; p38 inhibitor SB202190 25 μM) and then stimulated for 4h with 20 ng/ml PMA and 2 μM ionophore A23187 (PMA/I). Black triangles indicate increasing concentrations of DNase I (10-12 μg/ml). In A and B genomic DNA was used as a non-DNase I-digested control DNA sample.

To test whether the loss of DHS at the enhancer was associated with a reduction of GM-CSF mRNA levels, I performed a qRT-PCR analysis. First of all I verified the induction of GM-CSF gene expression after PMA/I in both cell lines. Treatment with PMA/I for 4 h strongly increased GM-CSF mRNA levels in both Jurkat and KG1a cells (Figure 3.10). The level of GM-CSF gene expressed in Jurkat and KG1a cells was about 2% of the level for GAPDH, which was much lower than the level measured above in T blast cells. In fact, cell lines do not always behave in the same way as primary cells and this could explain the difference in GM-CSF expression between the leukaemia cell lines and T blast cells. In both Jurkat and KG1a cells the combination of MEK inhibitor, PD98059 and p38 inhibitor, SB202190 decreased the PMA/I-induced GM-CSF gene expression down to control levels (Figure 3.10A and B). The p38 inhibitor alone (25 μM) reduced the PMA/I-induced GM-CSF gene expression down to the control level in both cell lines. Also the MEK inhibitor (50 μM) had a strong effect, since it reduced the PMA/I-induced GM-CSF gene expression by about 90%. The results obtained in the PCR analysis don't mirror the results from the DHSs analysis, where the single inhibitors were ineffective in reducing the DHS at the enhancer in Jurkat cells. However, the DHS is not a quantitative assay; moreover, the DHS band is weak and it is not easy to detect the changes in intensity. This discrepancy suggests that gene expression and chromatin remodelling are regulated via distinct mechanisms in Jurkat cells. This may indicate that the single inhibitors are sufficient to inhibit factors required for transcription at the promoter, but not for remodelling at the enhancer in Jurkat cells.

Figure 3.10 ***Effect of MEK and p38 inhibitors on PMA/I-induced GM-CSF gene expression in Jurkat and KG1a cells***

A

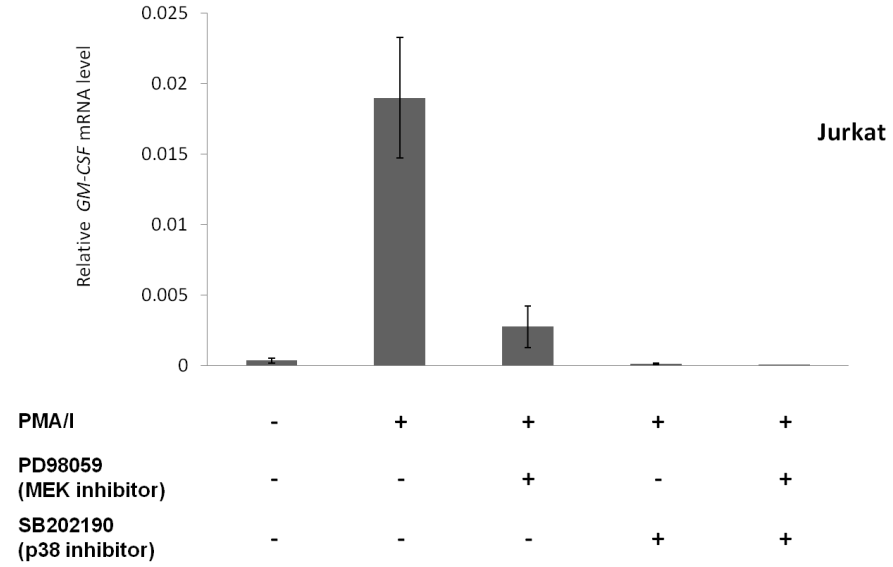

B

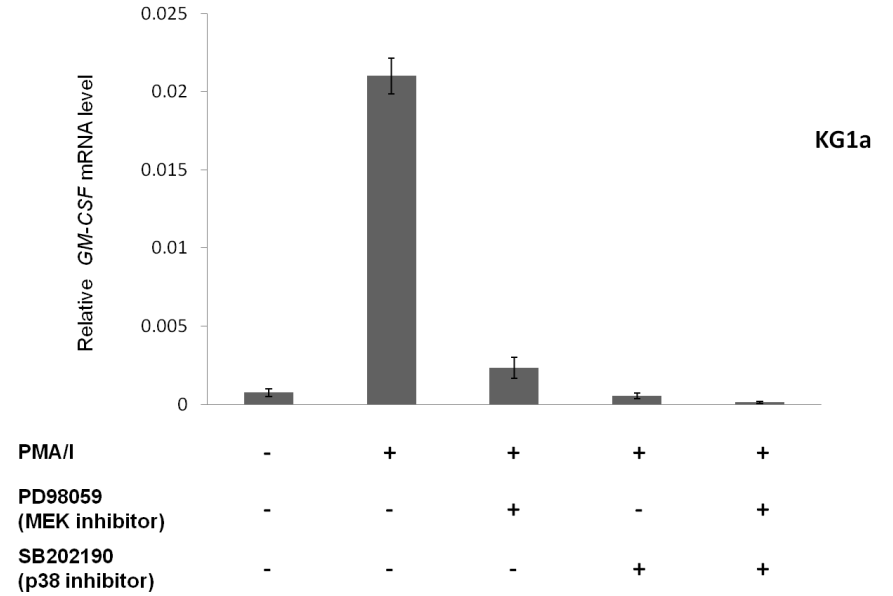

Effect of MEK and p38 inhibitors on PMA/I-induced GM-CSF mRNA levels in Jurkat (A) and KG1a cells (B). The analysis was performed by qRT-PCR. Treatments and concentrations are as above. The Y-axis shows expression relative to human GAPDH expression. Each bar represents the average of least three independent experiments. Error bars represent SE.

3.6 Two alternative MEK and p38 inhibitors (U0126 and SB203580) reduce the PMA/I-induced GM-CSF gene expression in Jurkat and KG1a cells

To test whether the effect shown by the inhibitors on PMA/I-induced GM-CSF gene expression was specifically related to MAPKs inhibition and not to a non specific effect on other pathways, I decided to test two alternative MEK and p38 inhibitors (U0126 and SB203580, respectively). I was particularly interested in finding a possible cooperation or synergism of the two chemicals in reducing the PMA/I-induced GM-CSF gene expression, as was seen with PD98059 and SB202190. To this end, I treated Jurkat and KG1a cells with increasing concentrations of both U0126 and SB203580 (1-10 μM) for 1 hour, before stimulating the cells with PMA and ionophore A23187 for 4 h. Then I extracted the mRNA and I evaluated the effect of the inhibitors on the PMA/I-induced GM-CSF gene expression by qRT-PCR (data not shown). I selected the doses which reduced GM-CSF gene expression by less than 50% and used these in combination. In Jurkat cells 1 μM U0126 (MEK inhibitor) and 0.5 μM SB203580 (p38 inhibitor) decreased PMA/I-induced GM-CSF expression by 40% and 35%, whereas their combination slightly decreased GM-CSF gene expression compared to the single inhibitors. In fact the combination of U0126 and SB203580 reduced the PMA/I-induced GM-CSF mRNA levels by about 60% (additive effect) (Figure 3.11A).

The effect of the two inhibitors together was more pronounced in KG1a cells. In fact the combination of 1.5 μM U0126 and 5 μM SB203580 reduced the PMA/I-induced GM-CSF mRNA levels by around 80%, whereas the single inhibitors reduced it by 35% and 10% respectively (synergistic effect). The combination of U0126 and SB203580 showed a more synergistic effect than the

PD98059/SB202190 combination in KG1a cells. In fact both 10 μM PD98059 and 5 μM SB202190 reduced PMA/I-induced GM-CSF gene expression by around 30-35%, whereas the combination decreased it by around 55% (Figure 3.11B). Interestingly, U0126 was effective at lower doses than the MEK inhibitor PD98059. U0126 reduced PMA/I-induced gene expression by around 35% at 1.5 μM, PD98059 led to the same reduction at 10 μM.

These results demonstrate that the effect of the chemicals in reducing PMA/I-induced GM-CSF gene expression is most likely due to a specific inhibition of the MEK/ERK and p38 MAPK pathways.

3.7 MAPK inhibitors selectivity in KG1a cells

Even though the chemicals I used are known as selective inhibitors, they might cross-react with different signal pathways and show non-specific effects, especially at high doses. To test the specificity of the inhibitors on the different MAPK pathways, I performed a Western Blot analysis, testing the effect of the MEK inhibitor PD98059 on p38 phosphorylation and the effect of the p38 inhibitor SB202190 on ERK1/2 phosphorylation in KG1a cells.

Figure 3.12 demonstrates that increasing concentrations (1-25 μM) of MEK inhibitor do not reduce PMA/I-induced p38 phosphorylation; likewise, the p38 inhibitor (used at concentrations between 10 and 50 μM) does not reduce PMA/I-induced ERK 1/2 phosphorylation. By contrast, small doses of SB202190 (1 μM) activated the MEK/ERK pathway, increasing ERK1/2 phosphorylation level by more than 100%, as previously reported by Hirosawa and colleagues [296].

Figure 3.11 ***Effect of U0126 and SB203580 inhibitors on Jurkat and KG1a cells***

A

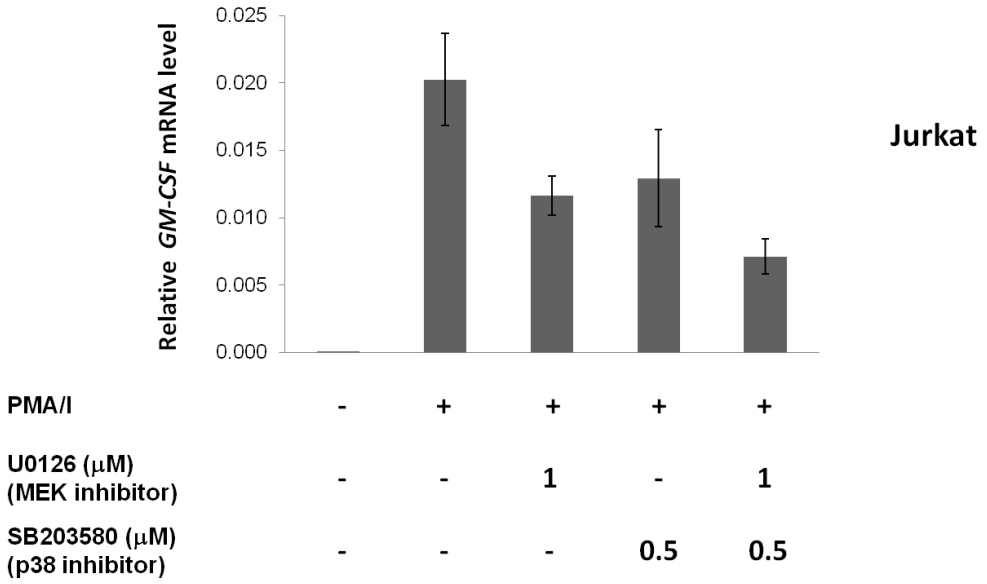

B

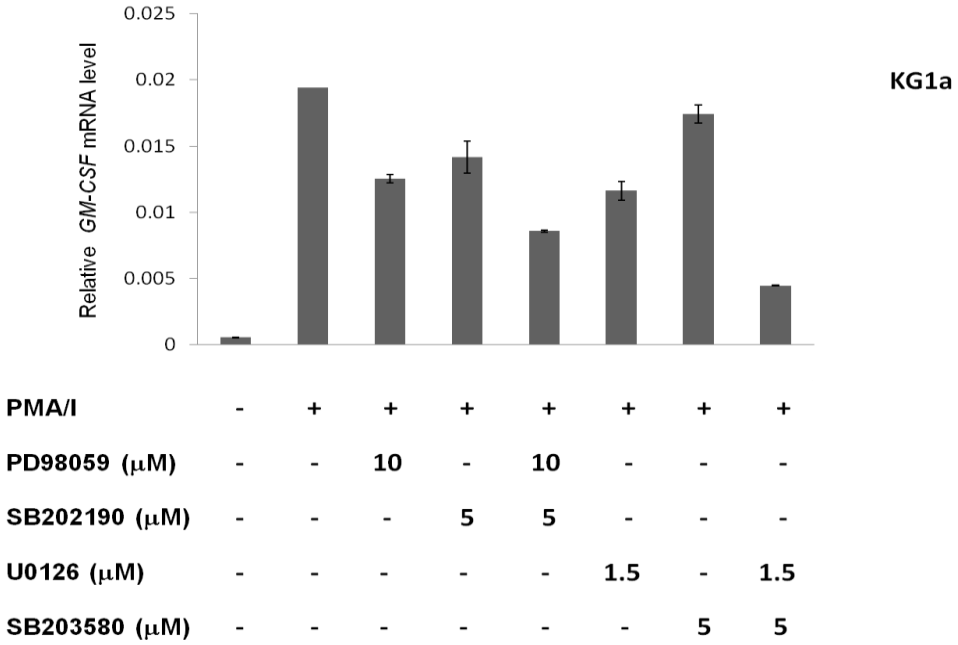

GM-CSF mRNA levels were measured by qRT-PCR in Jurkat (A) and KG1a (B) cells. Cells were pre-treated for 1 h with the indicated concentrations of MAPK inhibitors and then stimulated for 4h with 20 ng/ml PMA and 2 μM ionophore A23187 (PMA/I). The Y-axis shows expression relative to GAPDH gene. Each bar represents the average value of at least three biological replicates. Error bars represent SE.

Figure 3.12 ***MEK and p38 MAPK inhibitors cross-react in KG1a cells***

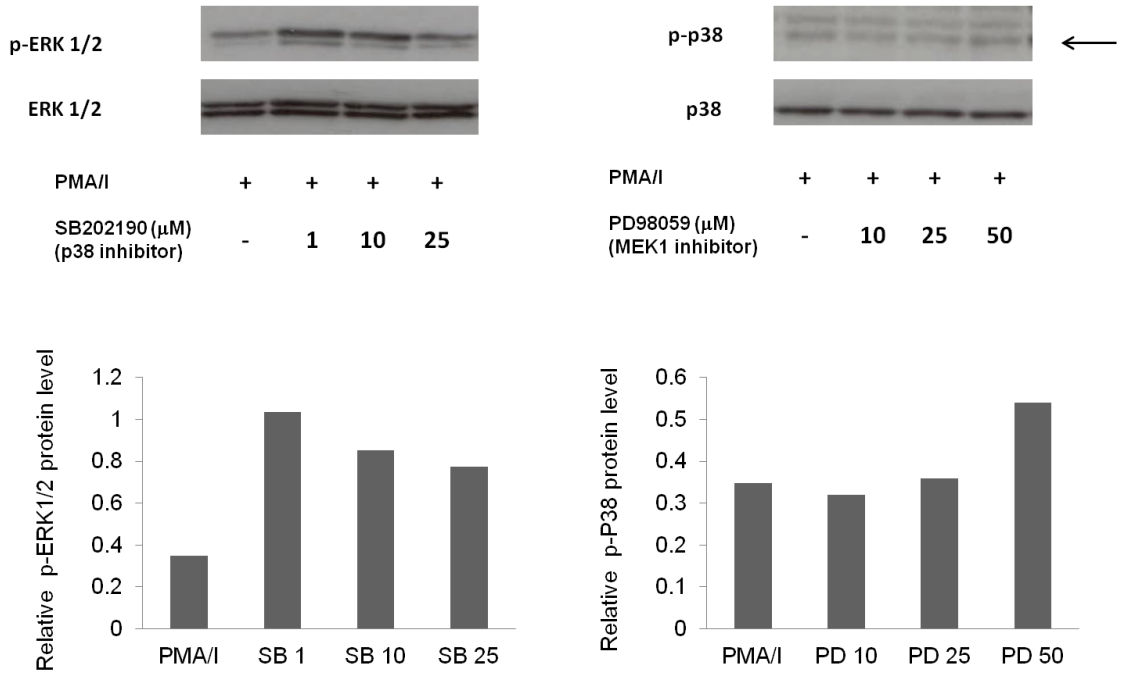

Western blot analysis of whole-cell lysates prepared from KG1a cells after 1h pre-treatment with inhibitors and 1h stimulation with 20 ng/ml PMA and 2 μM ionophore A23187 (PMA/I). A) Levels of PMA/I-induced ERK1/2 phosphorylation were evaluated after treatment with increasing doses of p38 inhibitor (1-25 μM), whereas levels of PMA/I-induced p38 phosphorylation were measured after increasing concentration of MEK inhibitor (10-50 μM). The arrow indicates the specific band for p38. % of phosphorylation represented by the histograms is relative to the level of total protein and is normalised to the % of phosphorylation shown by PMA/I-treated cells. The intensity of the bands and the % of phosphorylation was evaluated by using Image J software. A representative experiment of three biological replicates is shown.

ERK1/2 phosphorylation stayed high also after treatment with 10 μM and 25 μM SB202190. Similarly, MEK inhibitor activated p38 pathway, but just at high doses. In fact 50 μM PD98059 increased p38 phosphorylation by 50% compared to PMA/I-treated cells, whereas 10 and 25 μM PD98059 did not increase the PMA/I-induced p38 phosphorylation levels. These results are not surprising, since there is a complex cross-talk amongst the different MAPK pathways and the inhibition of one pathway may lead to a compensatory activation of a different one. On the contrary, neither PD98059 (10-50 μM) or SB202190 (1-25 μM) increased or decreased the level of phosphorylation of SAPK/JNK induced by PMA/I (Figure 3.13). However, in all these blots the untreated control is missing. An untreated control would have been essential to proof that the stimulation worked.

These results confirmed a strong interconnection between the MAPK pathways, especially between the MEK/ERK and the p38 pathways in KG1a cells and caution should be used when dealing with inhibitors, especially at high doses**.**

3.8 siRNA-mediated knockdown of ERK1/2 and p38 decreases GM-CSF mRNA level

Since I have already demonstrated that selective MAPK inhibitors could affect other MAPK pathways in a non specific manner, I wanted to verify that the results shown by the inhibitors on GM-CSF gene expression were specifically due to the inhibition of ERK1/2 and p38. In order to do this, I decided to measure the PMA/I-induced GM-CSF gene expression after knockdown of specific ERK1/2 and p38 proteins. The most targeted method to knockdown the MAPK proteins makes use of specific small-interfering RNAs (siRNAs).

Figure 3.13 ***MEK and p38 inhibitors don't cross-react with JNK pathway in KG1a cells***

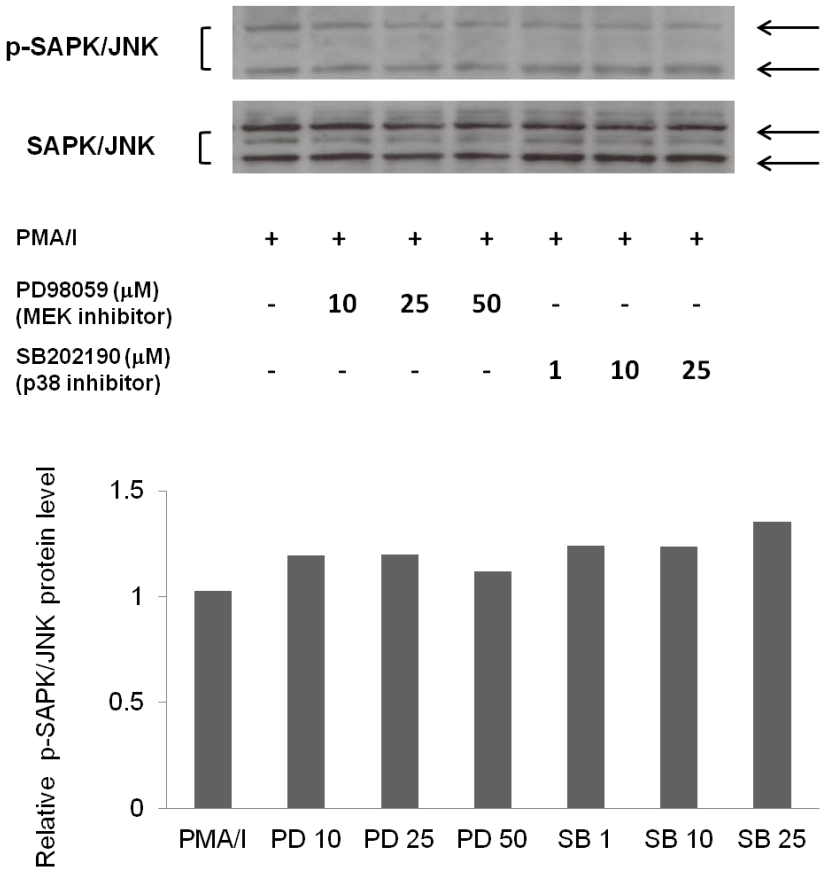

Western blot analysis of whole-cell lysates prepared from KG1a cells after 1h pre-treatment with inhibitors and 1h stimulation with 20 ng/ml PMA and 2 μM ionophore A23187 (PMA/I). PMA/I-induced SAPK/JNK phosphorylation levels after treatment with increasing doses of MEK and p38 inhibitors. % of phosphorylation represented by the histograms is relative to the level of total protein and is normalised to the % of phosphorylation shown by PMA/I-treated cells. The intensity of the bands and the % of phosphorylation was evaluated by using Image J software. A representative experiment of three biological replicates is shown.

Jurkat and KG1a cells were transfected via electroporation with either 100 nM universal negative control siRNA (siCTRL), or 100 nM siERK1/2 and sip38. The universal negative control siRNA has no homology to any known mammalian gene and it should have minimal non-specific effects on gene expression. After 48 hours transfection with siRNAs, cells were treated with PMA and ionophore A23187 (PMA/I) for 4 hours and then mRNA was extracted. To test the efficiency of siRNA-mediated knockdown, ERK1 and p38 mRNA levels were measured by qRT-PCR. I decided to first test ERK1 mRNA levels to verify the role of the ERK pathway in GM-CSF gene expression. GM-CFS mRNA levels were measured after verifying ERK1 and p38 significant silencing. In Jurkat cells ERK1 mRNA levels decreased by about 80% compared to siCTRL and this reduction corresponded to a decrease of GM-CSF gene expression by about 50%. Similarly, the reduction of p38 gene expression compared to the siCTRL (about 65%) corresponded to about 25-30% reduction of GM-CSF gene expression (Figure 3.14A). I achieved a similar level of ERK1/2 and p38 gene knockdown in KG1a cells and this resulted in a corresponding reduction of PMA/I-induced GM-CSF gene expression (Figure 3.14B). The effect of MAPK protein knockdown on GM-CSF gene expression was stronger in KG1a than in Jurkat cells, since GM-CSF mRNA levels decreased by about 65% and 50% after ERK1/2 and p38 knockdown compared to siCTRL. The reduction of GM-CSF gene expression after ERK1/2 knockdown was a little more effective than after p38 knockdown, similarly to the results obtained in Jurkat cells. This might be due to a slightly stronger reduction in ERK1 gene expression compared to p38 gene expression.

Figure 3.14 ***ERK1/2 and p38 siRNAs reduce PMA/I-induced GM-CSF mRNA levels in Jurkat cells***

A

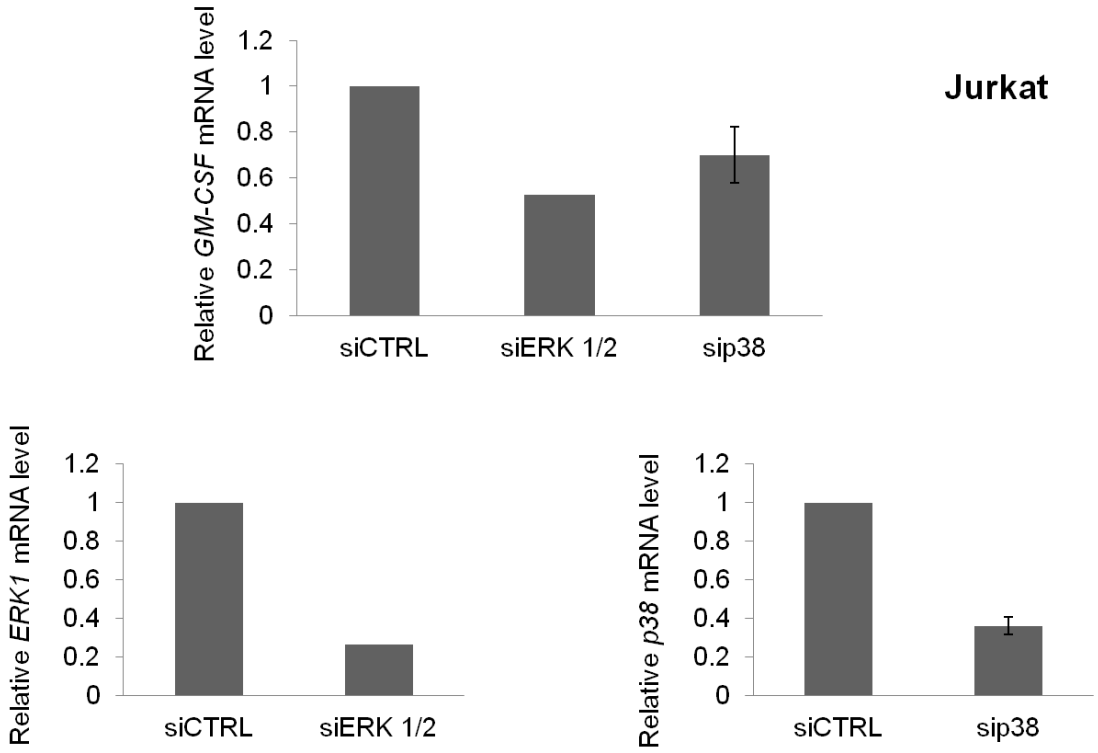

A) Jurkat cells were transfected with either 100 nM negative control siRNA (siCTRL) or 100 nM specific siERK1/2 and sip38; 48 hours after transfection, cells were treated with 20 ng/ml PMA and 2 μM ionophore A23187 (PMA/I) for 4 hours and then mRNA was extracted. GM-CSF mRNA levels, as well as ERK1 and p38 mRNA levels, were measured by qRT-PCR. The Y-axis shows expression normalised to GAPDH gene expression. mRNA levels are relative to siCTRL. Each bar represents the average value of two or three biological replicates. Error bars represent SE. Where error bars are not present values from a representative experiment are shown.

Figure 3.14 ***ERK1/2 and p38 siRNAs reduce PMA/I-induced GM-CSF mRNA levels in KG1a cells***

B

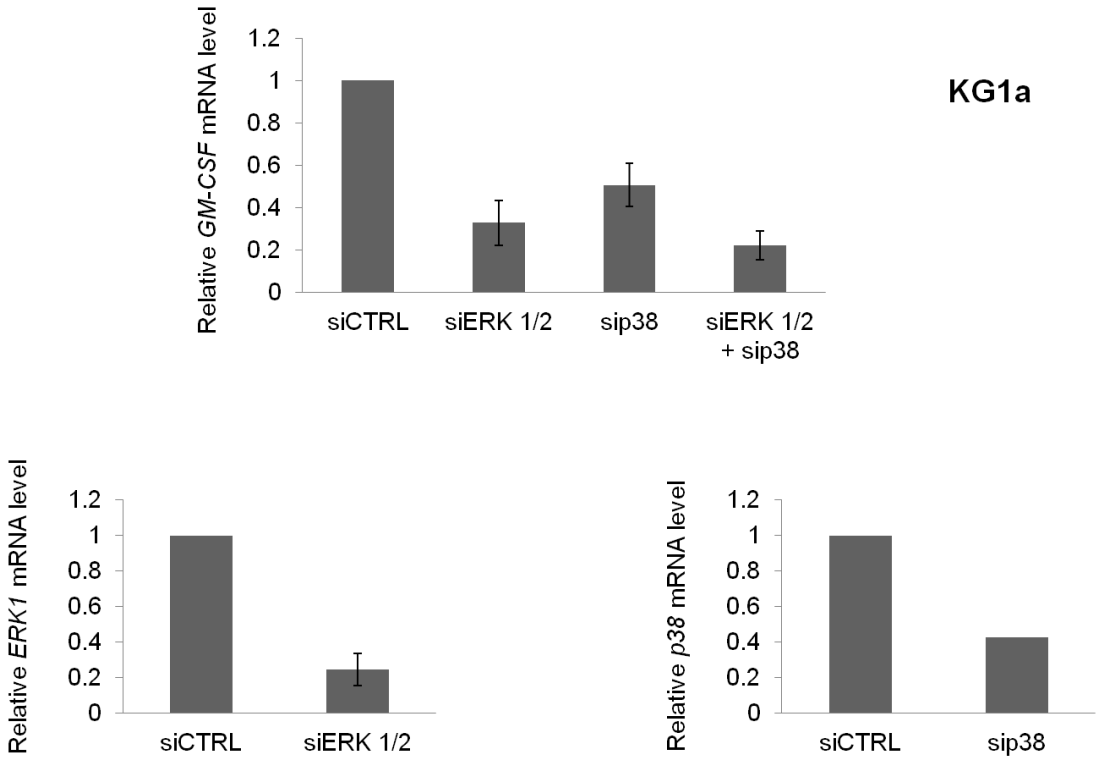

B) KG1a cells were transfected with either 100 nM negative control siRNA (siCTRL) or 100 nM specific siERK1/2 and sip38; after 48 hours from transfection cells were treated with 20 ng/ml PMA and 2 μM ionophore A23187 (PMA/I) for 4 hours and then mRNA was extracted. GM-CSF mRNA levels, as well as ERK1 and p38 mRNA levels, were measured by qRT-PCR. Y-axis shows expression normalised to GAPDH gene expression. mRNA levels are relative to siCTRL. Bars represent the average value of two or three biological replicates. Error bars represent SE. Where error bars are not present values from a representative experiment are shown.

Moreover, the use of both siERK1/2 and p38 at the same time led to a further reduction of PMA/I-induced GM-CSF gene expression compared to the use of single siRNAs in KG1a cells. I didn't achieve 100% knockdown of ERK1 and p38 gene expression but the corresponding reduction in GM-CSF mRNA levels was enough to show a specific role of ERK and p38 pathways in regulating PMA/I-induced GM-CSF gene expression. Maybe an analysis a longer time after transfection or a further transfection with siRNA would have been required to see a better knockdown of ERK1 and p38 mRNA.

Beyond mRNA knockdown, I also wanted to verify ERK1/2 and p38 protein knockdown. To do this, KG1a cells were transfected again via electroporation after 72 hours from the first transfection with either 100 nM siCTRL or specific MAPK siRNAs. Whole cell extracts were analysed by Western blot after one day (after a total of 96 h from the first transfection). Figure 3.15 shows that in KG1a cells ERK1 protein levels were reduced by 90% (the corresponding upper band in the Western Blot is barely visible), whereas ERK2 and p38 protein levels were reduced by around 75% respect to siCTRL. Analysis of the intensity of the bands was performed by using ImageJ software.

Figure 3.15 ***ERK1/2 and p38 siRNAs in KG1a cells***

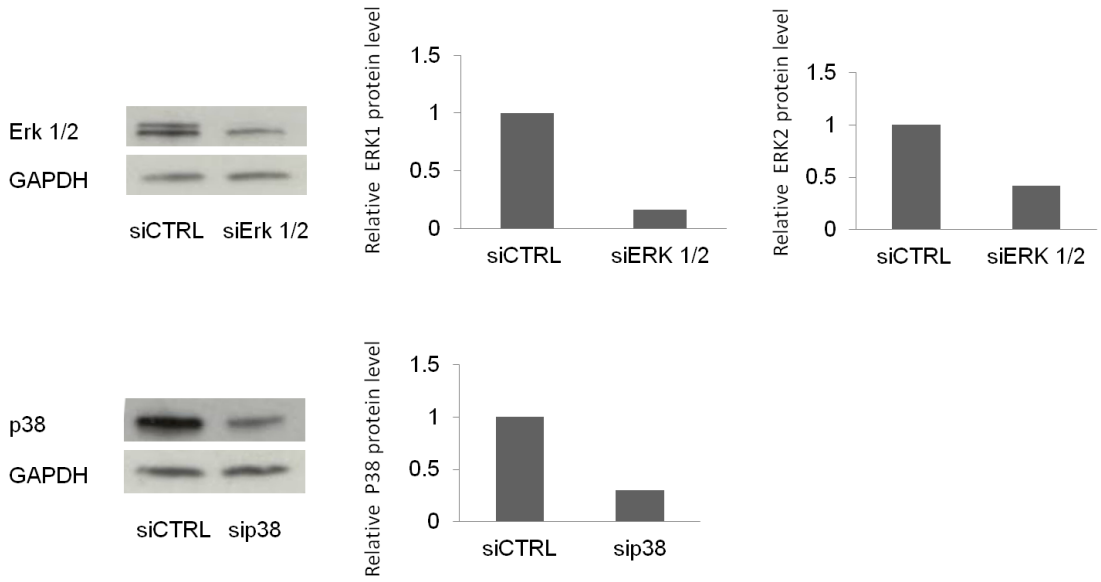

Western blot analysis of whole cell extracts from KG1a cells transfected with either 100 nM siCTRL or specific siMAPK (siERK1/2 or sip38). Cells were transfected via electroporation a second time after 72 hours from the first transfection. After one day (a total of 96 h from the initial transfection), whole cell proteins were extracted and the efficiency of ERK1/2 and p38 knockdown was evaluated. About 30 μg of proteins were loaded. GAPDH was used as loading control. The intensity of the bands was measured by using Image J software. The Y-axis shows the value of protein levels normalised to GAPDH and relative to siCTRL. One representative experiment is shown.

3.9 The JNK inhibitor SP600125 reduces the PMA/I-induced JNK phosphorylation and GM-CSF gene expression in Jurkat and KG1a cells

The reason why I focused on the use of MEK/ERK and p38 inhibitors is because high doses of JNK inhibitor SP600125 did not show any significant effect either in the reduction of PMA/I-induced GM-CSF gene expression or in the inhibition of DHS formation at the enhancer in T blast cells. This didn't exclude a possible effect of SP600125 on Jurkat and KG1a cells. Therefore, I tested the effect of SP600125 on the activation of JNK pathway and on its downstream protein c-Jun after treatment with PMA/I. The transcriptional activity of c-Jun is regulated by phosphorylation at Ser63 and Ser73 through SAPK/JNK [297]. c-Jun is preferably a JNK target, although it can be phosphorylated and activated also by ERK [298]. Therefore, I decided to measure the phosphorylation of c-Jun at Ser73 to verify the activation of JNK and/or ERK pathway in Jurkat and KG1a cells after treatment with PMA/I. For this purpose, I pre-treated both cell lines with 50 μM of the JNK inhibitor SP600125 for 1 hour and then I stimulated them for 2 hours with PMA/I. Figure 3.16 shows that PMA/I strongly increased both c-Jun protein levels and its phosphorylation at Ser73. In both cell lines, SP600125 50 μM, as well as the MEK inhibitor, PD90589 50 μM, greatly reduced c-Jun protein levels and completely abolished the PMA/I-induced c-Jun phosphorylation at Ser73 (just a weak band can be detected after PD98059 in KG1a cells). These results demonstrated that PMA/I treatment induces JNK activation in both Jurkat and KG1a cells and that the phosphorylation of c-Jun at Ser73 is dependent on both JNK and ERK MAPK pathways.

Figure 3.16 ***Effect of the MEK and JNK inhibitors on the PMA/I-induced c-Jun phosphorylation in Jurkat and KG1a cells***

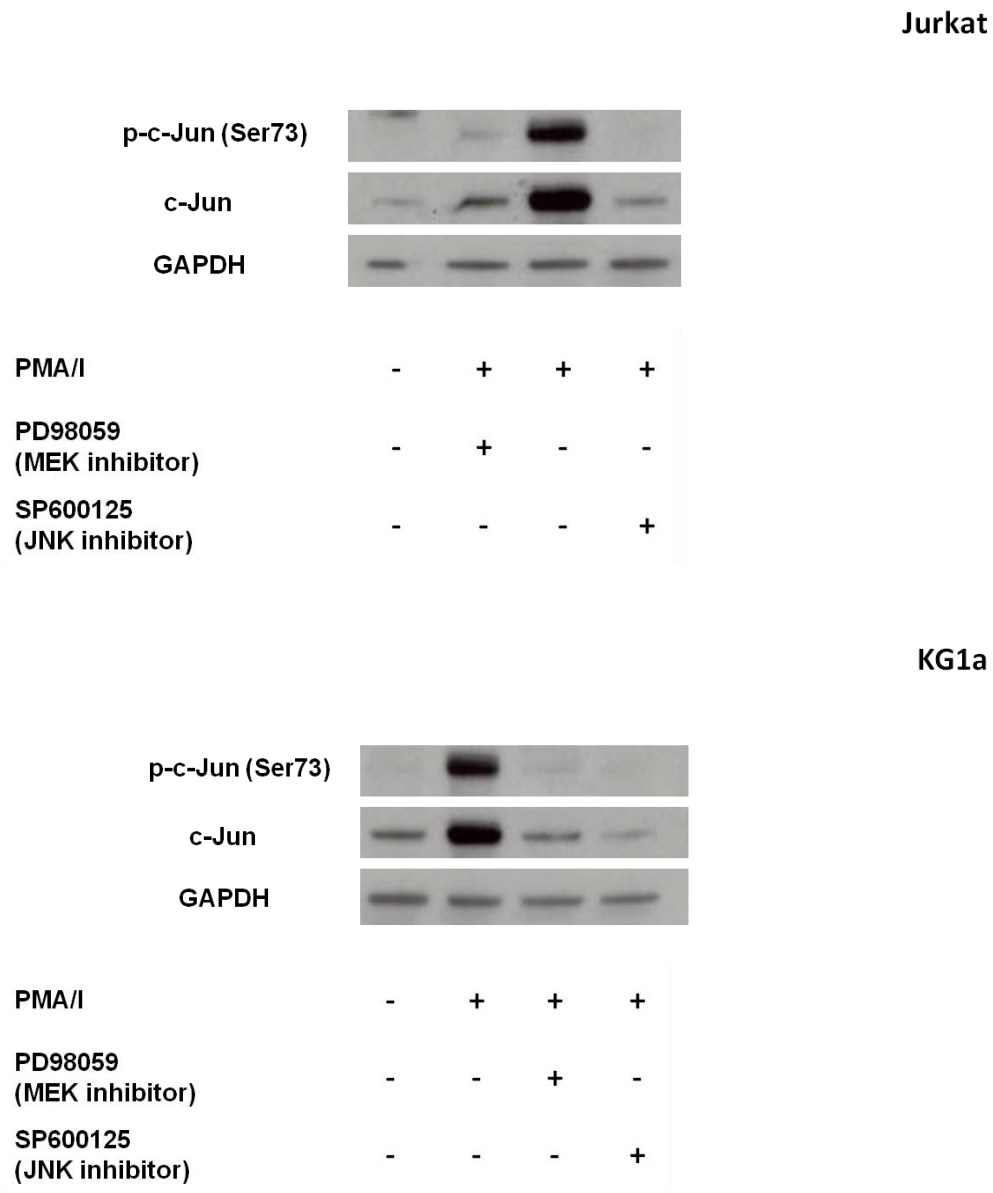

Effect of the JNK inhibitor, SP600125 on PMA/I-induced c-Jun phosphorylation at Ser73. Western blot analysis of whole-cell lysates prepared from Jurkat and KG1a cells after 1h pre-treatment with either the MEK inhibitor PD98059 (50 μM) or the JNK inhibitor, SP600125 (50 μM) and following 2h stimulation with 20 ng/ml PMA and 2 μM ionophore A23187 (PMA/I). A representative experiment of two biological replicates is shown.

Then, to test whether JNK activation was involved in the PMA/I-induced GM-CSF gene expression, I measured GM-CSF mRNA levels in both cell lines after treatment with the JNK inhibitor, SP600125. I pre-treated both cell lines for 1 h with increasing concentrations of SP600125 (5-50 μM) and then I stimulated them for 4h PMA/I. In Jurkat cells, both 5 and 20 μM SP600125 reduced PMA/I-induced GM-CSF gene expression by about 25%, whereas 50 μM decreased expression by around 90%. In KG1a cells, the JNK inhibitor was ineffective at 5 μM, whereas it reduced PMA/I-induced GM-CSF gene expression by 70% and 85% at 20 and 50 μM respectively (Figure 3.17).

These results show that JNK pathway seems to be involved in the regulation of GM-CSF gene expression induced by PMA/I in Jurkat and KG1a cell lines. Not surprisingly these results showed a different behaviour between primary cells (T blast cells) and cell lines, since in T blast cells 50 μM of the JNK inhibitor SP600125 didn't have more than 10% effect in reducing PMA/I-induced GM-CSF mRNA levels (see Figure 3.6).

3.10 The combination of MEK and p38 inhibitors reduces the PMA/I-induced AP-1 DNA binding in transgenic T blast cells, Jurkat and KG1a cells

So far I have demonstrated that in T blast cells, Jurkat and KG1a cells GM-CSF gene expression is in part dependent on the activation of MAPK pathways. These pathways lead to the activation of transcription factors that can interact with the IL-3/GM-CSF locus, thus inducing chromatin conformational changes as well as gene expression.

Figure 3.17 ***Effect of the JNK inhibitor, SP600125 on the PMA/I-induced GM-CSF expression in Jurkat and KG1a cells***

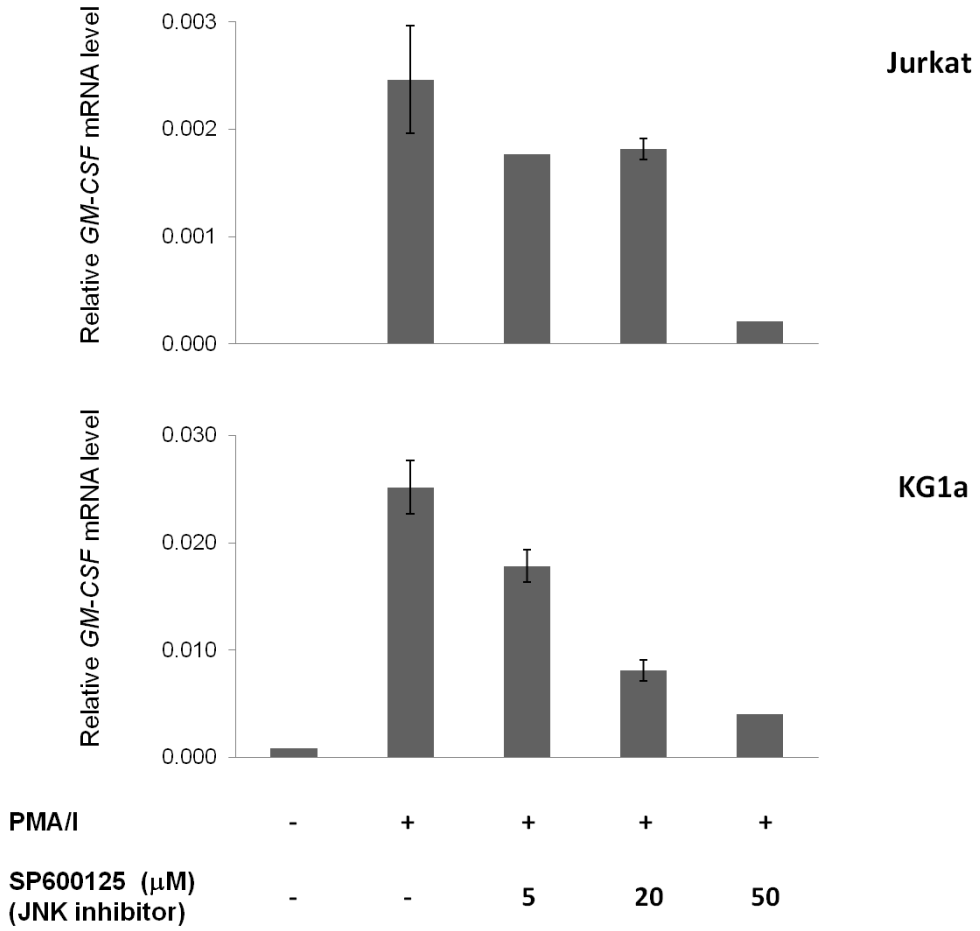

Effect of the JNK inhibitor, SP600125 on PMA/I-induced GM-CSF mRNA levels in Jurkat and KG1a cells. Cells were pre-treated for 1 h with increasing doses of SP600125 (5-50 μM) and then stimulated for 4h with 20 ng/ml PMA and 2 μM ionophore A23187 (PMA/I). The Y-axis shows expression relative to *GAPDH* gene expression. One representative experiment is shown. The bars are the average values of three technical replicates. Error bars represent SE.

One of these transcription factors is the Activating Protein 1 (AP-1). The -3 kb GM-CSF enhancer encompasses three composite NFAT/AP-1 binding sites and two of them have been demonstrated to be essential for the enhancer activity in T cells [276]. To test the AP-1 binding ability to the DNA after PMA/I treatment, I treated the cells for 2 h with PMA/I and prepared the nuclear extracts from treated and untreated cells before performing an Electrophoretic mobility shift assay (EMSA). The EMSA shows the ability of a protein, in this case AP-1, to bind a specific sequence of DNA, in this case an oligonucleotide probe from the Stromelysin gene containing a perfect AP-1 consensus sequence (TGAGTCA).

Figure 3.18 shows that the AP-1 DNA binding activity increased after only 2 h stimulation with PMA/I in T blast cells (A) as well as in Jurkat (B) and KG1a (C) cells. 1 h pre-treatment using a combination of the MEK inhibitor, PD98059 (50 μM) and the p38 inhibitor, SB202190 (25 μM) decreased AP-1 DNA binding activity in T blast cells and Jurkat cells and abolished it in KG1a cells. Treatments with single inhibitors were effective in KG1a cells but not in Jurkat or in T blast cells. Also the level of AP-1 binding in untreated cells was much higher in Jurkat than in KG1a cells.

AP-1 is a homodimer or heterodimer formed of proteins from the Jun family and the Fos family and the closely related activating transcription factors (ATFs), the cyclic AMP response element binding proteins (CREB) and the Maf subfamily [188]. I confirmed the specificity of the AP-1 band in EMSA by using a c-Fos antibody or c-Jun antibodies (supershift) and high concentrations of unlabelled oligo duplex (competitor). In fact the use of a specific antibody not only reduces the intensity of AP-1 binding to the DNA, but its binding to the protein:DNA complex makes the complex migrate with a slower mobility.

Figure 3.18 ***MAPK inhibitors effect on the PMA/I-induced AP-1 DNA binding***

A T blast cells

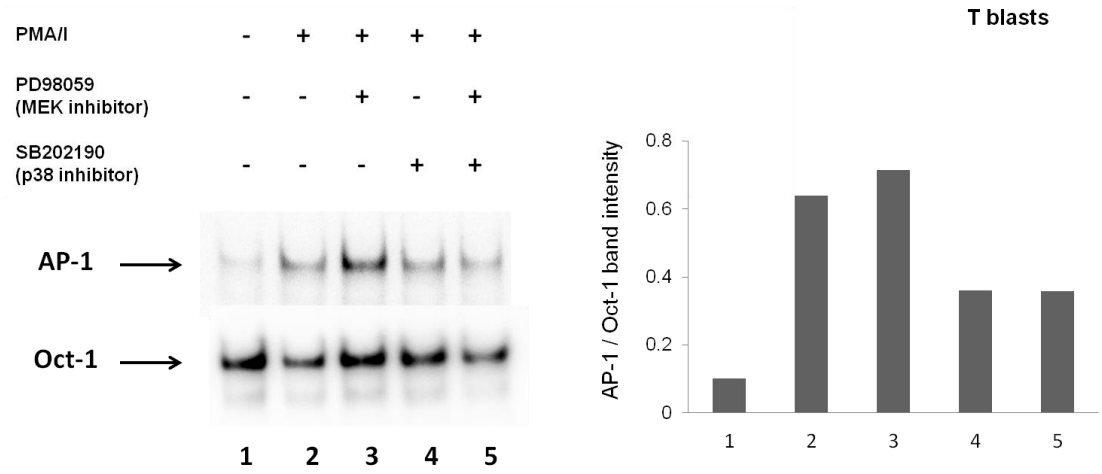

B Jurkat

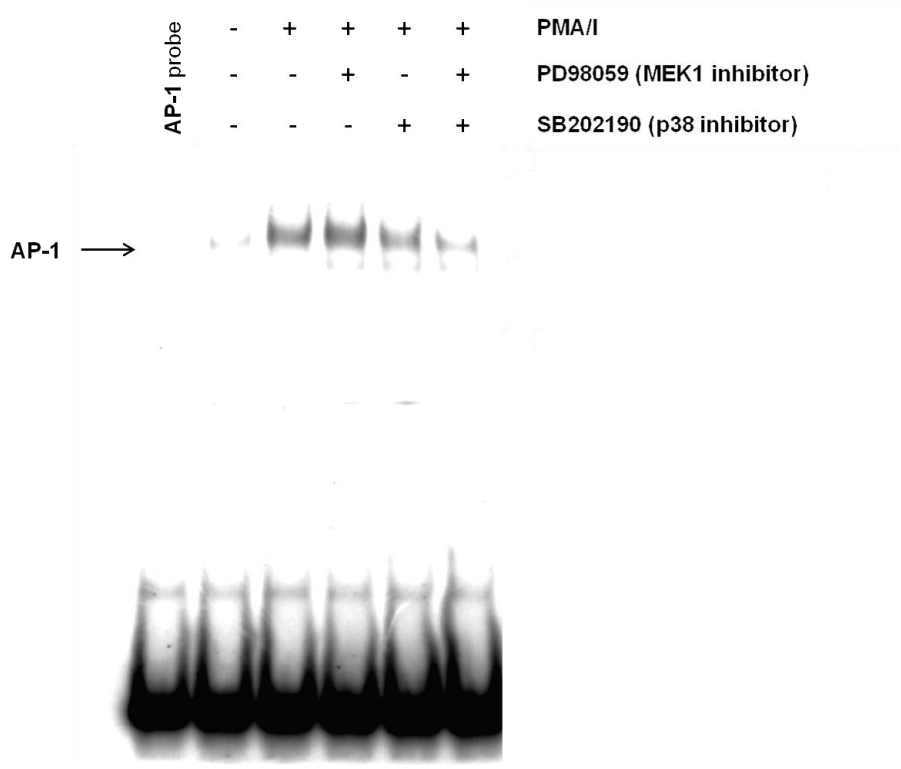

Figure 3.18 ***MAPK inhibitors effect on the PMA/I-induced AP-1 DNA binding***

C KG1a

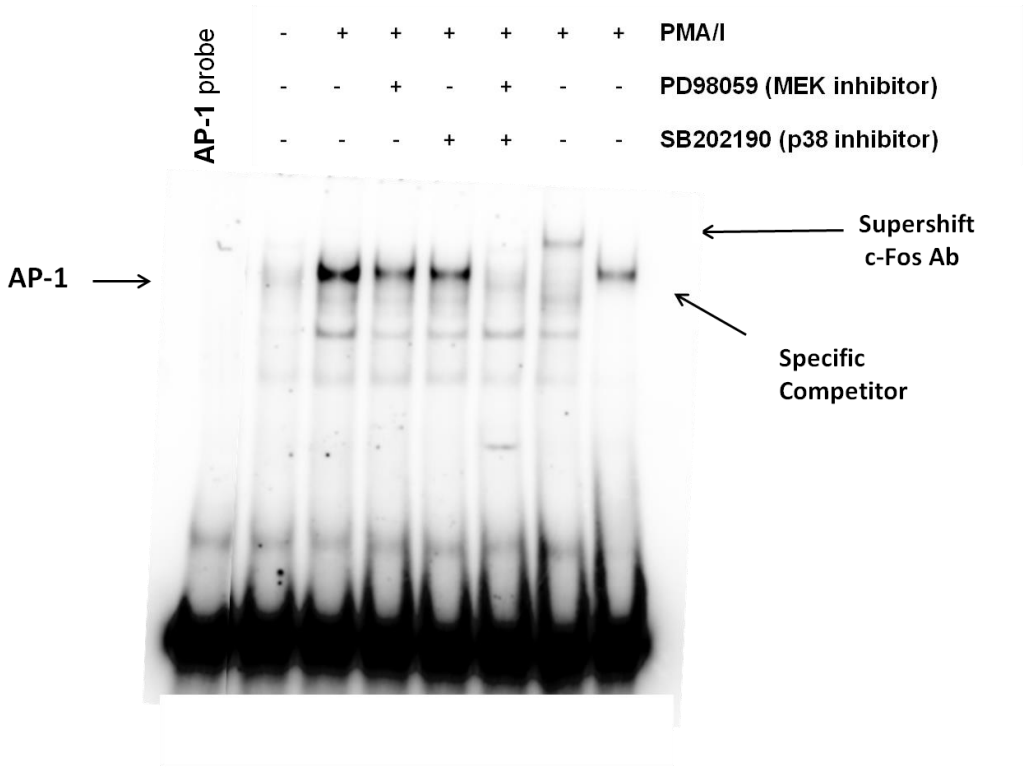

D

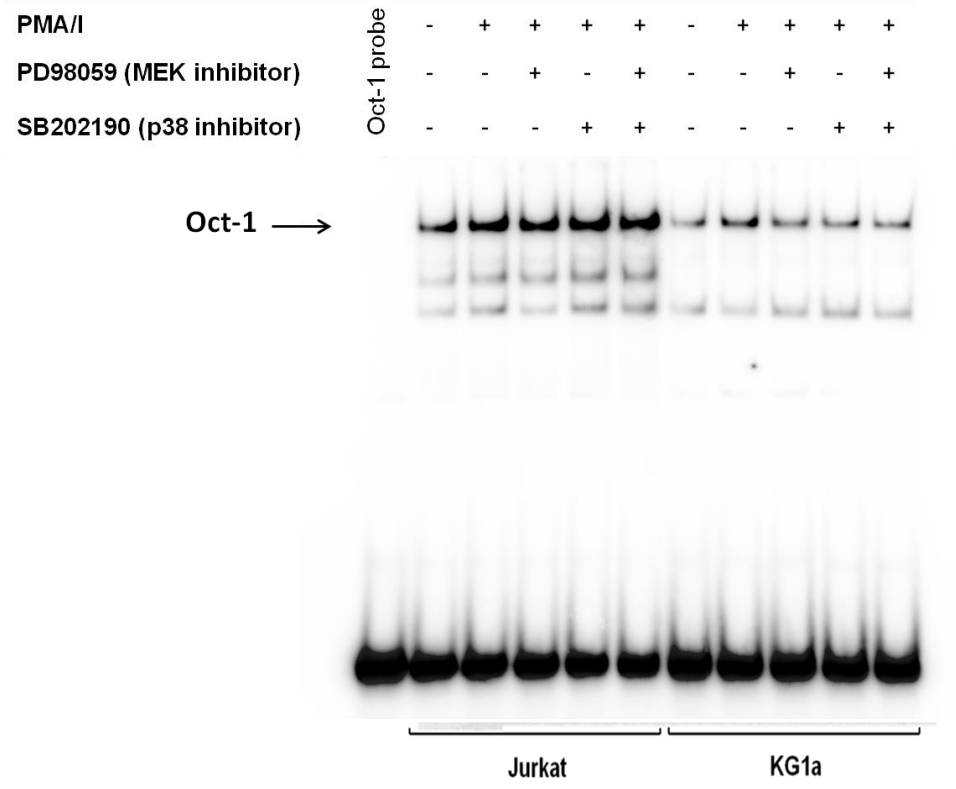

Figure 3.18 ***MAPK inhibitors effect on the PMA/I-induced AP-1 DNA binding***

E

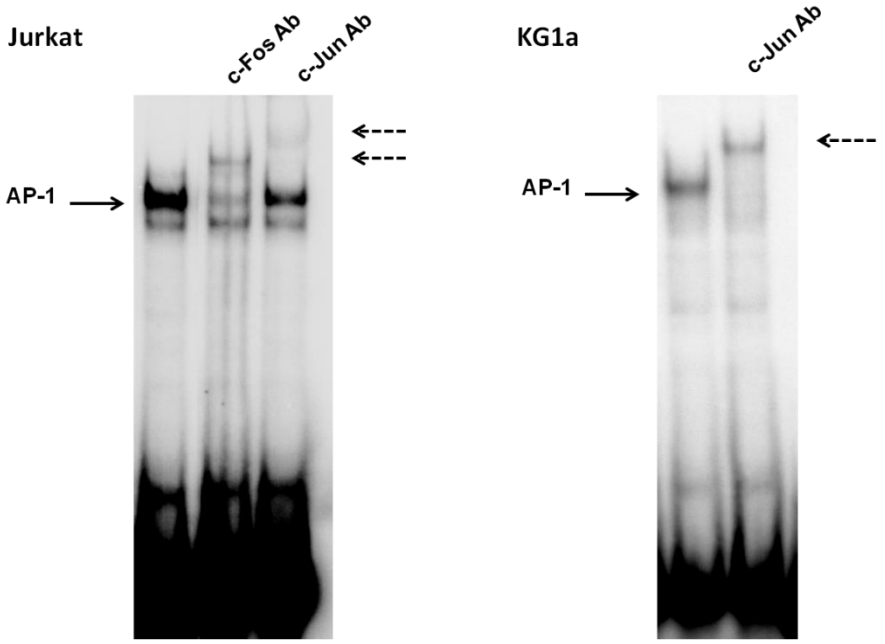

AP-1 EMSA assay performed on nuclear extracts of T blast cells (A), Jurkat (B) and KG1a cells (C). Cells were pre-treated for 1 h with the MEK inhibitor PD98059 (50 μM) and the p38 inhibitor SB202190 (25 μM), singularly or in combination and then stimulated for 2h with 20 ng/ml PMA and 2 μM ionophore A23187 (PMA/I). D) Oct-1 EMSA used as loading control for Jurkat and KG1a cells. In each lane 4 μg of nuclear extracts were used. E) AP-1 EMSA on nuclear extracts from Jurkat and KG1a cells treated with PMA/I. Nuclear extracts were pre-incubated with either c-Fos or c-Jun antibodies. Dashed arrows indicate supershift bands. One representative experiment for each EMSA is shown. Analysis of the bands intensity has been performed by Image J software.

Indeed, in Figure 3.18C and E a new band is detected above the specific one for AP-1. The competition with an unlabelled oligo duplex for the AP-1 binding reduced the intensity of the specific AP-1 band. I used an Oct-1 (octamer-binding protein-1) EMSA as loading control, since Oct-1 is a nuclear transcription factor that is constitutively expressed in the cells and it is not affected by any of the treatments (Figure 3.18D).

As described in section 3.8 for PMA/I-induced GM-CSF gene expression, I wanted to verify that the effect of the MAPK inhibitors on AP-1 DNA binding activity is due to the specific inhibition of MEK/ERK and p38 pathways, rather than to non-specific effects. To this end, I transfected KG1a cells via electroporation with either 200 nM siCTRL or 100 nM siERK1/2 together with 100 nM sip38. After 48 h from transfection I stimulated the cells for 2 h with PMA and ionophore A23187 (PMA/I) and then prepared the nuclear extracts. The AP-1 EMSA represented in Figure 3.19 shows that the combination of siERK1/2 and sip38 decreased AP-1 binding to the DNA by about 70% respect to the negative siCTRL.

These results demonstrated that the AP-1 binding ability to DNA induced by PMA/I is dependent on ERK and p38 MAPK pathways in KG1a cells and it is likely to be also dependent on them in T blast cells and Jurkat cells. However, additional siMAPK knockdown experiments would be required to verify this assumption.

Figure 3.19 ***Effect of siERK1/2 and sip38 on the PMA/I-induced AP-1 DNA binding in KG1a cells***

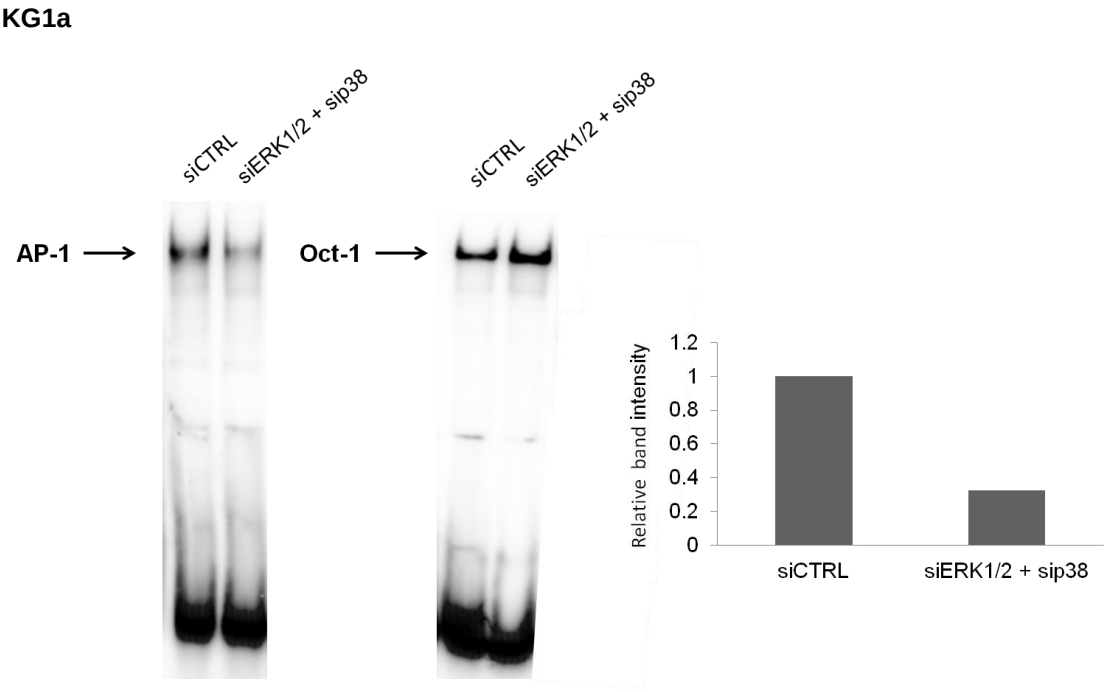

AP-1 and Oct-1 EMSA in KG1a cells treated with either 200 nM siCTRL or a combination of 100 nM siERK1/2 and 100 nM sip38. Analysis of the intensity of the bands was performed using Image J software. The Y-axis shows the levels of AP-1 binding normalised to Oct-1 and relative to the siCTRL. One representative experiment is shown.

3.11 c-Fos and c-Jun mRNA and protein expression increase after PMA/I treatment in T blast cells, Jurkat and KG1a cells

I already demonstrated that AP-1 is activated by PMA/I in T blast cells, Jurkat and KG1a cells and its binding to DNA is mediated by ERK and p38 MAPK pathways. Next, I wanted to study the protein composition of the AP-1 dimers. To this end, I measured the level of c-Fos and c-Jun mRNA and protein after PMA/I stimulation. c-Fos and c-Jun are immediate-early (IE) genes and are quickly expressed after stimulation. To find out the best timing of PMA/I stimulation in order to get the highest c-Fos and c-Jun gene expression, I treated KG1a cells with PMA/I for 30 min, 45 min, 1 hour and 2 hours. Results showed that the highest c-Fos mRNA levels were detected after 45 min, after which they decreased. Maximum c-Jun gene expression was reached after 2 hours, and its levels remained high after 4 hours (data not shown).

After finding the best time for gene induction in KG1a cells, I treated with PMA/I also T blast cells and Jurkat cells and measured c-Fos and c-Jun mRNA levels after 45 minutes and 2 hours, respectively, by qRT-PCR analysis. I detected a strong increase of c-Jun and especially c-Fos mRNA levels after PMA/I treatment in both T blast cells and the cell lines (Figure 3.20).

Next, I wanted to investigate the role of ERK and p38 pathways in the induction of c-Fos and c-Jun gene expression. Therefore, I pre-treated the cells for 1 h with the MEK inhibitor, PD98059 (50 μM) and the p38 inhibitor, SB202190 (25 μM), singularly and in combination.

The combination of the two inhibitors reduced both *FOS* and *JUN* mRNA to the levels measured in untreated cells. In T blast cells and Jurkat cells the single p38 inhibitor SB202190 decreased both PMA/I-induced *FOS* and *JUN* gene

expression by 25% and 40% respectively (Figure 3.20A and B). In KG1a cells, the p38 inhibitor was more effective, reducing both genes by around 50% compared to PMA/I treated cells (Figure 3.20C). On the contrary, the MEK inhibitor, PD98059 didn't reduce *JUN* mRNA levels in T blast cells and KG1a cells (Figure 3.20A and C, respectively). Pre-treatment of T blast cells with MEK inhibitor PD98059 even caused a small increase of the PMA/I-induced *JUN* expression. This effect might be due to a cross-talk among the different MAPK pathways, since I have already demonstrated that the inhibition of one of the pathways by using specific chemicals might lead to the activation of a different pathway. In Jurkat cells, MEK inhibitor was not effective in reducing *FOS* mRNA levels (Figure 3.20B). Interestingly, in KG1a and T blast cells *FOS* mRNA levels are at least 100 times higher than *JUN* mRNA levels after PMA/I stimulation, whereas in Jurkat cells they are comparable. However, these were measured at different times, and the levels may be balanced by other Fos and Jun family members that can compensate for *FOS* and *JUN*.

Figure 3.20 ***Effect of MAPK inhibitors on PMA/I-induced c-Fos and c-Jun gene expression***

A T blast cells

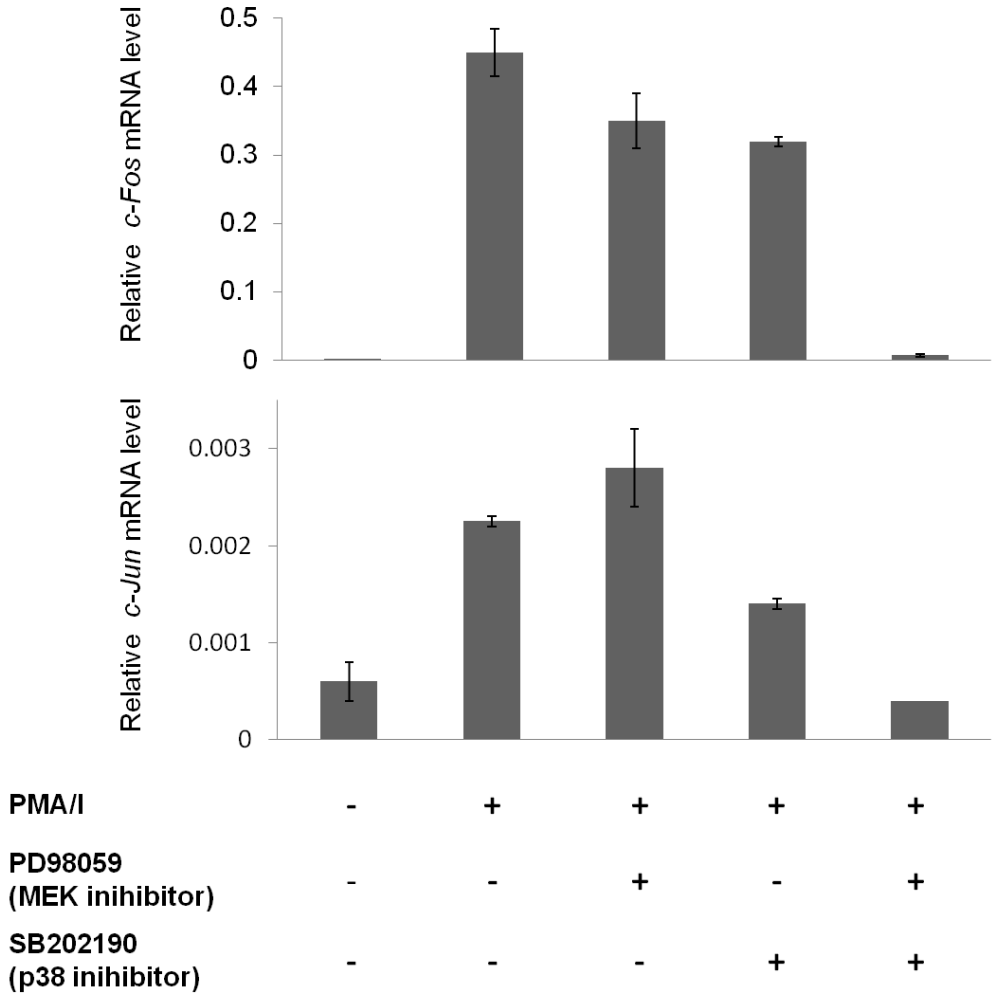

A) *FOS* and *JUN* mRNA levels measured by qRT-PCR in T blast cells after 1h pre-treatment with MAPK inhibitors (MEK inhibitor PD98059 50 μM and p38 inhibitor SB202190 25 μM), singularly or in combination, and stimulation with 20 ng/ml PMA and 2 μM ionophore A23187 (PMA/I) for 45' (*FOS*) or 2 h (*JUN*). The Y-axis shows expression relative to *GAPDH* gene expression. Each bar represents the average of three independent experiments, error bars represent SE.

Figure 3.20 ***Effect of MAPK inhibitors on PMA/I-induced c-Fos and c-Jun gene expression***

B Jurkat

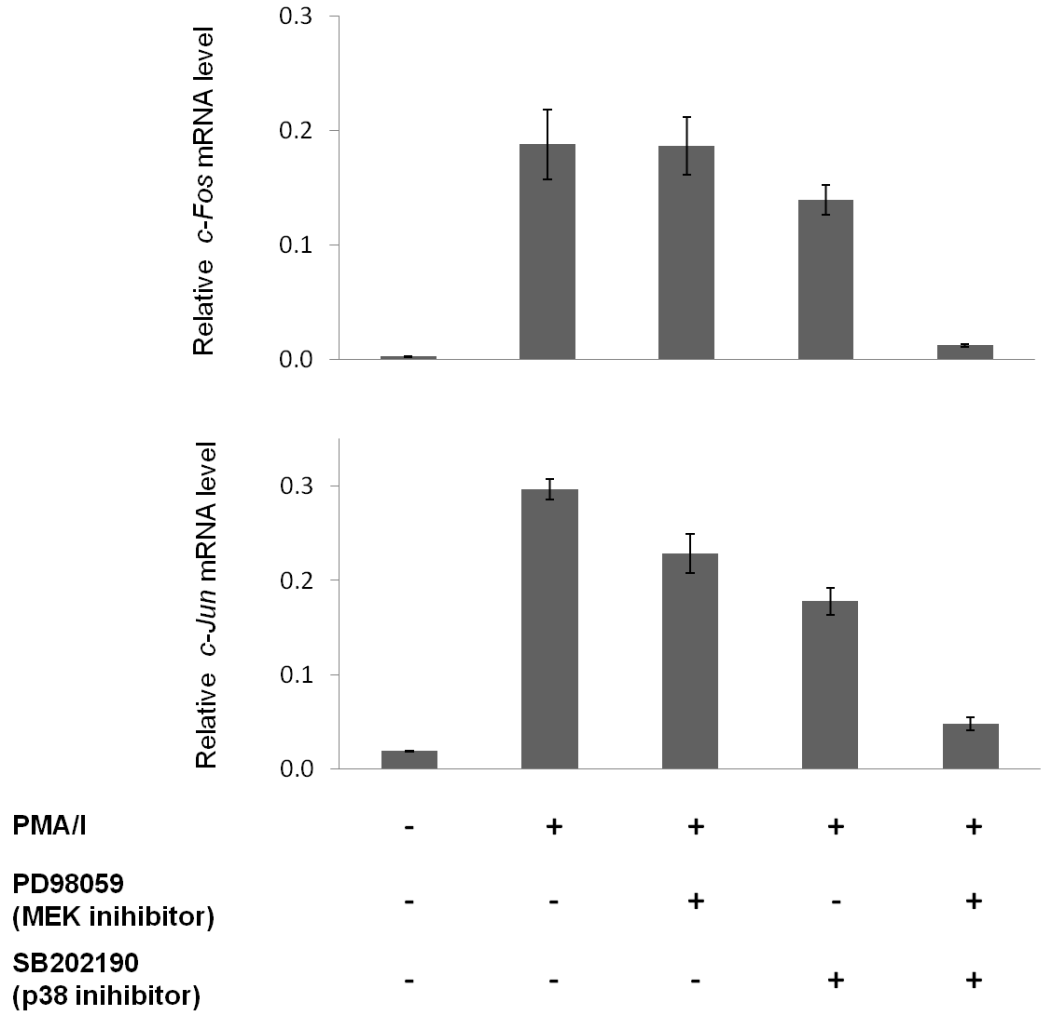

B) *FOS* and *JUN* mRNA levels measured by qRT-PCR in Jurkat cells after 1h pre-treatment with MAPK inhibitors (MEK inhibitor, PD98059 50 μM and p38 inhibitor, SB202190 25 μM), singularly or in combination, and stimulation with 20 ng/ml PMA and 2 μM ionophore A23187 (PMA/I) for 45' (*FOS*) or 2 h (*JUN*). The Y-axis shows expression relative to *GAPDH* gene expression. Each bar represents the average of three independent experiments, error bars represent SE.

Figure 3.20 ***Effect of MAPK inhibitors on the PMA/I-induced c-Fos and c-Jun gene expression***

C KG1a

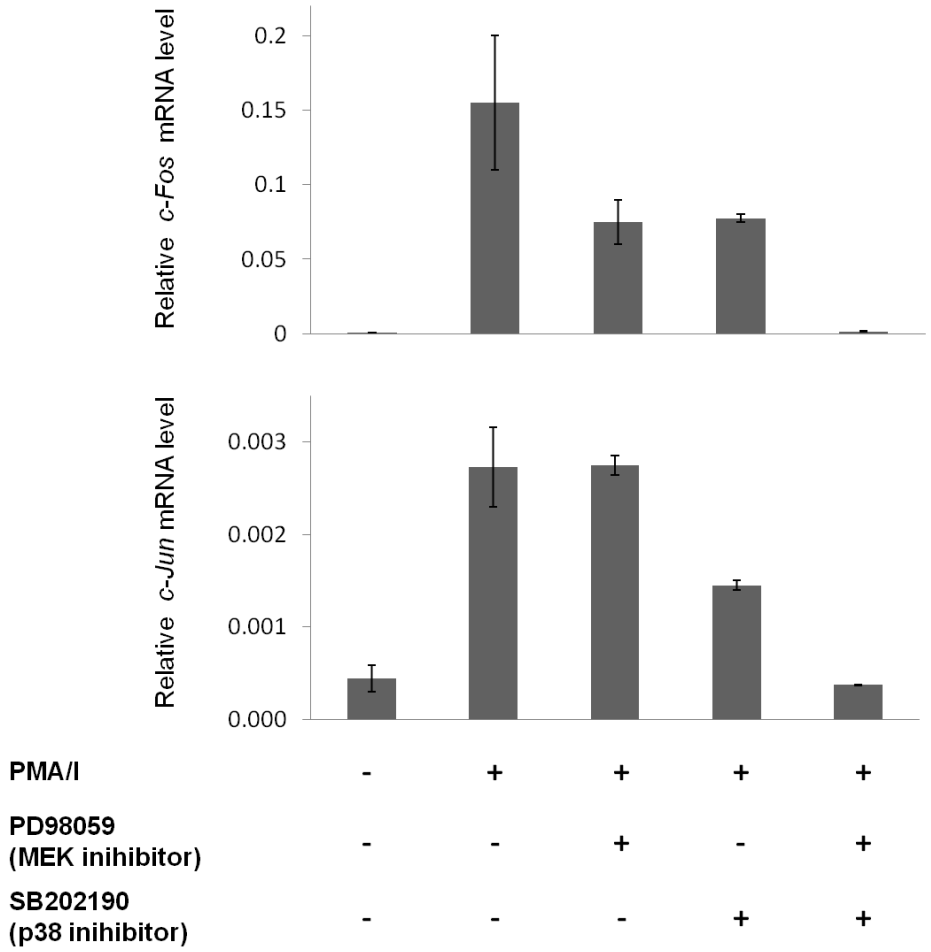

C) *FOS* and *JUN* mRNA levels measured by qRT-PCR in KG1a cells after 1h pre-treatment with MAPK inhibitors (MEK inhibitor, PD98059 50 μM and p38 inhibitor, SB202190 25 μM), singularly or in combination, and stimulation with 20 ng/ml PMA and 2 μM ionophore A23187 (PMA/I) for 45' (*FOS*) or 2 h (*JUN*). The Y-axis shows expression relative to *GAPDH* expression. Each bar represents the average of three independent experiments, error bars represent SE.

I wanted to confirm the results obtained in the qRT-PCR analysis by measuring c-Fos and c-Jun protein levels. Therefore, I performed a Western blot analysis. I pre-treated Jurkat and KG1a cells with the MEK inhibitor, PD98059 (50 μM) and the p38 inhibitor, SB202190 (25 μM), singularly and in combination and then I stimulated them for 1 h with PMA and ionophore A23187 (PMA/I). I detected the levels of c-Fos and c-Jun protein expression by using specific primary antibodies and I used GAPDH protein as loading control, because it is constitutive and its levels don't change upon any of the treatments used. As seen in gene expression analysis, PMA/I treatment increased also c-Fos and c-Jun protein levels. In both cell lines, pre-treatment with MEK and p38 inhibitor combination decreased both c-Fos and c-Jun genes down to the level of untreated cells (Figure 3.21A and B).

3.12 PMA/I treatment induces Elk1 phosphorylation in KG1a cells

Since I demonstrated that c-Fos expression is MEK/ERK-dependent in KG1a cells, I investigated whether the ERK downstream target, Elk1, could have a role in the regulation of c-Fos transcription. Elk1 is a transcription factor which can bind *FOS* promoter at serum responsive elements (SRE), activating its transcription [165]. Elk1 is mainly phosphorylated by ERK and JNK MAPKs but some studies demonstrated that it can also be phosphorylated by p38 upon its activation with different stimuli [186, 276, 299].

Figure 3.21 ***Effect of MAPK inhibitors on the PMA/I-induced c-Fos and c-Jun protein levels***

A Jurkat

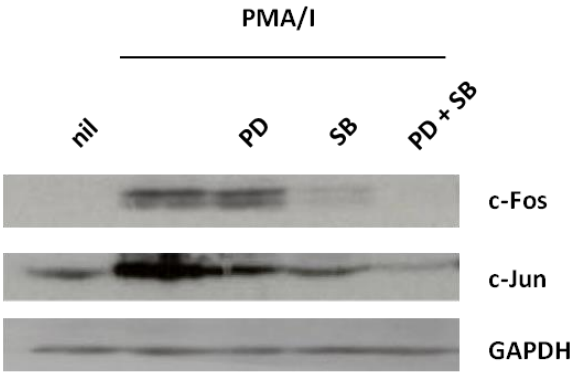

B KG1a

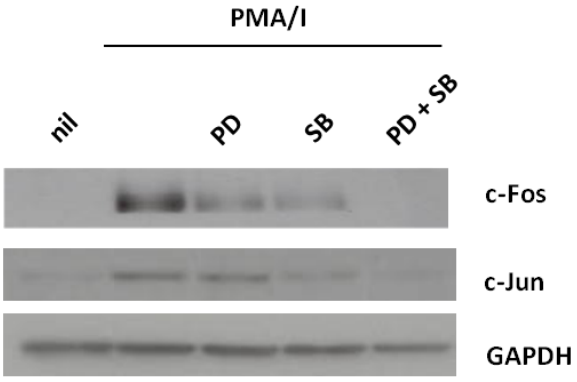

Western blotting of whole-cell lysates prepared from Jurkat (A) and KG1a (B) cells after 1h pre-treatment with MAPK inhibitors (MEK inhibitor PD98059 50 μM and p38 inhibitor SB202190 25 μM), singularly or in combination, and 1 h stimulation with 20 ng/ml PMA and 2 μM ionophore A23187 (PMA/I). *GAPDH* was used as loading control. A representative experiment of three biological replicates is shown.

In order to show a possible involvement of Elk1 in stimulated KG1a cells and also its putative role in *FOS* transcription I stimulated the cells for 1 h with PMA/I. Then I isolated whole-cell protein extracts and performed a Western blot analysis. PMA/I treatment induced the phosphorylation of Elk1, which was completely absent in untreated cells. Pre-treatment of cells with the MEK inhibitor PD98059 (50 μM) and with the combination of MEK and p38 inhibitors (50 μM and 25 μM respectively) seemed to completely abolish Elk1 phosphorylation (Figure 3.22A), whereas p38 did not show any effect. Therefore, the inhibitory effect shown by the combination of MAPK inhibitors seemed to be due to the MEK inhibitor only. It would be interesting to see whether also JNK inhibition could reduce PMA/I-induced Elk1 phosphorylation. From these results, I can conclude that PMA/I-induced Elk1 phosphorylation is ERK-mediated but not p38-mediated in KG1a cells. To check whether Elk1 could be responsible for an increase in *FOS* gene expression in KG1a cells, I performed a ChIP assay for Elk1, designing primers on the *FOS* promoter region, on PMA/I-stimulated cells for 1.5 h, with or without 1 h pre-treatment with the combination of MEK and p38 inhibitors (50 μM and 25 μM respectively). Subsequent qRT-PCR analysis showed that Elk1 enrichment at *FOS* promoter increased from 2.6 to 5.8 (over 100%) in PMA/I-treated cells and was almost completely reduced by the combination of inhibitors (Figure 3.22B). Values for Elk1 enrichment are expressed relative to Elk1 enrichment at the inactive *IVL* gene promoter. Since in Figure 3.22A I demonstrated that Elk1 phosphorylation is dependent only on MEK/ERK pathway, the effect of the MAPK inhibitors combination is most likely due to the MEK inhibitor only. A ChIP-qPCR on KG1a cells pre-treated with the single inhibitors would be useful to answer this question.

Figure 3.22 ***Elk1 phosphorylation increases in PMA/I-treated KG1a cells***

A

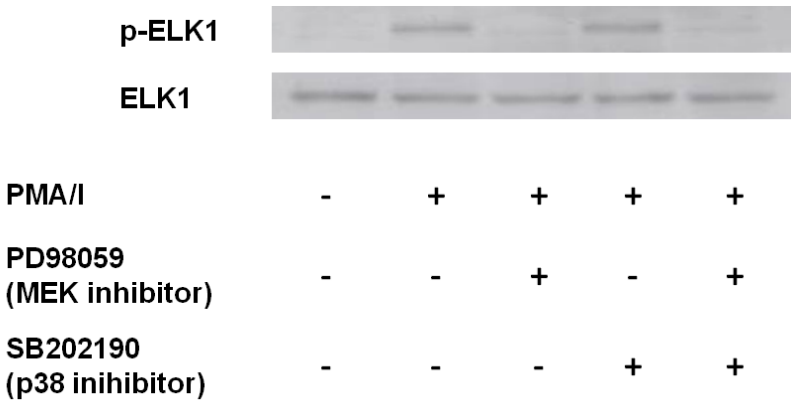

B

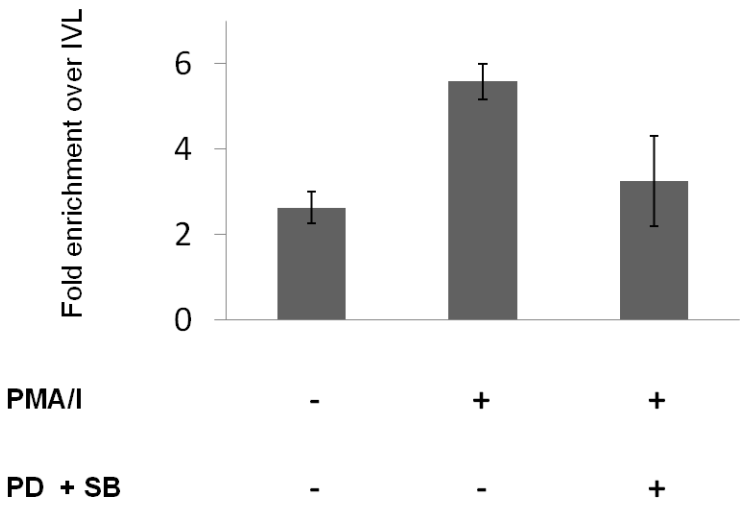

A) Western blot analysis of whole-cell lysates prepared from KG1a cells after 1h pre-treatment with MAPK inhibitors and 1h stimulation with 20 ng/ml PMA and 2 μM ionophore, A23187 (PMA/I). A representative experiment of three biological replicates is shown. B) ChIP-qPCR showing relative Elk1 enrichment at the *FOS* promoter in KG1a cells after 1.5 hours PMA/I stimulation and 1h pre-treatment with PD98059 (MEK inhibitor) and SB202190 (p38 inhibitor). The Y-axis shows Elk1 enrichment normalized to the IVL promoter as an inactive control. Eah bar represents the average value of three technical replicates. Error bars represent SE.

3.13 siRNA-mediated knockdown of c-Jun reduces GM-CSF mRNA level

Since I demonstrated that PMA/I-induced GM-CSF expression is associated with an increase of AP-1 DNA binding and an increase in mRNA levels of its components c-Fos and c-Jun, I used a siRNA against c-Jun to test its specific relevance in regulating GM-CSF gene expression.

KG1a cells were transfected with either 100 nM negative control siRNA (siRNA CTRL) or 100 nM *JUN* siRNA; after 48 hours from transfection cells were treated with PMA/I for 4 hours and mRNA was extracted to evaluate GM-CSF and *JUN* mRNA levels. RT-PCR analysis in Figure 3.23A shows that the reduction in *JUN* gene expression mirrored the reduction in GM-CSF gene expression (about 55% reduction compared to siCTRL treated cells), suggesting a requirement for *JUN* in GM-CSF gene activation.

I checked c-Jun protein knockdown by Western blot after 72 hours from transfection, after treating the cells for 2 h with PMA/I to induce *JUN* expression. Figure 3.23B shows that after 72 hours c-Jun protein levels were about 50% less than in siCTRL treated cells. It is notable that there is a correlation between the reduction in c-Jun protein/gene expression and the one in GM-CSF gene expression. It would be interesting to transfect the cells again or perform the analysis after longer time from transfection to reach a higher level of c-Jun knockdown and then see if there is a corresponding reduction in GM-CSF gene expression.

Figure 3.23 ***siRNA against c-Jun influences the PMA/I-induced GM-CSF gene expression in KG1a cells***

A

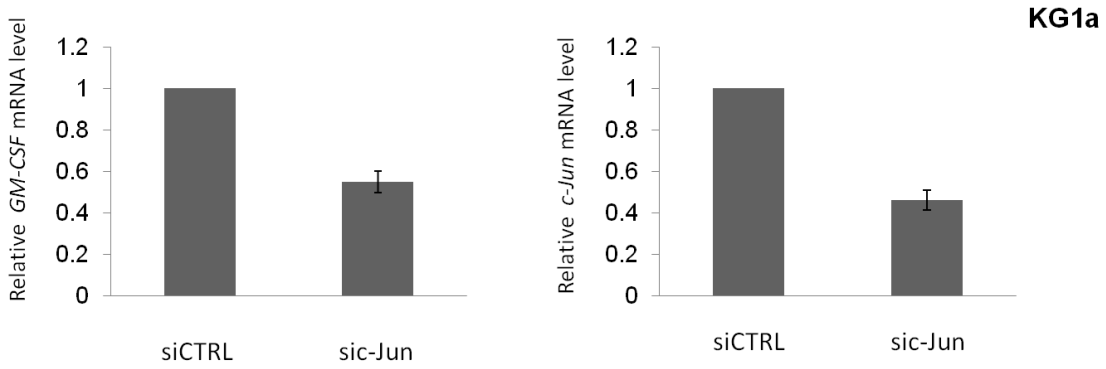

B

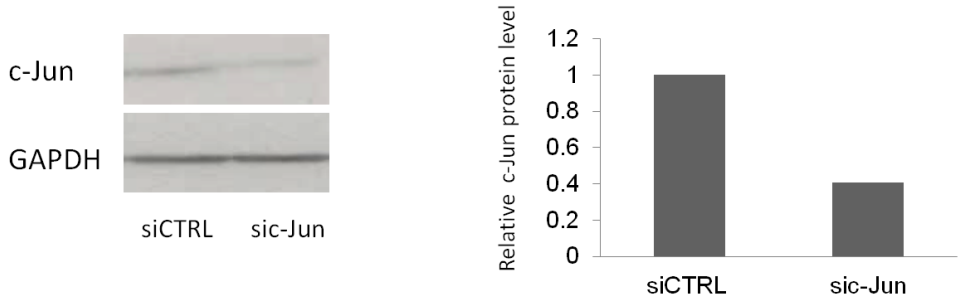

A) Cells were transfected with either 100 nM scrambled siRNA (CTRL) or 100 nM *JUN* siRNA; 48 hours after transfection, cells were treated for 4 hours with 20 ng/ml PMA and 2 μM ionophore, A23187 (PMA/I) and mRNA was extracted to measure *GM-CSF* and *JUN* mRNA levels in RT-PCR analysis. B) c-Jun protein knockdown was checked 72 hours after transfection, after treating the cells with PMA/I for 2 hours to induce c-Jun expression. Analysis of protein levels after transfection was performed by using Image J software by measuring the intensity of the bands and normalizing them to *GAPDH*. c-Jun protein levels are relative to siCTRL. One representative experiment is shown.

3.14. PMA/I stimulation induces gene expression of AP-1 components

After evaluating the effect of MAPK inhibitors on PMA/I-induced FOS and JUN gene expression, I decided to measure the level of expression of other AP-1 components in Jurkat and KG1a cell lines after treatment with PMA/I and whether this expression was affected by MAPK inhibitors. Therefore, I treated the cells for 1 h with PMA/I at the same doses used so far and I performed a qRT-PCR analysis to measure *FRA1* and *FRA2* gene expression (amongst the Fos proteins) and *JUNB* and *JUND* mRNA levels (amongst the Jun proteins) (Figure 3.24-25). Gene expression analysis revealed that in Jurkat cells PMA/I stimulation increased *FRA1* gene expression by approximately 15 fold compared to untreated cells, whereas *FRA2* gene expression increased by about 3.5 fold. PMA/I-induced *FRA1* and *FRA2* gene expression were decreased by the MEK inhibitor (50 μM) and the p38 inhibitor (25 μM) by around 50% and 75% respectively, whereas in combination these inhibitors reduced the mRNA levels down to the levels of untreated cells (Figure 3.24). In KG1a cells *FRA1* gene didn't show any significant increase after PMA/I stimulation, and none of the treatment with the inhibitors affected its expression. In contrast, *FRA2* mRNA levels in PMA/I-treated cells were about 2.5 times higher than in untreated cells. MAPK inhibitors alone reduced PMA/I-induced *FRA2* gene expression by around 40%, whereas in combination with p38 inhibitor, the mRNA levels were reduced down to the levels of untreated cells (Figure 3.25).

RT-PCR analysis of *JUN* transcripts revealed that *JUNB* and *JUND* gene expression increased in Jurkat cells after treatment with PMA/I by about 20 and 2.5 folds respectively, compared to untreated cells. The MEK inhibitor PD98059

and the p38 inhibitor SB202190 reduced *JUNB* and *JUND* gene expression by about 30 and 50% respectively, compared to the PMA/I-treated cells, whereas their combination reduced the mRNA levels down to the levels of untreated cells (Figure 3.24). In KG1a cells, PMA/I treatment increased *JUNB* and *JUND* mRNA levels by 10 and 2 folds respectively. The MEK inhibitor PD98059 and the p38 inhibitor SB202190 reduced *JUNB* mRNA levels by about 25% and 50% respectively, compared to the cells treated with PMA/I. In Jurkat cells, MAPK inhibitors alone decreased PMA/I-induced *JUND* gene expression by about 25%, but *t*-test statistical analysis revealed that this reduction is not significant. However, their combination reduced the *JUND* gene expression down to the levels of untreated cells, as seen so far for the expression of all the AP-1 components analysed, apart from *FRA1* in KG1a cells. It is notable that the effect of the combination of MEK and p38 inhibitors in reducing gene expression is always significant compared to the inhibitors alone, apart from the case of *JUND* gene expression in KG1a cells, where the effect of the combination is not significantly stronger than p38 inhibitor alone.

Interestingly, in both cell lines, *JUNB* and *JUND* mRNA levels were higher than *FRA1* and *FRA2* mRNA levels, even before PMA/I treatment.

These results demonstrate that PMA/I induced the expression of *FRA2*, *JUNB*, *JUND* in Jurkat and KG1a cells and also *FRA1* expression in Jurkat cells. Moreover, treatment of both cell lines with the combination of MEK and p38 inhibitors abolished the increase of gene expression induced by PMA/I.

FRA1, *FRA2*, *JUNB*, *JUND* mRNA levels were measured by RT-PCR in Jurkat cells after 1h pre-treatment with MAPK inhibitors (MEK inhibitor PD98059 50 μM and p38 inhibitor SB202190 25 μM) and 1 h stimulation with 20 ng/ml PMA and 2 μM ionophore A23187 (PMA/I). The Y-axis shows expression relative to *GAPDH* expression. Each bar represents the average of three independent experiments, error bars represent SE. n.s. = student's *t*-test value > 0.05 compared to p38 inhibitor alone.

Figure 3.24 ***AP-1 components mRNA levels after PMA/I treatment in Jurkat cells***

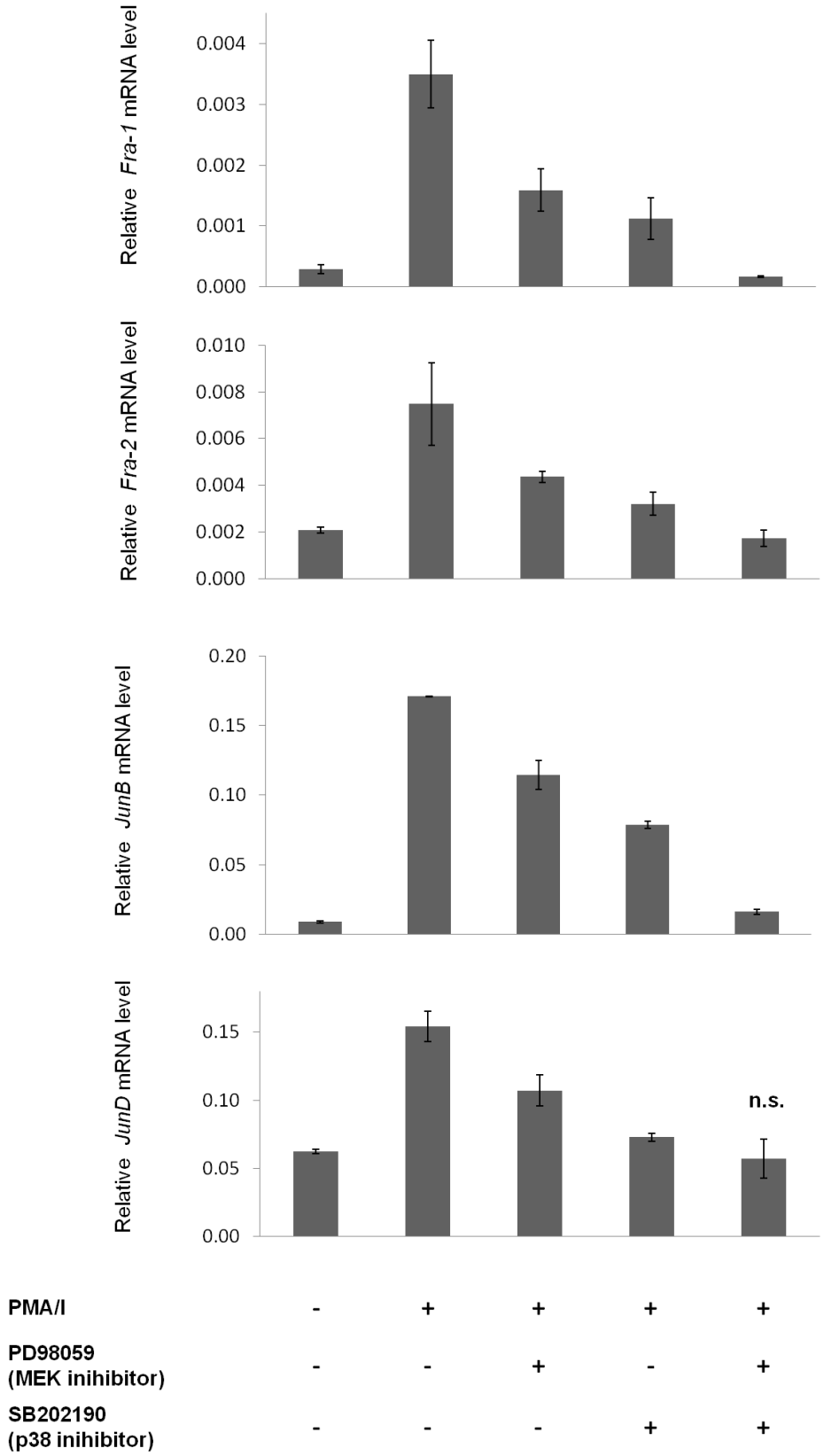

FRA1, *FRA2*, *JUNB*, *JUND* mRNA levels were measured by RT-PCR in KG1a cells after 1h pre-treatment with MAPK inhibitors (MEK inhibitor PD98059 50 μM and p38 inhibitor SB202190 25 μM) and 1 h stimulation with 20 ng/ml PMA and 2 μM ionophore A23187 (PMA/I). The Y-axis shows expression relative to *GAPDH* expression. Each bar represents the average of three independent experiments, error bars represent SE. n.s. = student's *t*-test value > 0.05 compared to p38 inhibitor alone.

Figure 3.25 ***AP-1 components mRNA levels after PMA/I treatment in KG1a cells***

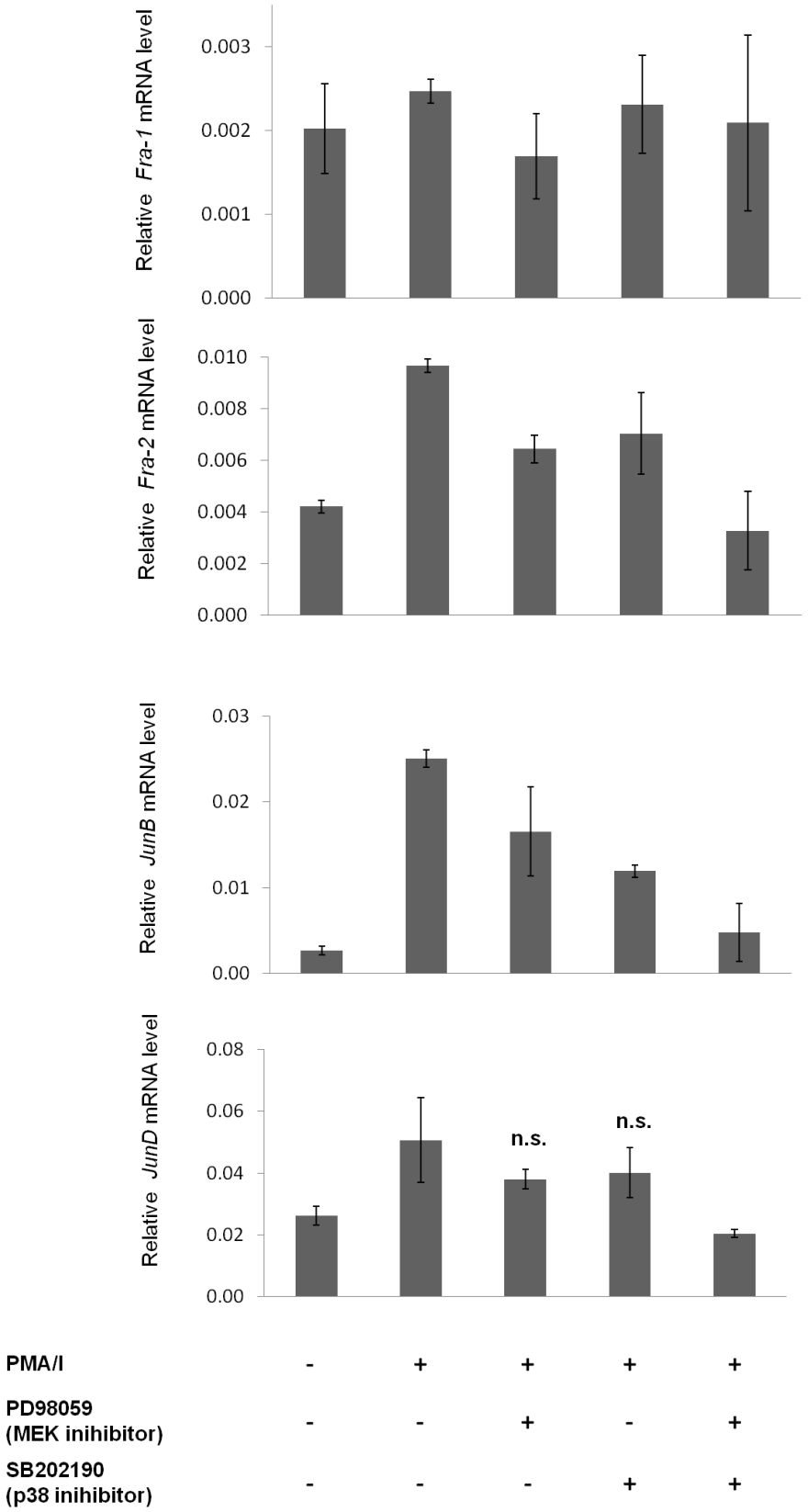

3.15 MAPK inhibitors reduce the PMA/I-mediated recruitment of c-Fos and c-Jun at the GM-CSF enhancer *in vivo*

Having demonstrated that PMA/I stimulation induces the AP-1 DNA binding *in vitro* in T blast cells, Jurkat and KG1a, and that the combination of MEK and p38 inhibitors is able to reduce it, I decided to verify the recruitment of c-Fos and c-Jun proteins to the GM-CSF enhancer *in vivo,* using chromatin immunoprecipitation (ChIP).

I performed c-Fos and c-Jun ChIP on the region of the GM-CSF enhancer containing the composite NFAT/AP1 binding site (GM420) on PMA/I-stimulated cells for 1.5 h, with or without 1 h pre-treatment with the combination of MEK and p38 inhibitors (50 μM and 25 μM respectively). qPCR analysis showed that c-Fos enrichment at GM-CSF enhancer increased by five and four times in PMA/I-treated KG1a and Jurkat cells, respectively, whereas c-Jun occupancy increased by about three fold in KG1a cells. c-Fos enrichment was completely abolished by the treatment with the combination of MEK and p38 inhibitors in both cell lines (Figure 3.26A and B), whereas c-Jun occupancy was reduced by about 50% (Figure 3.26A).

These results confirm the recruitment of AP-1 to the GM-CSF enhancer *in vivo* in KG1a-stimulated cells, and suggest that the effect is mediated by the ERK and p38 MAPK pathway.

Figure 3.26 ***PMA/I treatment induces the recruitment of c-Fos and c-Jun at the GM-CSF enhancer***

A KG1a

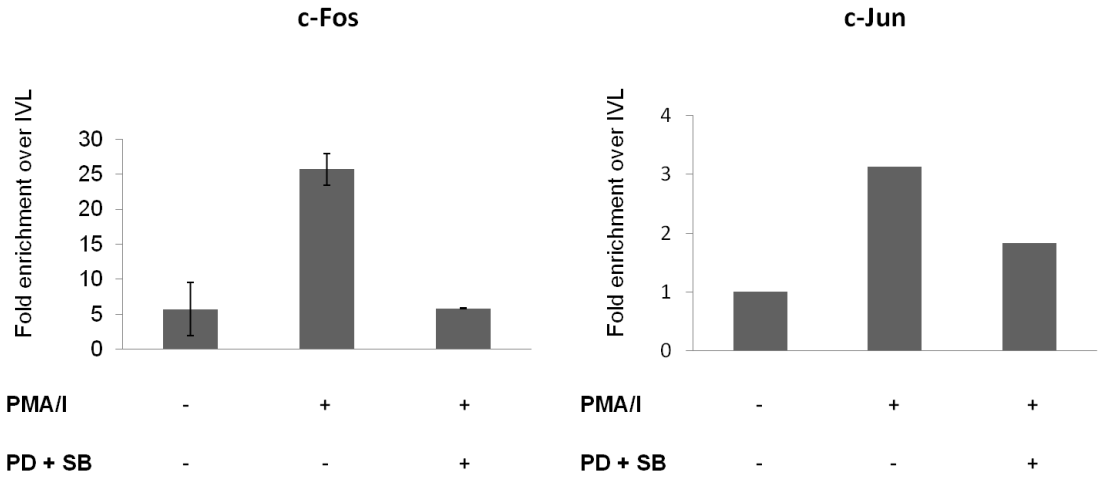

B Jurkat

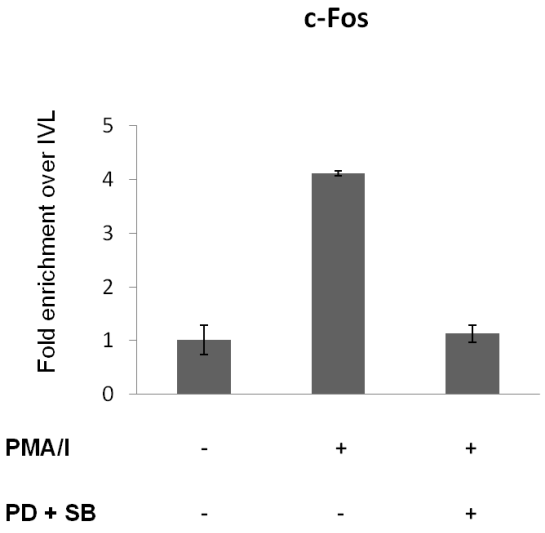

ChIP-qPCR showing relative c-Fos and c-Jun enrichment at the GM-CSF enhancer in KG1a (A) and Jurkat (B) cells after 1h pre-treatment with PD98059 50 μM (MEK inhibitor) and SB202190 25 μM (p38 inhibitor) followed by 1.5 h PMA/I stimulation. Parallel control IgG precipitations gave values comparable to background levels (not shown). Y-axis shows relative enrichment to the gene desert region IVL. In the c-Fos graph each bar represents the average of three independent biological experiments. Error bars represent SE. For the c-Jun, ChIP-qPCR one representative experiment is shown.

3.16 The p300 inhibitor C646 reduces PMA/I-induced GM-CSF gene expression

The results obtained so far demonstrated that AP-1 plays an important role in PMA/I-induced GM-CSF gene expression. Several reports showed that AP-1 can regulate gene transcription interacting with transcriptional co-activators such as p300, which has histone acetyltranferase activity [300, 301]. Hence, I investigated the putative role of p300 in the PMA/I-induced GM-CSF gene expression by pre-treating Jurkat and KG1a cells for 1 h with increasing doses (5-20 μM) of the specific p300 inhibitor, C646 [302] before stimulation. qRT-PCR analysis of GM-CSF mRNA levels revealed that in Jurkat cells 5 μM and 10 μM C646 reduced PMA/I-induced GM-CSF mRNA levels by about 50% and 90% respectively; 20 μM C646 completely abolished GM-CSF gene expression. In KG1a cells, the same doses were less effective than in Jurkat; in fact both 5 μM and 10 μM reduced PMA/I-induced GM-CSF gene expression by about 40%, whereas 20 μM reduced it by about 65% (Figure 3.27).

These results confirm a role of p300 in regulating PMA/I-induced GM-CSF gene expression in KG1a and Jurkat cells.

Figure 3.27 ***The p300 inhibitor C646 reduces the PMA/I-induced GM-CSF gene expression in Jurkat and KG1a cells***

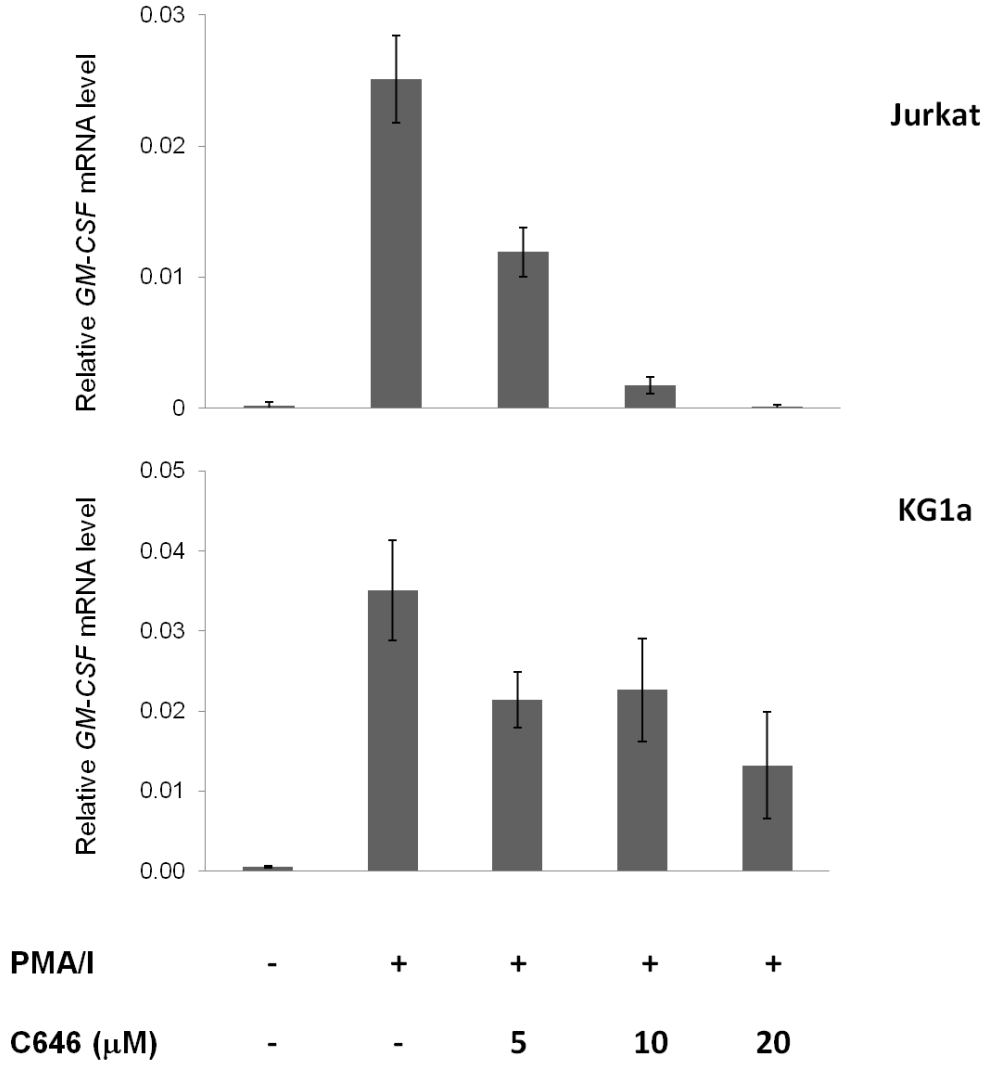

qRT-PCR showing GM-CSF gene expression after pre-treatment of Jurkat and KG1a cells with increasing doses of C646 and an induction with 20 ng/ml PMA and 2 μM ionophore, A23187 (PMA/I) for 4 hours. The y-axis shows GM-CSF gene expression relative to *GAPDH* expression. Each bar represents the average of at least two independent biological experiments and error bars represent SE.

3.17 PMA/I stimulation recruits p300 to the GM-CSF enhancer and increases histone H3 acetylation levels in Jurkat and KG1a cells

Since the results obtained so far suggest an involvement of p300 in the regulation of PMA/I-induced GM-CSF gene expression and since p300 has been demonstrated to interact with AP-1 [300, 301], I decided to perform a ChIP assay to evaluate p300 recruitment to the GM-CSF enhancer at the NFAT/AP-1 site (GM420). Moreover, p300 is also known to be an excellent chromatin marker of enhancers [137, 303].

I treated the cells for 1.5 h with the same doses of PMA/I used so far for all the experiments, with or without 1 h pre-treatment with the combination of MEK inhibitor, PD98059 (50 μM) and p38 inhibitor, SB202190 (25 μM). In both cell lines p300 occupancy strongly increased after PMA/I stimulation. The enrichment was about 8 fold in Jurkat cells and about 90 times in KG1a cells, compared to untreated cells. Pre-treatment with MAPK inhibitors combination reduced the levels of p300 occupancy by 90% in KG1a cells and down to the level of untreated cells in Jurkat cells (Figure 3.28A and B).

These results suggest that PMA/I treatment stimulates the recruitment of p300 to the GM-CSF enhancer via MAPK signalling pathways.

Figure 3.28 ***PMA/I treatment induces the recruitment of p300 to the GM-CSF enhancer***

A Jurkat

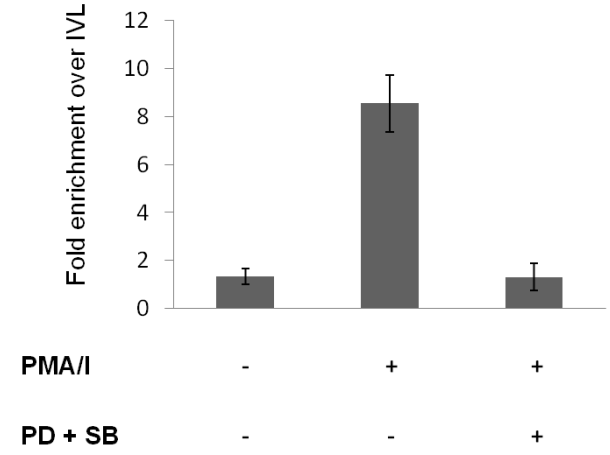

B KG1a

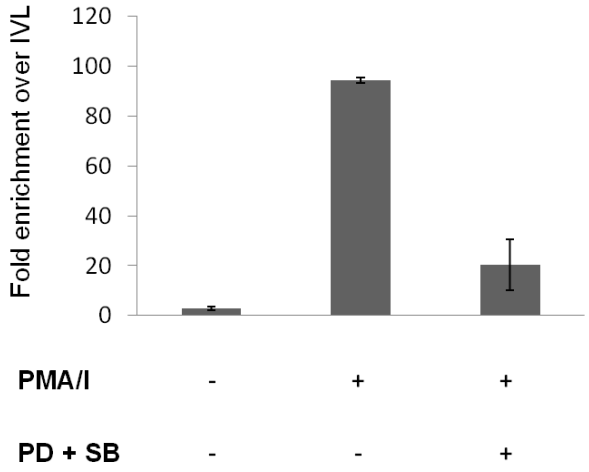

ChIP-qPCR showing relative p300 enrichment at the GM-CSF enhancer in Jurkat (A) and KG1a (B) cells after 1h pre-treatment with PD98059 (MEK inhibitor) and SB202190 (p38 inhibitor) and following stimulation with 20 ng/ml PMA and 2 μM ionophore A23187 (PMA/I) for 1.5 h. Parallel control IgG precipitations gave values comparable to background levels (not shown). The Y-axis shows relative enrichment to the gene desert region IVL. Each bar represents the average of at least three independent experiments. Error bars represent SE.

p300 is known to have histone acetyltranferase activity [300, 301]. H3 Lysine 27 acetylation (H3K27ac) is a marker of active enhancers and it is often observed at p300 positive enhancers [304].

For this reason, I decided to perform a ChIP assay for H3K27ac at the GM-CSF enhancer, at the same site used for p300 and AP-1 ChIP (GM420), and also a global H3 acetylation, since p300 can acetylate other histone residues [305, 306].

In KG1a cells, the levels of H3K27ac increased by approximately three fold after PMA/I stimulation, and they were reduced down to the control level by the combination of MEK and p38 inhibitors (Figure 3.29A). These results were confirmed in Jurkat cells, although the increase of H3K27 acetylation induced by PMA/I was less pronounced than in KG1a cells (only 50% compared to untreated cells) (Figure 3.29B).

Finally, in KG1a cells the use of an anti-acetyl-histone H3 antibody revealed that PMA/I induced an increase of global acetylation by 100% at the nucleosome H3 flanking the DHS at the enhancer; once again the enrichment was strongly reduced by the combination of MEK and p38 inhibitors (Figure 3.29A).

The qRT-PCR analyses of the ChIP assay for transcription factor binding expressed the enrichment at the GM-CSF enhancer relative to IVL. In the ChIP assay for histone marks the results are normalized to total H3.

These results demonstrate that PMA/I treatment induces the acetylation of H3 and H3K27ac at the GM-CSF locus, confirming it has characteristics of an active enhancer, and the PMA/I-induced acetylation seems to be MAPK dependent.

Figure 3.29 ***PMA/I treatment increases H3 acetylation levels in KG1a and Jurkat cells***

A KG1a

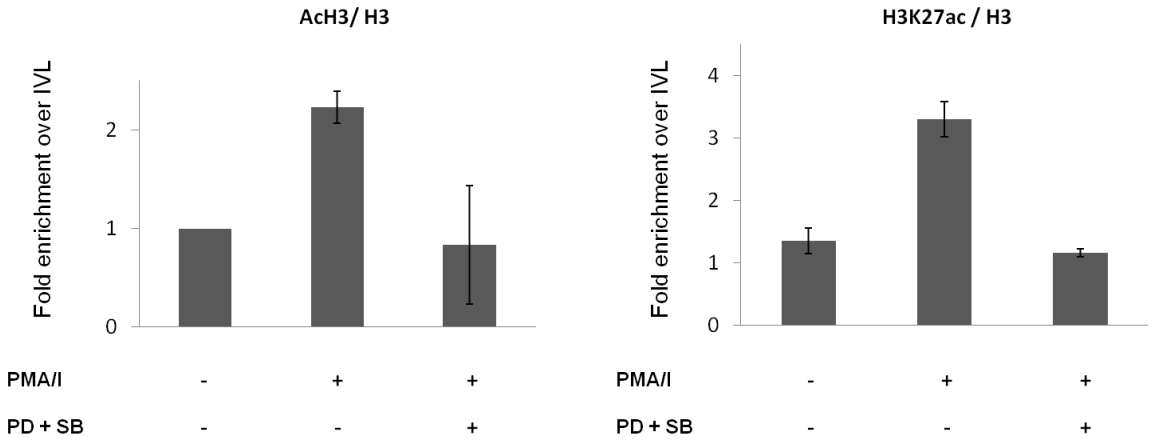

B Jurkat

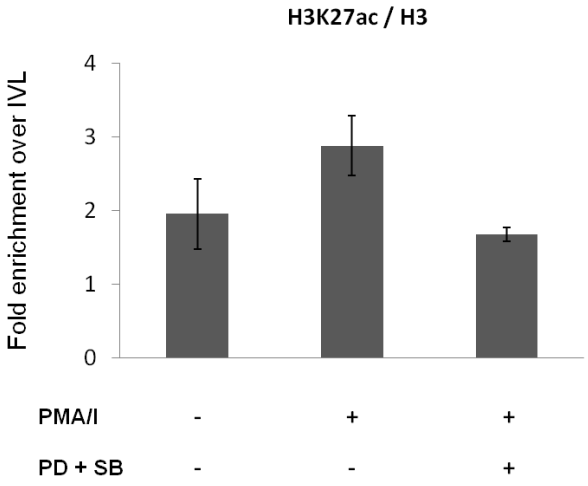

ChIP-qPCR showing relative H3K27ac/H3 and global H3 acetylation enrichment at the GM-CSF enhancer in KG1a (A) and Jurkat (B) cells after 1h pre-treatment with PD98059 (MEK inhibitor) and SB202190 (p38 inhibitor) and following stimulation with 20 ng/ml PMA and 2 μM ionophore A23187 (PMA/I) for 1.5 h. Parallel control IgG precipitations gave values comparable to background levels (not shown). Results are normalized to total H3 levels and the Y-axis shows the relative enrichment to the gene desert region IVL. Each bar represents the average of three independent experiments. Error bars represent SE.

3.18 The p300 inhibitor C646 fails to inhibit the PMA/I-induced chromatin remodelling at GM-CSF enhancer in Jurkat and KG1a cells

Since the results obtained so far demonstrate that PMA/I recruits p300 to the GM-CSF enhancer *in vivo,* I wondered whether its specific inhibition by C646 could change the chromatin conformation at the GM-CSF enhancer. To test this, I performed a DHSs analysis of cells stimulated with PMA/I with or without pre-treatment for 1 h with C646. I used 10 μM C646 in Jurkat cells and 20 μM C646 in KG1a cells, which were found to reduce PMA/I-induced GM-CSF gene expression by 90% and 50% respectively (see Figure 3.27). In the DHSs analysis, I used DNase I-digested nuclei isolated from untreated cells or cells treated with PMA/I and PMA/I + C646 inhibitor, using the same strategy as before. As already seen in previous experiments PMA/I treatment induced a strong DHS at the enhancer in both cell lines, but pre-treatment with the p300 inhibitor C646 failed to reduce this (Figure 3.30). These results suggest that p300 could be recruited by other transcription factors after the formation of the DHS, therefore its inhibition might not influence the chromatin conformation at the GM-CSF enhancer after PMA/I treatment or p300 is not needed for HS formation.

3.19 The combination of MEK and p38 MAPK inhibitors decreases the PMA/I-induced phosphorylation of MSK1 in Jurkat and KG1a cells

So far I focused on the combination of MEK and p38 inhibitors (PD98059 an SB202190 respectively) because, amongst all the different combinations of MAPK inhibitors tested (including the ones using the JNK inhibitor SP600125),

these were the most effective in reducing the PMA/I-induced GM-CSF gene expression and chromatin remodelling at the GM-CSF enhancer.

Figure 3.30 ***Effect of the p300 inhibitor C646 on the PMA/I-induced chromatin remodelling at the GM-CSF enhancer***

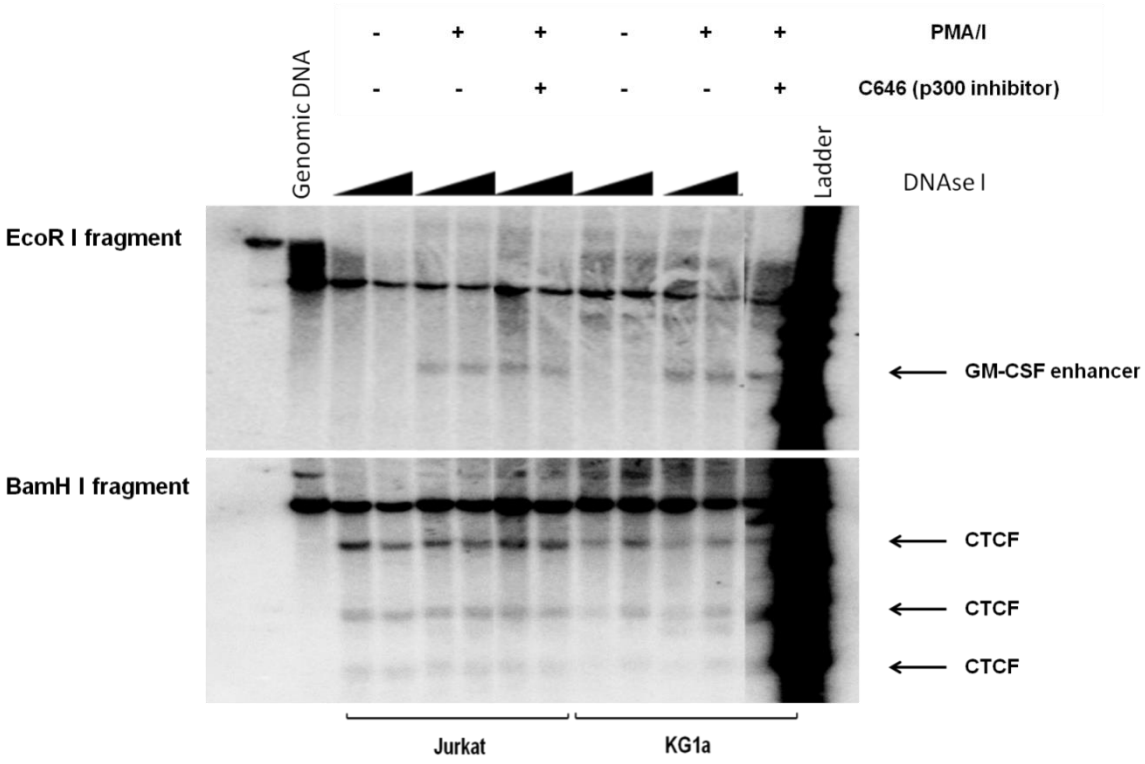

Mapping of DHSs within GM-CSF enhancer and promoter in a 9.4 kb EcoR I fragment and in a 4.6 kb BamH I fragment downstream of the IL3 gene showing three constitutive CTCF sites. Cells were pre-treated with C646 for 1h and then stimulated for 4h with 20 ng/ml PMA and 2 μM ionophore, A23187 (PMA/I). Black triangles indicate increasing concentrations of DNase I (8 and 10 μg/μl) and genomic DNA serves as control. Just one dose of DNAse I (10 μg/μl) is represented for KG1a cells pre-treated with C646.

One of the reasons why the combination of MEK and p38 inhibitors resulted the highest effect in my model system could be because MEK/ERK pathway have mutual downstream target proteins, including the mitogen- and stress-activated protein kinase MSK1/2. MSK1/2 are nuclear serine/threonine protein kinases which can phosphorylate several substrates including NF-κB [203], histone H3 [307] and CREB [308, 309], mediating the transcriptional activation of several genes. MSK1/2 can be phosphorylated at Thr581 by either ERK or p38 MAPKs [310, 311].

In order to investigate whether MSK1 is phosphorylated in response to stimulation with PMA/I and whether this phosphorylation is mediated by both ERK and p38 pathways, I performed a Western blot analysis using 30 μg of whole cell extract isolated from Jurkat or KG1a cells. I used primary antibodies against either the phosphorylated form of MSK1 (Phospho-Thr581) or the total form, which should recognise both modified and unmodified protein. As represented in Figure 3.31, untreated cells (both Jurkat and KG1a cells) show an insignificant level of MSK1 phosphorylation, which is considerably increased by PMA/I treatment. Interestingly, in both cell lines the phosphorylation of MSK1 decreased upon MEK and p38 inhibitor pre-treatment and was completely abolished by the combination of the two. In Jurkat cells it seemed that the two inhibitors had about the same effect in reducing MSK1 phosphorylation, whereas in KG1a cells the MEK inhibitor PD98059 seemed to be more effective. The amount of total MSK1 should not change upon these different treatments and in fact it remained about constant in this analysis. However a GAPDH would have been a better loading control.

These results demonstrate that PMA/I stimulation induce MSK1 phosphorylation in Jurkat and KG1a cells and this phosphorylation is ERK and p38-dependent.

Figure 3.31 ***PMA/I treatment phosphorylates MSK1 in Jurkat and KG1a cells***

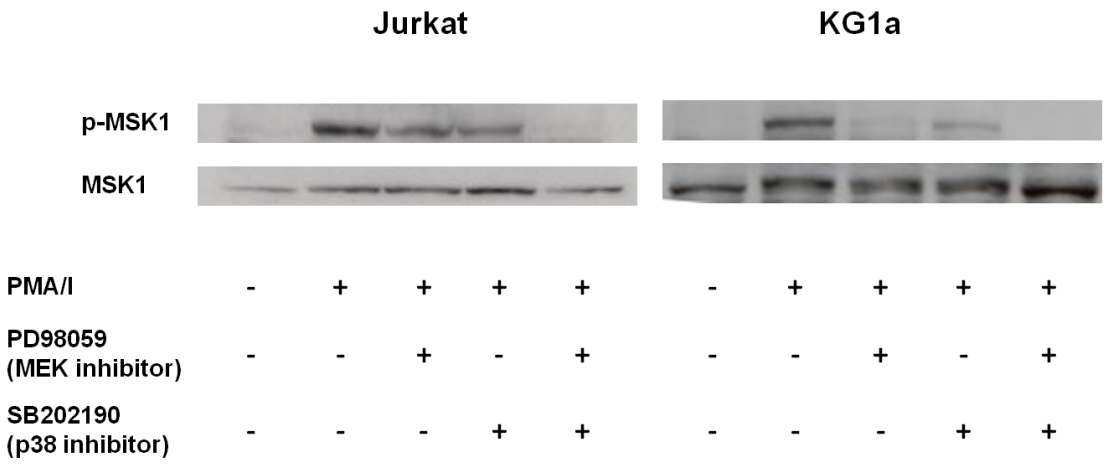

Western blotting of whole-cell lysates prepared from Jurkat and KG1a cells after 1h pre-treatment with MAPK inhibitors and 1h stimulation with 20 ng/ml PMA and 2 μM ionophore A23187 (PMA/I). A representative experiment of three biological replicates is shown.

3.20 MSK1 knockdown reduces the PMA/I-induced GM-CSF gene expression and inhibits chromatin remodelling at the GM-CSF enhancer in Jurkat and KG1a cells

Since I demonstrated that the single MEK and p38 inhibitors reduced MSK1 phosphorylation and their combination completely abrogated MSK1 phosphorylation, I decided to investigate the role of this kinase in PMA/I-induced GM-CSF gene expression and chromatin remodelling in Jurkat and KG1a cell lines. In order to do this, I used the MSK inhibitor H89, at concentrations previously described in the literature [312, 313]. This compound is known to inhibit also Protein Kinase A (PKA), which is activated via cAMP [314].

In order to test the effect of MSK on PMA/I-induced GM-CSF gene expression, I pre-treated Jurkat and KG1a with 10 μM H89 for 1 h, before PMA/I stimulation for 4 hours. H89 reduced the PMA/I-induced GM-CSF mRNA levels in Jurkat cells by approximately 85%. The same concentration inhibited PMAI-induced GM-CSF gene expression by 50% in KG1a cells, suggesting that other downstream components of MAPK signalling may be involved in GM-CSF gene regulation in these cell line (Figure 3.32).

From these results it seems that MSK plays an important role in the regulation of GM-CSF gene in Jurkat and KG1a cells. However, H89 is a chemical that can also inhibit PKA kinase and, as for other drugs, it might show off target effects. For these reasons, I used a specific siRNA to knockdown MSK1 expression in KG1a cells.

Figure 3.32 ***Effect of the MSK1 inhibitor H89 on the PMA/I-induced GM-CSF gene expression in Jurkat and KG1a cells***

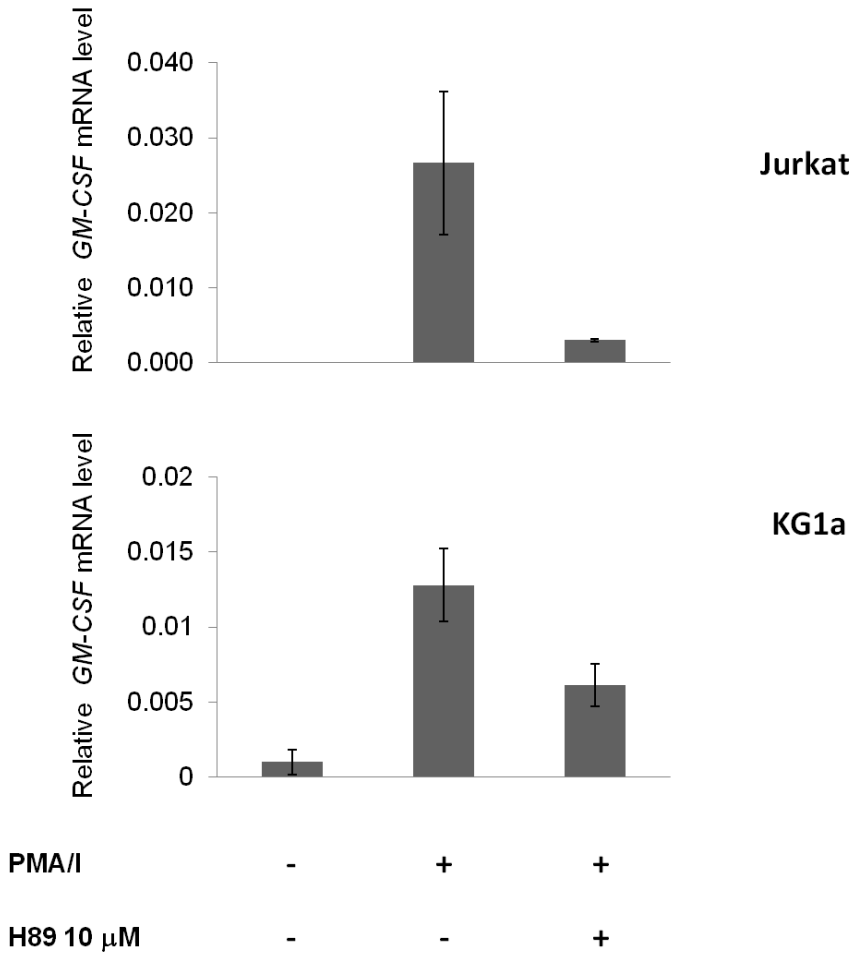

qRT-PCR showing GM-CSF gene expression after pre-treatment of Jurkat and KG1a cells with H89 10 μM for 1 h and an induction with 20 ng/ml PMA and 2 μM ionophore A23187 (PMA/I) for 4 hours. The Y-axis shows GM-CSF gene expression relative to *GAPDH* expression. Each bar represents the average of at least two independent repeats and the error bars represent SE.

As described in section 3.8 to knockdown ERK1/2 and p38, I transfected the cells with either 100 nM of negative control siRNA (siCTRL) or 100 nM specific siRNA against MSK1. 48 hours after transfection, I treated the cells with PMA/I; after 4 hours I extracted the mRNA and I measured both GM-CSF and MSK1 gene expression, to check the level of knockdown. Figure 3.33A shows that a 90% reduction of MSK1 gene expression is achieved by siMSK1 (compared to siCTRL) corresponding to about a 50% reduction in PMA/I-induced GM-CSF gene expression, confirming the results obtained by the use of the H89 inhibitor. I also measured the levels of MSK1 protein after siRNA transfection by Western Blot analysis (Figure 3.33B). 72 h after transfection, I achieved only 60% reduction compared to siCTRL. To obtain a further knockdown, I could have transfected again the cells with the siRNA and waited for longer time, as I previously did for ERK1/2 and p38. However, the level of knockdown was satisfactory for a gene expression analysis.

These results confirmed an important role of MSK1 in the regulation of PMA/I-GM-CSF gene expression in my model systems.

Given the inhibitory effect shown by the MSK inhibitor H89 on PMA/I-induced gene expression, I wondered whether H89 can also reduce PMA/I-induced chromatin remodelling at the GM-CSF enhancer.

I performed a Southern blot using the same strategy as before, mapping the DHSs in an EcoR I and BamH I fragment in DNase I-digested samples. Cells were either treated only with PMA/I for 4 h or pre-treated for 1 h with 10 μM H89 before stimulation. Untreated cells were used as control. In this analysis, the two cell lines showed different results. In fact the treatment with H89 resulted in a loss of the DHS in Jurkat cells whereas it did not affect DHS formation in KG1a cells (Figure 3.34).

Figure 3.33 ***Effect of siMSK1 on PMA/I-induced GM-CSF gene expression in KG1a cells***

A

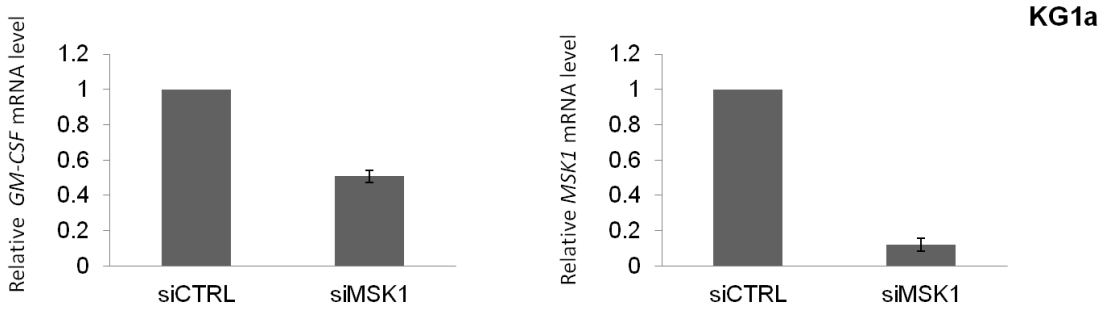

B

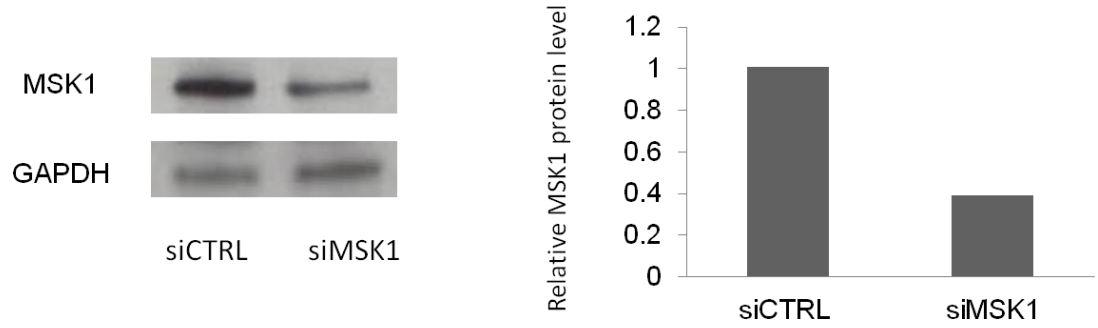

A) KG1a cells were transfected with either 100 nM siRNA (siCTRL) or 100 nM MSK1 siRNA; 48 hours after transfection, cells were treated for 4 hours PMA/I and mRNA was extracted to evaluate GM-CSF and MSK1 mRNA levels. B) MSK1 protein knockdown was checked 72 hours after transfection by Western Blot analysis. The intensity of the bands was analysed using ImageJ software. One representative experiment is shown.

Figure 3.34 ***Effect of MSK1 on the PMA/I-induced chromatin remodelling at the GM-CSF enhancer in Jurkat and KG1a cells***

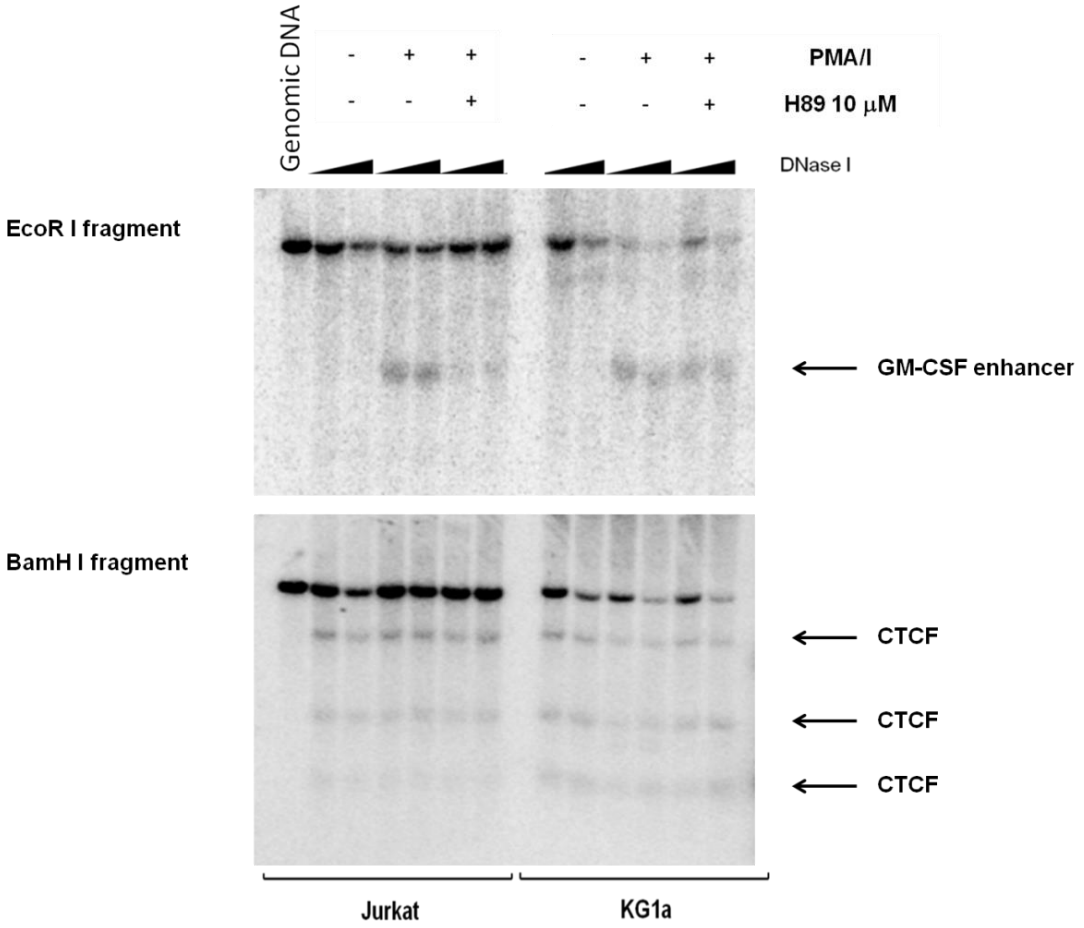

Mapping of DHSs within the GM-CSF enhancer and promoter in a 9.4 kb EcoR I fragment and in a 4.6 kb BamH I fragment downstream of the IL3 gene showing three constitutive CTCF sites. Jurkat and KG1a cells were pre-treated with H89 for 1 h and then stimulated for 4h with PMA/I. Black triangles indicate increasing concentrations of DNase I and genomic DNA serves as control.

These results suggest that, in the two cell lines, two different mechanisms control chromatin remodelling at the GM-CSF enhancer after PMA/I stimulation, and that one of these is independent of MSK1.

3.21 Cross-talk between MAPK and NF-κB signalling

So far I studied the involvement of MAPK pathways in PMA-induced GM-CSF gene expression. I found that MEK/ERK and p38 pathways are essential in the regulation of PMA/I-induced GM-CSF gene regulation in Jurkat and KG1a leukaemic cell lines, and their action is mediated by their mutual downstream target MSK1. MSK1 represents an important junction between MAPK and NF-κB pathways. In fact, MSK1 has been known to activate NF-κB through the phosphorylation of p65 subunit at Ser276 [315]. This phosphorylation promotes the recruitment of the co-activator p300/CBP [316], followed by the acetylation of both NF-κB p65 at Lys314 and histones at the NF-κB bound promoters [243]. In order to find a possible connection between the MAPK and NF-κB pathways in the regulation of PMA/I-induced GM-CSF gene expression, I performed a Western blot analysis to measure the phosphorylation of NF-κB p65 at Ser276 in Jurkat and KG1a cells.

Figure 3.35 shows that PMA/I treatment induces NF-κB phosphorylation at Ser276 in both cell lines. Cells were also pre-treated with MEK and p38 inhibitors alone or in combination as previously described in order to investigate how these pathways could interfere with NF-κB signalling pathways. The MEK/p38 inhibitors in combination were more effective in reducing p65 phosphorylation at Ser276 compared to the single inhibitors. These results are

very similar to the ones observed on MSK1 phosphorylation (Figure 3.31), indicating that MSK1 could be the kinase responsible for Ser276 phosphorylation. To further confirm this speculation, I repeated the Western blot to measure the level of phosphorylation of p65 at Ser276 in PMA/I-stimulated cells pre-treated with MSK1 inhibitor H89 (10 μM). In both cell lines, treatment with H89 abrogated the phosphorylation of Ser276 (Figure 3.35).

These results suggest that ERK and p38 MAPK pathways could be responsible for PMA/I-induced NF-κB activation through MSK1.

However, phosphorylation of p65 at Ser276 occurs in the nucleus and is not the only way NF-κB is activated. Inactive NF-κB is bound to its inhibitor I-κB in the cytoplasm. Activation of the NF-κB canonical pathway leads to the phosphorylation of I-κB and its degradation by the proteasome, whereas the p65 subunit undergoes phosphorylation at different sites. The most common site of phosphorylation is Ser536, which is accompanied by the translocation of p65 to the nucleus, where it can activate gene transcription [211, 212]. In several solid tumours and haematological malignancies NF-κB is already active and phosphorylated at this site in untreated cells [317, 318].

To investigate whether NF-κB is already active in untreated Jurkat and KG1a cells, I measured the phosphorylation of p65 at Ser536 using the same whole-cell lysates from cells either treated or not with the inhibitors. In KG1a cells NF-κB was already phosphorylated at Ser536 before stimulation with PMA/I, whereas in Jurkat cells this phosphorylation was almost entirely inducible. Neither the single MEK and p38 inhibitors nor their combination significantly decreased the NF-κB phosphorylation level in Jurkat cells (Figure 3.36).

Figure 3.35 ***H89 decreases the PMA/I-induced NF-κB phosphorylation at Ser276 in Jurkat and KG1a cells***

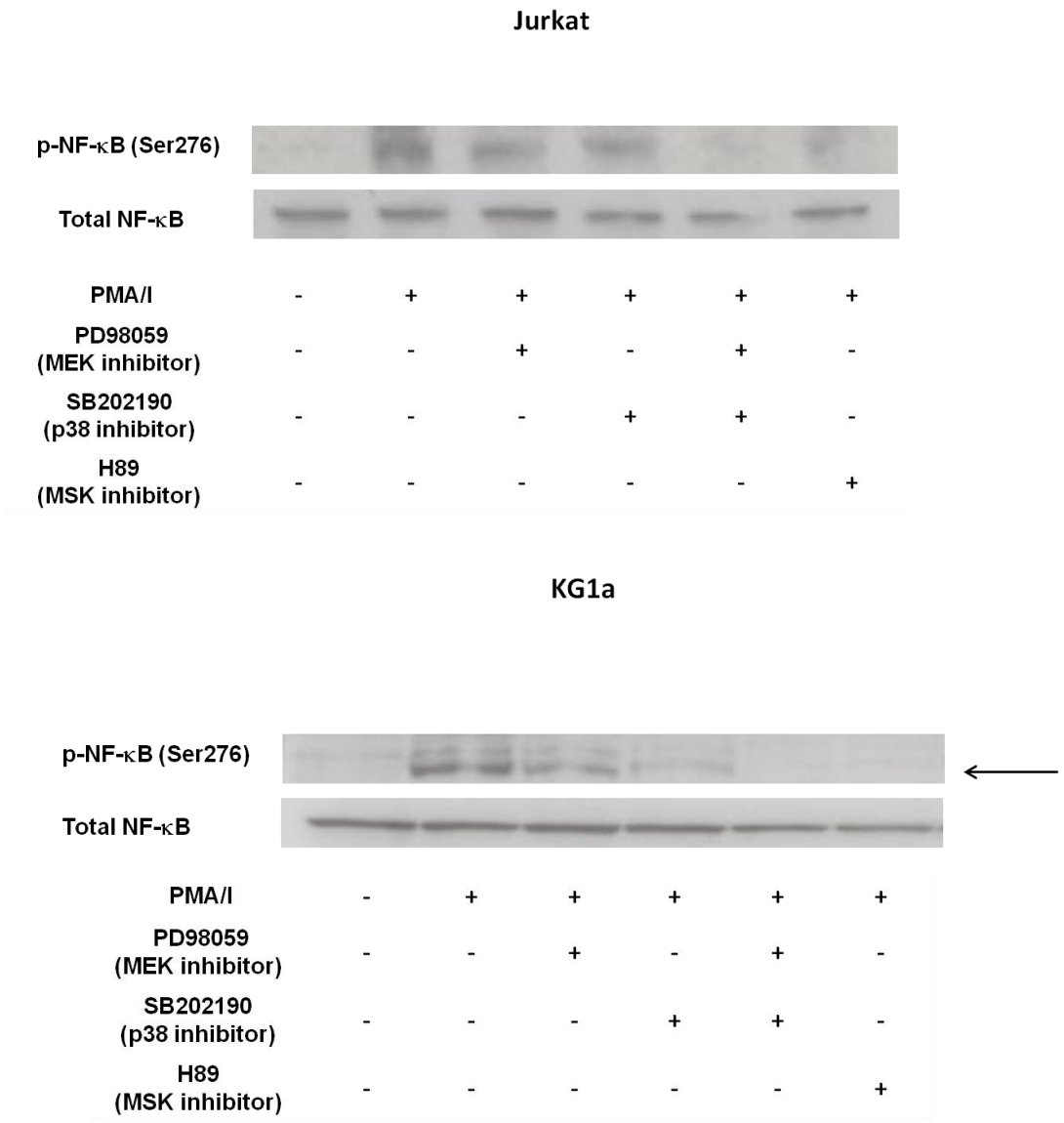

Western blotting of whole-cell lysates prepared from Jurkat and KG1a cells after 1h pre-treatment with inhibitors and 1h stimulation with PMA/I. The arrow indicates the specific band. A representative experiment of three biological replicates is shown.

Figure 3.36 ***Effect of the combination of the MEK and p38 inhibitors on the PMA/I-induced NF-κB phosphorylation in Jurkat and KG1a cells***

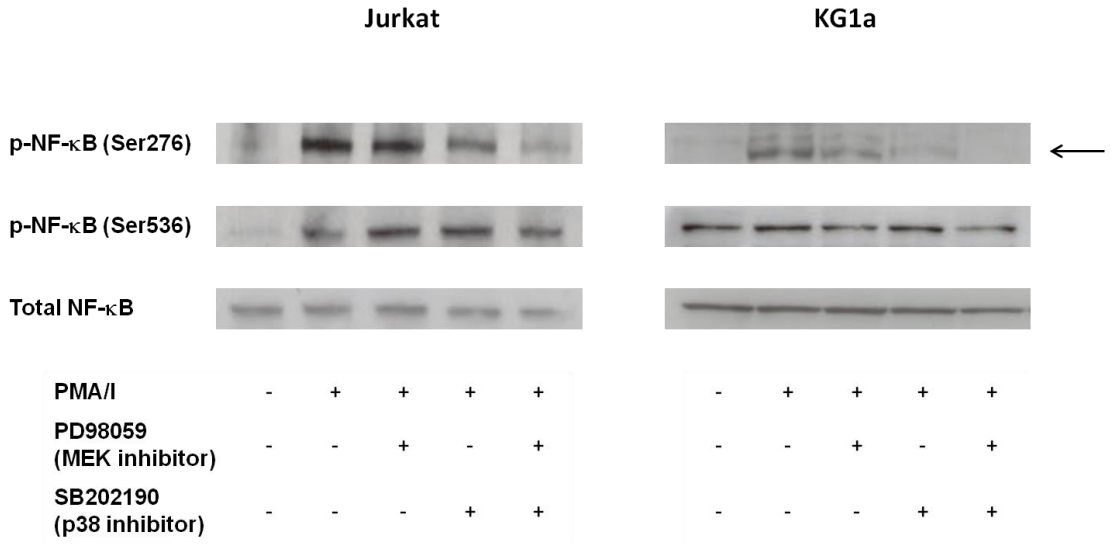

Western blotting of whole-cell lysates prepared from Jurkat and KG1a cells after 1h pre-treatment with inhibitors as before and 1h stimulation with PMA/I. A representative experiment of three biological replicates is shown. The arrow indicates the specific band for p-NF-κB (Ser276).

In KG1a cells it seems that the MEK inhibitor PD98059 slightly decreased the p65 phosphorylation, as well as the combination of MEK/p38 inhibitor, probably due to the effect of the MEK inhibitor only.

These results show that NF-κB pathway is activated by PMA/I treatment in Jurkat and KG1a cells. This activation is mediated by p65 phosphorylation at Ser276 and Ser536 in Jurkat cells, but only by its phosphorylation at Ser276 in KG1a cells.

3.22 The NF-κB pathway is involved in the PMA/I-induced GM-CSF gene expression and chromatin remodelling at the -3 kb GM-CSF enhancer

Results shown so far imply that PMA/I activates NF-κB through its phosphorylation at Ser276 and this activation seems to be mediated by MSK1. The GM-CSF promoter encompasses an NF-κB site and the GM-CSF enhancer also contains a NF-κB/NFAT binding motif, suggesting that NF-κB pathway might have a role in GM-CSF gene regulation.

Unpublished data from luciferase assays performed in Peter Cockerill's laboratory showed that modification of the κB/NFAT binding site at GM220 significantly decreases the enhancer activity in Jurkat cells. Holloway et al. [319] already demonstrated the importance of NF-κB in the GM-CSF promoter chromatin remodelling, showing that NF-κB recruits Brg1-containing complexes to the promoter in T cells and that low levels of NF-κB in the nucleus lead to a reduction in GM-CSF gene transcription.

For all these reasons I decided to inhibit the canonical NF-κB pathway by using the proteasome inhibitor MG132 during PMA/I-induced GM-CSF gene expression.

I pre-treated Jurkat and KG1a cells with increasing doses of MG132, prior stimulation for 4 hours with PMA/I, in order to find doses capable at significantly reducing PMA/I-induced GM-CSF gene expression. qRT-PCR analysis in Figure 3.37 shows that 1 μM MG132 almost totally inhibited the PMA/I-induced GM-CSF mRNA levels in Jurkat whereas a dose of 5 μM was required to reduce gene expression down to the level of untreated cells. MG132 seemed to be less effective in KG1a cells, because 1 μM ad 2.5 μM decreased GM-CSF gene expression by 70% and 85% respectively, whereas only the highest concentration tested (5 μM) completely abolished the GM-CSF gene expression induced by PMA/I. These results confirm the involvement of NF-κB pathways in PMA/I-induced GM-CSF gene expression in Jurkat and KG1a cells.

In order to test the effect of the proteasome inhibitor MG132 on the PMA/I-induced chromatin remodelling at GM-CSF enhancer, I mapped the DHSs in an EcoR I fragment in DNase I-digested nuclei by Southern blot as described previously. I pre-treated Jurkat and KG1a cells for 1 h with 1 μM and 5 μM MG132 respectively, doses shown to completely (or almost completely) inhibit the PMA/I-induced GM-CSF expression. As I observed previously after treatment with the MSK inhibitor H89, the two cell lines showed different results. In fact, treatment with MG132 resulted in a loss of the DHS at the GM-CSF enhancer in Jurkat, whereas it did not affect DHS formation in KG1a cells (Figure 3.38).

These results suggest again that, in the two cell lines, two different protein complexes might be present at the GM-CSF enhancer after PMA/I stimulation and confirm an important role for NF-κB pathway in the regulation of chromatin remodelling at the GM-CSF enhancer induced by PMA/I in Jurkat T cells.

Figure 3.37 ***Effect of the proteasome inhibitor MG132 on the PMA/I-induced GM-CSF gene expression in Jurkat and KG1a cells***

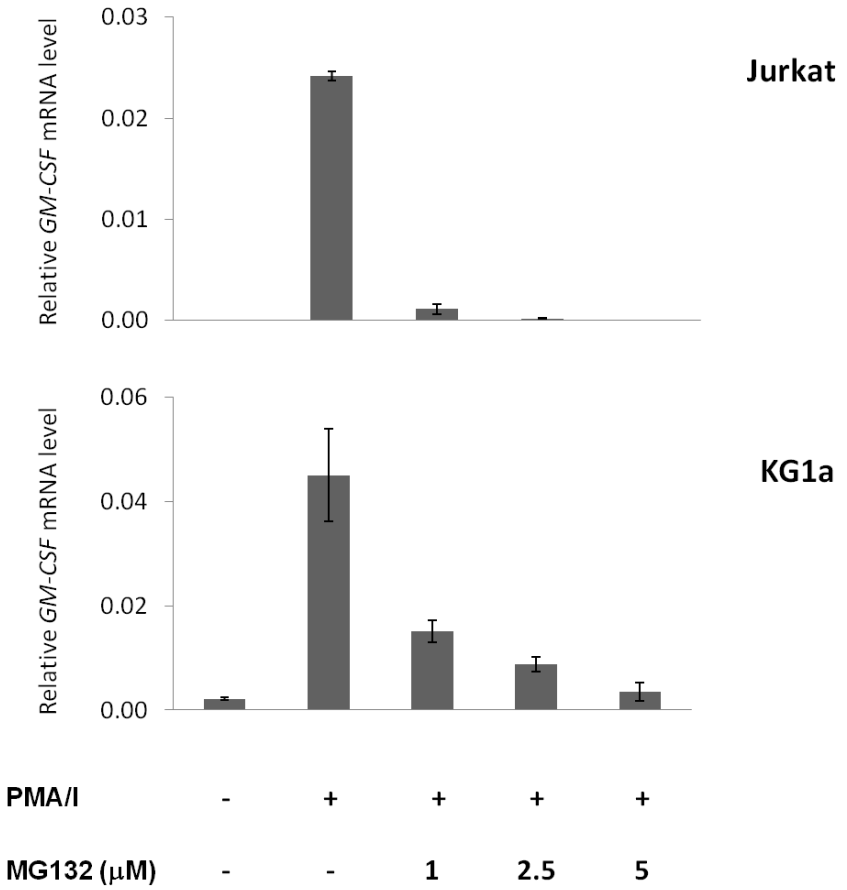

qRT-PCR showing GM-CSF gene expression after pre-treatment of Jurkat and KG1a cells with increasing doses of MG132 and an induction with 20 ng/ml PMA and 2 μM ionophore A23187 (PMA/I) for 4 hours. The y-axis shows GM-CSF gene expression relative to *GAPDH* gene expression. Each bar represents the average of three independent repeats and the error bars represent SE.

Figure 3.38. ***Effect of the proteasome inhibitor MG132 on the PMA/I-induced chromatin remodelling at the GM-CSF enhancer in Jurkat and KG1a cells***

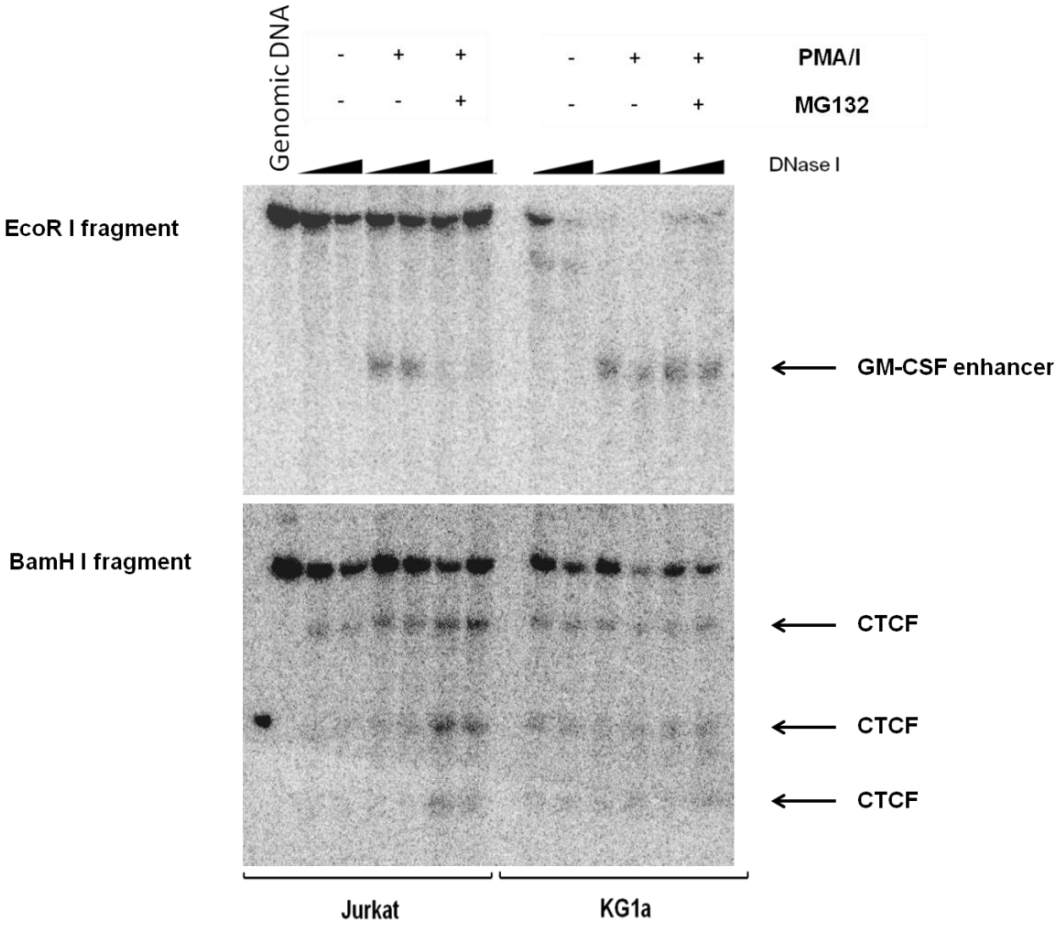

Mapping of DHSs within GM-CSF enhancer and promoter in a 9.4 kb EcoR I fragment and in a 4.6 kb BamH I fragment downstream of the IL3 gene showing three constitutive CTCF sites. Cells were pre-treated with MG132 (1 μM for Jurkat and 5 μM for KG1a) for 1h and then stimulated for 4h with 20 ng/ml PMA and 2 μM ionophore A23187 (PMA/I). Black triangles indicate increasing concentrations of DNase I; genomic DNA was used as control.

3.23 MSK1 and NF-κB are recruited at the GM-CSF enhancer by treatment with PMA/I in KG1a cells

In previous sections, I demonstrated a connection between MAPK pathways and NF-κB pathways, showing that MSK1 phosphorylates p65 at Ser276 in PMA/I-stimulated cells and also that MAPK inhibitors can reduce this phosphorylation. Since the GM-CSF enhancer encompasses a NFAT/κB binding site (GM220), I wondered whether the two transcription factors could be recruited to the GM-CSF enhancer after PMA/I induction. To answer this question, I performed a ChIP assay on KG1a cells either treated with PMA/I or pre-treated with inhibitors as described previously. Untreated cells were used as control. In KG1a cells, both MSK1 and NF-κB occupancy increased by about five fold after PMA/I stimulation, compared to untreated cells. Treatment with MEK and p38 MAPK inhibitors in combination reduced the level of enrichment down to the level of untreated cells (Figure 3.39A). MSK1 occupancy was measured at the NF-κB binding site within the enhancer (GM220) and treatment with the MSK inhibitor H89 reduced NF-κB occupancy at this site by about 70% (similar to the combination of MAPK inhibitors). This might suggest a direct interaction between the two transcription factors. Since I demonstrated that MSK1 phosphorylates NF-κB at Ser276 and this phosphorylation promotes the recruitment of the co-activator p300/CBP [243], I next performed a ChIP analysis to test whether the MSK1 inhibitor H89 had an effect on the PMA/I-induced p300 recruitment to the enhancer at GM220. The inhibitory effect shown by H89 (about 55% compared to PMA/I-treated cells) demonstrates that MSK1 is likely to induce recruitment of p300 at the GM220 (NFAT/κB site), probably through the phosphorylation of NF-κB p65 at Ser276 (Figure 3.39B).

Figure 3.39 ***MSK1 and NF-κB p65 are recruited at the GM-CSF enhancer by PMA/I stimulation in KG1a cells***

A

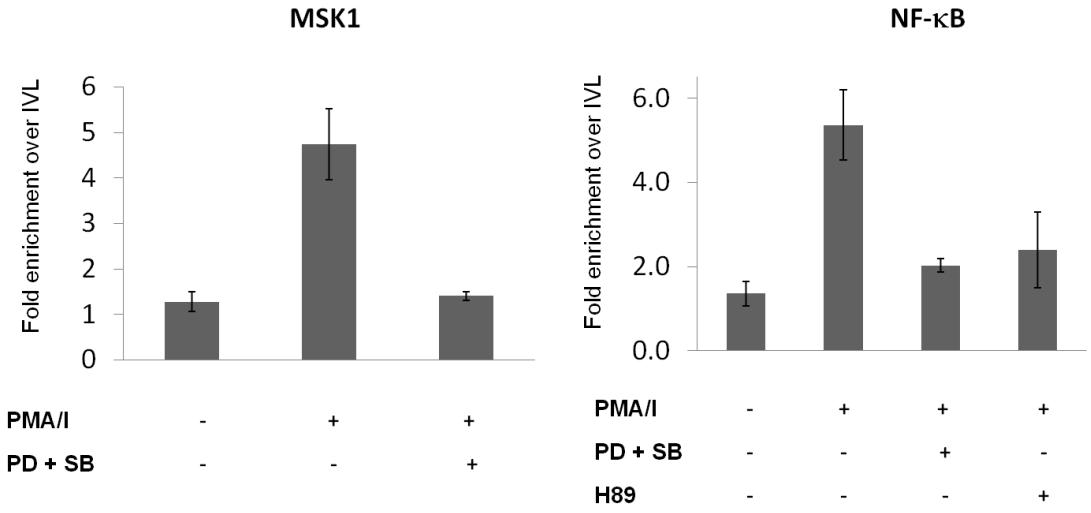

B

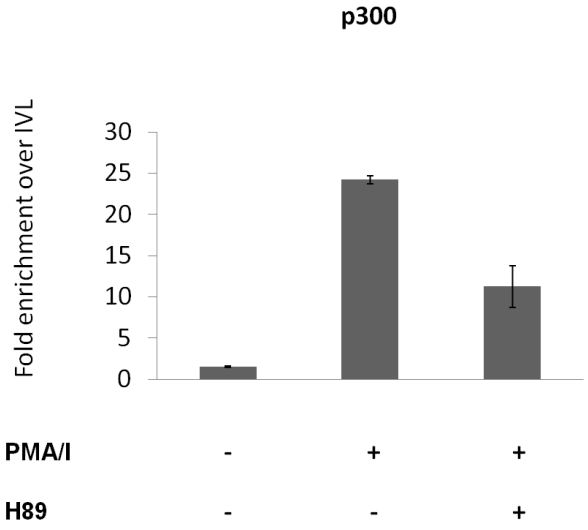

ChIP-qPCR showing relative A) MSK1, NF-κB p65 and B) p300 enrichment at the GM-CSF enhancer in KG1a cells after 1.5 hours PMA/I stimulation and 1h pre-treatment with H89 (MSK1 inhibitor) or with the combination of PD98059 (MEK inhibitor) and SB202190 (p38 inhibitor). Parallel control IgG precipitations gave values comparable to background levels (not shown). The Y-axis shows relative enrichment compared to IVL. Each bar represents the average of at least three independent experiments. Error bars represent SE.

3.24. MSK1 does not seem to be responsible for the PMA/I-induced *FOS* gene transcription in Jurkat and KG1a cells

I previously showed that PMA/I treatment increases the expression of several AP-1 components, including *FOS*, and this increase is MAPK-dependent. I also showed that some of the effects of the combination of MEK and p38 inhibitor on PMA/I-induced GM-CSF gene expression are mediated by their mutual target MSK1. MSK1 have been reported to phosphorylate H3 at Ser10 at *FOS* promoter, inducing its transcriptional activation [320, 321]. Therefore, I wonder whether MSK1 could be in part responsible for the increase in *FOS* transcription mediated by PMA/I. To investigate this, I measured the levels of *FOS* gene expression by qRT-PCR. I pre-treated the cells for 1 h with MSK inhibitor H89 (10 μM) before PMA/I stimulation for 45 minutes. Treatment with H89 not only failed to decrease *FOS* gene expression (Figure 3.40), but it seemed to cause a small increase in KG1a cells, albeit not significant.

I also performed an EMSA to check whether the H89 inhibitor can reduce the PMA/I-induced AP-1 binding already demonstrated in the cell lines. In Jurkat cells, treatment with H89 decreased the PMA/I-induced AP-1 binding whereas it didn't show any inhibitory effect on KG1a cells (Figure 3.41A and B). The reduction in AP-1 DNA binding in Jurkat could be due to an inhibitory effect of MSK1 on different components of AP-1, or it could be mediated by PKA, since also this kinase is inhibited by H89.

These results show that the PMA/I-mediated increase of *FOS* expression seems not to be mediated by MSK1 in both cell lines. On the contrary, MSK1 or PKA (H89 is also a PKA inhibitor) seem to regulate the induction of AP-1 in Jurkat cells. Further analysis would be needed to verify this hypothesis and also to find out which AP-1 components are involved.

Figure 3.40 ***H89 fails to reduce FOS gene expression in Jurkat and KG1a cells***

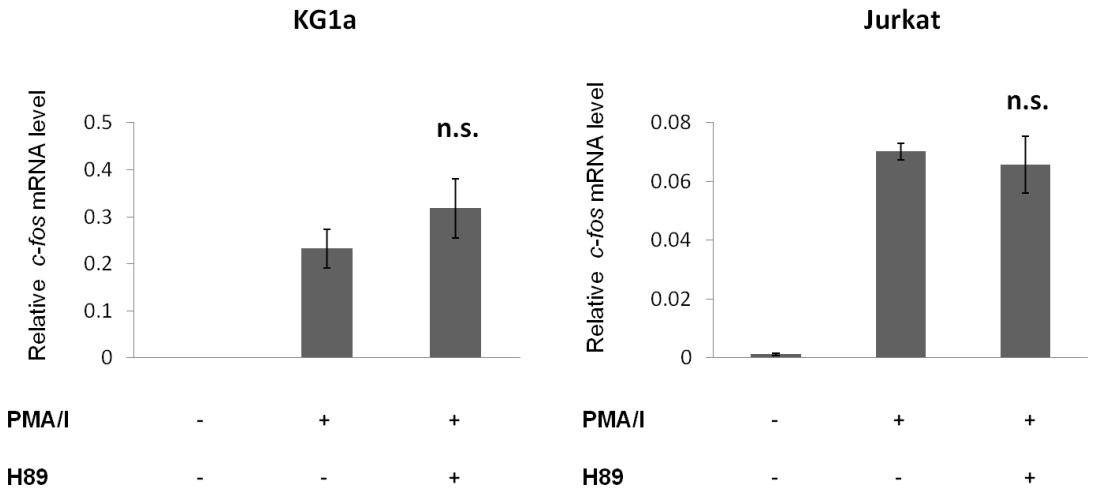

qRT-PCR showing GM-CSF gene expression after pre-treatment of Jurkat and KG1a cells with H89 10 μM for 1h and an induction with 20 ng/ml PMA and 2 μM ionophore A23187 (PMA/I) for 45 minutes. The y-axis shows GM-CSF gene expression relative to *GAPDH* gene expression. Each bar represents the average of at least three independent repeats and the error bars represent SE. n.s. = student's *t*-test value > 0.05 between the group of samples treated with PMA/I and the ones pre-treated with H89.

Figure 3.41 ***H89 effect on the PMA/I-induced AP-1 DNA binding ability***

A Jurkat

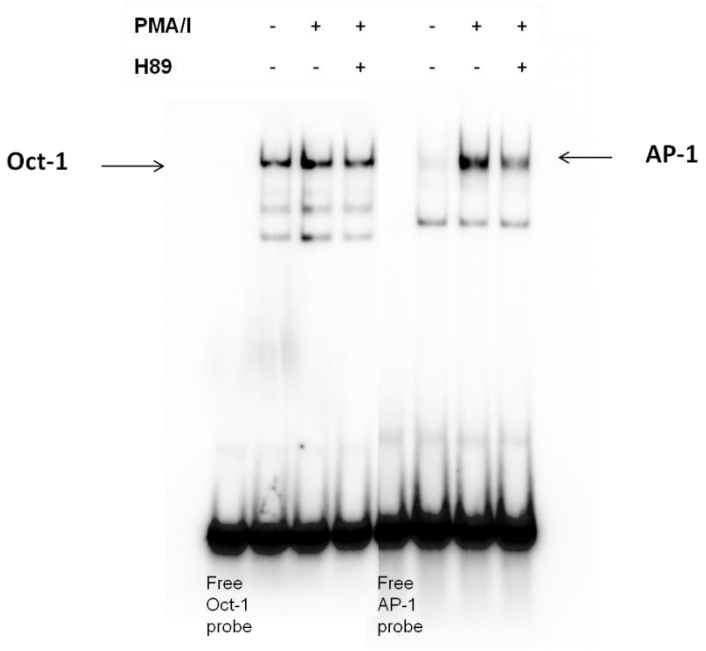

B KG1a

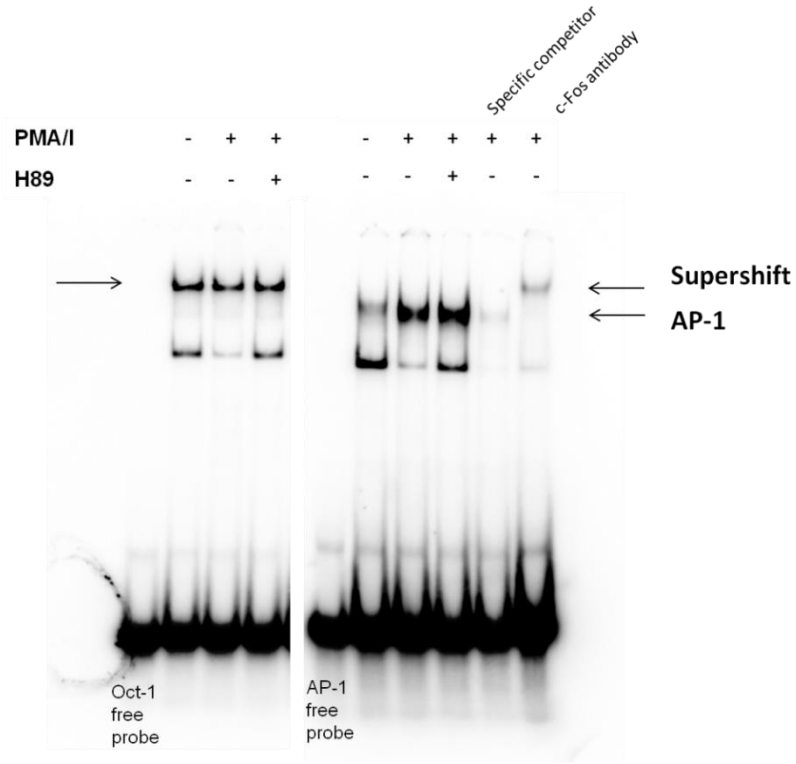

EMSA assay to detect AP-1 binding performed on nuclear extracts of Jurkat (A) and KG1a (B) cells. The EMSA to detect Oct-1 binding was performed as loading control. In B) the supershift assay has been performed using a specific c-Fos antibody**.**

3.25 MAPK inhibitors and CsA do not induce chromatin remodelling in HEL cells but inhibit the PMA/I-induced GM-CSF gene expression

So far I used as model for GM-CSF regulation three different cell types (Jurkat, KG1a and murine T blast cells) which all show an inducible DHS at the GM-CSF enhancer. In contrast to these cell types, untreated erythroleukaemic HEL cells already show a constitutive DHS at the enhancer, as has been observed in a high proportion of AML cells from patients (unpublished data from the Cockerill laboratory). These cells also have a DHS between -4.1 and -4.3 kb, as has also been observed in cells derived from AML patients [246].

To get an idea of which signalling pathways mediate the creation of this DHS, I treated HEL cells for 4h and 8h with MAPK inhibitors and Cyclosporin A (CsA), a calcineurin phosphatase inhibitor, testing concentrations already used on the other cell lines. Then I performed a Southern blot analysis, using the strategy already described, mapping the DHSs in an EcoR I in DNase I-digested samples. Results showed that none of the drugs used inhibited the constitutive DHSs at the enhancer or at -4.1 kb (Figure 3.42). Since HEL cells don't express high levels of the GM-CSF gene, I had to stimulate them with PMA/I for 4h after 1h pre-treatment with the inhibitors, as already described. Treatment with PMA/I led to over 100 fold induction in GM-CSF gene expression. Surprisingly CsA and the p38 inhibitor SB202190 decreased GM-CSF gene expression down to control levels (Figure 3.43), whereas the MEK inhibitor PD98059 reduced it by around 80%. The effect of the MEK and p38 inhibitor together couldn't be determined because p38 inhibitor alone already abolished GM-CSF gene expression. Lower doses of both inhibitors should have been used to estimate

their possible cooperative/synergistic effect on the reduction of GM-CSF mRNA levels.

Figure 3.42 ***Effect of inhibitors on GM-CSF chromatin structure in HEL cells***

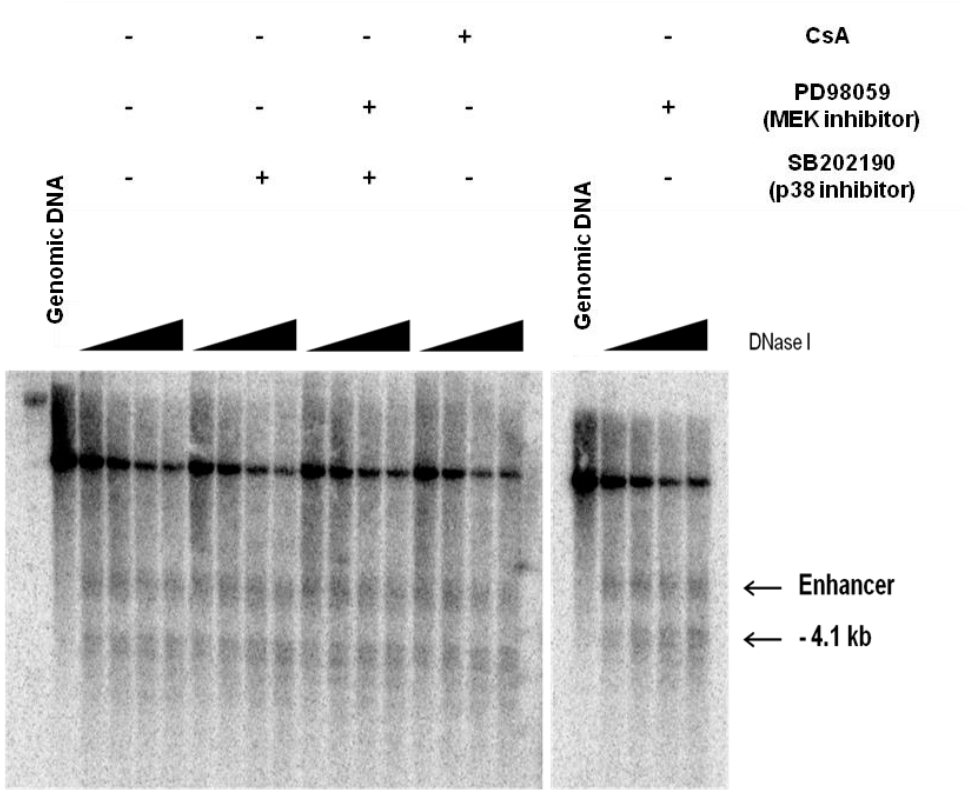

Mapping of DHSs within the GM-CSF enhancer in a 9.4 kb EcoR I fragment. HEL cells were treated with the inhibitors for 8h (MEK1 inhibitor, PD98059 50 μM, p38 inhibitor, SB202190 25 μM, CsA 0.1 μM).

Figure 3.43 ***Effect of inhibitors on GM-CSF gene expression in HEL cells***

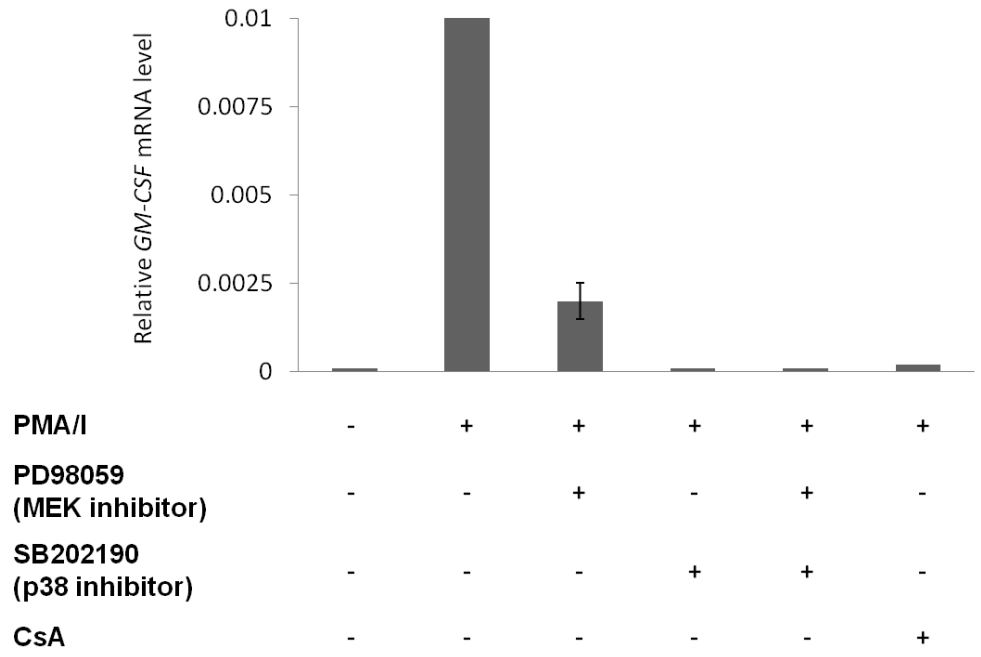

qRT-PCR analysis to measure human GM-CSF mRNA levels after 1h pre-treatment of HEL cells with MAPK inhibitors (MEK inhibitor, PD98059 50 μM, p38 inhibitor, SB202190 25 μM) or CsA 0.1 μM and 4h stimulation with 20 ng/ml PMA and 2 μM ionophore A23187 (PMA/I). GM-CSF gene expression is relative to *GAPDH* expression. Each bar represents the average of at least three independent repeats. Error bars represent SE.

These results demonstrate that GM-CSF transcription is MAPK and Ca^{2+} dependent, whereas its chromatin remodelling at the enhancer is not, suggesting distinct mechanisms of regulation in HEL cells.

3.26 RUNX1 is present at both -3 kb and -4.1 kb DHSs in HEL cells

The GM-CSF enhancer is also known to interact with the constitutively expressed factor RUNX1, but only after induction of the DHS in other cell types where the DHS is inducible [280]. The DHS at -4.1 kb also contains several potential RUNX1 binding motifs which have not been investigated in previous studies.

Since neither the treatment with MAPK inhibitors nor CsA inhibited chromatin remodelling at -3 kb and/or -4.1kb DHS in HEL cells, I decided to perform a ChIP assay at both sites to verify the presence of the transcription factor RUNX1, whose recruitment is likely to be independent on MAPK and Ca^{2+} signalling pathways. Results confirmed the presence of RUNX1 at both DHSs (Figure 3.44). RUNX1 occupancy at the -4.1 kb DHS was comparable to the one measured at the upstream PU.1 enhancer, used as positive control. In fact the PU.1 enhancer element is bound by RUNX1 at multiple sites and this binding is essential for enhancer activity [322, 323].

These results suggest a completely different composition of the protein complex present at the GM-CSF enhancer in HEL cells compared to cells where the DHS is inducible (e.g. T blasts, Jurkat and KG1a cells) and this might be the reason why in HEL cells the DHS at the GM-CSF enhancer is not sensitive to either MAPK inhibitors or the Ca^{2+} signalling inhibitors CsA. This same pattern may exist in AML cells where these two DHSs are observed.

Figure 3.44 ***RUNX1 occupancy at -3 kb and -4.1 kb DHSs in HEL cells***

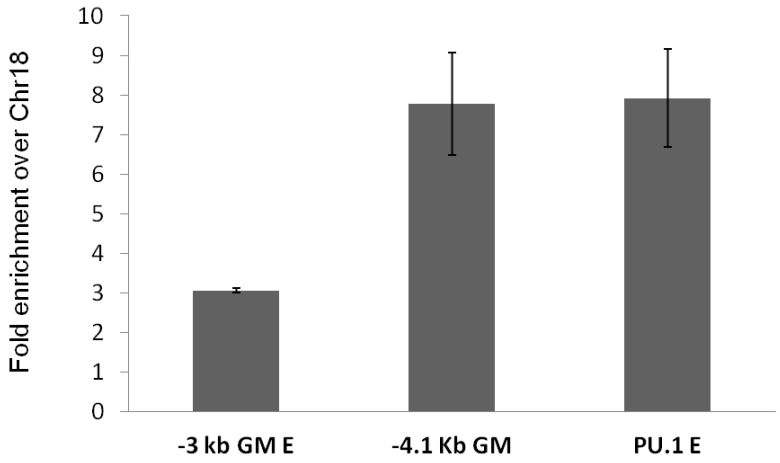

ChIP-qPCR showing relative RUNX1 enrichment at the -3 kb enhancer (E) and -4.1 kb DHSs in the GM-CSF locus in HEL cells. Parallel control IgG precipitations gave values comparable to background levels (not shown). The Y-axis shows relative enrichment compared to the gene desert region Chr18. Bars represents the average of at least three independent experiments. Error bars represent SE.

4. DISCUSSION

In this study I investigated the role of signalling pathways in the regulation of the IL-3/GM-CSF locus, analysing in particular the expression and chromatin structure of the GM-CSF gene. The models I used were activated T blast cells, which normally produce GM-CSF when stimulated, plus the Jurkat T-ALL-derived cell line and the KG1a AML-derived cell line, which can both be induced to express GM-CSF. We wanted to gain an understanding of pathways that activate the GM-CSF locus because several papers [259-261] demonstrated that AML blast cells produce high levels of GM-CSF, which can in turn activate its own receptor to support blast cell growth and proliferation in an autocrine or paracrine way. In some cases of AML, GM-CSF production may be the result of the constitutive activation of a surface receptor such as FLT3 of cKIT, or components of signalling pathways such as RAS. In KG1a cells, the -3 kb GM-CSF enhancer is inducible upon stimulation with PMA and a calcium ionophore (PMA/I) and this is associated with an increase of GM-CSF mRNA levels. The enhancer is also inducible in activated T blast cells and in the leukaemic cell line Jurkat. T cells were used in this study to find similarities and differences in the regulation of GM-CSF gene between normal blood cells and leukaemic cells. The T blast cells used in this study were derived from transgenic mice, which contain six copies of an Age I fragment encompassing the entire IL3/GM-CSF locus and for this reason produce high levels of GM-CSF following TCR activation. Jurkat cells are derived from a T-ALL leukaemia and they have been used over the years to better understand the TCR signalling, because of their similarities with primary T cells [324]. The activation of kinase signal pathways, mediated by PMA, along with the Ca^{2+}-dependent signal pathway triggered by

calcium ionophore, induces a robust TCR activation response, with a strong production of IL-2 and an increase of the free intracellular Ca^{2+} concentration [325, 326]. A similar TCR artificial stimulation can be achieved by using a combination of antibodies anti-CD3 and anti-CD28. The choice to use PMA/I was based on the results obtained by Smeets et al. [327], who showed that PMA/I treatment induces a stronger activation of MAPK pathways together with a stronger and faster release of intracellular Ca^{2+} in Jurkat cells, compared to a CD3/CD28 stimulation. A more pronounced response is in fact ideal to study the effect of inhibitors. According to Smeet's study the nuclear translocation of NF-κB is similar upon the two different stimulations.

In all the three models, I verified the phosphorylation of ERK, p38 and JNK MAPKs after treatment with PMA/I. I then tested different inhibitors, alone or in combination, to find which pathways are more relevant to GM-CSF gene regulation, in terms of transcription and chromatin remodelling.

Cockerill at al. [289] have already demonstrated that the DHS at the GM-CSF enhancer is highly inducible in T cells and is inhibited by CsA. In this study I demonstrated that another inhibitor of the Ca^{2+} signal pathways, the NFAT inhibitor 11R-VIVIT, did not reduce the DHS at the enhancer in T blast cells when used at 10 μM. Both CsA and 11R-VIVIT lead to the inhibition of the NFAT signalling pathway, preventing the transcription of cytokine genes, including GM-CSF [328, 329]. CsA is a chemical compound which strongly inhibits calcineurin phosphatase activity, whereas 11R-VIVIT is a cell-permeable peptide which inhibits the interaction between NFAT and calcineurin, resulting in competitive inhibition of NFAT signalling pathway. The presence of 11 residues of arginine (11R) improves cell permeability. However, 11R-VIVIT does not affect calcineurin phosphatase activity nor does it interfere with

calcineurin-dependent pathways, such as NF-κB pathway [278]. CsA has been demonstrated to interfere with the calcineurin-dependent NF-κB activation by inhibiting the transcriptional induction of the p50 subunit and the c-Rel protein and by reducing IκB degradation [330]. The 11R-VIVIT NFAT selective specificity could explain why this compound showed a very weak effect in reducing GM-CSF gene expression and chromatin remodelling at the enhancer in T blast cells. My results are in contrast with the observations of Aramburu et al. [278], who demonstrated that transfection of Jurkat cells with GFP-VIVIT greatly reduced the PMA/I-dependent GM-CSF gene expression. However, Aramburu tested the compound on a cell line, whereas I tested it on activated T blasts and this could explain the different results. After a first analysis of the Ca^{2+} signalling pathway, I focused on the kinase activation induced by PMA/I.

I first verified the phosphorylation of the three main MAPK pathways (MEK/ERK, p38 and JNK) before and after treatment with PMA/I. Western blot analysis showed a PMA/I-induced phosphorylation of the three proteins. However, low levels of ERK1/2 and p38 phosphorylation were already detectable in T blasts, maybe due to the fact that cells were cultured in presence of IL-2, which has mitogenic effects and is able to activate MAPK signalling. Instead, the leukaemia cell line KG1a showed high levels of p38 phosphorylation, as already demonstrated by Kale et al. [295], in line with the observation that cancer cells often show constitutive activation of signalling pathways. Jurkat cells seemed to show constitutive low levels of JNK/SAPK phosphorylation.

Previous studies already demonstrated that treatment with PMA/I leads to a stronger activation of p38 and JNK MAPKs, compared to PMA alone, at least in Jurkat cells, whereas ERK1/2 activation is comparable [327]. Importantly, KG1a

cells do not differentiate upon PMA/I treatment, which is distinct from the similar myelomonocytic $CD34^+$ KG1 cells, which instead differentiate into dendritic-like cells [331].

In this study MAPK inhibitors reduced the PMA/I-induced GM-CSF gene expression and chromatin remodelling at the enhancer. In fact, in Jurkat and KG1a cells, high doses of single MAPK inhibitors greatly decreased PMA/I-induced GM-CSF gene expression. In primary transgenic T blast cells the single inhibitors were less effective than in cell lines. The p38 inhibitor, SB202190 was the most effective in reducing GM-CSF mRNA levels whereas high doses of the JNK inhibitor, SP600125 were almost ineffective. The results obtained from western blot analysis do not give precise information about the total amount of MAPK proteins in the cells, but it can be speculated that the poor efficacy of SP600125 on T blast cells could be in part due to the predominant activation of MEK/ERK and p38 in response to PMA/I treatment.

Amongst the combinations tried, the combination of MEK plus p38 inhibitors showed the strongest effect in reducing GM-CSF gene expression. DHS analysis in T blast cells demonstrated that the combination of MEK and p38 inhibitors reduced the formation of the DHS at the GM-CSF enhancer by around 50%. Interestingly, the addition of JNK inhibitor, SP600125 to this combination did not increase this effect. The same inhibitory effect on PMA/I-induced GM-CSF gene expression and chromatin remodelling was also confirmed in Jurkat cells and KG1a cells.

DHS analysis of the three cell models showed different effects of the inhibitors on the DHS located 4.5 kb downstream of the IL-3 promoter. This region has been demonstrated to be inducible in myeloid progenitor cells and Jurkat cells and it represents a non-coding promoter in Jurkat cells [264]. In this study, I

demonstrated that the +4.5 kb DHS could be detected in T blast cells prior to any stimulation (although PMA/I treatment clearly enhanced chromatin remodelling) and it was partially inhibited by CsA; on the other hand, the DHS was completely inhibited by the combination of MEK and p38 inhibitors in KG1a cells, but not in T blast cells. These results showed again a further difference between activated T cells and myeloid cells in GM-CSF gene regulation. Further experiments would be needed to find out the role of this DHS in myeloid cells and which signalling pathways are involved in its regulation.

Although high doses of the JNK inhibitor SP600125 could reduce the PMA/I-induced GM-CSF gene expression and also the PMA/I-induced c-Jun phosphorylation in Jurkat and KG1a cells, I decided to keep studying the combination of MEK and p38 inhibitors in the cell lines because of its powerful effect shown on T blast cells. In fact it is not unusual to find different results between primary cells and cell lines, which often carry gene mutations/translocations or show constitutively activation of protein signalling pathways.

To make sure that the reduction of GM-CSF gene expression was due to the specific inhibition of MAPK pathways and not to off-target effects of the inhibitors, I also used specific ERK1/2 and p38 siRNAs as well as two alternative MEK and p38 inhibitors, U0126 and SB203580. Caution has to be used when dealing with chemical compounds because these ‘specific’ inhibitors might also act on other kinases. SB202190 and its close relative SB203580 have been used in numerous of reports to study the physiological roles of p38*α* and p38*β* MAPKs [332]. Although these compounds are still used, more recent studies showed that they can inhibit other kinases with similar or greater potency [333]. SB203580 also inhibits c-Raf and GSK3 *in vitro* [334]. Bain and

colleagues [332] reported that, at the same dose, SB202190 is slightly more effective than SB203580 in inhibiting p38*α* and p38*β* MAPK activity. In terms of selectivity, in the same study both SB202190 and SB203580 were reported to inhibit in part JNK activity, but not ERK1 and ERK2. A slight reduction of MEK and ERK1/2 activity was reported for SB203580. PD98059 and U0126 are non-competitive inhibitors that interact mainly with the complex enzyme-substrate, thus preventing the phosphorylation of MEK and/or the conformational change that leads to the activated kinase [335, 336]. In their study, Ahn and colleagues compared the activity of PD98059 and U0126 and they found that U0126 inhibited MEK1 kinase activity at a lower concentration than PD98059 [337]. These findings are in line with the results obtained in KG1a cells because, as shown in Figure 3.11, I used a lower dose of U0126 compared to PD98059 to inhibit GM-CSF gene expression. In terms of selectivity, these two MEK inhibitors seem not to interfere significantly with either p38 or JNK activity. Just a small inhibitory effect on JNK2 kinase activity was reported by U0126 [332]. In this study neither the MEK inhibitor PD98059 nor p38 inhibitor SB202190 decreased JNK phosphorylation in KG1a cells. On the contrary, inhibition of the MEK/ERK pathway seemed to stimulate the p38 pathway and *vice versa*. A similar effect was already reported by Hirosawa at al., who demonstrated that SB202190 was able to activate MEK/MAPK to stimulate the growth of leukaemia cells [296].

To further avoid any possible effect due to the non-specificity or cross-reactivity of the inhibitors, I decided to also knockdown ERK and p38 pathways by using siRNAs. The inhibition of the PMA/I-induced GM-CSF gene expression obtained with the use of siRNAs mirrored the ones obtained with MEK and p38 inhibitors,

concluding that in Jurkat and KG1a leukaemia models the PMA/I-induced GM-CSF gene expression is MEK/ERK and p38 MAPK-dependent.

As already mentioned, essential for GM-CSF enhancer activity is the cooperation between the Ca^{2+} signalling pathway, mediated by NFAT, and the kinase signalling pathways, mediated by AP-1. The AP-1 family of transcription factors assemble as homodimers and heterodimers of Jun, Fos or activating transcription factors (ATFs). Jun and ATF can form both heterodimers and homodimers, but Fos cannot form homodimers. Jun-Jun and Jun-Fos dimers prefer to bind to the PMA-responsive element TGA(C/G)TCA. Jun-ATF and ATF dimers preferentially bind to the cAMP-responsive element TGACGTCA (CRE) [338]. Fos-Jun heterodimers have higher stability than Jun-Jun homodimers and therefore they have an increased DNA binding activity [339]. ATF-2 and c-Fos are mainly p38 and ERK targets. The activation of ERK and its downstream targets such as 90K-ribosomal S6 kinase (RSK) leads to the phosphorylation of multiple residues in the carboxy-terminal transactivation domain of c-Fos, which results in its increased protein stability and transcriptional activity [340, 341]. Moreover ERK can phosphorylate and activate Elk1, which binds the serum responsive element (SRE) at the *FOS* promoter, stimulating its transcriptional activity [165]. p38 MAPK [186] and JNK have also been reported to phosphorylate Elk1 upon their activation by different stimuli [299]. In this study, I demonstrated that PMA/I stimulation induces Elk1 phosphorylation in KG1a cells and this phosphorylation is ERK-dependent but not p38-dependent. It is likely, therefore, that Elk1 binding to the *FOS* promoter is responsible for the increase of *FOS* gene expression in KG1a cells. c-Jun is preferably a JNK target, although it can be phosphorylated and activated also by ERK [298] and p38 [342]. My results showed that in both KG1a and Jurkat cells the PMA/I-

mediated c-Jun phosphorylation is both ERK- and JNK-dependent (Figure 3.16). Phosphorylation of Ser63 and Ser73 in the c-Jun transactivation domain are known to increase c-Jun activity [343, 344]. The formation of the more stable Jun-Fos heterodimer is likely prevented when both MEK and p38 pathways are inhibited and this might in part explain why these two pathways are so relevant for GM-CSF gene regulation in the models used in this study. In fact results from qRT-PCR analysis demonstrated that the two inhibitors synergistically decreased both *FOS* and *JUN* gene expression in activated T blast cells and leukaemia cell lines. Interestingly, whereas p38 inhibitor reduced both c-Fos and c-Jun expression (both protein and mRNA level) in all the three cell models, MEK inhibitor had no effect on *JUN* expression in either T blast cells or KG1a cells- Moreover, whereas it did not reduce *FOS* expression in Jurkat cells. This might in part explain the stronger effect of p38 inhibitor in reducing GM-CSF gene expression. The controversial results shown in Figure 3.16A, where a significant decrease in c-Jun expression is detected after PD98059 treatment, might be explained by the different duration of PMA/I stimulation. It is possible that the reduction in c-Jun expression could be appreciated after a longer PMA/I stimulation (2 hours or longer). It is also notable that there are different mRNA levels between the PMA/I-induced *FOS* and *JUN* in the different cell types. Jurkat cells showed a similar level of *FOS* and *JUN* gene expression after PMA/I stimulation, whereas T blast cells and KG1a cells showed a strong predominance of *FOS* gene expression over *JUN* gene. However, both c-Fos and c-Jun proteins could be detected in the EMSA supershift assay in the two cell lines, indicating that they are both responsible for AP-1 DNA binding.

However, in this study, I didn't investigate the possibility of p38 to phosphorylate and activate c-Jun, as previously demonstrated by Humar et al. [342] in T lymphocytes. This could explain why the p38 inhibitor SB202190 decreases *JUN* expression levels. AP-1 relevance on GM-CSF gene regulation has been confirmed by the siRNA-mediated c-Jun knockdown, which caused a significant decrease in the PMA/I-induced GM-CSF gene expression.

I also measured the mRNA level of other Fos and Jun family proteins. The combination of MEK and p38 inhibitors was more effective on Jurkat than KG1a cells in inhibiting the expression of AP-1 proteins and this could in part explain why they showed a stronger effect also in reducing GM-CSF mRNA levels in Jurkat cell line.

After measuring mRNA expression of AP-1 components, I performed an EMSA assay to test the AP-1 DNA binding ability to the DNA. My results showed that PMA/I treatment strongly induced the AP-1 binding to the DNA and this was reduced by the combination of MEK and p38 inhibitors in T blast cells, Jurkat and KG1a cells. The EMSA band representing AP-1 binding to DNA in untreated T blast cells and KG1a cells reflects the activation of MAPK pathways in these cell types. However, the intensity of the bands seen in EMSA and western blots, and sometimes even their presence, are highly dependent on the duration of exposure of the membrane. In fact c-Jun protein levels are already detectable in untreated Jurkat cells and this could suggest a possible constitutive activation of the JNK pathway. On the other hand, neither c-Fos nor c-Jun protein was detected in untreated KG1a cells, despite the high levels of p38 phosphorylation already detected. However, to better study the activation of these signalling pathways, an analysis of the MAPK protein kinases activity and c-Fos and c-Jun phosphorylation should be performed.

The AP-1 EMSA analysis were performed using an oligonucleotide duplex probe derived from the stromelysin gene containing the perfect AP-1 consensus sequence TGAGTCA. A more specific analysis should be conducted by using an oligonucleotide spanning either just the AP-1 site from the GM330 enhancer region (also containing a perfect AP-1 binding motif) or one of the composite NFAT/AP-1binding motifs, such as the GM420 region.

Both in Jurkat cells and in T blast cells, the single inhibitors did not significantly reduce AP-1 binding to the DNA (especially the MEK inhibitor), whereas they had a stronger effect in KG1a cells. The ineffectiveness of the MEK inhibitor in T blast cells and in Jurkat cells mirrors could be due to the fact that PD98059 did not reduce neither the PMA/I-induced *JUN* gene expression in T blast cells nor the induced *FOS* gene expression in Jurkat cells. PD98059 did not reduce *FOS* protein levels in Jurkat cells either, whereas it was more effective in KG1a cells and this could explain why this inhibitor reduced AP-1 DNA binding in KG1a cells but not in Jurkat cells. On the other hand, the p38 inhibitor SB202190 was more effective in reducing *FOS* and *JUN* mRNA and protein levels in both cell lines and this might explain why it had a stronger effect than the MEK inhibitor in reducing the level of PMA/I-induced AP-1 DNA binding activity.

ChIP analysis showed that treatment with PMA/I leads to the recruitment of both c-Fos and c-Jun to chromatin *in vivo* and this was reduced by the combination of MEK and p38 inhibitors. These results suggest that PMA/I treatment induces GM-CSF gene expression and chromatin remodelling at the enhancer via ERK1/2 and p38 MAPK-dependent AP-1 activation. This study complements earlier work showing that the calcium-dependent induction of NFAT was also required for GM-CSF gene expression and chromatin

remodelling [289], and it helps to explain the inhibitory actions of transcription and translation inhibitors observed in this study.

Since several reports showed that AP-1 can regulate gene transcription by interacting with the histone acetyltranferase p300 [300, 301], I investigated the putative role of p300 in the PMA/I-induced GM-CSF gene expression by using its specific inhibitor, C646. Results from qRT-PCR analysis confirmed that PMA/I-induced GM-CSF gene expression is dependent on p300 in Jurkat cells and KG1a cells. I also demonstrated that p300 is recruited at GM-CSF enhancer *in vivo* after PMA/I stimulation and this is associated with an increase of global histone H3 acetylation in KG1a cells and H3K27 acetylation in both cell lines. H3K27ac has been reported to mark active enhancers and has been often observed at p300 positive enhancers [304]. However, the p300 inhibitor, C646 failed to reduce the DHS at the enhancer, suggesting that p300 is recruited to chromatin by other transcription factors after the DHS is formed.

The strong effect of the combination of MEK and p38 inhibitors seen in this study could be in part explained by the fact that both MEK/ERK and p38 pathways can activate the nuclear kinases MSK1/2. MSK1/2 are nuclear serine/threonine protein kinases which can phosphorylate several substrates, including NF-κB [203], histone H3 [307] and CREB [308, 309], mediating the transcriptional activation of several genes. My results showed that MSK1 is strongly phosphorylated by PMA/I treatment and this phosphorylation is mediated by both ERK and p38 MAPKs. I demonstrated that MSK1 is likely to be involved in PMA/I-induced GM-CSF gene expression, by showing that both the MSK/PKA H89 inhibitor and a specific MSK1 siRNA reduced GM-CSF mRNA levels. The effect of MSK1 inhibition on the PMA/I-induced GM-CSF gene expression seemed to be stronger in Jurkat cells than in KG1a cells. In

fact, treatment with the MSK inhibitor H89 decreased gene expression just by 50%, against the 80-90% reduction obtained after the treatment with MEK1 and p38 inhibitors, suggesting the involvement of other transcription factors in addition to AP-1 in the KG1a model.

Moreover, H89 reduced the induction of the DHS at the GM-CSF enhancer in Jurkat cells but not in KG1a cells, suggesting the presence of different protein complexes in the two models. This is not surprising, since in myeloid cells other transcription factors are involved in the regulation of GM-CSF gene, including GATA factors [281]. Further ChIP analysis of myeloid transcription factors would help to better understand the composition of these two different protein complexes.

MSK1/2 phosphorylate the NF-κB p65 subunit at Ser276 leading to NF-κB activation [315]. This phosphorylation promotes the recruitment of the co-activator p300/CBP [316], followed by the acetylation of both NF-κB p65 at Lys314 and histones at the NF-κB bound promoters [243]. Both the GM-CSF promoter and enhancer encompass a NF-κB binding motif. Moreover, unpublished data from luciferase assays performed in the Cockerill lab showed that mutation of the NF-κB motif at the enhancer reduces the enhancer activity.

For all these reasons I decided to investigate the role of NF-κB in the regulation of GM-CSF gene expression, focusing especially on its cross-talk with MAPK signalling pathways. Holloway et al. [319] already demonstrated the importance of NF-κB in chromatin remodelling at the GM-CSF promoter, showing that NF-κB recruits Brg1-containing complexes to the promoter in T cells *in vitro* and that low levels of NF-κB in the nucleus lead to a reduction in GM-CSF gene transcription. Here, I confirmed the role of NF-κB on gene transcription in both

cell lines by using the proteasome inhibitor MG132. The canonical activation of NF-κB pathway consists in the phosphorylation of Iκ-B by the IKK kinases. This phosphorylation causes the detachment of Iκ-B from NF-κB, leading to the degradation of Iκ-B by the proteasome and the release of p50-p65 heterodimer into the nucleus where it binds to specific κB sites within the promoter and enhancer regions of NF-κB target genes [211, 212]. The proteasome inhibitor MG132 is known to prevent IκB degradation and the translocation of NF-κB p65 to the nucleus; this caused a decrease of GM-CSF mRNA levels in a dose-dependent way. On the other hand, as observed after H89 treatment, MG132 reduced the intensity of the DHS at the enhancer in Jurkat cells but not in KG1a cells, further suggesting the presence of two different protein complexes in the two cell lines. Moreover, the fact that H89 and MG132 inhibited PMA/I-induced GM-CSF gene expression but not chromatin remodelling at the enhancer may indicate that these two chemicals are sufficient to inhibit factors required for transcription at the promoter, but not for remodelling at the enhancer in KG1a cells. In order to address this question it would be interesting to investigate whether both p65 and MSK1 are recruited at the GM-CSF promoter after PMA/I treatment and verify their interaction. In fact, their interaction could explain why both H89 and MG132 reduced GM-CSF mRNA levels but neither of them inhibited chromatin remodelling at the enhancer. However, MG132 doesn't affect only p65, but inhibits the degradation of all the proteins regulated through the proteasome system, including several MAPK targets. For this reason MG132 is not the best chemical to study NF-κB pathway. My data should be confirmed using additional inhibitors or more specific p65 siRNAs.

I also demonstrated that NF-κB was phosphorylated at Ser276 upon PMA/I stimulation and that this phosphorylation was dependent on MAPKs. In fact the pattern of NF-κB phosphorylation strongly correlated with MSK1 phosphorylation; NF-κB phosphorylation was reduced by MAPKs inhibitors and abrogated by either the MEK/p38 inhibitors combination or the MSK1 inhibitor H89. These results suggest that MSK1 is likely to be the major factor responsible for NF-κB phosphorylation at Ser276 after PMA/I stimulation in Jurkat cells and KG1a cells and a cross-talk between MAPK and NF-kB in GM-CSF gene regulation can be speculated. A hypothetical model is represented in Figure 4.1.

However, a possible role of PKA cannot be excluded, since it can also phosphorylate p65 at Ser276 and it can be inhibited by H89. To address this question, experiments should be conducted after transfection of the cells with a kinase-dead mutant of MSK1.

NF-κB was already phosphorylated at Ser536 in the KG1a model, as in several forms of solid tumours and haematological malignancies [317, 345]. The weak reduction of p65 phosphorylation observed in KG1a after treatment with MEK inhibitor and the combination of MEK and p38 inhibitors could be mediated by the inhibition of the downstream serine/threonine kinase ribosomal S6 kinase 1 (RSK1). In fact RSK1 has been demonstrated to phosphorylate NF-κB in different models and upon different stimuli [318, 346, 347]. It would be interesting to test this hypothesis by measuring the phosphorylation levels of RSK1 after PMA/I treatment and inhibitors.

Although both the MSK1 inhibitor H89 and the proteasome inhibitor MG132 failed to reduce the intensity of the DHS, ChIP analysis confirmed the presence

in vivo of both MSK1 and NF-κB p65 at the enhancer. Their occupancy was reduced by the combination of MEK and p38 inhibitors and NF-κB recruitment was inhibited also by the MSK1 inhibitor H89, suggesting that phosphorylation of Ser276 could increase p65 binding to chromatin *in vivo* [348].

Figure 4.1. ***Hypothetical model of PMA/I-induced GM-CSF gene activation in Jurkat and KG1a cells***

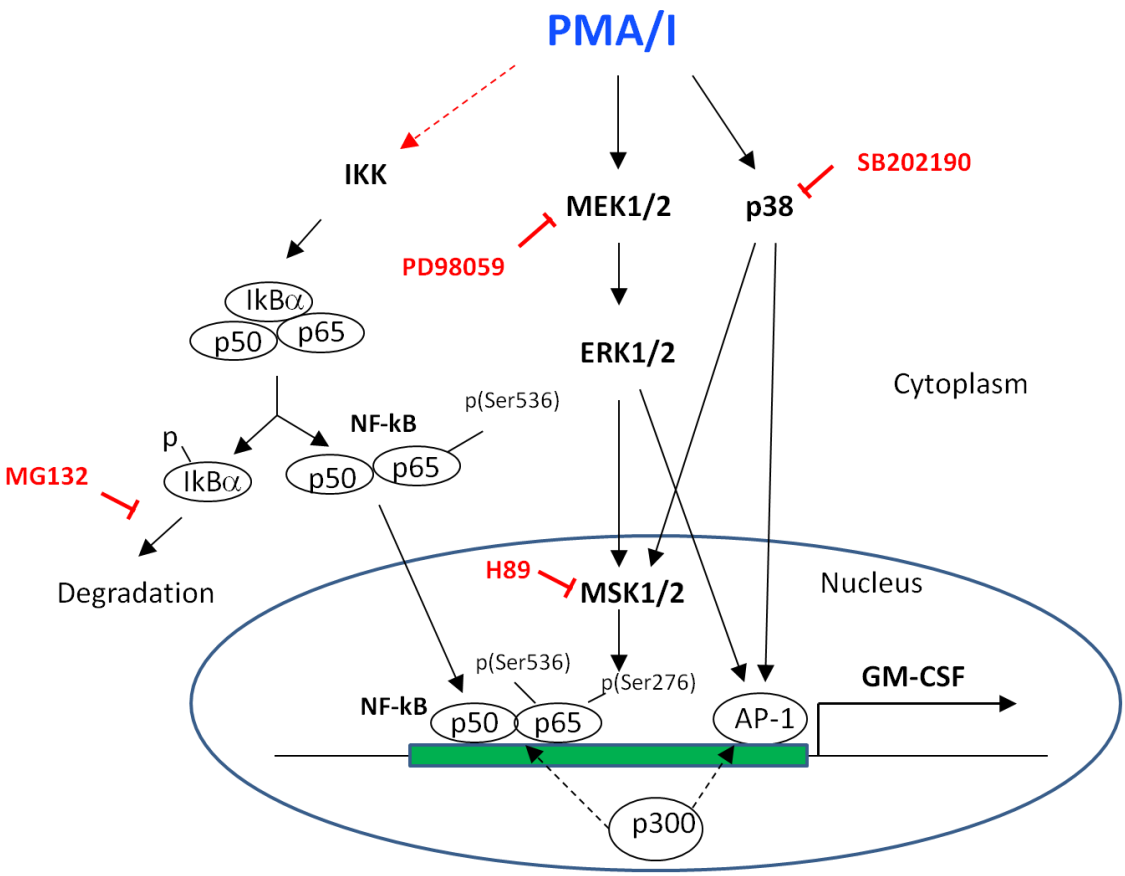

PMA/I activate ERK and p38 MAPK signalling pathways, leading to the activation of AP-1, which binds the GM-CSF enhancer (represented as a green rectangle). The ERK and p38 mutual transcription factor MSK phosphorylates p65, which is also recruited to the enhancer. A cross-talk between MAPK and NF-κB signalling pathways seems essential for the PMA/I-induced GM-CSF gene activation. Most likely PMA/I stimulation activates NF-κB pathway also through IKK in Jurkat cells (red dashed arrow), whereas this pathway is constitutively activated in KG1a cells. p300 is also recruited to the GM-CSF enhancer by PMA/I; however, further studies are needed to verify its association with AP-1 and/or NF-κB. The inhibitors used in this study are written in red.

However, these results don't give any information about p65 nuclear localisation. In fact, Carpenter and colleagues demonstrated that H89 inhibited p65 DNA binding ability *in vitro* without reducing its translocation to the nucleus [349]. An immunocytochemical staining would be needed to address this question.

H89 also inhibited the occupancy of p300 to the enhancer. My results suggest that MSK1 is likely to recruit p300 at the enhancer, probably through the phosphorylation of NF-κB p65 at Ser276. However, ChIP analysis showed that p300 was recruited to the GM-CSF enhancer both at the GM420 (NFAT/AP-1 binding motif) and GM220 site (κB motif). Co-immunoprecipitation and time course analysis would be required to define the interaction amongst the different transcription factors and the sequence of events which leads to the creation of the DHS at the enhancer.

MSK1 is also involved in chromatin remodelling and histone modifications, being able to phosphorylate Ser10 and Ser28 on histone H3. Ser10 phosphorylation has been shown to occur at the promoter of several immediate early (IE) genes in mammalian cells, including c-Fos and c-Jun, in response to mitogenic stimulation or cellular stress [315] and this phosphorylation induces gene transcription [320]. In this regard, since our results showed that PMA/I treatment increased AP-1 activity, I investigated whether MSK1 could be in part responsible for the increased c-Fos transcription. In both Jurkat and KG1a cell lines treatment with the MSK1 inhibitor H89 failed to decrease c-Fos gene expression as well as the AP-1 binding ability to the DNA in KG1a. My results showed that the increase in c-Fos expression seems not to be mediated by MSK1. The small reduction in AP-1 DNA binding in Jurkat cells could be due to an inhibitory effect of MSK1 on different components of AP-1, like c-Jun or

ATF-2. In fact, Aggeli and colleagues [312] demonstrated that phospho-MSK1 is able to form a complex with either phospho-c-Jun or phospho-ATF-2 and in their model H89 decreased the AP-1 activity induced by oxidative stress.

MAPK-mediated phosphorylation of both Ser10 and Ser28 has been shown also after PMA stimulation in mouse embryonic fibroblast cells [350]. However, histone H3 phosphorylation is not always related to transcriptional activation, but it is dependent on promoter context [351]. Lau et al. [207] demonstrated that phosphorylation at Ser28 on histone H3 by MSK1 can antagonize Polycomb silencing at targeted genes reducing the amount of H3K27me3 at the promoter and thereby promoting the activities of H3K27 HATs. The two modifications H3K27ac/Ser28ph are directly associated with the transcription-initiating form of RNA Polymerase II. Therefore, by inhibiting both MEK/ERK and p38 pathways, the effect of MSK1 on gene activation and accessibility might be lost. Histone modification and RNA Pol II ChIP analysis would be required to confirm this hypothesis.

In this study I also investigated the effect of MAPK inhibitors on a different model of leukaemia. With this purpose I used HEL cells as model of human erythroleukaemia. In contrast to Jurkat and KG1a cells, HEL cells showed a constitutive DHS at the GM-CSF enhancer and a second DHS at 4.1 kb upstream of the GM-CSF promoter. Neither MAPK inhibitors nor CsA were able to inhibit the two DHSs, whereas all the chemicals, singularly, greatly decreased the PMA/I-induced GM-CSF gene expression. It is possible that 8 hours treatment wasn’t long enough to inhibit the constitutive DHSs, but it is also possible that NFAT and AP-1 are not the only transcription factors responsible for the creation of these DHSs. In fact both DHSs contain also RUNX1 motifs and, by ChIP analysis, I demonstrated that RUNX1 bound chromatin at both

sites, especially at the -4.1kb DHS. These data demonstrated that GM-CSF gene transcription and chromatin remodelling at the enhancer are regulated via distinct mechanisms in HEL cells. From these results I can conclude that PMA/I-induced GM-CSF gene expression and its chromatin structure are regulated differently in different models of leukaemia.

Unpublished data from the Cockerill lab revealed that, similarly to the HEL cells and other types of myeloid leukaemia, a few AML patient samples showed the presence of a DHS at the GM-CSF enhancer before any stimulation. It would be interesting to test the efficacy of MAPK and other inhibitors in reducing GM-CSF gene expression and chromatin remodelling in AML primary cells, especially in those types of AML carrying specific chromosomal mutations or translocations. In fact, cell lines represent just a model of study and the stimulation with PMA/I an artificial way to induce GM-CSF gene transcription. Different stimuli (i.e. CD3/CD28 stimulation) could lead to a slightly different activation of signal pathways, in terms of entity and duration. Morever, this study on GM-CSF gene regulation could represent the starting point for a genome-wide DHS analysis on AML samples, in order to find specific remodelled target genes and to investigate which transcription factors and signalling pathways are responsible for their regulation.

In conclusion my study demonstrates a fundamental role for MAPK (especially MEK/ERK and p38) and NF-κB signalling pathways in mediating the PMA/I-induced GM-CSF gene transcription and chromatin remodelling in T blast cells and leukaemia cell lines showing an inducible DHS at the -3kb enhancer. In particular, I showed a crucial role of the AP-1 transcription factor in the PMA/I-induced GM-CSF gene expression and an interesting connection between MAPK and NF-κB pathways through MSK1. Consequently, these pathways

might represent potential targets for the treatment of AML cases where aberrant DHSs exist. However, other types of leukaemia could be regulated differently and different signalling pathways might be activated according to the presence of particular mutations or chromosomal abnormalities; for this purpose, further studies on primary cells or different leukaemia cell lines should be carried out.

5. LIST OF REFERENCES

1. Orkin, S.H., *Diversification of haematopoietic stem cells to specific lineages.* Nature reviews. Genetics, 2000. **1**(1): p. 57-64.

2. Osawa, M., et al., *Long-term lymphohematopoietic reconstitution by a single CD34-low/negative hematopoietic stem cell.* Science, 1996. **273**(5272): p. 242-5.

3. Christensen, J.L. and I.L. Weissman, *Flk-2 is a marker in hematopoietic stem cell differentiation: a simple method to isolate long-term stem cells.* Proceedings of the National Academy of Sciences of the United States of America, 2001. **98**(25): p. 14541-6.

4. Laiosa, C.V., M. Stadtfeld, and T. Graf, *Determinants of lymphoid-myeloid lineage diversification.* Annual review of immunology, 2006. **24**: p. 705-38.

5. Kondo, M., I.L. Weissman, and K. Akashi, *Identification of clonogenic common lymphoid progenitors in mouse bone marrow.* Cell, 1997. **91**(5): p. 661-672.

6. Kondo, M., I.L. Weissman, and K. Akashi, *Identification of clonogenic common lymphoid progenitors in mouse bone marrow.* Cell, 1997. **91**(5): p. 661-72.

7. Akashi, K., et al., *A clonogenic common-myeloid progenitor that gives rise to all myeloid lineages.* Nature, 2000. **404**(6774): p. 193-197.

8. Manz, M.G., et al., *Dendritic cell potentials of early lymphoid and myeloid progenitors.* Blood, 2001. **97**(11): p. 3333-41.

9. Adolfsson, J., et al., *Identification of Flt3+ lympho-myeloid stem cells lacking erythro-megakaryocytic potential a revised road map for adult blood lineage commitment.* Cell, 2005. **121**(2): p. 295-306.

10. Fauci, A.S., et al., *Harrison's Principles of Internal Medicine, 17th edition.* . The McGraw-Hill Companies, Inc.

11. Cedar, H. and Y. Bergman, *Epigenetics of haematopoietic cell development.* Nature reviews. Immunology, 2011. **11**(7): p. 478-88.

12. Lai, A.Y. and M. Kondo, *T and B lymphocyte differentiation from hematopoietic stem cell.* Seminars in immunology, 2008. **20**(4): p. 207-12.

13. Lai, A.Y. and M. Kondo, *Asymmetrical lymphoid and myeloid lineage commitment in multipotent hematopoietic progenitors.* The Journal of experimental medicine, 2006. **203**(8): p. 1867-73.

14. Peschon, J.J., et al., *Early lymphocyte expansion is severely impaired in interleukin 7 receptor-deficient mice.* The Journal of experimental medicine, 1994. **180**(5): p. 1955-60.

15. von Freeden-Jeffry, U., et al., *Lymphopenia in interleukin (IL)-7 gene-deleted mice identifies IL-7 as a nonredundant cytokine.* The Journal of experimental medicine, 1995. **181**(4): p. 1519-26.

16. Mercer, E.M., Y.C. Lin, and C. Murre, *Factors and networks that underpin early hematopoiesis.* Seminars in immunology, 2011. **23**(5): p. 317-25.

17. Scott, E.W., et al., *Requirement of transcription factor PU.1 in the development of multiple hematopoietic lineages.* Science, 1994. **265**(5178): p. 1573-7.

18. Spooner, C.J., et al., *A recurrent network involving the transcription factors PU.1 and Gfi1 orchestrates innate and adaptive immune cell fates.* Immunity, 2009. **31**(4): p. 576-86.

19. DeKoter, R.P., H.J. Lee, and H. Singh, *PU.1 regulates expression of the interleukin-7 receptor in lymphoid progenitors.* Immunity, 2002. **16**(2): p. 297-309.

20. Georgopoulos, K., *Haematopoietic cell-fate decisions, chromatin regulation and ikaros.* Nature reviews. Immunology, 2002. **2**(3): p. 162-74.

21. Bain, G., et al., *E2A proteins are required for proper B cell development and initiation of immunoglobulin gene rearrangements.* Cell, 1994. **79**(5): p. 885-92.

22. Lin, H. and R. Grosschedl, *Failure of B-cell differentiation in mice lacking the transcription factor EBF.* Nature, 1995. **376**(6537): p. 263-7.

23. Gisler, R. and M. Sigvardsson, *The human V-preB promoter is a target for coordinated activation by early B cell factor and E47.* Journal of immunology, 2002. **168**(10): p. 5130-8.

24. Nutt, S.L., et al., *Essential functions of Pax5 (BSAP) in pro-B cell development: difference between fetal and adult B lymphopoiesis and reduced V-to-DJ recombination at the IgH locus.* Genes & development, 1997. **11**(4): p. 476-91.

25. Pridans, C., et al., *Identification of Pax5 target genes in early B cell differentiation.* Journal of immunology, 2008. **180**(3): p. 1719-28.

26. Benz, C. and C.C. Bleul, *A multipotent precursor in the thymus maps to the branching point of the T versus B lineage decision.* The Journal of experimental medicine, 2005. **202**(1): p. 21-31.

27. Godfrey, D.I., et al., *A developmental pathway involving four phenotypically and functionally distinct subsets of CD3-CD4-CD8- triple-negative adult mouse thymocytes defined by CD44 and CD25 expression.* Journal of immunology, 1993. **150**(10): p. 4244-52.

28. Germain, R.N., *T-cell development and the CD4-CD8 lineage decision.* Nature reviews. Immunology, 2002. **2**(5): p. 309-22.

29. Borgulya, P., et al., *Development of the CD4 and CD8 lineage of T cells: instruction versus selection.* The EMBO journal, 1991. **10**(4): p. 913-8.

30. Radtke, F., et al., *Deficient T cell fate specification in mice with an induced inactivation of Notch1.* Immunity, 1999. **10**(5): p. 547-58.

31. Ting, C.N., et al., *Transcription factor GATA-3 is required for development of the T-cell lineage.* Nature, 1996. **384**(6608): p. 474-8.

32. Georgescu, C., et al., *A gene regulatory network armature for T lymphocyte specification.* Proceedings of the National Academy of Sciences of the United States of America, 2008. **105**(51): p. 20100-5.

33. Huang, G., et al., *PU.1 is a major downstream target of AML1 (RUNX1) in adult mouse hematopoiesis.* Nature genetics, 2008. **40**(1): p. 51-60.

34. Huang, Y. and R.L. Wange, *T cell receptor signaling: beyond complex complexes.* The Journal of biological chemistry, 2004. **279**(28): p. 28827-30.

35. Nel, A.E., *T-cell activation through the antigen receptor. Part 1: signaling components, signaling pathways, and signal integration at the T-cell antigen receptor synapse.* The Journal of allergy and clinical immunology, 2002. **109**(5): p. 758-70.

36. Nel, A.E. and N. Slaughter, *T-cell activation through the antigen receptor. Part 2: role of signaling cascades in T-cell differentiation, anergy, immune senescence, and development of immunotherapy.* The Journal of allergy and clinical immunology, 2002. **109**(6): p. 901-15.

37. Hogan, P.G., et al., *Transcriptional regulation by calcium, calcineurin, and NFAT.* Genes & development, 2003. **17**(18): p. 2205-32.

38. Macian, F., *NFAT proteins: key regulators of T-cell development and function.* Nature reviews. Immunology, 2005. **5**(6): p. 472-84.

39. Teixeiro, E., et al., *T cell receptor-mediated signal transduction controlled by the beta chain transmembrane domain: apoptosis-deficient cells display unbalanced mitogen-activated protein kinases activities upon T cell receptor engagement.* The Journal of biological chemistry, 2002. **277**(6): p. 3993-4002.

40. Gorentla, B.K. and X.P. Zhong, *T cell Receptor Signal Transduction in T lymphocytes.* Journal of clinical & cellular immunology, 2012. **2012**(Suppl 12): p. 5.

41. Schmitz, M.L. and D. Krappmann, *Controlling NF-κB activation in T cells by costimulatory receptors.* Cell Death Differ, 2006. **13**(5): p. 834-42.

42. Jerome, K.R., *Viral modulation of T-cell receptor signaling.* Journal of virology, 2008. **82**(9): p. 4194-204.

43. DeKoter, R.P. and H. Singh, *Regulation of B lymphocyte and macrophage development by graded expression of PU.1.* Science, 2000. **288**(5470): p. 1439-41.

44. Zhang, D.E., et al., *Absence of granulocyte colony-stimulating factor signaling and neutrophil development in CCAAT enhancer binding protein alpha-deficient mice.* Proceedings of the National Academy of Sciences of the United States of America, 1997. **94**(2): p. 569-74.

45. Iwasaki, H., et al., *The order of expression of transcription factors directs hierarchical specification of hematopoietic lineages.* Genes & development, 2006. **20**(21): p. 3010-21.

46. Shivdasani, R.A., et al., *A lineage-selective knockout establishes the critical role of transcription factor GATA-1 in megakaryocyte growth and platelet development.* The EMBO journal, 1997. **16**(13): p. 3965-73.

47. Hasserjian, R.P., *Acute myeloid leukemia: advances in diagnosis and classification.* International journal of laboratory hematology, 2013. **35**(3): p. 358-66.

48. Kelly, L.M. and D.G. Gilliland, *Genetics of myeloid leukemias.* Annual review of genomics and human genetics, 2002. **3**: p. 179-98.

49. Doepfner, K.T., D. Boller, and A. Arcaro, *Targeting receptor tyrosine kinase signaling in acute myeloid leukemia.* Critical reviews in oncology/hematology, 2007. **63**(3): p. 215-30.

50. Steffen, B., et al., *The molecular pathogenesis of acute myeloid leukemia.* Critical reviews in oncology/hematology, 2005. **56**(2): p. 195-221.

51. Takahashi, S., *Current findings for recurring mutations in acute myeloid leukemia.* Journal of hematology & oncology, 2011. **4**: p. 36.

52. Shih, A.H., et al., *The role of mutations in epigenetic regulators in myeloid malignancies.* Nature reviews. Cancer, 2012. **12**(9): p. 599-612.

53. Naoe, T. and H. Kiyoi, *Gene mutations of acute myeloid leukemia in the genome era.* International journal of hematology, 2013. **97**(2): p. 165-74.

54. Mitani, K., *Chromosomal abnormalities and oncogenes.* International journal of hematology, 1996. **63**(2): p. 81-93.

55. Nakamura, T., et al., *ALL-1 is a histone methyltransferase that assembles a supercomplex of proteins involved in transcriptional regulation.* Molecular cell, 2002. **10**(5): p. 1119-28.

56. Hug, B.A. and M.A. Lazar, *ETO interacting proteins.* Oncogene, 2004. **23**(24): p. 4270-4.

57. Lam, K. and D.E. Zhang, *RUNX1 and RUNX1-ETO: roles in hematopoiesis and leukemogenesis.* Frontiers in bioscience, 2012. **17**: p. 1120-39.

58. Di Croce, L., et al., *Methyltransferase recruitment and DNA hypermethylation of target promoters by an oncogenic transcription factor.* Science, 2002. **295**(5557): p. 1079-82.

59. Di Croce, L., *Chromatin modifying activity of leukaemia associated fusion proteins.* Human molecular genetics, 2005. **14 Spec No 1**: p. R77-84.

60. Fazi, F., et al., *Heterochromatic gene repression of the retinoic acid pathway in acute myeloid leukemia.* Blood, 2007. **109**(10): p. 4432-40.

61. Deneberg, S., *Epigenetics in myeloid malignancies.* Methods in molecular biology, 2012. **863**: p. 119-37.

62. Melki, J.R., et al., *Increased DNA methyltransferase expression in leukaemia.* Leukemia : official journal of the Leukemia Society of America, Leukemia Research Fund, U.K, 1998. **12**(3): p. 311-6.

63. Gama-Sosa, M.A., et al., *The 5-methylcytosine content of DNA from human tumors.* Nucleic acids research, 1983. **11**(19): p. 6883-94.

64. Van Vlierberghe, P. and A. Ferrando, *The molecular basis of T cell acute lymphoblastic leukemia.* The Journal of clinical investigation, 2012. **122**(10): p. 3398-406.

65. Weng, A.P., et al., *Activating mutations of NOTCH1 in human T cell acute lymphoblastic leukemia.* Science, 2004. **306**(5694): p. 269-71.

66. Hebert, J., et al., *Candidate tumor-suppressor genes MTS1 (p16INK4A) and MTS2 (p15INK4B) display frequent homozygous deletions in primary cells from T- but not from B-cell lineage acute lymphoblastic leukemias.* Blood, 1994. **84**(12): p. 4038-44.

67. Chen, Q., et al., *The tal gene undergoes chromosome translocation in T cell leukemia and potentially encodes a helix-loop-helix protein.* The EMBO journal, 1990. **9**(2): p. 415-24.

68. Xia, Y., et al., *TAL2, a helix-loop-helix gene activated by the (7;9)(q34;q32) translocation in human T-cell leukemia.* Proceedings of the National Academy of Sciences of the United States of America, 1991. **88**(24): p. 11416-20.

69. Boehm, T., et al., *The rhombotin family of cysteine-rich LIM-domain oncogenes: distinct members are involved in T-cell translocations to human chromosomes 11p15 and 11p13.* Proceedings of the National Academy of Sciences of the United States of America, 1991. **88**(10): p. 4367-71.

70. Su, X., et al., *Transforming potential of the T-cell acute lymphoblastic leukemia-associated homeobox genes HOXA13, TLX1, and TLX3.* Genes, chromosomes & cancer, 2006. **45**(9): p. 846-55.

71. Erikson, J., et al., *Deregulation of c-myc by translocation of the alpha-locus of the T-cell receptor in T-cell leukemias.* Science, 1986. **232**(4752): p. 884-6.

72. Clappier, E., et al., *The C-MYB locus is involved in chromosomal translocation and genomic duplications in human T-cell acute leukemia (T-ALL), the translocation defining a new T-ALL subtype in very young children.* Blood, 2007. **110**(4): p. 1251-61.

73. Palomero, T., et al., *Mutational loss of PTEN induces resistance to NOTCH1 inhibition in T-cell leukemia.* Nature medicine, 2007. **13**(10): p. 1203-10.

74. Van Vlierberghe, P., et al., *ETV6 mutations in early immature human T cell leukemias.* The Journal of experimental medicine, 2011. **208**(13): p. 2571-9.

75. Lacronique, V., et al., *A TEL-JAK2 fusion protein with constitutive kinase activity in human leukemia.* Science, 1997. **278**(5341): p. 1309-12.

76. Lee, T.I. and R.A. Young, *Transcription of eukaryotic protein-coding genes.* Annual review of genetics, 2000. **34**: p. 77-137.

77. Fuda, N.J., M.B. Ardehali, and J.T. Lis, *Defining mechanisms that regulate RNA polymerase II transcription in vivo.* Nature, 2009. **461**(7261): p. 186-92.

78. Thomas, M.C. and C.M. Chiang, *The general transcription machinery and general cofactors.* Critical reviews in biochemistry and molecular biology, 2006. **41**(3): p. 105-78.

79. Kurokawa, R., M.G. Rosenfeld, and C.K. Glass, *Transcriptional regulation through noncoding RNAs and epigenetic modifications.* RNA biology, 2009. **6**(3): p. 233-6.

80. Leach, K.M., et al., *Reconstitution of human β-Globin locus control region hypersensitive sites in the absence of chromatin assembly.* Mol Cell Biol, 2001. **21**(8): p. 2629-2640.

81. Cockerill, P.N., *Structure and function of active chromatin and DNase I hypersensitive sites.* The FEBS journal, 2011. **278**(13): p. 2182-210.

82. Gross, D.S. and W.T. Garrard, *Nuclease hypersensitive sites in chromatin.* Annual review of biochemistry, 1988. **57**: p. 159-97.

83. Gross, D.S. and W.T. Garrard, *Nuclease Hypersensitive Sites in Chromatin.* Annu Rev Biochem, 1988. **57**(1): p. 159-197.

84. Bonifer, C., *Developmental regulation of eukaryotic gene loci: which cis-regulatory information is required?* Trends Genet, 2000. **16**(7): p. 310-315.

85. Struhl, K., et al., *Activation and repression mechanisms in yeast.* Cold Spring Harbor symposia on quantitative biology, 1998. **63**: p. 413-21.

86. Sandelin, A., et al., *Mammalian RNA polymerase II core promoters: insights from genome-wide studies.* Nature reviews. Genetics, 2007. **8**(6): p. 424-36.

87. Ponjavic, J., et al., *Transcriptional and structural impact of TATA-initiation site spacing in mammalian core promoters.* Genome biology, 2006. **7**(8): p. R78.

88. Yang, C., et al., *Prevalence of the initiator over the TATA box in human and yeast genes and identification of DNA motifs enriched in human TATA-less core promoters.* Gene, 2007. **389**(1): p. 52-65.

89. Deng, W. and S.G. Roberts, *TFIIB and the regulation of transcription by RNA polymerase II.* Chromosoma, 2007. **116**(5): p. 417-29.

90. Kutach, A.K. and J.T. Kadonaga, *The downstream promoter element DPE appears to be as widely used as the TATA box in Drosophila core promoters.* Mol Cell Biol, 2000. **20**(13): p. 4754-4764.

91. Kadonaga, J.T., *The DPE, a core promoter element for transcription by RNA polymerase II.* Exp Mol Med, 2002. **34**(4): p. 259-64.

92. Smale, S.T., *Core promoters: active contributors to combinatorial gene regulation.* Genes Dev, 2001. **15**(19): p. 2503-2508.

93. Ogbourne, S. and T.M. Antalis, *Transcriptional control and the role of silencers in transcriptional regulation in eukaryotes.* The Biochemical journal, 1998. **331 (Pt 1)**: p. 1-14.

94. Blackwood, E.M. and J.T. Kadonaga, *Going the distance: a current view of enhancer action.* Science, 1998. **281**(5373): p. 60-3.

95. Hatzis, P. and I. Talianidis, *Dynamics of enhancer-promoter communication during differentiation-induced gene activation.* Molecular cell, 2002. **10**(6): p. 1467-77.

96. Valenzuela, L. and R.T. Kamakaka, *Chromatin insulators.* Annual review of genetics, 2006. **40**: p. 107-38.

97. Lobanenkov, V.V., et al., *A novel sequence-specific DNA binding protein which interacts with three regularly spaced direct repeats of the CCCTC-motif in the 5'-flanking sequence of the chicken c-myc gene.* Oncogene, 1990. **5**(12): p. 1743-53.

98. Farrell, C.M., A.G. West, and G. Felsenfeld, *Conserved CTCF insulator elements flank the mouse and human beta-globin loci.* Molecular and cellular biology, 2002. **22**(11): p. 3820-31.

99. Recillas-Targa, F., et al., *Position-effect protection and enhancer blocking by the chicken beta-globin insulator are separable activities.* Proceedings of the

National Academy of Sciences of the United States of America, 2002. **99**(10): p. 6883-8.

100. Chung, J.H., M. Whiteley, and G. Felsenfeld, *A 5' element of the chicken beta-globin domain serves as an insulator in human erythroid cells and protects against position effect in Drosophila.* Cell, 1993. **74**(3): p. 505-14.

101. Prioleau, M.N., et al., *An insulator element and condensed chromatin region separate the chicken beta-globin locus from an independently regulated erythroid-specific folate receptor gene.* The EMBO journal, 1999. **18**(14): p. 4035-48.

102. Recillas-Targa, F., A.C. Bell, and G. Felsenfeld, *Positional enhancer-blocking activity of the chicken beta-globin insulator in transiently transfected cells.* Proceedings of the National Academy of Sciences of the United States of America, 1999. **96**(25): p. 14354-9.

103. Holwerda, S.J. and W. de Laat, *CTCF: the protein, the binding partners, the binding sites and their chromatin loops.* Philosophical transactions of the Royal Society of London. Series B, Biological sciences, 2013. **368**(1620): p. 20120369.

104. Schmidt, D., et al., *Waves of retrotransposon expansion remodel genome organization and CTCF binding in multiple mammalian lineages.* Cell, 2012. **148**(1-2): p. 335-48.

105. Lee, B.K. and V.R. Iyer, *Genome-wide studies of CCCTC-binding factor (CTCF) and cohesin provide insight into chromatin structure and regulation.* The Journal of biological chemistry, 2012. **287**(37): p. 30906-13.

106. Lutz, M., et al., *Transcriptional repression by the insulator protein CTCF involves histone deacetylases.* Nucleic acids research, 2000. **28**(8): p. 1707-13.

107. Yusufzai, T.M., et al., *CTCF tethers an insulator to subnuclear sites, suggesting shared insulator mechanisms across species.* Molecular cell, 2004. **13**(2): p. 291-8.

108. Luscombe, N.M., et al., *An overview of the structures of protein-DNA complexes.* Genome biology, 2000. **1**(1): p. REVIEWS001.

109. Auble, D.T., et al., *Molecular analysis of the SNF2/SWI2 protein family member MOT1, an ATP-driven enzyme that dissociates TATA-binding protein from DNA.* Molecular and cellular biology, 1997. **17**(8): p. 4842-51.

110. Knoepfler, P.S. and R.N. Eisenman, *Sin meets NuRD and other tails of repression.* Cell, 1999. **99**(5): p. 447-50.

111. Kornberg, R.D. and Y. Lorch, *Twenty-five years of the nucleosome, fundamental particle of the eukaryote chromosome.* Cell, 1999. **98**(3): p. 285-94.

112. Luger, K., et al., *Crystal structure of the nucleosome core particle at 2.8 A resolution.* Nature, 1997. **389**(6648): p. 251-60.

113. Zlatanova, J., S.H. Leuba, and K. van Holde, *Chromatin structure revisited.* Critical reviews in eukaryotic gene expression, 1999. **9**(3-4): p. 245-55.

114. Elgin, S.C., *Heterochromatin and gene regulation in Drosophila.* Current opinion in genetics & development, 1996. **6**(2): p. 193-202.

115. Maeshima, K. and M. Eltsov, *Packaging the genome: the structure of mitotic chromosomes.* Journal of biochemistry, 2008. **143**(2): p. 145-53.

116. Wang, G.G., C.D. Allis, and P. Chi, *Chromatin remodeling and cancer, Part II: ATP-dependent chromatin remodeling.* Trends in molecular medicine, 2007. **13**(9): p. 373-80.

117. Hake, S.B., A. Xiao, and C.D. Allis, *Linking the epigenetic 'language' of covalent histone modifications to cancer.* British journal of cancer, 2004. **90**(4): p. 761-9.

118. Plass, C., et al., *Mutations in regulators of the epigenome and their connections to global chromatin patterns in cancer.* Nature reviews. Genetics, 2013. **14**(11): p. 765-80.

119. Kouzarides, T., *Chromatin modifications and their function.* Cell, 2007. **128**(4): p. 693-705.

120. Jenuwein, T. and C.D. Allis, *Translating the histone code.* Science, 2001. **293**(5532): p. 1074-80.

121. Bhaumik, S.R., E. Smith, and A. Shilatifard, *Covalent modifications of histones during development and disease pathogenesis.* Nature structural & molecular biology, 2007. **14**(11): p. 1008-16.

122. Bhaumik, S.R., E. Smith, and A. Shilatifard, *Covalent modifications of histones during development and disease pathogenesis.* Nat Struct Mol Biol, 2007. **14**(11): p. 1008-1016.

123. Pena, P.V., et al., *Molecular mechanism of histone H3K4me3 recognition by plant homeodomain of ING2.* Nature, 2006. **442**(7098): p. 100-3.

124. Wysocka, J., et al., *A PHD finger of NURF couples histone H3 lysine 4 trimethylation with chromatin remodelling.* Nature, 2006. **442**(7098): p. 86-90.

125. Arzate-Mejia, R.G., D. Valle-Garcia, and F. Recillas-Targa, *Signaling epigenetics: novel insights on cell signaling and epigenetic regulation.* IUBMB life, 2011. **63**(10): p. 881-95.

126. Steward, M.M., et al., *Molecular regulation of H3K4 trimethylation by ASH2L, a shared subunit of MLL complexes.* Nature structural & molecular biology, 2006. **13**(9): p. 852-4.

127. Wang, Z., et al., *Combinatorial patterns of histone acetylations and methylations in the human genome.* Nature genetics, 2008. **40**(7): p. 897-903.

128. Kimura, H., *Histone modifications for human epigenome analysis.* Journal of human genetics, 2013. **58**(7): p. 439-45.

129. Nowak, S.J. and V.G. Corces, *Phosphorylation of histone H3: a balancing act between chromosome condensation and transcriptional activation.* Trends in genetics : TIG, 2004. **20**(4): p. 214-20.

130. Macdonald, N., et al., *Molecular basis for the recognition of phosphorylated and phosphoacetylated histone h3 by 14-3-3.* Molecular cell, 2005. **20**(2): p. 199-211.

131. Shilatifard, A., *Chromatin modifications by methylation and ubiquitination: implications in the regulation of gene expression.* Annual review of biochemistry, 2006. **75**: p. 243-69.

132. Bannister, A.J., et al., *Selective recognition of methylated lysine 9 on histone H3 by the HP1 chromo domain.* Nature, 2001. **410**(6824): p. 120-4.

133. Munari, F., et al., *Methylation of lysine 9 in histone H3 directs alternative modes of highly dynamic interaction of heterochromatin protein hHP1beta with the nucleosome.* The Journal of biological chemistry, 2012. **287**(40): p. 33756-65.

134. Cao, R., Y. Tsukada, and Y. Zhang, *Role of Bmi-1 and Ring1A in H2A ubiquitylation and Hox gene silencing.* Molecular cell, 2005. **20**(6): p. 845-54.

135. Eskeland, R., et al., *Ring1B compacts chromatin structure and represses gene expression independent of histone ubiquitination.* Molecular cell, 2010. **38**(3): p. 452-64.

136. Orford, K., et al., *Differential H3K4 methylation identifies developmentally poised hematopoietic genes.* Developmental cell, 2008. **14**(5): p. 798-809.

137. Heintzman, N.D., et al., *Distinct and predictive chromatin signatures of transcriptional promoters and enhancers in the human genome.* Nature genetics, 2007. **39**(3): p. 311-8.

138. Barski, A., et al., *High-resolution profiling of histone methylations in the human genome.* Cell, 2007. **129**(4): p. 823-37.

139. Li, B., M. Carey, and J.L. Workman, *The role of chromatin during transcription.* Cell, 2007. **128**(4): p. 707-19.

140. Klose, R.J. and Y. Zhang, *Regulation of histone methylation by demethylimination and demethylation.* Nature reviews. Molecular cell biology, 2007. **8**(4): p. 307-18.

141. Wu, S.C. and Y. Zhang, *Active DNA demethylation: many roads lead to Rome.* Nature reviews. Molecular cell biology, 2010. **11**(9): p. 607-20.

142. Okano, M., et al., *DNA methyltransferases Dnmt3a and Dnmt3b are essential for de novo methylation and mammalian development.* Cell, 1999. **99**(3): p. 247-57.

143. Hermann, A., R. Goyal, and A. Jeltsch, *The Dnmt1 DNA-(cytosine-C5)-methyltransferase methylates DNA processively with high preference for hemimethylated target sites.* The Journal of biological chemistry, 2004. **279**(46): p. 48350-9.

144. Tahiliani, M., et al., *Conversion of 5-methylcytosine to 5-hydroxymethylcytosine in mammalian DNA by MLL partner TET1.* Science, 2009. **324**(5929): p. 930-5.

145. Goll, M.G. and T.H. Bestor, *Eukaryotic cytosine methyltransferases.* Annual review of biochemistry, 2005. **74**: p. 481-514.

146. Baubec, T. and D. Schubeler, *Genomic patterns and context specific interpretation of DNA methylation.* Current opinion in genetics & development, 2014. **25C**: p. 85-92.

147. Deaton, A.M. and A. Bird, *CpG islands and the regulation of transcription.* Genes & development, 2011. **25**(10): p. 1010-22.

148. Biterge, B. and R. Schneider, *Histone variants: key players of chromatin.* Cell and tissue research, 2014.

149. Hake, S.B. and C.D. Allis, *Histone H3 variants and their potential role in indexing mammalian genomes: the "H3 barcode hypothesis".* Proceedings of the National Academy of Sciences of the United States of America, 2006. **103**(17): p. 6428-35.

150. Malik, H.S. and S. Henikoff, *Phylogenomics of the nucleosome.* Nature structural biology, 2003. **10**(11): p. 882-91.

151. Martens, J.A. and F. Winston, *Recent advances in understanding chromatin remodeling by Swi/Snf complexes.* Current opinion in genetics & development, 2003. **13**(2): p. 136-42.

152. Ooi, L., et al., *BRG1 chromatin remodeling activity is required for efficient chromatin binding by repressor element 1-silencing transcription factor (REST) and facilitates REST-mediated repression.* The Journal of biological chemistry, 2006. **281**(51): p. 38974-80.

153. Corona, D.F. and J.W. Tamkun, *Multiple roles for ISWI in transcription, chromosome organization and DNA replication.* Biochimica et biophysica acta, 2004. **1677**(1-3): p. 113-9.

154. Shimono, K., et al., *Microspherule protein 1, Mi-2beta, and RET finger protein associate in the nucleolus and up-regulate ribosomal gene transcription.* The Journal of biological chemistry, 2005. **280**(47): p. 39436-47.

155. Kobor, M.S., et al., *A protein complex containing the conserved Swi2/Snf2-related ATPase Swr1p deposits histone variant H2A.Z into euchromatin.* PLoS biology, 2004. **2**(5): p. E131.

156. Dong, C., R.J. Davis, and R.A. Flavell, *MAP kinases in the immune response.* Annual review of immunology, 2002. **20**: p. 55-72.

157. Schaeffer, H.J. and M.J. Weber, *Mitogen-activated protein kinases: specific messages from ubiquitous messengers.* Molecular and cellular biology, 1999. **19**(4): p. 2435-44.

158. Geest, C.R. and P.J. Coffer, *MAPK signaling pathways in the regulation of hematopoiesis.* Journal of leukocyte biology, 2009. **86**(2): p. 237-50.

159. Junttila, M.R., S.P. Li, and J. Westermarck, *Phosphatase-mediated crosstalk between MAPK signaling pathways in the regulation of cell survival.* FASEB journal : official publication of the Federation of American Societies for Experimental Biology, 2008. **22**(4): p. 954-65.

160. Vermeulen, L., et al., *The versatile role of MSKs in transcriptional regulation.* Trends in biochemical sciences, 2009. **34**(6): p. 311-8.

161. Pages, G., et al., *Defective thymocyte maturation in p44 MAP kinase (Erk 1) knockout mice.* Science, 1999. **286**(5443): p. 1374-7.

162. Saba-El-Leil, M.K., et al., *An essential function of the mitogen-activated protein kinase Erk2 in mouse trophoblast development.* EMBO reports, 2003. **4**(10): p. 964-8.

163. Ross, S.E., et al., *Phosphorylation of C/EBPalpha inhibits granulopoiesis.* Molecular and cellular biology, 2004. **24**(2): p. 675-86.

164. Mori, M., et al., *Activation of extracellular signal-regulated kinases ERK1 and ERK2 induces Bcl-xL up-regulation via inhibition of caspase activities in erythropoietin signaling.* Journal of cellular physiology, 2003. **195**(2): p. 290-7.

165. Zarubin, T. and J. Han, *Activation and signaling of the p38 MAP kinase pathway.* Cell research, 2005. **15**(1): p. 11-8.

166. Mudgett, J.S., et al., *Essential role for p38alpha mitogen-activated protein kinase in placental angiogenesis.* Proceedings of the National Academy of Sciences of the United States of America, 2000. **97**(19): p. 10454-9.

167. Arai, H., et al., *Functional regulation of TEL by p38-induced phosphorylation.* Biochemical and biophysical research communications, 2002. **299**(1): p. 116-25.

168. Uddin, S., et al., *Differentiation stage-specific activation of p38 mitogen-activated protein kinase isoforms in primary human erythroid cells.* Proceedings of the National Academy of Sciences of the United States of America, 2004. **101**(1): p. 147-52.

169. Geest, C.R., et al., *p38 MAP kinase inhibits neutrophil development through phosphorylation of C/EBPalpha on serine 21.* Stem cells, 2009. **27**(9): p. 2271-82.

170. Sabapathy, K., et al., *c-Jun NH2-terminal kinase (JNK)1 and JNK2 have similar and stage-dependent roles in regulating T cell apoptosis and proliferation.* The Journal of experimental medicine, 2001. **193**(3): p. 317-28.

171. Nagata, Y., E. Nishida, and K. Todokoro, *Activation of JNK signaling pathway by erythropoietin, thrombopoietin, and interleukin-3.* Blood, 1997. **89**(8): p. 2664-9.

172. Bonnesen, B., et al., *MEK kinase 1 activity is required for definitive erythropoiesis in the mouse fetal liver.* Blood, 2005. **106**(10): p. 3396-404.

173. Nagata, Y., et al., *Activation of p38 MAP kinase and JNK but not ERK is required for erythropoietin-induced erythroid differentiation.* Blood, 1998. **92**(6): p. 1859-69.

174. Sasaki, T., et al., *The stress kinase mitogen-activated protein kinase kinase (MKK)7 is a negative regulator of antigen receptor and growth factor receptor-induced proliferation in hematopoietic cells.* The Journal of experimental medicine, 2001. **194**(6): p. 757-68.

175. Johnson, D.E., *Src family kinases and the MEK/ERK pathway in the regulation of myeloid differentiation and myeloid leukemogenesis.* Advances in enzyme regulation, 2008. **48**: p. 98-112.

176. Towatari, M., et al., *Constitutive activation of mitogen-activated protein kinase pathway in acute leukemia cells.* Leukemia : official journal of the Leukemia Society of America, Leukemia Research Fund, U.K, 1997. **11**(4): p. 479-84.

177. Shahjahan, M., et al., *p38 mitogen-activated protein kinase has different degrees of activation in myeloproliferative disorders and myelodysplastic syndromes.* American journal of clinical pathology, 2008. **130**(4): p. 635-41.

178. Raitano, A.B., et al., *The Bcr-Abl leukemia oncogene activates Jun kinase and requires Jun for transformation.* Proceedings of the National Academy of Sciences of the United States of America, 1995. **92**(25): p. 11746-50.

179. Elsasser, A., et al., *The fusion protein AML1-ETO in acute myeloid leukemia with translocation t(8;21) induces c-jun protein expression via the proximal AP-1 site of the c-jun promoter in an indirect, JNK-dependent manner.* Oncogene, 2003. **22**(36): p. 5646-57.

180. Hartman, A.D., et al., *Constitutive c-jun N-terminal kinase activity in acute myeloid leukemia derives from Flt3 and affects survival and proliferation.* Experimental hematology, 2006. **34**(10): p. 1360-76.

181. Klein, A.M., E. Zaganjor, and M.H. Cobb, *Chromatin-tethered MAPKs.* Current opinion in cell biology, 2013. **25**(2): p. 272-7.

182. Hu, S., et al., *Profiling the human protein-DNA interactome reveals ERK2 as a transcriptional repressor of interferon signaling.* Cell, 2009. **139**(3): p. 610-22.

183. Chen, Y.J., Y.N. Wang, and W.C. Chang, *ERK2-mediated C-terminal serine phosphorylation of p300 is vital to the regulation of epidermal growth factor-induced keratin 16 gene expression.* The Journal of biological chemistry, 2007. **282**(37): p. 27215-28.

184. Simone, C., et al., *p38 pathway targets SWI-SNF chromatin-remodeling complex to muscle-specific loci.* Nature genetics, 2004. **36**(7): p. 738-43.

185. Kim, K.Y. and D.E. Levin, *Mpk1 MAPK association with the Paf1 complex blocks Sen1-mediated premature transcription termination.* Cell, 2011. **144**(5): p. 745-56.

186. Ferreiro, I., et al., *The p38 SAPK is recruited to chromatin via its interaction with transcription factors.* The Journal of biological chemistry, 2010. **285**(41): p. 31819-28.

187. Zhang, H.M., et al., *Mitogen-induced recruitment of ERK and MSK to SRE promoter complexes by ternary complex factor Elk-1.* Nucleic acids research, 2008. **36**(8): p. 2594-607.

188. Lopez-Bergami, P., E. Lau, and Z. Ronai, *Emerging roles of ATF2 and the dynamic AP1 network in cancer.* Nature reviews. Cancer, 2010. **10**(1): p. 65-76.

189. Reddy, S.P. and B.T. Mossman, *Role and regulation of activator protein-1 in toxicant-induced responses of the lung.* American journal of physiology. Lung cellular and molecular physiology, 2002. **283**(6): p. L1161-78.

190. Angel, P. and M. Karin, *The role of Jun, Fos and the AP-1 complex in cell-proliferation and transformation.* Biochimica et biophysica acta, 1991. **1072**(2-3): p. 129-57.

191. Chinenov, Y. and T.K. Kerppola, *Close encounters of many kinds: Fos-Jun interactions that mediate transcription regulatory specificity.* Oncogene, 2001. **20**(19): p. 2438-52.

192. Yokoyama, K., et al., *C-Fos regulation by the MAPK and PKC pathways in intervertebral disc cells.* PloS one, 2013. **8**(9): p. e73210.

193. Piech-Dumas, K.M., et al., *The cAMP responsive element and CREB partially mediate the response of the tyrosine hydroxylase gene to phorbol ester.* Journal of neurochemistry, 2001. **76**(5): p. 1376-85.

194. Whitmarsh, A.J. and R.J. Davis, *Transcription factor AP-1 regulation by mitogen-activated protein kinase signal transduction pathways.* Journal of molecular medicine, 1996. **74**(10): p. 589-607.

195. Dhanasekaran, N. and E. Premkumar Reddy, *Signaling by dual specificity kinases.* Oncogene, 1998. **17**(11 Reviews): p. 1447-55.

196. Chen, R.H., et al., *Phosphorylation of c-Fos at the C-terminus enhances its transforming activity.* Oncogene, 1996. **12**(7): p. 1493-502.

197. Skinner, M., et al., *Transcriptional activation and transformation by FosB protein require phosphorylation of the carboxyl-terminal activation domain.* Molecular and cellular biology, 1997. **17**(5): p. 2372-80.

198. Gruda, M.C., et al., *Regulation of Fra-1 and Fra-2 phosphorylation differs during the cell cycle of fibroblasts and phosphorylation in vitro by MAP kinase affects DNA binding activity.* Oncogene, 1994. **9**(9): p. 2537-47.

199. Murakami, M., et al., *Phosphorylation and high level expression of Fra-2 in v-src transformed cells: a pathway of activation of endogenous AP-1.* Oncogene, 1997. **14**(20): p. 2435-44.

200. Tomas-Zuber, M., et al., *C-terminal elements control location, activation threshold, and p38 docking of ribosomal S6 kinase B (RSKB).* The Journal of biological chemistry, 2001. **276**(8): p. 5892-9.

201. Sands, W.A. and T.M. Palmer, *Regulating gene transcription in response to cyclic AMP elevation.* Cellular signalling, 2008. **20**(3): p. 460-6.

202. Wiggin, G.R., et al., *MSK1 and MSK2 are required for the mitogen- and stress-induced phosphorylation of CREB and ATF1 in fibroblasts.* Molecular and cellular biology, 2002. **22**(8): p. 2871-81.

203. Vermeulen, L., et al., *Transcriptional activation of the NF-kappaB p65 subunit by mitogen- and stress-activated protein kinase-1 (MSK1).* The EMBO journal, 2003. **22**(6): p. 1313-24.

204. Quivy, V. and C. Van Lint, *Regulation at multiple levels of NF-kappaB-mediated transactivation by protein acetylation.* Biochemical pharmacology, 2004. **68**(6): p. 1221-9.

205. Vicent, G.P., et al., *Induction of progesterone target genes requires activation of Erk and Msk kinases and phosphorylation of histone H3.* Molecular cell, 2006. **24**(3): p. 367-81.

206. Duncan, E.A., et al., *The kinases MSK1 and MSK2 are required for epidermal growth factor-induced, but not tumor necrosis factor-induced, histone H3 Ser10 phosphorylation.* The Journal of biological chemistry, 2006. **281**(18): p. 12521-5.

207. Lau, P.N. and P. Cheung, *Histone code pathway involving H3 S28 phosphorylation and K27 acetylation activates transcription and antagonizes polycomb silencing.* Proceedings of the National Academy of Sciences of the United States of America, 2011. **108**(7): p. 2801-6.

208. Tiwari, V.K., et al., *A chromatin-modifying function of JNK during stem cell differentiation.* Nature genetics, 2012. **44**(1): p. 94-100.

209. Braun, T., et al., *Targeting NF-kappaB in hematologic malignancies.* Cell death and differentiation, 2006. **13**(5): p. 748-58.

210. Karin, M., et al., *NF-kappaB in cancer: from innocent bystander to major culprit.* Nature reviews. Cancer, 2002. **2**(4): p. 301-10.

211. Henkel, T., et al., *Rapid proteolysis of I kappa B-alpha is necessary for activation of transcription factor NF-kappa B.* Nature, 1993. **365**(6442): p. 182-5.

212. Palombella, V.J., et al., *The ubiquitin-proteasome pathway is required for processing the NF-kappa B1 precursor protein and the activation of NF-kappa B.* Cell, 1994. **78**(5): p. 773-85.

213. Hoesel, B. and J.A. Schmid, *The complexity of NF-kappaB signaling in inflammation and cancer.* Molecular cancer, 2013. **12**: p. 86.

214. Dunn, G.P., L.J. Old, and R.D. Schreiber, *The three Es of cancer immunoediting.* Annual review of immunology, 2004. **22**: p. 329-60.

215. Liou, G.Y. and P. Storz, *Reactive oxygen species in cancer.* Free radical research, 2010. **44**(5): p. 479-96.

216. Wang, Y., et al., *Akt/Ezrin Tyr353/NF-kappaB pathway regulates EGF-induced EMT and metastasis in tongue squamous cell carcinoma.* British journal of cancer, 2014. **110**(3): p. 695-705.

217. Jayakumar, T., et al., *Anti-cancer Effects of CME-1, a Novel Polysaccharide, Purified from the Mycelia of Cordyceps sinensis against B16-F10 Melanoma Cells.* Journal of cancer research and therapeutics, 2014. **10**(1): p. 43-9.

218. Xie, T.X., et al., *Constitutive NF-kappaB activity regulates the expression of VEGF and IL-8 and tumor angiogenesis of human glioblastoma.* Oncology reports, 2010. **23**(3): p. 725-32.

219. Ben-Neriah, Y. and M. Karin, *Inflammation meets cancer, with NF-kappaB as the matchmaker.* Nature immunology, 2011. **12**(8): p. 715-23.

220. Pflueger, D., et al., *Discovery of non-ETS gene fusions in human prostate cancer using next-generation RNA sequencing.* Genome research, 2011. **21**(1): p. 56-67.

221. Garg, A. and B.B. Aggarwal, *Nuclear transcription factor-kappaB as a target for cancer drug development.* Leukemia : official journal of the Leukemia Society of America, Leukemia Research Fund, U.K, 2002. **16**(6): p. 1053-68.

222. Breccia, M. and G. Alimena, *NF-kappaB as a potential therapeutic target in myelodysplastic syndromes and acute myeloid leukemia.* Expert opinion on therapeutic targets, 2010. **14**(11): p. 1157-76.

223. Lee, C.H., et al., *NF-kappaB as a potential molecular target for cancer therapy.* BioFactors, 2007. **29**(1): p. 19-35.

224. Munzert, G., et al., *Constitutive NF-kappab/Rel activation in philadelphia chromosome positive (Ph+) acute lymphoblastic leukemia (ALL).* Leukemia & lymphoma, 2004. **45**(6): p. 1181-4.

225. Baumgartner, B., et al., *Increased IkappaB kinase activity is associated with activated NF-kappaB in acute myeloid blasts.* Leukemia : official journal of the Leukemia Society of America, Leukemia Research Fund, U.K, 2002. **16**(10): p. 2062-71.

226. Estrov, Z., et al., *Phenylarsine oxide blocks interleukin-1beta-induced activation of the nuclear transcription factor NF-kappaB, inhibits proliferation, and induces apoptosis of acute myelogenous leukemia cells.* Blood, 1999. **94**(8): p. 2844-53.

227. Chen, F.E., et al., *Crystal structure of p50/p65 heterodimer of transcription factor NF-kappaB bound to DNA.* Nature, 1998. **391**(6665): p. 410-3.

228. Wan, F. and M.J. Lenardo, *Specification of DNA binding activity of NF-kappaB proteins.* Cold Spring Harbor perspectives in biology, 2009. **1**(4): p. a000067.

229. Calao, M., et al., *A pervasive role of histone acetyltransferases and deacetylases in an NF-kappaB-signaling code.* Trends in biochemical sciences, 2008. **33**(7): p. 339-49.

230. Sasaki, C.Y., et al., *Phosphorylation of RelA/p65 on serine 536 defines an I{kappa}B{alpha}-independent NF-{kappa}B pathway.* The Journal of biological chemistry, 2005. **280**(41): p. 34538-47.

231. Ryo, A., et al., *Regulation of NF-kappaB signaling by Pin1-dependent prolyl isomerization and ubiquitin-mediated proteolysis of p65/RelA.* Molecular cell, 2003. **12**(6): p. 1413-26.

232. Sundar, I.K., et al., *Mitogen- and stress-activated kinase 1 (MSK1) regulates cigarette smoke-induced histone modifications on NF-kappaB-dependent genes.* PloS one, 2012. **7**(2): p. e31378.

233. Lin, C.C., et al., *Thrombin induces inducible nitric oxide synthase expression via the MAPK, MSK1, and NF-kappaB signaling pathways in alveolar macrophages.* European journal of pharmacology, 2011. **672**(1-3): p. 180-7.

234. Jacks, K.A. and C.A. Koch, *Differential regulation of mitogen- and stress-activated protein kinase-1 and -2 (MSK1 and MSK2) by CK2 following UV radiation.* The Journal of biological chemistry, 2010. **285**(3): p. 1661-70.

235. Nowak, D.E., et al., *RelA Ser276 phosphorylation is required for activation of a subset of NF-kappaB-dependent genes by recruiting cyclin-dependent kinase 9/cyclin T1 complexes.* Molecular and cellular biology, 2008. **28**(11): p. 3623-38.

236. Zhong, H., R.E. Voll, and S. Ghosh, *Phosphorylation of NF-kappa B p65 by PKA stimulates transcriptional activity by promoting a novel bivalent*

interaction with the coactivator CBP/p300. Molecular cell, 1998. **1**(5): p. 661-71.

237. Yang, Z., et al., *Recruitment of P-TEFb for stimulation of transcriptional elongation by the bromodomain protein Brd4.* Molecular cell, 2005. **19**(4): p. 535-45.

238. Nicodeme, E., et al., *Suppression of inflammation by a synthetic histone mimic.* Nature, 2010. **468**(7327): p. 1119-23.

239. Chen, L.F., Y. Mu, and W.C. Greene, *Acetylation of RelA at discrete sites regulates distinct nuclear functions of NF-kappaB.* The EMBO journal, 2002. **21**(23): p. 6539-48.

240. Chen, L., et al., *Duration of nuclear NF-kappaB action regulated by reversible acetylation.* Science, 2001. **293**(5535): p. 1653-7.

241. Kiernan, R., et al., *Post-activation turn-off of NF-kappa B-dependent transcription is regulated by acetylation of p65.* The Journal of biological chemistry, 2003. **278**(4): p. 2758-66.

242. Saccani, S., S. Pantano, and G. Natoli, *Two waves of nuclear factor kappaB recruitment to target promoters.* The Journal of experimental medicine, 2001. **193**(12): p. 1351-9.

243. Chen, L.F., et al., *NF-kappaB RelA phosphorylation regulates RelA acetylation.* Molecular and cellular biology, 2005. **25**(18): p. 7966-75.

244. Metcalf, D., *Hematopoietic cytokines.* Blood, 2008. **111**(2): p. 485-91.

245. Lotem, J. and L. Sachs, *Cytokine control of developmental programs in normal hematopoiesis and leukemia.* Oncogene, 2002. **21**(21): p. 3284-94.

246. Cockerill, P.N., et al., *The human granulocyte-macrophage colony-stimulating factor gene is autonomously regulated in vivo by an inducible tissue-specific enhancer.* Proceedings of the National Academy of Sciences of the United States of America, 1999. **96**(26): p. 15097-102.

247. Nicola, N.A., *Hemopoietic cell growth factors and their receptors.* Annual review of biochemistry, 1989. **58**: p. 45-77.

248. Dexter, T.M. and E. Spooncer, *Growth and Differentiation in the Hemopoietic System.* Annu Rev Cell Biol, 1987. **3**(1): p. 423-441.

249. Kobayashi, M., et al., *Interleukin-3 is significantly more effective than other colony- stimulating factors in long-term maintenance of human bone marrow-derived colony-forming cells in vitro.* Blood, 1989. **73**(7): p. 1836-1841.

250. Hara, T. and A. Miyajima, *Function and signal transduction mediated by the interleukin 3 receptor system in hematopoiesis.* Stem cells, 1996. **14**(6): p. 605-18.

251. Ihle, J.N., *STATs: signal transducers and activators of transcription.* Cell, 1996. **84**(3): p. 331-4.

252. Sato, N., et al., *Signal transduction by the high-affinity GM-CSF receptor: two distinct cytoplasmic regions of the common beta subunit responsible for different signaling.* The EMBO journal, 1993. **12**(11): p. 4181-9.

253. Russell, N.H., *Autocrine growth factors and leukaemic haemopoiesis.* Blood reviews, 1992. **6**(3): p. 149-56.

254. Kelleher, C., et al., *Synergism between recombinant growth factors, GM-CSF and G-CSF, acting on the blast cells of acute myeloblastic leukemia.* Blood, 1987. **69**(5): p. 1498-503.

255. Hoang, T., et al., *Interleukin 1 enhances growth factor-dependent proliferation of the clonogenic cells in acute myeloblastic leukemia and of normal human primitive hemopoietic precursors.* The Journal of experimental medicine, 1988. **168**(2): p. 463-74.

256. Bradbury, D., et al., *Interleukin-1 is one factor which regulates autocrine production of GM-CSF by the blast cells of acute myeloblastic leukaemia.* British journal of haematology, 1990. **76**(4): p. 488-93.

257. Hoang, T., et al., *Tumor necrosis factor alpha stimulates the growth of the clonogenic cells of acute myeloblastic leukemia in synergy with granulocyte/macrophage colony-stimulating factor.* The Journal of experimental medicine, 1989. **170**(1): p. 15-26.

258. Hoang, T., et al., *Interleukin-6 enhances growth factor-dependent proliferation of the blast cells of acute myeloblastic leukemia.* Blood, 1988. **72**(2): p. 823-6.

259. Young, D.C. and J.D. Griffin, *Autocrine secretion of GM-CSF in acute myeloblastic leukemia.* Blood, 1986. **68**(5): p. 1178-81.

260. Cheng, G.Y., et al., *Structure and expression of genes of GM-CSF and G-CSF in blast cells from patients with acute myeloblastic leukemia.* Blood, 1988. **71**(1): p. 204-8.

261. Kaufman, D.C., et al., *Enhanced expression of the granulocyte-macrophage colony stimulating factor gene in acute myelocytic leukemia cells following in vitro blast cell enrichment.* Blood, 1988. **72**(4): p. 1329-32.

262. Oster, W., et al., *Participation of the cytokines interleukin 6, tumor necrosis factor-alpha, and interleukin 1-beta secreted by acute myelogenous leukemia blasts in autocrine and paracrine leukemia growth control.* The Journal of clinical investigation, 1989. **84**(2): p. 451-7.

263. Kluck, P.M., et al., *Order of human hematopoietic growth factor and receptor genes on the long arm of chromosome 5, as determined by fluorescence in situ hybridization.* Annals of hematology, 1993. **66**(1): p. 15-20.

264. Baxter, E.W., et al., *The inducible tissue-specific expression of the human IL-3/GM-CSF locus is controlled by a complex array of developmentally regulated enhancers.* Journal of immunology, 2012. **189**(9): p. 4459-69.

265. Stoecklin, G., S. Hahn, and C. Moroni, *Functional hierarchy of AUUUA motifs in mediating rapid interleukin-3 mRNA decay.* J Biol Chem, 1994. **269**(46): p. 28591-28597.

266. Shaw, G. and R. Kamen, *A conserved AU sequence from the 3' untranslated region of GM-CSF mRNA mediates selective mRNA degradation.* Cell, 1986. **46**(5): p. 659-667.

267. Cockerill, P.N., *Mechanisms of transcriptional regulation of the human IL-3/GM-CSF locus by inducible tissue-specific promoters and enhancers.* Critical reviews in immunology, 2004. **24**(6): p. 385-408.

268. Duncliffe, K.N., et al., *A T cell-specific enhancer in the interleukin-3 locus is activated cooperatively by Oct and NFAT elements within a DNase I-hypersensitive site.* Immunity, 1997. **6**(2): p. 175-85.

269. Hawwari, A., et al., *The human IL-3 locus is regulated cooperatively by two NFAT-dependent enhancers that have distinct tissue-specific activities.* Journal of immunology, 2002. **169**(4): p. 1876-86.

270. Shoemaker, S.G., R. Hromas, and K. Kaushansky, *Transcriptional regulation of interleukin 3 gene expression in T lymphocytes.* Proceedings of the National Academy of Sciences of the United States of America, 1990. **87**(24): p. 9650-4.

271. Mathey-Prevot, B., et al., *Positive and negative elements regulate human interleukin 3 expression.* Proceedings of the National Academy of Sciences of the United States of America, 1990. **87**(13): p. 5046-50.

272. Bert, A.G., et al., *Reconstitution of T cell-specific transcription directed by composite NFAT/Oct elements.* Journal of immunology, 2000. **165**(10): p. 5646-55.

273. Bowers, S.R., et al., *A conserved insulator that recruits CTCF and cohesin exists between the closely related but divergently regulated interleukin-3 and granulocyte-macrophage colony-stimulating factor genes.* Molecular and cellular biology, 2009. **29**(7): p. 1682-93.

274. Mirabella, F., et al., *The human IL-3/granulocyte-macrophage colony-stimulating factor locus is epigenetically silent in immature thymocytes and is progressively activated during T cell development.* Journal of immunology, 2010. **184**(6): p. 3043-54.

275. Johnson, B.V., et al., *Granulocyte-macrophage colony-stimulating factor enhancer activation requires cooperation between NFAT and AP-1 elements and is associated with extensive nucleosome reorganization.* Molecular and cellular biology, 2004. **24**(18): p. 7914-30.

276. Cockerill, P.N., et al., *Human granulocyte-macrophage colony-stimulating factor enhancer function is associated with cooperative interactions between AP-1 and NFATp/c.* Molecular and cellular biology, 1995. **15**(4): p. 2071-9.

277. Rao, A., C. Luo, and P.G. Hogan, *Transcription factors of the NFAT family: regulation and function.* Annual review of immunology, 1997. **15**: p. 707-47.

278. Aramburu, J., et al., *Affinity-driven peptide selection of an NFAT inhibitor more selective than cyclosporin A.* Science, 1999. **285**(5436): p. 2129-33.

279. Cockerill, G.W., et al., *Regulation of granulocyte-macrophage colony-stimulating factor and E-selectin expression in endothelial cells by cyclosporin A and the T-cell transcription factor NFAT.* Blood, 1995. **86**(7): p. 2689-98.

280. Bowers, S.R., et al., *Runx1 binds as a dimeric complex to overlapping Runx1 sites within a palindromic element in the human GM-CSF enhancer.* Nucleic acids research, 2010. **38**(18): p. 6124-34.

281. Bert, A.G., et al., *A modular enhancer is differentially regulated by GATA and NFAT elements that direct different tissue-specific patterns of nucleosome positioning and inducible chromatin remodeling.* Molecular and cellular biology, 2007. **27**(8): p. 2870-85.

282. Cakouros, D., et al., *A NF-kappa B/Sp1 region is essential for chromatin remodeling and correct transcription of a human granulocyte-macrophage colony-stimulating factor transgene.* Journal of immunology, 2001. **167**(1): p. 302-10.

283. Shang, C., et al., *Nuclear factor of activated T cells contributes to the function of the CD28 response region of the granulocyte macrophage-colony stimulating factor promoter.* International immunology, 1999. **11**(12): p. 1945-56.

284. Schonwasser, D.C., et al., *Activation of the mitogen-activated protein kinase/extracellular signal-regulated kinase pathway by conventional, novel, and atypical protein kinase C isotypes.* Molecular and cellular biology, 1998. **18**(2): p. 790-8.

285. Nomura, N., et al., *Phorbol 12-myristate 13-acetate-activated protein kinase C increased migratory activity of subconjunctival fibroblasts via stress-activated protein kinase pathways.* Molecular vision, 2007. **13**: p. 2320-7.

286. Rana, T.M., *Illuminating the silence: understanding the structure and function of small RNAs.* Nature reviews. Molecular cell biology, 2007. **8**(1): p. 23-36.

287. Brown, K., et al., *Mutual regulation of the transcriptional activator NF-kappa B and its inhibitor, I kappa B-alpha.* Proceedings of the National Academy of Sciences of the United States of America, 1993. **90**(6): p. 2532-6.

288. Pfeifhofer-Obermair, C., N. Thuille, and G. Baier, *Involvement of distinct PKC gene products in T cell functions.* Frontiers in immunology, 2012. **3**: p. 220.

289. Cockerill, P.N., et al., *The granulocyte-macrophage colony-stimulating factor/interleukin 3 locus is regulated by an inducible cyclosporin A-sensitive enhancer.* Proceedings of the National Academy of Sciences of the United States of America, 1993. **90**(6): p. 2466-70.

290. Zhang, B., et al., *The calcineurin-NFAT pathway allows for urokinase receptor-mediated beta3 integrin signaling to cause podocyte injury.* Journal of molecular medicine, 2012. **90**(12): p. 1407-20.

291. Vieira, L., et al., *Three-way translocation (X;20;16)(p11;q13;q23) in essential thrombocythemia implicates NFATC2 in dysregulation of CSF2 expression and megakaryocyte proliferation.* Genes, chromosomes & cancer, 2012. **51**(12): p. 1093-108.

292. Fuertes, M.B., et al., *Regulated expression of galectin-1 during T-cell activation involves Lck and Fyn kinases and signaling through MEK1/ERK, p38 MAP kinase and p70S6 kinase.* Molecular and cellular biochemistry, 2004. **267**(1-2): p. 177-85.

293. Li, Y.Q., et al., *Regulation of lymphotoxin production by the p21ras-raf-MEK-ERK cascade in PHA/PMA-stimulated Jurkat cells.* Journal of immunology, 1999. **162**(6): p. 3316-20.

294. Song, H., et al., *IL-18 enhances ULBP2 expression through the MAPK pathway in leukemia cells.* Immunology letters, 2008. **120**(1-2): p. 103-7.

295. Kale, V.P., *Differential activation of MAPK signaling pathways by TGF-beta1 forms the molecular mechanism behind its dose-dependent bidirectional effects on hematopoiesis.* Stem cells and development, 2004. **13**(1): p. 27-38.

296. Hirosawa, M., et al., *The p38 pathway inhibitor SB202190 activates MEK/MAPK to stimulate the growth of leukemia cells.* Leukemia research, 2009. **33**(5): p. 693-9.

297. Davis, R.J., *Signal transduction by the JNK group of MAP kinases.* Cell, 2000. **103**(2): p. 239-52.

298. Leppa, S., et al., *Differential regulation of c-Jun by ERK and JNK during PC12 cell differentiation.* The EMBO journal, 1998. **17**(15): p. 4404-13.

299. Whitmarsh, A.J., et al., *Integration of MAP kinase signal transduction pathways at the serum response element.* Science, 1995. **269**(5222): p. 403-7.

300. Lin, C.C., et al., *Upregulation of COX-2/PGE2 by ET-1 mediated through Ca2+-dependent signals in mouse brain microvascular endothelial cells.* Molecular neurobiology, 2014. **49**(3): p. 1256-69.

301. Lee, I.T., et al., *TNF-alpha induces cytosolic phospholipase A2 expression in human lung epithelial cells via JNK1/2- and p38 MAPK-dependent AP-1 activation.* PloS one, 2013. **8**(9): p. e72783.

302. Bowers, E.M., et al., *Virtual ligand screening of the p300/CBP histone acetyltransferase: identification of a selective small molecule inhibitor.* Chemistry & biology, 2010. **17**(5): p. 471-82.

303. Blow, M.J., et al., *ChIP-Seq identification of weakly conserved heart enhancers.* Nature genetics, 2010. **42**(9): p. 806-10.

304. Creyghton, M.P., et al., *Histone H3K27ac separates active from poised enhancers and predicts developmental state.* Proceedings of the National Academy of Sciences of the United States of America, 2010. **107**(50): p. 21931-6.

305. Di Cerbo, V., et al., *Acetylation of histone H3 at lysine 64 regulates nucleosome dynamics and facilitates transcription.* eLife, 2014. **3**: p. e01632.

306. Bedford, D.C. and P.K. Brindle, *Is histone acetylation the most important physiological function for CBP and p300?* Aging, 2012. **4**(4): p. 247-55.

307. Thomson, S., et al., *The nucleosomal response associated with immediate-early gene induction is mediated via alternative MAP kinase cascades: MSK1 as a potential histone H3/HMG-14 kinase.* The EMBO journal, 1999. **18**(17): p. 4779-93.

308. Gustin, J.A., et al., *Tumor necrosis factor activates CRE-binding protein through a p38 MAPK/MSK1 signaling pathway in endothelial cells.* American journal of physiology. Cell physiology, 2004. **286**(3): p. C547-55.

309. Darragh, J., et al., *MSKs are required for the transcription of the nuclear orphan receptors Nur77, Nurr1 and Nor1 downstream of MAPK signalling.* The Biochemical journal, 2005. **390**(Pt 3): p. 749-59.

310. Bruck, N., et al., *A coordinated phosphorylation cascade initiated by p38MAPK/MSK1 directs RARalpha to target promoters.* The EMBO journal, 2009. **28**(1): p. 34-47.

311. Brami-Cherrier, K., et al., *Role of the ERK/MSK1 signalling pathway in chromatin remodelling and brain responses to drugs of abuse.* Journal of neurochemistry, 2009. **108**(6): p. 1323-35.

312. Aggeli, I.K., C. Gaitanaki, and I. Beis, *Involvement of JNKs and p38-MAPK/MSK1 pathways in H2O2-induced upregulation of heme oxygenase-1 mRNA in H9c2 cells.* Cellular signalling, 2006. **18**(10): p. 1801-12.

313. Kefaloyianni, E., C. Gaitanaki, and I. Beis, *ERK1/2 and p38-MAPK signalling pathways, through MSK1, are involved in NF-kappaB transactivation during oxidative stress in skeletal myoblasts.* Cellular signalling, 2006. **18**(12): p. 2238-51.

314. Delghandi, M.P., M. Johannessen, and U. Moens, *The cAMP signalling pathway activates CREB through PKA, p38 and MSK1 in NIH 3T3 cells.* Cellular signalling, 2005. **17**(11): p. 1343-51.

315. Arthur, J.S., *MSK activation and physiological roles.* Frontiers in bioscience : a journal and virtual library, 2008. **13**: p. 5866-79.

316. Mukherjee, S.P., et al., *Analysis of the RelA:CBP/p300 interaction reveals its involvement in NF-kappaB-driven transcription.* PLoS biology, 2013. **11**(9): p. e1001647.

317. Kim, J.Y., et al., *NF-kappaB activation is related to the resistance of lung cancer cells to TNF-alpha-induced apoptosis.* Biochemical and biophysical research communications, 2000. **273**(1): p. 140-6.

318. Bohuslav, J., et al., *p53 induces NF-kappaB activation by an IkappaB kinase-independent mechanism involving phosphorylation of p65 by ribosomal S6 kinase 1.* The Journal of biological chemistry, 2004. **279**(25): p. 26115-25.

319. Holloway, A.F., et al., *Changes in chromatin accessibility across the GM-CSF promoter upon T cell activation are dependent on nuclear factor kappaB proteins.* The Journal of experimental medicine, 2003. **197**(4): p. 413-23.

320. Shimada, M., et al., *cAMP-response element-binding protein (CREB) controls MSK1-mediated phosphorylation of histone H3 at the c-fos promoter in vitro.* The Journal of biological chemistry, 2010. **285**(13): p. 9390-401.

321. Chadee, D.N., et al., *Increased Ser-10 phosphorylation of histone H3 in mitogen-stimulated and oncogene-transformed mouse fibroblasts.* The Journal of biological chemistry, 1999. **274**(35): p. 24914-20.

322. Rosenbauer, F., et al., *Acute myeloid leukemia induced by graded reduction of a lineage-specific transcription factor, PU.1.* Nature genetics, 2004. **36**(6): p. 624-30.

323. Ptasinska, A., et al., *Depletion of RUNX1/ETO in t(8;21) AML cells leads to genome-wide changes in chromatin structure and transcription factor binding.* Leukemia : official journal of the Leukemia Society of America, Leukemia Research Fund, U.K, 2012. **26**(8): p. 1829-41.

324. Abraham, R.T. and A. Weiss, *Jurkat T cells and development of the T-cell receptor signalling paradigm.* Nature reviews. Immunology, 2004. **4**(4): p. 301-8.

325. Cantrell, D.A., et al., *T lymphocyte activation signals.* Ciba Foundation symposium, 1992. **164**: p. 208-18; discussion 218-22.

326. Randriamampita, C. and A. Trautmann, *Ca2+ signals and T lymphocytes; "New mechanisms and functions in Ca2+ signalling".* Biology of the cell / under the auspices of the European Cell Biology Organization, 2004. **96**(1): p. 69-78.

327. Smeets, R.L., et al., *Molecular pathway profiling of T lymphocyte signal transduction pathways; Th1 and Th2 genomic fingerprints are defined by TCR and CD28-mediated signaling.* BMC immunology, 2012. **13**: p. 12.

328. Northrop, J.P., et al., *NF-AT components define a family of transcription factors targeted in T-cell activation.* Nature, 1994. **369**(6480): p. 497-502.

329. Tourneur, E., et al., *Cyclosporine A impairs nucleotide binding oligomerization domain (Nod1)-mediated innate antibacterial renal defenses in mice and human transplant recipients.* PLoS pathogens, 2013. **9**(1): p. e1003152.

330. Crabtree, G.R., *Calcium, calcineurin, and the control of transcription.* The Journal of biological chemistry, 2001. **276**(4): p. 2313-6.

331. St Louis, D.C., et al., *Evidence for distinct intracellular signaling pathways in CD34+ progenitor to dendritic cell differentiation from a human cell line model.* Journal of immunology, 1999. **162**(6): p. 3237-48.

332. Bain, J., et al., *The selectivity of protein kinase inhibitors: a further update.* The Biochemical journal, 2007. **408**(3): p. 297-315.

333. Godl, K., et al., *An efficient proteomics method to identify the cellular targets of protein kinase inhibitors.* Proceedings of the National Academy of Sciences of the United States of America, 2003. **100**(26): p. 15434-9.

334. Hall-Jackson, C.A., et al., *Effect of SB 203580 on the activity of c-Raf in vitro and in vivo.* Oncogene, 1999. **18**(12): p. 2047-54.

335. Alessi, D.R., et al., *PD 098059 is a specific inhibitor of the activation of mitogen-activated protein kinase kinase in vitro and in vivo.* The Journal of biological chemistry, 1995. **270**(46): p. 27489-94.

336. Davies, S.P., et al., *Specificity and mechanism of action of some commonly used protein kinase inhibitors.* The Biochemical journal, 2000. **351**(Pt 1): p. 95-105.

337. Ahn, N.G., et al., *Pharmacologic inhibitors of MKK1 and MKK2.* Methods in enzymology, 2001. **332**: p. 417-31.

338. Karin, M., Z. Liu, and E. Zandi, *AP-1 function and regulation.* Current opinion in cell biology, 1997. **9**(2): p. 240-6.

339. Smeal, T., et al., *Different requirements for formation of Jun: Jun and Jun: Fos complexes.* Genes & development, 1989. **3**(12B): p. 2091-100.

340. Murphy, L.O., et al., *Molecular interpretation of ERK signal duration by immediate early gene products.* Nature cell biology, 2002. **4**(8): p. 556-64.

341. Monje, P., et al., *Regulation of the transcriptional activity of c-Fos by ERK. A novel role for the prolyl isomerase PIN1.* The Journal of biological chemistry, 2005. **280**(42): p. 35081-4.

342. Humar, M., et al., *The mitogen-activated protein kinase p38 regulates activator protein 1 by direct phosphorylation of c-Jun.* The international journal of biochemistry & cell biology, 2007. **39**(12): p. 2278-88.

343. Pulverer, B.J., et al., *Phosphorylation of c-jun mediated by MAP kinases.* Nature, 1991. **353**(6345): p. 670-4.

344. Smeal, T., et al., *Oncogenic and transcriptional cooperation with Ha-Ras requires phosphorylation of c-Jun on serines 63 and 73.* Nature, 1991. **354**(6353): p. 494-6.

345. Kordes, U., et al., *Transcription factor NF-kappaB is constitutively activated in acute lymphoblastic leukemia cells.* Leukemia : official journal of the Leukemia Society of America, Leukemia Research Fund, U.K, 2000. **14**(3): p. 399-402.

346. Xu, S., et al., *Angiotensin II modulates interleukin-1beta-induced inflammatory gene expression in vascular smooth muscle cells via interfering with ERK-NF-kappaB crosstalk.* Biochemical and biophysical research communications, 2011. **410**(3): p. 543-8.

347. Kim, K.W., et al., *Extracellular signal-regulated kinase/90-KDA ribosomal S6 kinase/nuclear factor-kappa B pathway mediates phorbol 12-myristate 13-acetate-induced megakaryocytic differentiation of K562 cells.* The Journal of biological chemistry, 2001. **276**(16): p. 13186-91.

348. Reber, L., et al., *Ser276 phosphorylation of NF-kB p65 by MSK1 controls SCF expression in inflammation.* PloS one, 2009. **4**(2): p. e4393.

349. Carpenter, O.L. and S. Wu, *Regulation of MSK1-Mediated NF-kappaB Activation Upon UVB Irradiation.* Photochemistry and photobiology, 2013.

350. Soloaga, A., et al., *MSK2 and MSK1 mediate the mitogen- and stress-induced phosphorylation of histone H3 and HMG-14.* The EMBO journal, 2003. **22**(11): p. 2788-97.

351. Johansen, K.M. and J. Johansen, *Regulation of chromatin structure by histone H3S10 phosphorylation.* Chromosome research : an international journal on the molecular, supramolecular and evolutionary aspects of chromosome biology, 2006. **14**(4): p. 393-404.